Acta Universitatis Szegediensis

Acta Biologica Szegediensis

Volume 65,
Number 2,
2021

University of Szeged, Szeged, Hungary

http://abs.bibl.u-szeged.hu/index.php/abs

Acta Biologica Szegediensis

Volume 65(2):133-143, 2021
Acta Biologica Szegediensis
http://abs.bibl.u-szeged.hu/index.php/abs

DOI:10.14232/abs.2021.2.133-143

ARTICLE

Molecular, micromorphological and anatomical study of rangeland species of *Atriplex* (Chenopodiaceae) in Iran

Abolfazl Tahmasebi

Department of Range and Watershed Management, Faculty of Agriculture and Natural Resources, Gonbad Kavous University, Gonbad, Iran.

ABSTRACT *Atriplex*, as the largest genus of the Chenopodiaceae, is well known for its taxonomic complexity resulting from overlapping morphological characters. This halophytic perennial is distributed in salty and dry soils of Eurasia, America and Australia. *Atriplex* is one of the most widely cultivated rangeland species in Iran, which improves and revitalizes the rangelands. These unique characteristics of *Atriplex* make it a valuable plant. The present study is the first micromorphological investigation of this genus in Iran. In this study, the molecular evidence, micromorphological and anatomical structure of four species of *Atriplex* have been considered to evaluate their relationships. The basic shape of the pollen grains in most taxa is subprolate, however prolate and spheroidal pollen grains were recorded for *A. lentiformis* and *A. canescens*. One type of trichome (glandular) is described. Here, among the glandular trichomes, density and size of trichomes are considered as valuable characteristics. Micromorphology of epidermis illustrated three types of epidermal cells including puzzle-shaped, polygonal and irregular. Stem cross sections showed rounded shape, but the margins are different between four species. Using nuclear and plastid markers (nrDNA ITS and *rpl*32-*trn*$L_{(UAG)}$), we reconstructed phylogenetic relationships within four species of *Atriplex*. This data set was analyzed by phylogenetic methods including Bayesian inference, maximum likelihood and maximum parsimony. In phylogenetic analyses, all members of four species formed a well-supported clade (PP = 1; ML/BS = 100/100), divided into three major subclades (I, II and III). The results of the present study showed the usefulness of micromorphological, anatomical and molecular characteristics in taxon delimitation at specific levels.

KEY WORDS

anatomical structure
Atriplex
Iran
molecular
pollen
trichome

ARTICLE INFORMATION

Submitted
14 May 2021
Accepted
21 September 2021
***Corresponding author**
E-mail: ab_tahmasebi@gonbad.ac.ir

Introduction

Chenopodiaceae, as the largest family of the Caryophyllales (Cuenoud et al. 2002), contains 110 genera with 1700 species. They are predominantly found in arid to semiarid, saline and agricultural habitats in temperate and subtropical regions (Grigore 2012; Grigore et al. 2014). However, this family is very problematic from a taxonomical point of view and several attempts were recorded to clarify its position within Caryophyllales, and especially the phylogenetic relationships between Amaranthaceae and Chenopodiaceae (Kadereit et al. 2003). Angiosperm Phylogeny Group II (2003), APG III (2009) and APG IV (2016) do not recognize Chenopodiaceae as a separate family from Amaranthaceae, instead only the second is being maintained. Although all morphological characters seem to overlap in Chenopodiaceae and Amaranthaceae s. str., the familial status of the Chenopodiaceae is accepted in recent taxonomic treatments (Sukhorukov 2014; Hernández-Ledesma et al. 2015; Sukhorukov et al. 2019).

Atriplex L. (Atripliceae) can complete its life cycle in saline soils and can be used optimally if there are proper management plans. *Atriplex* species are known for complex genetics, rapid evolutionary rates and high tolerance to xeric, saline, and contaminated soils. It contains several distinguishable species by their morphology, cycle of development and ecological adaptation (Barrow and Osuna 2002). *Atriplex* is the largest genus of the Chenopodiaceae including 260 species in the world (Sukhorukov and Danin 2009) with 18 species in the Flora Iranica region (Hedge 1753). It is mainly distributed in arid and semiarid regions of Eurasia, America and Australia (Sukhorukov and Danin 2009). It is crucial that *Atriplex* species are endowed with an aerial and root-like biomass in the arid and semi-arid regions. The species of *Atriplex* are annual, perennial herbs, subshrubs, or shrubs. The species are often covered with bladder-like hairs that later

Figure 1. Natural habitat of studied species in East North of Iran.

collapse, and rarely with long trichomes. They constitute an efficient tool and relatively little expensive in the struggle against erosion and the desertification (Essafi et al. 2006). In South Africa, the genus seems to be less diverse, however in this region and in South America, it has not been extensively studied so far.

The evolution of C4 photosynthesis has played an important role in the evolutionary success of the genus because the bulk of *Atriplex* species perform C4 photosynthesis. *Atriplex* has typical Kranz anatomy with a layer of bundle sheath cells surrounding each vascular bundle and radially arranged palisade cells (Kadereit et al. 2010). This Atriplicoid leaf type (Carolin et al. 1975) occurs in two variants, viz. the *Atriplex halimus* L. and the *A. dimorphostegia* Kar. & Kir. types, respectively (Khatib 1959; Kadereit et al. 2003). Mozafar and Goodin (1970) studied vesiculated hairs in *A. halimus* as a mechanism for salt tolerance. Troughton and Card (1973) examined the anatomy of *A. buchananii* (Kirk) Kirk ex Cheeseman leaves in New Zealand. The previous phytochemical analyses of some *Atriplex* spp. reported the presence of several classes of secondary metabolites such as saponins, glycosides, flavonoids, tannins, terpenoids, alkaloids, and proteins (Ksouri et al. 2012). Khaniki et al (2012) examined anatomical structure of leaves and stems in *Chenopodium* L. and *Atriplex* in South Khorasan Province. Foliar anatomy of three species of Chenopodiaceae family including *Chenopodium album* L., *Kochia prostrate* L. and *Noaea mucronata* (Forssk.) Asch. & Schweinf. were studied by Zarinkamar (2006). Lu et al. (2018a) investigated the pollen morphological characters of 13 genera and 24 species of the Chenopodiaceae. Molecular phylogeny of Atripliceae (Chenopodioideae, Chenopodiaceae) including *Atriplex* and its implications for systematics, biogeography, flower and fruit evolution and the origin of C4 photosynthesis has been done by Kadereit et al. (2010). *Atriplex* is a rather polymorphic genus with fruiting bract morphology that has many transitional character states, the delimitation from its relative genera has always been problematic (Wilson 1984).

Due to the structural adaptations of this genus to environmental conditions (Kadereit et al. 2010), it was decided to examine the rangeland species of *Atriplex*. Proper knowledge of plant species is essential in the ecosystem and the type of management that should be applied in rangelands.

Table 1. List of species used in the study along with localities and vouchers.

Taxa	Collection data (all samples are from Iran)	GenBank accession no. ITS/rpl32-trnL(UAG)
A. canescens (Pursh) Nutt.	Golestan: Gonbad Kavous, Chapar Qoymeh, Tahmasebi, 803298, GKUH	LC631597/ LC631609
A. canescens	Golestan: Gonbad Kavous, Chapar Qoymeh, Tahmasebi, 803297, GKUH	LC631598 / LC631610
A. canescens	Golestan: Gonbad Kavous, Chapar Qoymeh, Tahmasebi, 803299, GKUH	LC631599 / LC631611
A. lentiformis (Torr.) S.Wats.	Golestan: Gonbad Kavous, Agh Abad, Tahmasebi, 803292, GKUH	LC631588 / LC631600
A. lentiformis	Golestan: Gonbad Kavous, Agh Abad, Tahmasebi, 803290, GKUH	LC631589 / LC631601
A. lentiformis	Golestan: Gonbad Kavous, Agh Abad, Tahmasebi, 803279, GKUH	LC631590 / LC631602
A. halimus L.	Golestan: Gonbad Kavous, Chapar Qoymeh, Tahmasebi, 803270, GKUH	LC631594 / LC631606
A. halimus	Golestan: Gonbad Kavous, Chapar Qoymeh, Tahmasebi, 803273, GKUH	LC631595 / LC631607
A. halimus	Golestan: Gonbad Kavous, Chapar Qoymeh, Tahmasebi, 803289, GKUH	LC631596 / LC631608
A. leucoclada Boiss.	Golestan: Gonbad Kavous, Agh Abad, Tahmasebi, 803278, GKUH	LC631591 / LC631603
A. leucoclada	Golestan: Gonbad Kavous, Agh Abad, Tahmasebi, 803295, GKUH	LC631592 / LC631604
A. leucoclada	Golestan: Gonbad Kavous, Agh Abad, Tahmasebi, 803296, GKUH	LC631593 / LC631605

GKUH: Gonbad Kavous University Herbarium

Table 2. Pollen morphological characters for the examined taxa of *Atriplex*.

Taxon	Length of polar axis (µm ±SD)	Length of equatorial axis (µm ± SD)	P/E	Shape	Colpus length (µm±SD)	Colpus width (µm±SD)	Ornamentation
A. canescens	21.55±1.48	18.77±0.43	1.14	Spheroidal	18.60±0.12	1.23±0.05	granulate
A. canescens	21.05±1.17	19.65±0.27	1.07	Spheroidal	18.80±0.09	1.14±0.01	granulate
A. canescens	22.05±1.17	18.65±0.27	1.07	Spheroidal	17.80±0.09	1.25±0.01	granulate
A. lentiformis	28.75±2.03	18.37±0.32	1.56	Prolate	20.70±0.15	1.75±0.09	microperforate
A. lentiformis	23.65±1.19	19.43±0.35	1.21	Prolate	19.16±0.16	1.74±0.04	microperforate
A. lentiformis	26.79±1.18	19.67±0.29	1.36	Prolate	21.96±0.07	1.63±0.01	microperforate
A. halimus	38.73±1.31	27.35±0.34	1.41	Subprolate	26.36±0.21	2.85±0.03	microechinate
A. halimus	34.65±1.36	22.43±0.31	1.54	Subprolate	25.10±0.16	2.70±0.01	microechinate
A. halimus	36.75±0.41	24.47±0.44	1.50	Subprolate	24.98±0.12	2.34±0.07	microechinate
A. leucoclada	37.64±0.34	25.35±0.17	1.48	Subprolate	25.49±0.28	2.45±0.04	Granulate-microechinate
A. leucoclada	35.44±0.38	23.65±0.28	1.49	Subprolate	25.70±0.19	2.78±0.06	Granulate-microechinate
A. leucoclada	35.44±0.38	23.65±0.28	1.49	Subprolate	25.70±0.19	2.78±0.06	Granulate-microechinate

There is no comprehensive micromorphological, anatomical and molecular study covering rangeland species of *Atriplex* in Iran. Therefore, the main objective of this study is to provide a detailed investigation and description of trichomes, pollen and epidermis micromorphology of the rangeland species of *Atriplex*. This has been mainly investigated by scanning electron microscopy (SEM) to determine whether this data is valuable in the taxonomy of the genus and delimitation of the species. Furthermore, micromorphology of epidermis, trichomes, and pollen of these species are described for the first time. The specific objectives of this study were as follows: (1) to find morphological characters that could be useful for the diagnosis of taxa; (2) to study the species relationship; (3) to assess the value of micromorphological, anatomical and molecular characters in rangeland species of *Atriplex* in Iran.

Materials and methods

Morphological methods

In the present study, 12 specimens of four *Atriplex* species were collected from different locations in North Iran (Fig. 1) and preserved in the Gonbad Kavous University Herbarium (GKUH). Identification of specimens was carried out based on Flora Iranica (Hedge 1753). The list of voucher specimens and details of localities are given in Table 1. Palynological studies on pollens of *Atriplex canescens* (Pursh) Nutt., *A. lentiformis* (Torr.) S.Wats., *A. halimus* and *A. leucoclada* Boiss. were made using a light microscope (LM) (Olympus, Vanox AHBS3) with a DP12 digital camera and a scanning electron microscope (SEM; Tescan, Vega-3 LMU). For SEM investigations, the pollen grains were transferred directly to double-sided tape affixed stubs and were sputter-coated with gold plates. The applied terminology based on Punt et al. (2007). For LM studies, the samples were acetolyzed following Erdtman's technique (Erdtman 1952). The pollen samples were obtained from freshly collected herbarium specimens. The measurements were based on at least 30 pollen grains per specimen. The characters of pollen grains of the studied species are summarized in Table 2. Trichome micromorphological characters of four species of *Atriplex* were investigated. Samples were removed from Gonbad Kavous University Herbarium (GKUH): To check the consistency of trichome types in different parts of a certain taxa, trichomes of stem and leaves were first investigated with stereomicroscope. Scanning electron microscopic studies were only made on leaf samples. Small pieces of leaves were fixed on aluminum stubs using double-sided adhesive and coated with a thin layer of gold-palladium. The SEM micrographs were taken in a SEM (Tescan, Vega-3 LMU) at an accelerating voltage of 15-22 kV at Research Institute of Razi (Tehran, Iran). The descriptive terminology mainly follows Salmaki et al. (2009); Zamfirache et al. (2009); Osman (2012), with some modifications. A list of voucher specimens used in this study is presented in Table 1.

Anatomical methods

The materials for anatomical studies were fixed in the field with formalin-acetic acid-alcohol (FAA). Four cross-sections were measured for each sample to assess the consistency of anatomical characters. All materials were boiled for 15 min and then fixed in Carnoy solution (alcohols to acetic acid in proportion 3:1). Handmade cross-sections were obtained from the stem using commercial razor blades. The cross-sections were obtained using carmine and methylene green double staining methods. Subsequently, the materials were washed in distilled water

Table 3. Leaf epidermal anatomical features of *Atriplex*.

Taxon	Cell shape*	Anticlinal walls	Stomata index (mm^2)	Stomata density (mm^2)	Stomata size (μm)	Stomata type
A. canescens	Puz	Zip	7 ±0.01	191.70±2.3	49.62×42.24	Anomocytic
A. canescens	Puz	Zip	9±0.04	198.50±4.3	46.31×40.43	Anomocytic
A. canescens	Puz	Zip	7 ±0.02	189.32±3.3	52.41×46.34	Anomocytic
A. lentiformis	Puz	Str	11±0.09	120.25±2.1	71.32×66.24	Anomocytic
A. lentiformis	Puz	Str	11±0.02	107.18±1.4	62.45×53.14	Anomocytic
A. lentiformis	Puz	Str	12±0.03	132.23±1.2	61.41×54.32	Anomocytic
A. halimus	Pol	Sin	14±0.04	151.16±3.2	82.43×65.30	Anomocytic
A. halimus	Pol	Sin	13±0.01	147.19±2.5	75.25×51.20	Anomocytic
A. halimus	Pol	Sin	14±0.04	158.14±4.2	80.42×52.33	Anomocytic
A. leucoclada	Irr	Wa	13±0.07	125.28±1.7	53.40×62.30	Anomocytic
A. leucoclada	Irr	Wa	12±0.09	110.19±3.5	55.41×55.34	Anomocytic
A. leucoclada	Irr	Wa	13±0.04	123.14±4.2	52.35×66.30	Anomocytic

*Irr: Irregular; Pol: Polygonal; Puz: Puzzle-shaped; Sin: Sinuous; Str: Straight; Wa: Wavy; Zip: Zip-shaped.

(1 minute) and dehydrated through an ethyl alcohol (70%) and were mounted on microscopic glass slides. Slide sections were studied and photographed.

Epidermis studies on leaves of *A. canescens*, *A. lentiformis*, *A. halimus* and *A. leucoclada* were made using a scanning electron microscope (SEM; Tescan, Vega-3 LMU). Small pieces of leaves were fixed on aluminum stubs using double-sided adhesive and coated with a thin layer of gold-palladium. The SEM micrographs were taken in a SEM (Tescan, Vega-3 LMU) at an accelerating voltage of 15-22 kV at Research Institute of Razi (Tehran, Iran). Some characters (stomata length/weight, number of stomata, number of epidermal cells) were measured with Image Tools ver. 3.0 and AxioVision 4.8. (Table 3).

Molecular methods

Taxon sampling

A sampling includes plants from 12 specimens and four species of *Atriplex* were chosen as an ingroup for nrDNA ITS and *rpl*32-*trn*$L_{(UAG)}$. *Halimione verucifera* Aellen was chosen as an outgroup following previous molecular phylogenetic studies (Kadereit et al. 2010). A list of all the taxa used in this study and the sources, voucher information and GenBank accession numbers are given in Table 1.

DNA extraction, PCR and sequencing

Total genomic DNA was extracted from dried leaf materials deposited in Gonbad Kavous University Herbarium (GKUH), using the Kit method. The nrDNA ITS (Nuclear ribosomal DNA Internal Transcribed Spacer) region was amplified using the primers ITS5m of Sang et al. (1995) and ITS4 of White et al. (1990). The *rpl*32-*trn*$L_{(UAG)}$ spacer was amplified using the rpl32-F and trn$L_{(UAG)}$ primers described in Shaw et al. (2007). PCR amplification of the DNA regions followed procedures described in detail by Naderi Safar et al. (2014). The quality of PCR products was checked by electrophoresis in 1% agarose gels in 1 × TAE (pH 8) buffer and were photographed with a UV gel documentation system (UVItec, Cambridge, UK). PCR products along with the same primers were sent for Sanger sequencing at Macrogen (Seoul, South Korea) through Pishgam (Tehran, Iran).

Sequence alignment

Combined dataset was aligned using the web-based version of MUSCLE (Edgar 2004 at http://www.ebi.ac.uk/Tools/msa/muscle/) under default parameters followed by manual adjustment. The alignment of the dataset required the introduction of numerous single and multiple-base indels (insertions/deletions). Positions of indels were treated as missing data for the ITS and *rpl*32-*trn*$L_{(UAG)}$ datasets.

Phylogenetic inferences

Parsimony method

Maximum parsimony (MP) analyses were conducted using PAUP* version 4.0a157 (Swofford 2002). The heuristic search option was employed for the combined dataset using tree bisection-reconnection (TBR) branch swapping, with 1000 replications of random addition sequence and an automatic increase in the maximum number of trees. Uninformative characters were excluded from the analyses. Branch support values (MPBS) were estimated using a full heuristic search with 1000 bootstrap replicates (Felsenstein 1985) each with simple addition sequence.

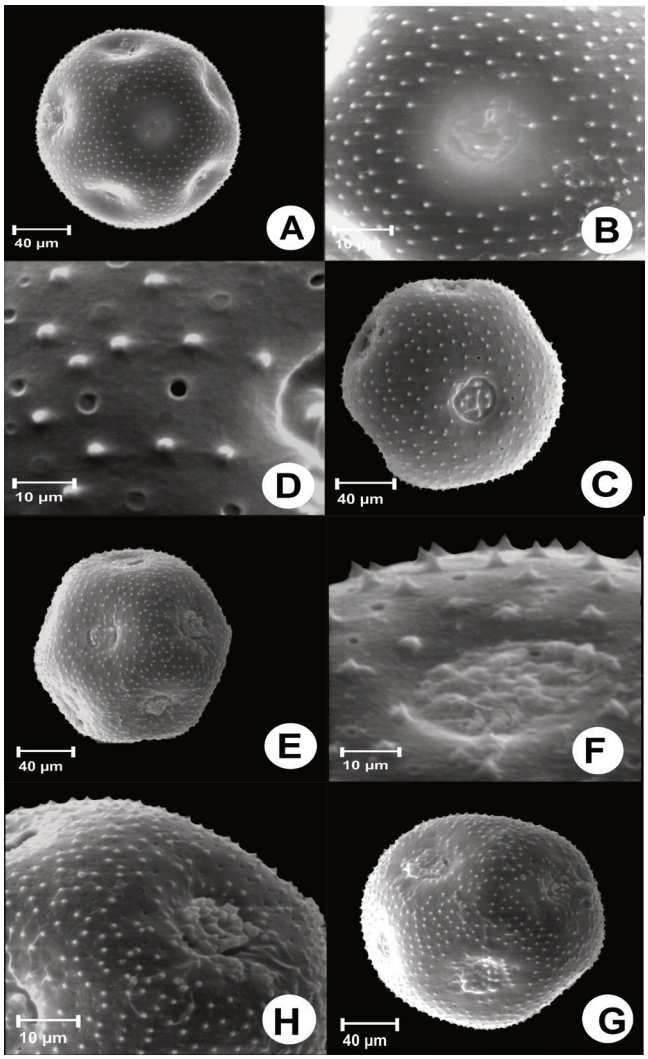

Figure 2. Scanning electron micrographs (SEM) of pollen surface in *Atriplex*. (A, B) *A. canescens*, (C, D) *A. lentiformis*, (E, F) *A. halimus*, (G, H) *A. leucoclada*.

Likelihood method

Maximum likelihood (ML) analyses were carried out using the RAxML-HPC2 on XSEDE (8.2.8) at the CIPRES Science Gateway. Bootstrap values (LBS) were calculated in RAxML-HPC2 based on 1000 replicates with one search replicate per bootstrap replicate.

Bayesian inference

For Bayesian inference (BI) analyses, models of sequence evolution were selected using the program MrModeltest version 2.3 (Nylander 2004) based on the Akaike information criterion (AIC) (Posada and Buckley 2004). This program indicated a GTR+I+G model for the combined dataset. BI analyses were performed using MrBayes version 3.2 (Ronquist et al. 2012) on the CIPRES Science Gateway (Cyber infrastructure for Phylogenetic Research cluster) (Miller et al. 2010, https://www.phylo.org) for the dataset. Bayesian analyses were performed, with default priors (uniform priors) and the best-fit model of sequence evolution for dataset, with two runs of ten million generations and four simultaneous chains (one cold and three heated with a heating parameter of 0.2), by saving trees every 100 generations. The trees sampled after discarding 25% as "burn-in" were collected to build a 50% majority rule consensus phylogram were used to calculate posterior probability values (PP). Tree visualization was carried out using Tree View version 1.6.6 (Page 2001).

Results

Pollen morphology

The pollen grains of the studied species revealed some variations and separated four species of *Atriplex*. All palynological structures and measurements for the examined species concerning pollen type from polar view, polar (P) and equatorial (E) measurements, P/E ratio, colpus length and width, pollen shape and exine ornamentation are shown in Table 2. Selected SEM micrographs of the pollens and their surfaces are shown in Fig. 2. Generally, type of pollen grain aperture is observed subprolate among studied species (Fig. 2). The length of the polar and equatorial axis was found useful in separating four species. Polar axis (P) length of pollen grains varied from the smallest size for *A. canescens* (21.05 µm) to the largest size for *A. halimus* (38.73 µm). The equatorial axis (E) length of pollen grains ranged from the smallest size in *A. lentiformis* (18.37 µm) to the largest size in *A. halimus* (27.35 µm). The shape classes are based on the ratio between the length of polar axis (P) and equatorial diameter (E) (Erdtman 1952). The P/E ratio ranged from 1.07 to 1.56, therefore the pollen shape is subprolate in *A. leucoclada* and *A. halimus* but prolate in *A. lentiformis* and spheroidal in *A. canescens* were also seen. The ornamentation of tectum is granulated in *A. canescens* (Fig. 2B), microperforate in *A. lentiformis* (Fig. 2D), microechinate in *A. halimus* (Fig. 2F) and is granulate-microechinate in *A. leucoclada* (Fig. 2H).

Trichome morphology

One basic type of trichome can be distinguished on the leaf surface of the studied taxa including glandular. Selected SEM micrographs of common trichome types are presented in Fig. 3. Some trichome characters which provide appropriate variation for taxa discrimination including the length of stalk, number of trichome cells (unicellular, bi-cellular or multi-cellular) and the density of trichome cells. A considerable variation is observed among the glandular trichomes. Based on the observed

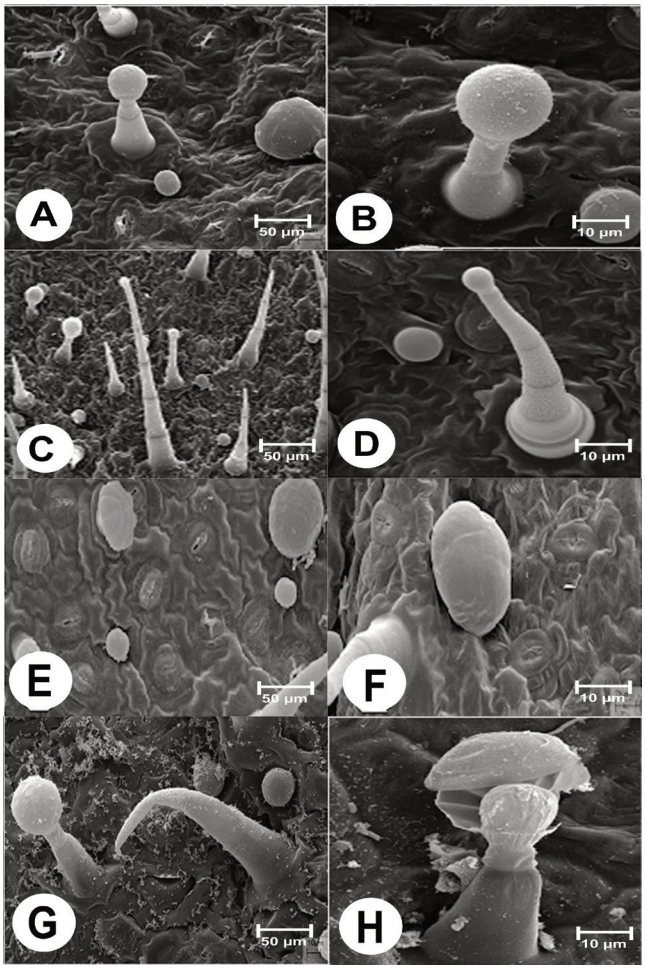

Figure 3. Scanning electron micrographs (SEM) of trichome in *Atriplex*. (A, B) *A. canescens*, (C, D) *A. lentiformis*, (E, F) *A. halimus*, (G, H) *A. leucoclada*.

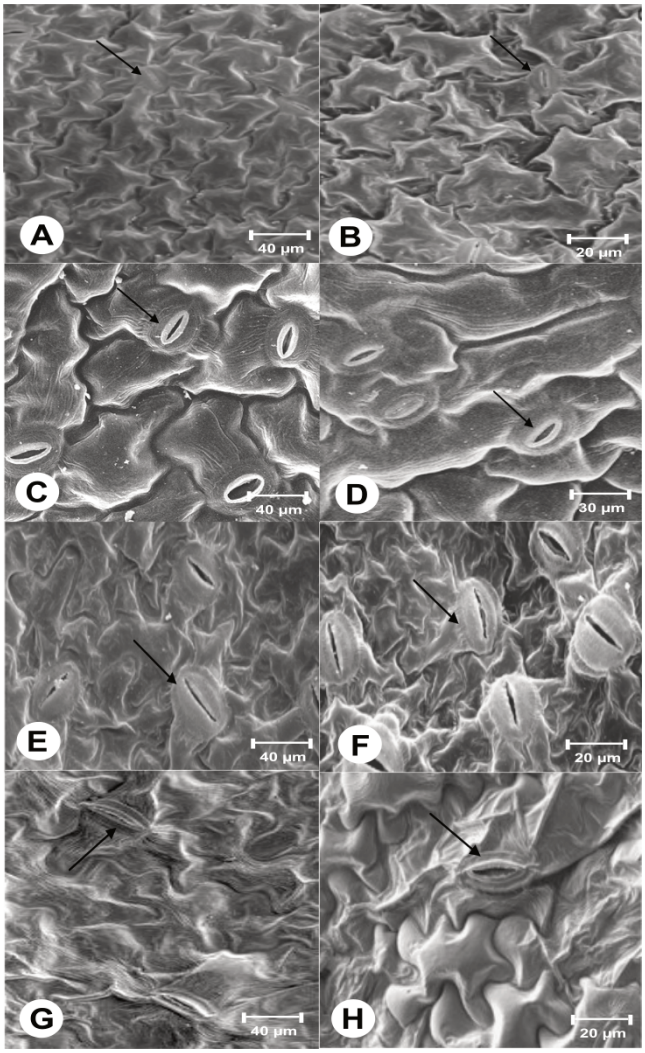

Figure 4. Epidermal cells on leaves: shape, size, anticlinal wall and stomata under Scanning electron micrographs (SEM) in *Atriplex*. (A, B) *A. canescens*, (C, D) *A. lentiformis*, (E, F) *A. halimus*, (G, H) *A. leucoclada*.

variations, glandular trichomes can be divided into two subtypes covering short stalked (e.g., *A. halimus*; Figs. 3E and 3F) and long stalked (e.g., *A. lentiformis*; Figs. 3C and 3D). Stalks of trichomes can be unicellular (e.g., *A. leucoclada*, Figs. 3G and 3H), bi-cellular (e.g., *A. canescens*, Figs. 3A and 3B) or multi-cellular (e.g., *A. lentiformis*, Figs. 3C and 3D). All the glandular trichomes in our study were unbranched. Some features of unbranched glandular trichomes including size, shape and number of cells in trichome provide useful diagnostic characters for recognizing examined taxa. The size of unbranched glandular trichomes varied from short (up to 100 µm, e.g., *A. halimus*; Figs. 3E and 3F) to long (200 to 600 µm, e.g., *A. lentiformis*, Figs. 3C and 3D).

Epidermal cell description

Epidermal and stomata characters of the leaves, such as cell shape, anticlinal wall patterns, stomata index, density, size and type were examined (Table 3). Three types of epidermal cells including puzzle-shaped, polygonal and irregular cells can be seen. Anticlinal walls have been observed the wavy, sinuous, straight and zip-shaped. Puzzle-shaped cells with zip-shaped and straight anticlinal walls on the adaxial leaf side of *A. canescens* and *A. lentiformis* were seen (Figs. 4B and 4D). Polygonal cells with sinuous cell walls were seen in *A. halimus* (Fig. 4F). Abaxial leaf epidermal cells were irregular, with wavy anticlinal walls in *A. leucoclada* (Fig. 4H). All studied specimens were of the anomocytic stomata type (Figs. 4C). The largest stomatal size was observed in *A. halimus* (Figs. 4E and 4F) and the smallest was observed in *A. canescens* (Figs. 4A and 4B). The maximum stomatal density was registered in *A. canescens* (Table 3).

Table 4. Dataset and tree statistics from single and combined analysis of the regions.

Total sample	nrDNA ITS	*rpl*32-*trn*L$_{(UAG)}$	ITS+*rpl*32-*trn*L$_{(UAG)}$
Number of sequences	13	13	13
Number of ingroup sequences	12	12	12
Alignment length [bp]	627	1278	1905
Number of parsimony- informative characters	106	140	324
Number of MPTs	16	23	29
Length of MPTs	74	87	94
Consistency index (CI)	0.68	0.67	0.64
Retention index (RI)	0.78	0.88	0.91
Evolutionary model selected (under AIC)	SYM+I+G	GTR+G	GTR+I+G

Anatomical study

Selected LM micrographs of cross-sections of the stem are presented in Figure 5. Most characters show significant variability between four species but were constant among different specimens of each studied species.

Stem anatomy

Stem cross sections showed rounded shape with wavy and straight margins (e.g., *A. halimus* in Fig. 5E and *A. canescens* in Fig. 5A). The epidermis is composed of single layered cells. The collenchyma tissue is located under the epidermis of the stem. They are 4-5-layered in four species. The cortex tissue is composed of 4-5-layered parenchyma cells. Vascular bundles are arranged in a single circle. The shape and number of vascular bundles are different. The number of vascular bundles is 10-14 with U-shaped and V-shaped outline (e.g., *A. canescens* in Fig. 5A and *A. halimus* in Fig. 5F). The xylem is surrounded by sclerenchymatous cells. Druse crystals were mainly distributed in the mesophyll and were densely distributed in *A. halimus* (Fig. 5F), but sparsely in *A. canescens* (Fig. 5A).

Phylogenetic analysis

Detailed information about alignment characteristics, selected model of nucleotide substitution, as well as tree statistics from the combined analysis of the nrDNA ITS and *rpl*32-*trn*L$_{(UAG)}$ regions, are summarized in Table 4. The aligned nrDNA ITS and *rpl*32-*trn*L$_{(UAG)}$ matrix comprised 627 and 1278 characters, respectively. The maximum parsimony, maximum likelihood and Bayesian analyses of the combined data produced congruent trees and gave similar results. All members of this genus form a well-supported clade (PP = 1, ML/BS = 100/100) (Fig. 6). The *Atriplex* clade is composed of three subclades. Subclade I includes the specimens of *A. canescens* (PP = 0.98, ML/BS = 99/100) and the subclade II (PP = 0.89, ML/BS = 100/94) comprises the specimens of *A. lentiformis* and the subclade III (PP = 0.97, ML/BS = 84/86) contains the rest of the species of *Atriplex* (*A. halimus* and A. *leucoclada*) (Fig. 6).

Discussion

About 15% of Iranian lands are affected by salinity. The rangeland species of *Atriplex*, such as *A. canescens*,

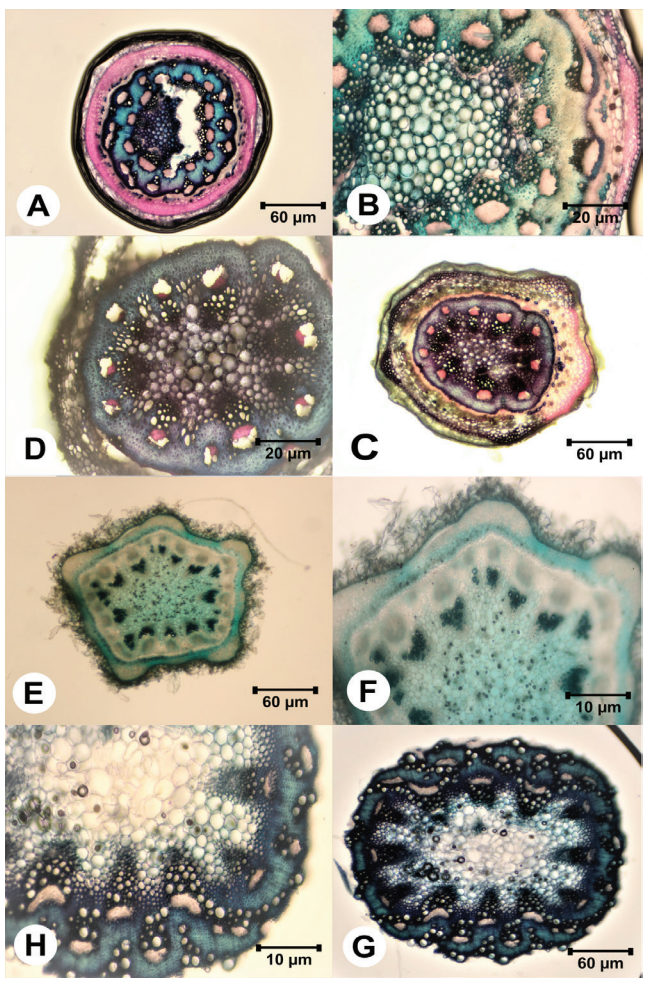

Figure 5. Transverse sections of stem in *Atriplex*. (A, B) *A. canescens*, (C, D) *A. lentiformis*, (E, F) *A. halimus*, (G, H) *A. leucoclada*.

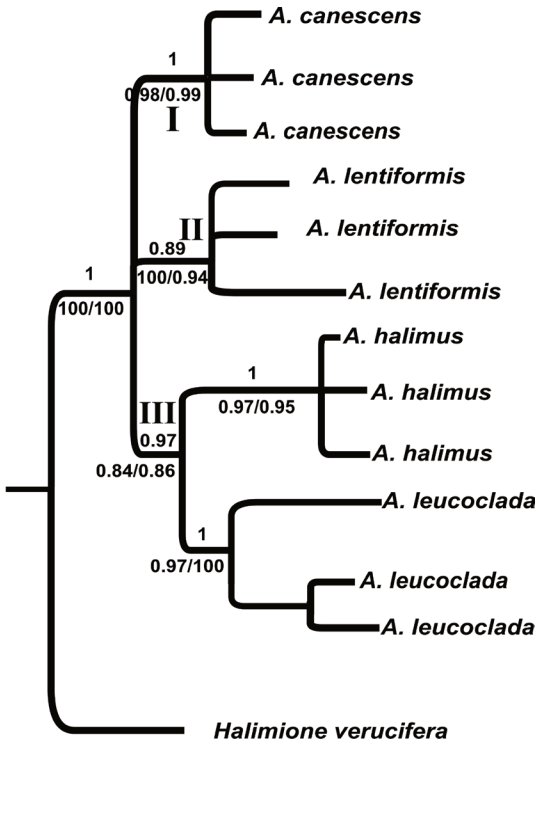

Figure 6. 50% majority rule consensus tree resulting from the Bayesian phylogenetic analysis of the nrDNA ITS and *rpl*32-*trn*L$_{(UAG)}$ datasets. Numbers of the branches are posterior probability (PP) from the BI and bootstrap support (BS) values from a MP and ML analysis, respectively (values <50 % were not shown).

A. halimus, A. lentiformis and *A. leucoclada* are notable for planting in saline soils. *Atriplex* is a halophyte plant distributed in dry and saline regions of different parts of Iran. While there are studies on cultivation (Moghadam 1973), cultivation methods (Henteh 1990), nutritional value (Ranjbar Fardiee 1991), growth (Eskandari 1995) and karyotype (Amoiee and Ahmadian 1995), *Atriplex* has gained little attention in previous micromorphological and phylogenetic studies. Hence, this study presents the first comprehensive investigation of rangeland species of *Atriplex* in Iran. Micro-morphological evaluation of the *Atriplex* species has shown the diagnostic value of these characters. Most of the pollen micromorphological features, such as pore diameter, pore number and pore membrane ornamentation, have been used to separate the different taxa of Chenopodiaceae at the generic level by SEM (scanning electron microscopy), although pore number and diameter are visible by LM (light microscopy) (Hao et al. 1989; Olvera et al. 2006; Perveen and Qaiser 2012; Lu et al. 2018a, 2018b). In previous studies, pollen size was used as a criterion to differentiate pollen types (Hao et al. 1989; Perveen and Qaiser 2012; Lu et al. 2018a). However, pollen size is excluded from Chenopodiaceae pollen classification, as Pan (1993) pointed out that it could be influenced by humidity in different habitats. Despite the general similarity of the pollen throughout Atripliceae (Olvera et al. 2006), our observations indicate that pollen micromorphology is a valuable source in taxonomic re-evaluations within the genus.

So far, no micromorphological study has been performed on trichomes of leaf surface in *Atriplex* species and this study is the first study to investigate the characteristics of trichomes in studied species. In a study by El Ghazali et al. (2016) on the stem epidermis in Chenopodiaceae, salt sacs were found in all species of *Atriplex*, *Obione*, *Halimione* Aellen, and in some species of *Salsola* L. and *Chenopodium*. The trichomes in these plants show a great variety in terms single-celled or multi-celled, tuberous and dense, and therefore this trait can be beneficial in the distinction of *Atriplex* species. *Atriplex canescens* species have medium density tuberous multicellular trichomes. Different specimens of *A. lentiformis* have very long density hairs with small glands at the end of them. *Atriplex leucoclada* species have single-celled hairs as glandular hairs with low density. The hairs in *A. halimus* are very short and have a very large salt gland. These hairs have no base and possess a medium density, and these results are in accordance with the study of Mozafar and Goodin (1970). They concluded that the salt concentration in vesicle hairs of *A. halimus* is higher than leaf saponin. These vesicles hairs have played a very crucial role in removing toxins and salts from the leaves, parenchyma and vascular bundles. In all *Atriplex* species, salt bladders occur (Schirmer and Breckle 1982; Carolin 1983; Reimann and Breckle 1988) and by a specialized mechanism of salt removal from leaves, they prevent dangerous accumulation of toxic salt levels (Mozafar and Goodin 1970; Osmond et al. 1980). The leaves of the most *Atriplex* species, particularly from field plants, are replete with bladders. In mature leaves, the salt bladders collapse and produce a thick layer all over the leaf surface. According to Smaoui (1971), salt bladders in *A. halimus* are numerous and their development occurs during leaf life. This thick layer of salt bladders constitutes a nearly impenetrable surface and often shows crystal deposits identified as sodium chloride (Osmond et al. 1980; Bennert and Schmidt 1983).

So far, no comprehensive study has been performed on the epidermis of *Atriplex* species and the current study is the first research on the characteristics of the epidermis and stomata in this genus. The characteristics of the epidermis examined by scanning electron microscopy in *Atriplex* species show a variety of micromorphological features. The epidermis acts as a barrier against mechani-

cal damage, insects, excessive light and lack of water (El Ghazali et al. 2016). The type of stomata in all species of this genus is anomocytic, which is consistent with the study of Khaniki et al. (2012). Locality and habitats of the species also significantly affect the stomata density. In woodland habitats, it mostly forms a dense ground cover occupying large areas and comprising many individuals (Metcalfe 1950). High stomata density was observed in *A. canescens* and *A. halimus* and low density in *A. lentiformis* and *A. leucoclada*. Stomata have a considerable role as valuable differentiating characters at various levels of plant ecology, taxonomy and physiology (Amini et al. 2019). Furthermore, the stomata type, density and structure have been affected by plant physiology, water efficiency and biomass (Luo and Zhou 2001). Generally, plants have different strategies to cope with ecological factors. The findings in the current study are in accordance with other studies relating to the stomata and structure (Miller 1983). The limited anatomical studies have been performed in the *Atriplex* genus, including the study of Khaniki et al. (2012). The cross section of the stem in the species of *Atriplex* is round and the non-woody pericycle is seen as a layer. In accordance with the studies of Khaniki et al. (2012), the vascular bundles are scattered in parenchymal tissue.

Kaderiet et al. (2003) studied the phylogenetic relationships of Amaranthaceae and Chenopodiaceae families based on *rbcl* chloroplast marker, but this marker could not distinct between the two families. In this study, phylogenetic analysis showed studied species with very high support are monophyletic (PP = 1, ML/BS = 100, MP/BS = 100). Studies on *Atriplex* showed that, specimens of *A. canescens* were isolated from specimens of *A. lentiformis* with high support (PP = 99, MLBS = 98, MPBS = 100). *Atriplex canescens* has a highly variable form and readily hybridizes with several other species in the *Atriplex* genus. This species is adapted to variable edaphical and environmental conditions (Mansen *et al.* 2004). In current study, this species is placed in a distinct subclade. Molecular study (nrDNA ITS, *atpB-rbcL* and *rbcl* sequences) conducted by Kaderiet et al. (2010), confirm close relationship between *A. halimus* and *A. leucoclada* and our results agreed with them. Relationships between specimens remained unresolved.

Conclusion

In conclusion, the present study was carried out to provide additional evidence for taxonomists and rangeland specialists. *Atriplex* is one of the mostly planted rangeland species in Golestan province (Iran), which improves and revitalizes the rangelands of the province. *Atriplex* is a valuable plant which tolerates fluctuation in salinity and stands higher levels of temperature. In some *Atriplex* species, such as *Atriplex canescens*, a great variety of vegetative forms has been observed. Also, these species have mixed with several other species in the genus *Atriplex*, which has caused the polyploidy phenomenon (increasing the number of chromosomes) and has created a very high adaptation to ecological and environmental conditions. These taxa differ in taxonomically important micromorphological and molecular characteristics. Due to low sequence divergence at the population level, AFLP or SSR markers, or RADs will be necessary for shedding further light on the relationships with more sampling at the population level. So micromorphological, molecular and anatomical studies will be aid for further research to identify and select suitable species of *Atriplex* in rangeland ecosystems.

Acknowledgements

The authors would like to thank Razi Institute (Tehran, Iran) staff for their assistance in scanning electron microscope, and all of persons who helped us in this research work. The present study was financially supported by Gonbad Kavous University, Gonbad (Iran).

References

Amini E, Nasrollahi F, Sattarian A, Haji Moradkhani M, Boozarpour S, Habibi M (2019) Micromorphological, anatomical and molecular study of *Hedera* species (Araliaceae) in Iran. Acta Biol Szeged 63:1-11.

Amoiee AM, Ahmadian Tehrani P (1995) Study karyotype of innatine *Atriplex* in Iran. Pajouhesh and Sazandegi No. 29.

APG II (2003) An update of the Angiosperm Phylogeny Group classification for the orders and families of flowering plants. APG II Bot J Linn Soc 141:399-436.

APG III (2009) An update of the Angiosperm Phylogeny Group classification for the orders and families of flowering plants. APG II Bot J Linn Soc 161:105-121.

APG IV (2016) An update of the Angiosperm Phylogeny Group classification for the orders and families of flowering plants: APG IV Bot J Linn Soc 181:1-20.

Barrow JR, Osuna P (2002) Phosphorus solubilization and uptake by dark septate fungi in fourwing saltbush, *Atriplex canescens* (Pursh) Nutt. J. Arid Environ. 51:449-459.

Bennert HW, Schmidt B (1983) On the osmoregulation in *Atriplex hymenelytra* (Torr.) Wats. (Chenopodiaceae). Oecologia 62:80-84.

Carolin RC, Jacobs SWL, Vesk M (1975) Leaf structure in Chenopodiaceae. Bot Jahrb Syst 95:226-255.

Carolin RC (1983) The trichomes of the Chenopodiaceae and Amaranthaceae. Bot Jahrb Syst 103:451-466.

Cuenoud P, Savolainen V, Chatrou LW, Powell M, Grayer RJ, Chase MW (2002) Molecular phylogenetics of Caryophyllales based on nuclear 18S rDNA and plastid rbcL, atpB, and matK DNA sequences. Am J Bot 89:132-144.

Edgar RC (2004) Muscle: multiple sequence alignment with high accuracy and high throughput. Nucleic Acids Res 32:1792-1797.

EL Ghazali GEB, AL Soqeer A, Abdalla WE (2016) Epidermal micro-morphological study on stems of members of the family Chenopodiaceae. App Ecol. Environ Res 14:623-633.

Erdtman G (1952) Pollen Morphology and Plant Taxonomy. Angiosperms. Chronica Botanica Co., Waltham, Massachusettes, Copenhagen.

Eskandari A (1995) Rule of pedological factors on growth and establishment of *Atriplex* species in Habib Abad (Esfahan province). Pajouhesh and Sazandegi No. 81.

Essafi NE, Mounsif M, Abousalim A, Bendaou M, Rachidai A, Gaboune F (2006) Impact of water stress on the fodder value of *Atriplex halimus* L. New Zealand. J Agric Res 49:321-329.

Felsenstein J (1985) Confidence limits on phylogenies: An approach using the bootstrap. Evolution 39:783-791.

Grigore MN (2012) Romanian Salt Tolerant Plants. Taxonomy and Ecology Edit. Technopress, Iasi.

Grigore MN, Ivanescu L, Toma C (2014) Halophytes. An integrative anatomical study. Springer, Cham, Heidelberg, New York, Dordrecht, London.

Hao HP, Zhang JT, Yan S (1989) Scanning electron microscope observation on the pollen grains of Chenopodiaceae. Acta Bot Sin 31:650-652.

Hedge C (1753) *Atriplex*. In Rechinger KH, Ed., Flora Iranica. Akademische Druck-U. Verlagsanstalt, Graz, Austria. pp 1-4.

Henteh A (1990) Investigation methods *Atriplex* planting in mohamadlo rangeland (Karaj province), M.Sc. Thesis, Natural Resources College of Tehran University.

Hernández-Ledesma P, Berendsohn WG, Borsch Th, von Mering S, Akhani H, Arias S, Castañeda-Noa I, Eggli U, Eriksson R, Flores-Olvera H, Fuentes-Bazán S, Kadereit G, Klak C, Korotkova N, Nyffeler R, Ocampo G, Ochoterena H, Oxelman B, Rabeler RK, Sanchez A, Schlumpberger BO, Uotila P (2015) A taxonomic backbone for the global synthesis of species diversity in the angiosperm order *Caryophyllales*. Willdenowia 45:281-383.

Kadereit G, Borsch T, Weising K, Freitag H (2003) Phylogeny of Amaranthaceae and Chenopodiaceae and the evolution of C4 photosynthesis. Int J Plant Sci 164:959-986.

Kadereit G, Mavrodiev EV, Zacharias EH, Sukhorukov AP (2010) Molecular phylogeny of Atripliceae (Chenopodioideae, Chenopodiaceae): Implications for systematics, biogeography, flower and fruit evolution, and the origin of C4 photosynthesis. Am J Bot 97:1664-1687.

Khaniki G, Falaki M, Lotfi Gharaei A, Asri Y (2012) Anatomical study of leaves and stems of *Chenopodium* L. and *Atriplex* L. species in South Khorasan province. Cell Mol Biotechnol 7:53-57.

Khatib A (1959) Contribution à l'étude systematique, anatomique, phylogénetique et écologique des Chénopodiacées de la Syrie. Ph.D. Dissertation, Montpellier University, Montpellier, France.

Ksouri R, Ksouri Megdiche W, Jallali I, Debez A, Magné C, Hiroko I, Abdelly C (2012) Medicinal halophytes: potent source of health promoting biomolecules with medical, nutraceutical and food applications. Crit Rev Biotechnol 32:289-326.

Lu KQ, Xie G, Li M, Li JF, Trivedi A, Ferguson DK, Yao YF, Wang YF (2018a). Pollen spectrum, a cornerstone for tracing the evolution of the eastern central Asian desert. Quat Sci Rev 186:111-122.

Lu KQ, Xie G, Li M, Li JF, Trivedi A, Ferguson DK, Yao YF, Wang YF (2018b) Data set of pollen morphological traits of 56 dominant species among desert vegetation in the eastern arid central Asia. Data Brief 18:1022-1046.

Luo Y, Zhou ZK (2001) Cuticle of *Quercus* sugen. *Cyclobalanopsis* (Oerst.) chneid. (Fagaceae). *Acta Phytophysiol* Sin 39:489-501.

Metcalfe CR, Chalk L (1950) Anatomy of the Dicotyledones. Vol. 1, Clarendon Press, Oxford, 243-245.

Miller EC (1983) Plant Physiology. McGrow Hill Book Company, New York, USA.

Miller MA, Pfeiffer W, Schwartz T (2010) Creating the CIPRES Science Gateway for Inference of Large Phylogenetic Trees. Proceedings of the Gateway Computing Environments Workshop (GCE), New Orleans, Louisiana. Piscataway: IEEE. 45-52.

Moghadam MR (1973) Study *Atriplex canescens* planting. IJNRR 29:32-43.

Mansen SB, Stevens R, Shaw NL (2004) Restoring Western Ranges and Wild Lands. USDA General Technical Report RMRSGTR 2:p 697.

Mozafar A, Goodin JR (1970) Vesiculated hairs: a mechanism for salt tolerance in *Atriplex halimus* L. Plant Physiol 45:62-65.

Naderi Safar K, Kazempour-Osaloo Sh, Maassoumi AA, Zarre Sh (2014) Molecular phylogeny of *Astragalus* section *Anthylloidei* (Fabaceae) inferred from nrDNA ITS and plastid *rpl*32-*trn*$L_{(UAG)}$ sequence data. Turkish J Bot 38:637-652.

Nylander JAA (2004) Mr Modeltest v2. Program distributed by the author. Evolutionary Biology Centre. Uppsala University, Uppsala.

Olvera HF, Fuentes-Soriano S, Martínez Hernández E (2006) Pollen morphology and systematics of Atripliceae (Chenopodiaceae). Grana 45:175-194.

Osman AK (2012) Trichome micromorphology of Egyptian *Ballota* (Lamiaceae) with emphasis on its systematic implication. Pak J Bot 44:33-46.

Osmond CB, Björkman D, Anderson DJ (1980) Physiological Processes in Plant Ecology. Towards a Synthesis with *Atriplex*. Ecological Studies 36. Springer-Verlag Berlin, Heidelberg

Page DM (2001) Tree View (Win32) version 1.6.6. Available: http://taxonomy.zoology.gla.ac.uk/rod/treeview.html.

Pan AD (1993) Studies on the pollen morphology of Chenopodiaceae from Xinjiang. Arid Land Geogr 16:22-27.

Perveen A, Qaiser M (2012) Pollen flora of Pakistan, LXX: Chenopodiaceae. Pak J Bot 44:1325-1333.

Posada D, Buckley TR (2004) Model selection and model averaging in phylogenetics: Advantages of akaike information criterion and Bayesian approaches over likelihood ratio tests. Syst Biol 53:793-808.

Punt W, Hoen PP, Blackmore S, Nilsson S, Thomas AL (2007) Glossary of pollen and spore terminology. Rev Palaeobot Palynol 143:1-81.

Ranjbar Fardoiee A (1991) Investigation nutritional value of *Atriplex canescens* and *Atriplex lentiformis* in different stage of enological, M.Sc. Thesis, Natural Resources College of Tehran University.

Reimann Ch, Breckle S (1988) Salt secretion in some *Chenopodium* species. Flora 180:289-296.

Ronquist F, Teslenko M, Mark P, Ayres DL, Darling A, Höhna S , Larget B, Liu L, Suchard MA, Huelsenbeck JP (2012) MrBayes 3.2:efficient Bayesian phylogenetic inference and model choice across a large model space. Syst Biol 61:539-542.

Salmaki Y, Zarre S, Jamzad Z, Bräuchler C (2009) Trichome micromorphology of Iranian *Stachys* (Lamiaceae) with emphasis on its systematic implication. Flora 204:371-381.

Sang T, Crawford DJ, Stuessy T (1995) Documentation of reticulate evolution in peonies (*Paeonia*) using internal transcribed spacer sequences of nuclear ribosomal DNA: implication for biogeography and concerted evolution. Proc Natl Acad Sci *USA* 92:6813-6817.

Schirmer U, Breckle SW (1982) The role of bladders for salt removal in some Chenopodiaceae (mainly *Atriplex* species). In Sen DN, Rajpurohit KS, Eds, Contributions to the Ecology of Halophytes. Tasks for Vegetation Science. Vol 2. Springer, Dordrecht.

Shaw J, Lickey EB, Schilling EE, Small RL (2007) Comparison of whole chloroplast genome sequences to choose noncoding regions for phylogenetic studies in angiosperms: the tortoise and the hare III. Am J Bot 94:275-288.

Smaoui A (1971) Différenciation des trichomes chez *Atriplex halimus*. L. C R Acad Sci, Sér D 273:1268-1271.

Sukhorukov A, Danin A (2009) Flora Mediterranea. Taxonomic notes on *Atriplex* sect. Teutliopsis and sect. *Atriplex* in Israel and Syria. 19:15-23.

Sukhorukov AP (2014) The carpology of the Chenopodiaceae with reference to the phylogeny, systematics and diagnostics of its representatives. Grif & Co., Tula.

Sukhorukov AP, Liu P, Kushunina M (2019) Taxonomic revision of Chenopodiaceae in Himalaya and Tibet. Phytokeys 116:1-141.

Swofford DL (2002) PAUP*: Phylogenetic Analysis Using Parsimony (*and Other Methods), Version 4.0b10. Sunderland: Sinauer Associates.

Troughton HK, Card A (1973) Leaf anatomy of *Atriplex buchananii*. NZ J Bot 12:167-177.

White TJ, Bruns T, Lee S, Taylor J (1990) Amplification and direct sequencing of fungal ribosomal RNA genes for phylogenetics. 315-322. In Innis MA, Gelfand DH, Sninsky JJ, White TJ, Eds. PCR Protocols: A Guide to Methods and Applications. Academic Press, San Diego.

Wilson PG (1984) Chenopodiaceae. 81-317. In George AS, Ed, Flora of Australia. Vol 4. Phytolaccaceae to Chenopodiaceae. Australian Government Publishing Service, Canberra, Australia.

Zamfirache MM, Burzo I, Olteanu IGZ, Ştefan M, Badea ML, Padurariu C, Gales RC, Adumitresei L, Lamban C, Truţă E, Stanescu I (2009) Glandular trichomes and essential oil constituents of *Perovskia artiplicifolia* Benth. Anal Şti Univ "Al I Cuza" Secţ 2 A. Genet Biol Mol 10:73-80.

Zarinkamar F (2006) Foliar anatomy of Chenopodiaceae family and xerophyte adaptation. Iran J Bot 11:175-185.

Acta Biologica Szegediensis

Volume 65(2):145-162, 2021
Acta Biologica Szegediensis
http://abs.bibl.u-szeged.hu/index.php/abs

DOI:10.14232/abs.2021.2.145-162

ARTICLE

Evaluation of rice (*Oryza sativa* L.) genotypes grown under combined salinity and submergence stresses based on vegetative stage phenotyping

Kaniz Fatema[1], Md Rasel[1]*, Mirza Mofazzal Islam[2], Shamsun Nahar Begum[2], Md. Golam Azam[3], Mohammad Anwar Hossain[1]*, Lutful Hassan[1]

[1]Department of Genetics and Plant Breeding, Faculty of Agriculture, Bangladesh Agricultural University, Mymensingh-2202, Bangladesh
[2]Plant Breeding Division, Bangladesh Institute of Nuclear Agriculture, Mymensingh-2202, Bangladesh
[3]Pulses Research Center, Bangladesh Agricultural Research Institute, Ishurdi, Pabna-6620, Bangladesh

ABSTRACT Sixteen rice genotypes were screened against combined salinity and submergence stresses to find out potential salt-submergence tolerant genotypes. Rice seedlings were subjected to submergence stress including two salinity levels viz., EC-6 dSm^{-1} and EC-8 dSm^{-1} for 10 days. Imposition of combined stress considerably decreased the growth parameters in rice seedlings, however *ACM-18*, *ACM-35,* and *RC-251* demonstrated the maximum value for growth attributes such as leaf live (%), root and shoot length, plant fresh and dry biomass. The results of correlation and regression revealed a significant and negative association of leaf lives (%), root length, fresh weight of root and shoot, and root dry weight with mean tolerance score under combined stress indicating their importance as the useful descriptors for the selection. Euclidean clustering was categorized the rice genotypes into three major clusters, i.e., A-susceptible, B-tolerant and moderately tolerant, and C-highly tolerant. Results of cluster analysis showed that the highly tolerant genotypes namely *ACM-18*, *ACM-35,* and *RC-251* were placed in the same cluster. Similar results were further confirmed by principal component analysis having the highly tolerant genotypes in the same group. Combining the morphological and multivariate analysis, *ACM-18*, *ACM-35,* and *RC-251* were selected as promising genotypes for developing high-yielding salt-submergence tolerant rice.
Acta Biol Szeged 65(2):145-162 (2021)

KEY WORDS
genetic diversity
principal component analysis
rice
salinity
submergence

ARTICLE INFORMATION
Submitted
9 May 2021
Accepted
20 August 2021
***Corresponding author**
E-mail: anwargpb@bau.edu.bd
rasel.gpb@bau.edu.bd

Introduction

Agriculture sector is facing different adverse conditions such as salinity, drought, submergence, and extreme temperature stress because of climate change (Shelley et al. 2016; Rahman et al. 2020). Among these, salinity is one of the most brutal environmental constraints that affect plant growth and development negatively. It is estimated that about 1125 million hectares (Mha) is affected by varying degrees of soil salinity which covers approximately 6.5% of the world's total land area (Parihar et al. 2015). Usually, soil salinity is caused by different natural processes or anthropogenic activities such as higher accumulation of soluble salts in the soil surface (Hussain et al. 2017). Moreover, the accumulation of excessive sodium ions with dominant anions of chloride and sulfate commanding high electrical conductivity of above 4 dSm^{-1} causes soil salinity (Ali et al. 2013). The higher procurement of salt in the soil is an intense problem that suppresses crop production in the coast-line areas, particularly in the low-lying developing countries around the world (Nicholls et al. 2007). The threat of soil salinity is also an extensive concern in the southern part of Bangladesh deteriorating the status of soil health and soil fertility leading to low agricultural production (Ahmed and Haider 2014). Approximately 53% of the coastal areas of Bangladesh are invaded by salinity stress which is roughly covering 50% of the country's average (Rahman and Ahsan 2001; Haque 2006). Since crop plants are unable to grow in the saline environment due to an imbalance of biological and biochemical functions, a significant proportion of agricultural land in the coastal belt remains fallow throughout the year (Rasel et al. 2019). Furthermore, soil salinity is frequently associated by water logging/submergence stress which also imbeds their eminent effects on plant growth and development (Yeo 1999; Singh 2015). Now a days, the biggest concern is the occurrence

of combined salinity and water logging stress is increasing throughout the globe because of acute irrigation practice in agricultural production systems, unexpected emergence of saline water tables, and intrusion of seawater in coastal environments (Hatton et al. 2003; Carter et al. 2006). Submergence stress regularly affects about 15 Mha of rainfed lowland areas especially in South and Southeast Asia (Neerja et al. 2007). In Bangladesh context, above one Mha of rice fields in the coastal areas suffer from prolonged partial flooding during the wet season every year (Ismail et al. 2010). This type of severe flooding can lead to complete inundation of the entire plant for up to 2 weeks and usually occurs at the early vegetative stage causing the hindrance of plants normal growth potential (Singh et al. 2014a).

Rice (*Oryza sativa* L.) is consumed as the most important food by more than 3.5 billion people around the world which supplies about 20 percent of the world's total dietary energy supply (Alexandratos and Jelle 2012; CGIAR 2016). Rice is also the dominant crop in the economic system of Bangladesh, and it is taken as the staple food for about 156 million people of the country (Shelley et al. 2016). In Bangladesh, the total land used for rice cultivation is approximately 10.83 Mha leading to an average production of 33.54 million metric tons per year (Kibria et al. 2017). However, currently the rice-based cropping systems are increasingly threatened by the salinity and submergence stress individually or simultaneously causing lower rice production in Bangladesh (Masutomi et al. 2009). On the other hand, existing modern high-yielding rice varieties of Bangladesh are susceptible to combined salt and submergence stress for which they cannot thrive the devastating effect of salinity stress with flash floods (Afrin et al. 2018; Bui et al. 2019). Thus, the development of high-yielding, multiple stress-tolerant varieties against salinity and submergence has a great importance that could provide farmers with the cost-effective options in saline-prone flood-affected areas for achieving food security and sustainable agriculture (Ismail et al. 2013; Singh et al. 2013).

Both water logging and salinity are pernicious to plant growth and yield in different ways (Singh 2017). The prevailing low osmotic potential in soil solution leading salt stress which causes nutritional imbalance, and specific ion effects in plant cells (Evelin et al. 2009). The growth and development of plants are adversely affected by the accumulation of excess salt in soil once the osmotic stress severely declines the uptake of water by roots (Munns and Tester 2008). Plant response to salt stress is very complicated and depends on numerous factors for instance type and concentration of the solutes, growth stage of the plant, the genetic potential of the plant and different environmental factors (Kordrostami et al. 2017). Usually, rice is relatively salt tolerant during seed germination, active tillering and, maturity stage but very sensitive at the seedling and early vegetative stage and thus, seedling vigor including leaf live (%), root length, shoot length, plant biomass and other growth traits are substantially affected and reduced under salt stress conditions (Singh and Flowers 2010; Hakim et al. 2014; Kumar et al. 2015). Besides these, salinity stress may also lead to membrane disorganization, toxic metabolites generation, photosynthesis inhibition, over-production of reactive oxygen species (ROS), and attenuated nutrient acquisition causing cell death (Chartzoulakis 2005; Sun et al. 2011; Rahman et al. 2020). Likewise salt stress, submergence stress also affects plant early growth stage and thus, reduces plant productivity to a great extent (Yadav et al. 2018). When salt stress is coupled with submergence stress, salinity can cause even greater damage to plants (Jackson and Ram 2003). For many plant species, when salinity and waterlogging happen together, Na^+ and/or Cl^- concentrations dramatically increase in shoots due to the entry of excess toxic ions into oxygen-deficient roots of plants (Barrett-Lennard 2003). Submergence situation for more than seven days can cause in the plants leaf rotting, loss of dry mass and lodging after the flood waterfall down (Goswami et al. 2015). In submergence condition, the availability of free O_2 around the roots is depleted and thus, hypoxia stress occurs which makes anaerobic metabolism in roots from an aerobic environment with the dramatic reductions of ATP synthesis (Teakle et al. 2006). Because of these changes, plants exhibit altered membrane transport, decreased conductance of stomata and decreased leaf water potentials, enhanced root senescence, reduced root and shoot length, and eventually caused the death of the whole plant (Barrett-Lennard 2003).

To find out multiple stress-tolerant genotypes, a proper screening technique is required with the selection of the appropriate developmental stage of plant (Ghosh et al. 2016). Usually, the seedling stage or vegetative stage of the rice plant is more affected by both salinity and submergence stress (Chunthaburee et al. 2016; Abedin et al. 2019). Thus, screening of rice genotypes for salinity or submergence tolerance at the early growth or vegetative stage can be undertaken using the parameters described as effective tolerant indices like leaf live (%), root length, shoot length, and plant biomass because variations in the genotypes on these stages are controlled by genetic components (Zeng et al. 2007; Ali et al. 2014). However, the combined effect of salinity and submergence stress on the vegetative stage of rice plants has rarely been examined (Rogers et al. 2011; Chen et al. 2013), thereby reflecting further study on rice plant at early growth stages in relation to multiple abiotic stresses like salinity and submergence are recommended (Yan et al. 2013).

Table 1. Modified standard evaluation score (SES) of visual salt injury for growth traits at the seedling stage of rice genotypes..

Score	Observation	Tolerance
1	Normal growth, no leaf symptoms	Highly tolerant (HT)
3	Nearly normal growth, but leaf tips of few leaves whitish and rolled	Tolerant (T)
5	Growth severely retarded, most leaves rolled; only a few are elongating	Moderately tolerant (MT)
7	Complete cessation of growth; most leaves dry; some plants dying	Susceptible (S)
9	Almost all plants dead or dying	Highly susceptible (HS)

Source: Gregorio et al. (1997)

Therefore, the present study has been undertaken to evaluate rice genotypes to explore their response to combined salinity and submergence stresses by assessing morphological traits at the late vegetative stage along with the classification of rice genotype employing hierarchical clustering and principal component analysis to identify robust salt-submergence tolerant rice genotype(s).

Materials and Methods

Plant materials and experimental design

A total of 16 rice genotypes (viz., *ACM-3, ACM-4, ACM-5, ACM-6, ACM-8, ACM-10, ACM-11, ACM-15, ACM-16, ACM-18, ACM-23, ACM-26, ACM-29, ACM-35, Binadhan-7,* and *RC-251*) collected from Bangladesh Institute of Nuclear Agriculture (BINA), Mymensingh-2202, Bangladesh and International Rice Research Institute (IRRI), together with two check genotypes viz., *RC-251* (positive check, both salinity and submergence tolerant), and *Binadhan-7* (negative check, both salinity and submergence susceptible) were used as plant materials in the present study. The experiment was conducted following completely randomized design with two factors (salinity and submergence) and three replications (each replication had 5 seedlings). Thus, the treatment combinations were as follows: control treatment, T_0 (distilled water), two stress treatments viz., T1 (EC-6 dSm^{-1} salinity level with complete submergence), and T_2 (EC-8 dSm^{-1} with complete submergence).

Plant culture and stress imposition

Initially, the uniform size rice seeds were sorted out and surface sterilized with 5% sodium hypochlorite and 0.1% mercuric chloride followed by three times washing with distilled water (dH_2O). Then, the seeds were kept in the oven at 50 °C for 2 days for breaking dormancy. The oven-treated seeds were soaked overnight with dH_2O and placed in the Petri dishes on a moist filter paper (50 seeds/petri dish) at room temperature (25 ± 2 °C) to induce germination. The 3-days old pre-germinated seeds were then sown in the seedbed for seedling growth. Seedbed was prepared by raising soil up to 5-10 cm from the field surfaces with the mixing of 8 kg cow dung properly. Afterwards, 30-days old seedlings were uprooted from the seedbed and transplanted in the previously prepared 15 cm in length and 11 cm in diameter sized perforated cotton fiber pots (3 seedlings in each pot). The pots were filled with silt loam soil having the following characteristics: pH of 6.2, electrical conductivity (EC) of 0.12 dSm^{-1}, cation exchange capacity of 8.5%, exchangeable Na^+ of 0.33 milliequivalent per 100 g soil, exchangeable K^+ of 0.15 cmol kg^{-1}, total nitrogen of 0.13%, organic carbon of 0.70%, and organic matter of 1.16%. The pots were placed in the trays (130 cm×75 cm×25 cm) filled with tap water (Ca^{2+} 3.2 mM, Mg^{2+} 0.50 mM, Na^+ 1 mM, K^+ 0.2 mM, $HCO3^-$ 5.0 mM, Cl^- 0.21 mM, SO_4^{2-} 0.08 mM, and P <0.002 mM), so that the fiber pots were half-drowned in tap water. After one week of transplanting, approximately one-third of urea (5 g), a full dose of phosphorus (4 g), and a full dose of potassium (3 g) fertilizers were applied on each of the pot at the optimal field application rates. The remaining urea (10 g) was applied later at 30^{th} and 50^{th} days of crop life span. Plants were kept in these normal water trays for 20 days for seedling establishment. Afterwards, the perforated pots with 50-days old seedlings were transferred from the trays into the large black tanks (16 pots per tank) containing salinized water solution. The salinized water solution was prepared by dissolving crude salt (sodium chloride with some trace minerals like potassium, iron, and zinc) with water. The water level for submergence stress treatment in the tank was maintained at 14 mm from the soil surface by adding tap water artificially. The rice seedlings were exposed to saline and complete submergence stress simultaneously for next 10 days. The EC and pH (6.5) of the salinized solution in the tank was kept constant and measured by an EC-meter (Hanna HI 4321) and pH-meter (Hanna HI 22111), respectively. Afterwards, plants were taken out from the drums and settled in the normal environmental condition until harvesting (day 70). The control plants were also grown in natural conditions without undergoing the salinity and submergence treatment with

Table 2. Combined analyses of variances among seven studied traits under in rice genotypes grown under combined salinity (6 $dSm^{-1}$and 8 dSm^{-1}) and submergence stress

Sources of variation	df	Mean sum squares						
		LL (%)	SL	RL	SFW	RFW	SDW	RDW
Genotypes (G)	15	5003.1***	2868.5***	345.0***	314.0***	6.32***	10.75***	0.44***
Treatments (T)	2	18095.1***	10489.9***	1354.2***	1321.5***	12.39***	71.04***	1.56***
G x T	30	916.3***	312.5***	20.03***	29.23***	0.55***	1.74***	0.06***
Error	64	36.11	4.18	1.02	1.18	0.01	0.01	0.01***
CV (%)	-	8.40	3.46	6.57	10.28	6.82	4.69	7.41***

'***' indicates significant at 0.001 level of probability, CV coefficient of variation, df degrees of freedom. The variables include LL (%) leaf live (%), RL root length (cm), SL shoot length (cm), RFW root fresh weight (mg), RDW root dry weight (mg), SFW shoot fresh weight (mg), and SDW shoot dry weight (mg).

well-drained conditions. The modified standard evaluation score (SES) was estimated at the late vegetative stage based on the visual symptoms of salt-submergence injury in 70-days old plants (IRRI, 1997) (Table 1). This scoring discriminated the susceptible genotypes from the tolerant and the moderately tolerant genotypes.

Data collection of morphological traits under normal and stress conditions

Different growth parameters were measured from 5 plants in each replication after 70th days of the plantation, and afterwards, the average value was taken. The leaf live (%) was measured by dividing the number of leaves live by the total number of leaves multiplied by hundred. The root length was measured from the shoot initiation to the root tip and shoot length was measured from the shoot initiation point to the tip of the plant by using a meter (m) scale. Immediately after harvesting, the shoot samples were separated from the root, and the fresh weight (mg) of root and shoot weight were taken carefully using an electric balance and afterwards, roots and shoots samples were separately enclosed in brown envelops (20 cm x 10 cm) and kept in an oven at 60 ℃ for five days. Then, the dry weight (mg) was also measured separately by using an electric balance.

Statistical analysis

The data obtained were analyzed by a two-way analysis of variance using Statistical Tool for Agricultural Research (STAR) (IRRI, Los Baños, Laguna, Philippines). The mean values were separated at the $p < 0.001$ level using the least significant difference (LSD) test and presented indicated by different alphabetical letters in the same column. The heat map and hierarchical clustering was performed by Biovinci considering the percent reduction values of growth traits of different genotypes under combined stress situations. PCA was conducted by using the STAR and the biplots were constructed with the first two PCA components *viz.,* PC1, and PC2 that explained the maximum variations exist among the datasets. The Pearson's correlation coefficients and regression coefficients among the studied traits were also calculated using the STAR and SPSS 22 software package, respectively. The genetic parameters such as phenotypic variance (σ^2p), genotypic variance (σ^2g), phenotypic co-efficient of variation (PCV), genotypic co-efficient of variation (GCV), heritability (h^2_b), and genetic advance (GA) for all the studied morphological traits were estimated following the method as previously described by Rasel et al. (2018).

Results

Growth characteristics changes in rice seedlings in response to combined salinity and submergence stresses

The analyses of variance (ANOVA) of different morphological parameters of 16 rice genotypes under combined salinity and submergence stresses indicated that the difference among genotypes for all the traits viz., leaf live (LL %), shoot length (SL), root length (RL), root fresh weight (RFW), shoot fresh weight (SFW), root dry weight (RDW), and shoot dry weight (SDW) were highly significant ($p < 0.001$) (Table 2). The interaction of salt-submergence stress decreased growth parameters of rice seedlings in all genotypes (Table 5). As three genotypes viz., *ACM-8, ACM-10*, and *Binadhan-7* were completely dead after 10-days of fully submergence stress in salinized water, the phenotypic traits for those genotypes were not measured (Table 4) and the percent reduction of all morphological parameters was maximum of 100% under stressed situations for those genotypes (Table 5). Rice seedlings showed more reduction of growth parameters with the increasing of salinity level in waterlogging condition. However, tolerant genotypes were least affected by imposed stress than susceptible genotypes for different agro-morphological traits. In the present study, the LL (%) was drastically reduced in *ACM-5* (T_1 59.4%, T_2 64.8%), *ACM-6* (T_1 37.4%, T_2 53.1%), and *ACM-16* (T_1 34.1%, T_2 34.6%) whereas minimum

Table 3. Ranking of rice genotypes for relative salt tolerance obtained from growth-related traits based on percent reduction.

Genotypes	Treatments	LL	SL	RL	SFW	RFW	SDW	RDW	Sum	MTS	Tolerance degree
ACM-3	T_1	1.00	3.00	3.00	3.00	1.00	1.00	5.00	2.42	4.56	MT
	T_2	1.00	5.00	9.00	5.00	9.00	9.00	9.00	6.71		
ACM-4	T_1	1.00	1.00	3.00	7.00	1.00	9.00	3.00	3.57	3.78	T
	T_2	1.00	1.00	5.00	9.00	1.00	9.00	9.00	5.00		
ACM-5	T_1	9.00	3.00	5.00	9.00	5.00	9.00	3.00	6.14	6.57	S
	T_2	9.00	5.00	5.00	9.00	7.00	9.00	5.00	7.00		
ACM-6	T_1	5.00	3.00	9.00	3.00	1.00	5.00	1.00	3.86	5.15	MT
	T_2	7.00	5.00	9.00	9.00	3.00	7.00	5.00	6.43		
ACM-8	T_1	9.00	9.00	9.00	9.00	9.00	9.00	9.00	9.00	9.00	HS
	T_2	9.00	9.00	9.00	9.00	9.00	9.00	9.00	9.00		
ACM-10	T_1	9.00	9.00	9.00	9.00	9.00	9.00	9.00	9.00	9.00	HS
	T_2	9.00	9.00	9.00	9.00	9.00	9.00	9.00	9.00		
ACM-11	T_1	1.00	3.00	1.00	1.00	3.00	1.00	1.00	1.57	2.99	T
	T_2	1.00	3.00	3.00	7.00	3.00	9.00	5.00	4.42		
ACM-15	T_1	3.00	1.00	5.00	7.00	3.00	9.00	1.00	4.14	4.86	MT
	T_2	5.00	3.00	7.00	9.00	3.00	9.00	3.00	5.57		
ACM-16	T_1	5.00	1.00	3.00	9.00	1.00	9.00	3.00	4.43	5.00	MT
	T_2	5.00	3.00	3.00	9.00	3.00	9.00	7.00	5.57		
ACM-18	T_1	1.00	1.00	1.00	3.00	1.00	3.00	1.00	1.57	2.42	HT
	T_2	1.00	1.00	7.00	5.00	3.00	5.00	1.00	3.28		
ACM-23	T_1	1.00	1.00	1.00	7.00	1.00	7.00	1.00	2.71	3.57	T
	T_2	3.00	5.00	3.00	9.00	1.00	9.00	1.00	4.43		
ACM-26	T_1	1.00	3.00	3.00	7.00	1.00	9.00	1.00	3.57	5.85	MT
	T_2	5.00	7.00	9.00	9.00	9.00	9.00	9.00	8.14		
ACM-29	T_1	1.00	3.00	5.00	5.00	5.00	7.00	1.00	3.86	5.58	MT
	T_2	3.00	5.00	7.00	9.00	9.00	9.00	9.00	7.29		
ACM-35	T_1	1.00	1.00	3.00	3.00	1.00	3.00	1.00	1.85	2.42	HT
	T_2	1.00	1.00	7.00	5.00	3.00	3.00	1.00	3.00		
Binadhan-7	T_1	9.00	9.00	9.00	9.00	9.00	9.00	9.00	9.00	9.00	HS
	T_2	9.00	9.00	9.00	9.00	9.00	9.00	9.00	9.00		
RC-251	T_1	1.00	1.00	1.00	3.00	1.00	1.00	1.00	1.28	1.99	HT
	T_2	1.00	3.00	1.00	7.00	1.00	1.00	5.00	2.71		

The treatments T_1 6 dSm^{-1} salinity level with complete submergence, and T_2 8 dSm^{-1} salinity level with complete submergence. Scoring range based on % reduction values of growth traits under stress conditions were count for 10-20%= score 1, 21-31%= score 3, 32-42%= score 5, 43-53%= score 7, and 54-64%= score 9; score 1,3,5,7 and 9 value was given according to IRRI standard protocol (1997), where score 1 denotes highly tolerant (HT), score 3 denotes tolerant (T), score 5 denotes moderately tolerant (MT), score 7 denotes susceptible (S), and score 9 denotes highly susceptible (HS). The variables include LL (%) leaf live (%), RL root length (cm), SL shoot length (cm), RFW root fresh weight (mg), RDW root dry weight (mg), SFW shoot fresh weight (mg), and SDW shoot dry weight (mg). MTS denotes mean tolerance score.

reduction was observed in *RC-251* (T_1 2.61%, T_2 7.17%), *ACM-35* (T_1 0.20%, T_2 9.60%), and *ACM-3* (T_1 5.79%, T_2 8.69%) when exposed to salt-submergence stress (Table 5). The severe curtailment of SL and RL were found in all the genotypes under combined submergence plus salt stress. However, some genotypes namely *RC-251, ACM-18,* and *ACM-35* displayed the highest root and shoot growth in salt-submergence stress situations (Table 4). Considering RL, the maximum reduction was found in *ACM-6* (69.6%), *ACM-26* (56.3%), *ACM-3* (55.4%) and the minimum reduction was observed in *ACM-11* (27.6%), and *ACM-23* (28.5%) like tolerant check *RC-251* (20.8%) at stagnant conditions with 8dSm^{-1}salinity level (Table 5). Similarly, the genotypes namely *ACM-35* (19.1%), *ACM-18* (20.3%), and *RC-251* (23.4%) also exhibited the least reduction for SL whereas maximum reduction was recorded in *ACM-26* (45.5%), *ACM-29* (42.8%), and *ACM-5* (40.0%) in combined waterlogging + 8dSm^{-1} salt treatments (Table 5). Under salinity-submergence stress, RFW and SFW in rice seedlings showed a differential response and significantly decreased in submerged rice plants with the increasing of salinity. However, some genotypes viz.,

Table 4. Performance of rice genotypes considering morphological traits at the late vegetative stage under salt-submergence stress and non-stressed conditions.

Genotypes	Treatment (T)	LL	SL	RL	SFW	RFW	SDW	RDW
ACM-3	T_0	98.0 ab	79.0 ab	24.6 b-e	12.72 f	3.59 b	2.59 h	1.05 a
	T_1	92.3 ab	60.0 c-f	18.6 b	10.0 cd	3.06 b	2.12 cd	0.65 cd
	T_2	89.5 a-c	53.0 b-d	11.0 ef	7.8 c-e	1.34 cd	0.93 ef	0.37 d
ACM-4	T_0	90.25ab	63.3 fg	25.5 bc	15.2 f	2.06 fg	3.11 fg	0.49 fg
	T_1	85.0 a-c	54.3 fg	17.0 b	8.07 d-f	1.98 cd	1.29 g	0.38 fg
	T_2	72.3 a-d	50.6 cd	16.0 bc	6.18 c-f	1.94 b	1.12 c-e	0.16e
ACM-5	T_0	100 a	71.6 c-e	18.6 h	15.8 de	2.22 ef	2.84 gh	0.51 fg
	T_1	40.5 f	54.0 g	12.0 c	6.32 ef	1.51 e	1.24 g	0.35 g
	T_2	35.1 g	43.0 ef	11.6 d-f	5.24 d-g	1.20 d	0.97 de	0.34 d
ACM-6	T_0	93.7 ab	76.0 a-c	29.0 a	16.5 de	1.90 fg	3.00 fg	0.49 fg
	T_1	58.6 e	56.1 e-g	11.1 c	11.29 c	1.65 e	1.90 d-f	0.46 ef
	T_2	43.9 fg	47.8 de	8.81 f	2.63 gh	1.47 cd	1.40 c	0.33 d
ACM-8	T_0	70.8 c	53.3 ij	8.25 j	2.60 i	1.06 i	1.12 k	0.59 ef
	T_1	0.00 g	0.00 i	0.00 d	0.00 g	0.00 g	0.00 h	0.00 h
	T_2	0.00 h	0.00 h	0.00 g	0.00 h	0.00 f	0.00 g	0.00 f
ACM-10	T_0	81.2 bc	57.3 hi	9.17 j	4.46 hi	1.52 h	1.42 j	0.46 g
	T_1	0.00 g	0.00 i	0.00d	0.00 g	0.00 g	0.00 h	0.00 h
	T_2	0.00 h	0.00 h	0.00 g	0.00 h	0.00 f	0.00 g	0.00 f
ACM-11	T_0	98.8 a	80.1 a	26.5 ab	30.0 a	2.74 d	5.94 a	0.94 c
	T_1	89.6 a-c	63.4 a-d	22.1 a	25.7 a	1.99 cd	5.30 a	0.83 ab
	T_2	86.4 a-c	61.9 a	19.1 a	17.0 a	1.89 b	2.44 b	0.59 ab
ACM-15	T_0	84.5 a-c	74.2 b-d	25.1 b-d	17.4 d	2.52 de	3.93 e	0.83 d
	T_1	59.6 e	66.5 ab	16.0 b	8.17 de	1.98 cd	1.72e f	0.73 bc
	T_2	54.2 ef	57.1 d-g	13.5 c-e	4.76 e-g	1.91 b	1.08 de	0.60 a
ACM-16	T_0	96.3 ab	76.1 a-c	22.5 d-g	23.8 bc	4.18 a	4.97 c	1.19 a
	T_1	63.4 de	65.0 a-c	16.8 b	9.12 c-e	3.83 a	1.62 f	0.87 a
	T_2	62.9 de	54.3 bc	15.8 bc	9.09 c	2.89 a	0.94 ef	0.60 cd
ACM-18	T_0	94.8 ab	78.5 ab	21.5 f-h	21.7 c	1.84 gh	4.39 d	0.58 ef
	T_1	91.9 ab	67.5 a	18.5 b	14.8 b	1.60 e	3.10 b	0.51 e
	T_2	80.9 c	62.5 a	11.5 d-f	12.6 b	1.39 cd	2.85 a	0.49 bc
ACM-23	T_0	97.0 ab	69.16 de	19.8 g-h	16.9 de	1.92 fg	4.12 de	0.63e
	T_1	79.4 b-d	65.1 a-c	16.1 b	9.13 c-e	1.67 de	2.17 cd	0.56de
	T_2	70.9b-e	42.5 ef	14.1 cd	4.84 e-g	1.54 c	0.90 ef	0.56 a-c
ACM-26	T_0	90.7 ab	75.1 a-c	22.1 e-g	22.3 bc	2.18 f	5.73 a	0.79 d
	T_1	72.4 c-e	55.5 e-g	17.0 b	11.29 c	2.06 c	1.93 de	0.64cd
	T_2	61.1 d-f	40.9 fg	9.67 f	3.28 fg	0.69 e	0.86 ef	0.16 e
ACM-29	T_0	93.3 ab	76.3 a-c	24.0 b-f	25.1 b	3.16 c	5.26 b	0.87 c
	T_1	80.8 bc	57.9 d-g	16.1 b	15.8 b	2.04 c	2.92 b	0.69 cd
	T_2	65.8 c-e	43.6 ef	11.3 d-f	3.33 fg	0.63 e	0.66 f	0.13 e
	T_0	98.6 a	68.1 ef	24.5 b-e	14.0 ef	1.93 fg	3.27 f	0.50 fg
ACM-35	T_1	98.4 a	60.9 b-e	16.0 b	10.7 cd	1.55 e	2.32 c	0.50 e
	T_2	89.1 a	55.1 bc	12.5 de	8.07 cd	1.47 cd	2.23 b	0.47 c
	T_0	100 a	59.1 gh	14.0 i	8.36 g	1.57 h	2.26 i	0.51 fg
Binadhan-7	T_1	0.00 g	0.00 i	0.00 d	0.00 g	0.00 g	0.00 h	0.00 h
	T_2	0.00 h	0.00 h	0.00 g	0.00 h	0.00 f	0.00 g	0.00 f
	T_0	91.9 ab	48.1 j	23.2 c-f	6.45 gh	0.97 i	1.56 j	0.33 h
RC-251	T_1	89.5 a-c	43.3 h	22.9 a	5.01 f	0.92 f	1.31 g	0.31 g
	T_2	85.3 ab	36.8 g	18.4 ab	3.57 fg	0.81 e	1.24 cd	0.21 e

Different letter within the column denotes the statistical significance difference among the mean values at $P < 0.05$. The treatments T_0 control, T_1 6 dSm^{-1} salinity level with complete submergence, and T_2 8 dSm-1 salinity level with complete submergence. The variables include LL (%) leaf live (%), RL root length (cm), SL shoot length (cm), RFW root fresh weight (mg), RDW root dry weight (mg), SFW shoot fresh weight (mg), and SDW shoot dry weight (mg).

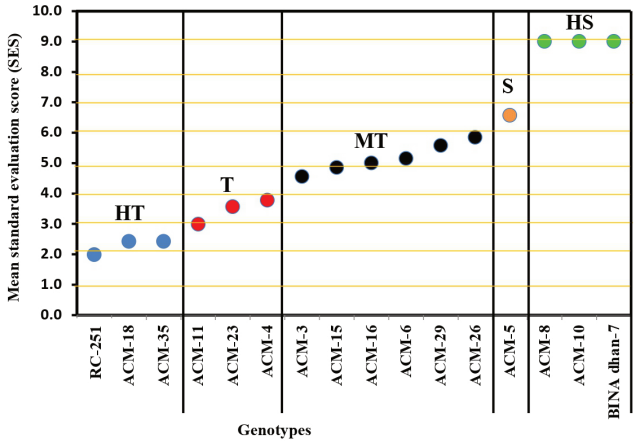

Figure 1. Evaluation of standard evaluation score (SES) in rice genotypes grown under combined salinity (6 dSm^{-1} and 8 dSm^{-1}) and waterlogging stress for 10 days at the late vegetative stage. Scoring range based on % reduction values of growth traits under stress conditions were count for 10-20% = score 1, 21-31%= score 3, 32-42% = score 5, 43-53% = score 7, and 54-64% = score 9; score 1,3,5,7 and 9 value was given according to IRRI standard protocol (1997), where score 1 denotes highly tolerant (HT), score 3 denotes tolerant (T), score 5 denotes moderately tolerant (MT), score 7 denotes susceptible (S), and score 9 denotes highly susceptible (HS). Table 3 showed the detailed parameters-wise scoring of rice genotypes under salt-submergence stress.

Categorizing of rice genotypes based on for mean salinity-submergence tolerance scores

Various degrees of phenotypic responses were reported in rice plants under salinity-submergence stress. Rice seedlings grown in the control condition showed normal growth and development whereas under stressed conditions, several impairments of salt-submergence induced injury such as yellowing and drying of leaves, reduction in root and shoot growths, and dying of seedlings were observed in the plants. Based on the morphological changes due to salinity-waterlogging stress, the rice genotypes were clustered into five groups viz., highly tolerant (mean tolerance score ≤2.5), tolerant (mean tolerance score ≤4.5), moderately tolerant (mean tolerance score ≤6.5), susceptible (mean tolerance score ≤8.5) and highly susceptible (mean tolerance score >8.5-9) (Table 3) following IRRI standard evaluation system (SES). After 10-days of combined stress induction, some plants were completely decayed and those were depicted as highly susceptible genotype viz., *ACM-8, ACM-10,* and *Binadhan-7* (Fig. 1). The genotypes namely *RC-251, ACM-18, and ACM-35* demonstrated the normal growth potential with the lowest mean tolerance score when both stresses is induced

ACM-35, ACM-4, ACM-23, and *ACM-3* minimized the reduction of RFW and SFW demonstrating higher fresh biomass likewise positive tolerant check *RC-251* when faced salt-submergence stress. In contrast, susceptible genotypes namely *ACM-5, ACM-16, ACM-26*, and *ACM-29* reflected the maximum reduction of RFW and SFW under combined stressed situations (Table 5). The results of the present investigation also showed the reduction of dry matter of rice plants in all genotypes under combined stressed conditions though tolerant genotypes exhibited less reduction of dry matter in comparison with susceptible genotypes (Table 5). When waterlogging with 8dSm^{-1} salt treatment is induced, the drastical reduction of root dry biomass was noted for *ACM-29* (84.6%), *ACM-26* (80.1%), and *ACM-4* (67.5%) whereas *ACM-35* (5.96%), *ACM-23* (11.1%), and *ACM-18* (15.5%) displayed the least reduction of root biomass compared to the other genotypes (Table 5). Similarly, the minimum reduction of shoot dry matter was also reported in *ACM-35* (T_1 29.0%, T_2 31.9%), and *ACM-18* (T_1 29.5%, T_2 35.2%) similar to positive check *RC-251* (T_1 15.6%, T_2 20.3%), whereas *ACM-26* (T_1 66.3%, T_2 85.0%), *ACM-16* (T_1 67.4%, T_2 81.1%), and *ACM-15* (T_1 56.3%, T_2 52.4%) reflected maximum shoot dry matter reduction under combined waterlogging + salt stress conditions (Table 5).

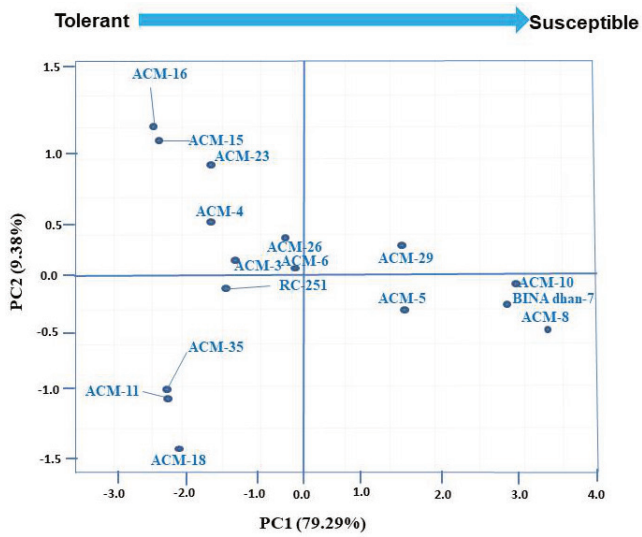

Figure 2. Hierarchical clustering and heatmap elucidating the genotype variable relationships. Color scale shows the intensity of the normalized mean values of different parameters. Clustering of rice genotypes considering percent reduction of growth parameters under combined salinity (6 dSm^{-1} and 8 dSm^{-1}) and submergence stress based on Euclidean distances grouped the genotypes into three clusters. Cluster-A includes *BINA dhan-7*, *ACM-8* and *ACM-10*; Cluster-B includes *ACM-5*, *ACM-6*, *ACM-15*, *ACM-16*, *ACM-26*, *ACM-29*, *ACM-3*, and *ACM-23*; Cluster-C includes *ACM-18*, *ACM-35*, *RC-251*, *ACM-4*, and *ACM-11*. The variables include LL (%) leaf live (%), RL root length (cm), SL shoot length (cm), RFW root fresh weight (mg), RDW root dry weight (mg), SFW shoot fresh weight (mg), and SDW shoot dry weight (mg).

Table 5. Percent reduction of growth parameters of 16 rice genotypes at the late vegetative stage under salt-submergence stress condition.

Genotypes	Treatment (T)	LL	SL	RL	SFW	RFW	SDW	RDW
ACM-3	T_1	5.79	24.0	24.3	20.7	14.7	18.0	37.7
	T_2	8.69	32.9	55.4	38.4	62.6	63.9	65.0
ACM-4	T_1	5.82	14.2	33.3	47.1	3.57	58.3	23.6
	T_2	19.8	20.0	37.2	59.5	5.83	63.9	67.5
ACM-5	T_1	59.4	24.6	35.7	60.2	32.2	56.5	30.2
	T_2	64.8	40.0	37.5	67.0	46.0	65.8	32.2
ACM-6	T_1	37.4	26.1	61.4	31.9	13.1	36.7	5.44
	T_2	53.1	37.0	69.6	84.1	22.7	53.3	32.6
ACM-8	T_1	100	100	100	100	100	100	100
	T_2	100	100	100	100	100	100	100
ACM-10	T_1	100	100	100	100	100	100	100
	T_2	100	100	100	100	100	100	100
ACM-11	T_1	9.35	20.8	16.3	14.2	27.3	10.7	11.3
	T_2	12.5	22.7	27.6	43.1	31.0	58.8	37.5
ACM-15	T_1	29.4	10.3	36.1	53.1	21.5	56.3	11.2
	T_2	35.7	22.9	46.2	72.6	24.3	72.4	27.0
ACM-16	T_1	34.1	14.6	25.1	61.7	8.22	67.4	26.6
	T_2	34.6	28.6	29.5	61.8	30.7	81.1	49.5
ACM-18	T_1	3.03	13.9	13.9	31.8	13.0	29.5	12.6
	T_2	14.6	20.3	46.5	41.9	24.2	35.2	15.5
ACM-23	T_1	18.1	5.88	18.4	46.2	13.1	47.3	10.1
	T_2	26.9	38.4	28.5	71.5	19.7	78.1	11.1
ACM-26	T_1	20.1	26.1	22.9	49.4	5.21	66.3	18.9
	T_2	32.6	45.5	56.3	85.3	68.4	85.0	80.1
ACM-29	T_1	13.4	24.1	32.6	36.9	35.2	44.5	20.3
	T_2	29.4	42.8	52.7	86.7	79.9	87.4	84.6
ACM-35	T_1	0.20	11.1	34.5	23.0	19.6	29.0	1.32
	T_2	9.60	19.1	48.6	42.3	23.6	31.9	5.96
Binadhan-7	T_1	100	100	100	100	100	100	100
	T_2	100	100	100	100	100	100	100
RC-251	T_1	2.61	9.79	1.26	22.3	4.83	15.6	6.06
	T_2	7.17	23.4	20.8	44.6	15.8	20.3	36.3

The treatments T_1 6 dSm^{-1} salinity level with complete submergence, and T_2 8 dSm^{-1} salinity level with complete submergence. %R' means percent reduction calculated as [(control value − salt treatment value)/control value × 100)]. Scoring range based on % reduction values of growth traits under stress conditions were count for 10-20%= score 1, 21-31%= score 3, 32-42% = score 5, 43-53% = score 7, and 54-64% = score 9; score 1,3,5,7 and 9 value was given according to IRRI standard protocol (1997), where score 1 denotes highly tolerant (HT), score 3 denotes tolerant (T), score 5 denotes moderately tolerant (MT), score 7 denotes susceptible (S), and score 9 denotes highly susceptible (HS). Table 3 showed the detailed parameters-wise scoring of rice genotypes. The variables include LL (%) leaf live (%), RL root length (cm), SL shoot length (cm), RFW root fresh weight (mg), RDW root dry weight (mg), SFW shoot fresh weight (mg), and SDW shoot dry weight (mg).

simultaneously and therefore, these were identified as highly tolerant whereas some other genotypes namely *ACM-11, ACM-23,* and *ACM-4* showed moderate to little injury symptoms under salt-submergence stress and consequently, these were regarded as tolerant genotypes (Fig. 1). The six genotypes viz., *ACM-3, ACM-15, ACM-16, ACM-6, ACM-29,* and *ACM-26* were identified as moderately tolerant as the seedling growth of those genotypes were partially inhibited under salinity-submergence stress conditions. Moreover, ACM-5 exhibited the greater reduction of growth traits having a higher mean tolerance score (6.57) in stressed conditions and therefore, it was depicted as a susceptible genotype (Fig. 1; Table 3).

The results of the cluster analysis

The heatmap and hierarchical clustering based on the percent reduction of growth traits under combined salinity and waterlogging stress using Euclidean distance grouped the 16 rice genotypes into three main clusters (Cluster-A, -B, and -C) (Fig. 2). The genotypes of the cluster-A are *Binadhan-7, ACM-8* and *ACM-10* which demonstrated the maximum reduction of growth traits and highest mean tolerance score (9.00) (Fig. 1; Table 3) under stressed conditions. Therefore, those genotypes

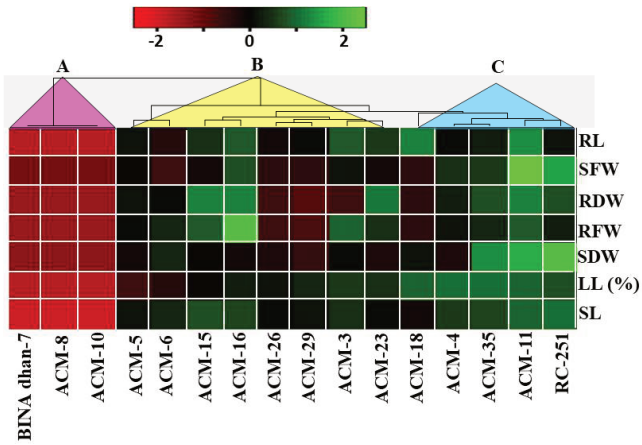

Figure 3. Loading plots of principal components 1 (PC1) and principal components 2 (PC2) of the PCA among 15 rice genotypes-based percent reduction of growth traits at the seedling stage under combined salinity (6 dSm^{-1} and 8 dSm^{-1}) and submergence stresses.

were regarded as highly susceptible genotypes. The distribution pattern of cluster analysis revealed maximum of eight genotypes viz., *ACM-5, ACM-6, ACM-15, ACM-16, ACM-26, ACM-29, ACM-3*, and *ACM-23* in cluster-B which showed differential response to salt-submergence tolerance under combined stress conditions such as *ACM-6, ACM-15, ACM-16, ACM-26, ACM-29, ACM-3* (moderately tolerant), *ACM-23* (tolerant) and ACM-5 (susceptible) (Fig. 2). The cluster-C had five genotypes and among them, ACM-18, ACM-35, and RC-251 displayed the least reduction of morphological parameters as well as the lowest mean tolerance score (≤2.5) (Fig. 1; Table 3) under combined stagnant and salinity stress, therefore these genotypes could be depicted as highly tolerant whereas rest two genotypes namely ACM-4, and ACM-11 were identified as tolerant genotypes (Fig. 2) as the heatmap showed that these genotypes had a lower reduction of growth traits as well as lower mean tolerance score (≤4.5) under salt-submergence stress situations (Fig. 1; Table 3).

The results of the principal component analysis (PCA)

Loading plots of principal component 1 (PC1) and principal component 2 (PC2) of the PCA among 16 rice genotypes based on the percent reduction of morphological attributes under combined salinity with waterlogging stress are presented in Fig. 3. In the present investigation, the PC1 from the PCA analysis explained about 79.29% of the total variation present in these genotypes, whereas PC2 describes 9.38% and the two components (PC1 and PC2) together explained 88.67% of data variability. The clustering patterns via PCA revealed that the genotypes viz., *ACM-11, ACM-35, ACM-18, and RC-251* which exhibited the least reduction of growth traits as well as the lowest mean tolerance score (Fig. 1; Table 3) under salinity-submergence stress, are grouped in the left lower side of the individual plot of PCA (Fig. 3). Therefore, those genotypes were identified as highly tolerant for salt-submergence stress. The genotypes namely *ACM-16, ACM-15, ACM-4, ACM-23, ACM-3, ACM-26* and *ACM-6* found in the left upper side of the biplot (Fig. 3) which showed lower growth reduction when combined salinity and submergence stress is imposed, and therefore these were regarded as tolerant and moderately tolerant genotypes based on the mean tolerance score (Fig. 1; Table 3). The genotypes grouped in the right lower side of biplot are *ACM-8, ACM-10, ACM-5,* and *Binadhan-7* (Fig. 3) depicted as susceptible genotypes because these genotypes demonstrated the maximum reduction of growth parameters under stress conditions having higher mean tolerance score (Fig. 1; Table 3). Besides, another genotype *ACM-29* which is grouped in the upper right side of the biplot exhibited lower growth reduction in waterlogging + NaCl treatment's, therefore it was regarded as a tolerant genotype according to the mean tolerance score (Fig. 1; Table 3).

Correlation and regression among different morphological attributes

To determine the most desirable traits for combined salt-submergence tolerance, Pearson's correlations were analyzed among different growth parameters of rice plants grown in saline condition with submergence stress (Table 6). The correlation matrix revealed a positive and significant correlation between all the growth traits in rice seedlings in submerged condition with both salinity levels. The highest positive and significant correlation was found between SFW and SDW ($r = 0.986^{**}$, $P < 0.01$), LL and RL ($r = 0.946^{**}$, $P < 0.01$), and RFW and RDW ($r = 0.895^{**}$, $P < 0.01$) at stagnant + 8dSm^{-1} salinity level whereas the least significant and positive correlation was observed in RFW with SDW at two different salinity level viz., at 6 dSm^{-1} salinity level ($r = 0.524^{**}$, $P < 0.05$), at stagnant 8 dSm^{-1} salinity level ($r = 0.556^{**}$, $P < 0.05$), and SFW with RFW ($r = 0.569^{**}$, $P < 0.05$) at 6 dSm^{-1} salinity level (Table 6). On the other hand, individual correlation of plants growth related traits, viz., LL ($r = -0.979^{**}$ & -0.818^{**}, $P < 0.01$), RL ($r = -0.858^{**}$ & -0.724^{**}, $P < 0.01$), SL ($r = -0.951^{**}$ & -0.808^{**}, $P < 0.01$), SFW ($r = -0.734^{*}$ & -0.650^{*}, $P < 0.05$), RFW ($r = -0.613^{**}$ & -0.613^{**}, $P < 0.05$), SDW ($r = -0.768^{**}$ & -0.811^{**}, $P < 0.01$), and RDW ($r = -0.722^{**}$ & -0.676^{**}, $P < 0.01$) showed negative and moderately significant correlation with mean tolerance score in both salinity levels with complete submergence situation (Table 6). There was a maximum negative and significant correlation observed between mean tolerance score with RFW ($r = 0.613^{**}$, $P < 0.01$) at waterlogging + 6 dSm^{-1} salinity level, RFW ($r = 0.613^{**}$, $P < 0.01$) at 8

Table 6. Correlation matrix among the morphological parameters under combined salinity (6 dSm^{-1} and 8 dSm^{-1}) and submergence stresses.

Traits	Treatment (T)	LL	SL	RL	SFW	RFW	SDW	RDW	MTS
LL (%)	T_1	1	0.875**	0.946**	0.730**	0.668**	0.748**	0.744**	-0.979**
	T_2	1	0.873**	0.871**	0.717**	0.637**	0.745**	0.644**	-0.818**
SL	T_1		1	0.881**	0.741**	0.818**	0.735**	0.891**	-0.858**
	T_2		1	0.851**	0.777**	0.830**	0.799**	0.815**	-0.724**
RL	T_1			1	0.726**	0.707**	0.747**	0.801**	-0.951**
	T_2			1	0.693**	0.779**	0.648**	0.706**	-0.808**
SFW	T_1				1	0.569*	0.986**	0.794**	-0.734**
	T_2				1	0.682**	0.844**	0.746**	-0.650**
RFW	T_1					1	0.524*	0.895**	-0.603*
	T_2					1	0.556*	0.847**	-0.613*
SDW	T_1						1	0.773**	-0.768**
	T_2						1	0.680**	-0.811**
RDW	T_1							1	-0.722**
	T_2							1	-0.676**

The treatments T_1 6 dSm^{-1} salinity level with complete submergence, and T_2 8 dSm^{-1} salinity level with complete submergence. MTS denote mean tolerance score. The variables include LL (%) leaf live (%), RL root length (cm), SL shoot length (cm), RFW root fresh weight (mg), RDW root dry weight (mg), SFW shoot fresh weight (mg), and SDW shoot dry weight (mg). '**' correlation is significant at 1% level of probability, and '*' correlation is significant at 5% level of probability.

dSm^{-1} salinity level and SDW (r = 0.676**, P < 0.05) at waterlogging + 8 dSm^{-1} salinity level (Table 6). Among the growth traits, LL (%), RL, SL, RDW, and SFW exhibited higher association with the mean tolerance score at higher salinity level (submergence + 8 dSm^{-1}) whereas RFW and SDW showed higher correlation with mean tolerance score at lower salinity level (submergence + 6 dSm^{-1}) (Table 6).

The multiple correlation coefficient (R) also demonstrated the positive and significant correlation between mean tolerance score (dependent variable) and growth parameters viz., LL (%), RL, SL, RFW, SFW, RDW, and SDW (independent variables) under combined stress of salinity and submergence (Table 7). However, the explained variation of mean tolerance score by independent variables was higher at 6 dSm^{-1} salinity level with complete submergence (R^2 = 0.959**, P < 0.01) in comparison with 8 dSm^{-1} with complete submergence (R^2 = 0.922**, P <0.01) (Table 7). The multiple regression lines were also analysed for each salinity level with submergence stress considering the constant value (mean tolerance score) and regression coefficients for morphological parameters such as LL (%), RL, SL, RFW, SFW, RDW, and SDW (Table 8). The results of the regression coefficients revealed that at 6 dSm^{-1} salinity with complete submergence conditions, only LL (%) had the negative and significant association with mean tolerance score (r = -0.054, **P < 0.01) whereas at 8 dSm^{-1} salinity with complete submergence, several traits such as LL (b = -0.042*, P < 0.05), RL (b = -0.170*, P < 0.05), RFW (b = -1.049*, P < 0.05), and RDW (b = -2.768**, P < 0.001) exhibited a significant and negative association with the mean tolerance score (Table 8). Bedsides, SL, and SFW had positive-significant association with the mean tolerance score at 8 dSm^{-1} salinity with complete waterlogging situations. However, RDW showed the non-significant association with the mean tolerance score in both salinity levels with waterlogging conditions (Table 8).

Table 7. Multiple correlation coefficients (R) between mean tolerance score (dependent variable) and morphological parameters (independent variables) at different salinity level (salinity (6 dSm^{-1} and 8 dSm^{-1}) with submergence stress.

Parameters	Treatments	
	6 dSm^{-1} salinity level with complete submergence	8 dSm^{-1} salinity level with complete submergence
R- value	0.989**	0.979**
R^2-value	0.959**	0.922**

'**' correlation is significant at 1% level of probability.

Table 8. Regression coefficients for different morphological parameters (independent variables) at different salinity level salinity (6 dSm^{-1} and 8 dSm^{-1}) with submergence stress and constant (dependent variable is mean tolerance score).

Traits	Regression coefficients	
	6 dSm^{-1} salinity level with complete submergence	8 dSm^{-1} salinity level with complete submergence
Constant (MTS)	9.011**	9.064***
%LL	-.054**	-.042*
SL	-.011^{NS}	.118**
RL	-.091^{NS}	-.170*
SFW	.141^{NS}	.275**
RFW	.366^{NS}	-1.049*
SDW	-.782^{NS}	-2.768***
RDW	-.116^{NS}	-2.626^{NS}

MTS denote mean tolerance score. The variables include LL (%) leaf live (%), RL root length (cm), SL shoot length (cm), RFW root fresh weight (mg), RDW root dry weight (mg), SFW shoot fresh weight (mg), and SDW shoot dry weight (mg).
'**' correlation is significant at 1% level of probability, and '*' correlation is significant at 5% level of probability.

Measurement of genetic variability, heritability, and genetic advance among the morphological parameters

A wide range of genotypic and phenotypic variance was observed in the agronomic traits of rice seedlings (Table 9). In the present study, the phenotypic co-efficient of variation (PCV) was higher than the genotypic co-efficient of variation (GCV) for all the traits. Among the traits, shoot fresh weight (100% & 100.9%), shoot dry weight (88.8% & 88.9%), and root fresh weight (86.8% & 87.1%) exhibited high estimates of GCV and PCV respectively whereas the lowest phenotypic GCV and PCV were observed for leaf live (%) (57.7% & 58.3%), and shoot length (58.7% & 58.8%) (Table 9). All the studied traits in this experiment exhibited high heritability ranging from 97.9% to 99.7% and the highest value was recorded in shoot dry weight (99.7%), shoot length (99.6%), and root fresh weight (99.3%) (Table 9). The highest genetic advance (GA) was found in leaf live (%) (82.9) and shoot length (63.5) whereas the lowest value was found in root dry weight (0.78) (Table 9).

Discussion

Due to the adverse climatic change, a considerable number of agricultural lands in the world are simultaneously affected by multiple environmental stresses such as salinity and waterlogging combination is most common among them. Waterlogging and salinization both have several individual or simultaneous physical, chemical, and biological effects on plant and soil which can influence plant growth potential negatively and can decrease the usability of the fields (Boling et al. 2007; Singh 2014b). The influential mode of salinity stress on the plant growth and development are well documented (Munns and Tester 2008), but the interaction effects of salt stress with waterlogging stress on plant growth are not fully revealed in rice crops like most of the plants (Colmer and Flowers 2008; Gill et al. 2019). In the present study, therefore an attempt has been made to examine the response of 16 rice genotypes

Table 9. Estimation of genetic parameters for the morphological parameters in 16 rice genotypes.

Traits	σ^2g	σ^2p	GCV (%)	PCV (%)	h^2_b (%)	GA
LL (%)	1656.0	1691.0	57.7	58.3	97.9	82.9
SL	955.0	958.3	58.7	58.8	99.6	63.5
RL	114.6	115.6	70.0	70.3	99.1	21.9
SFW	104.3	105.4	100	100.9	98.9	20.9
RFW	2.103	2.116	86.8	87.1	99.3	2.97
SDW	3.581	3.590	88.8	88.9	99.7	3.89
RDW	0.146	0.148	78.9	79.2	99.1	0.78

σ^2g genotypic variance, σ^2p phenotypic variance, GCV genotypic coefficient of variation, PCV phenotypic coefficient of variation, h^2_b narrow sense heritability, and GA genetic advance. The variables include LL (%) leaf live (%), RL root length (cm), SL shoot length (cm), RFW root fresh weight (mg), RDW root dry weight (mg), SFW shoot fresh weight (mg), and SDW shoot dry weight (mg).

grown under combined salinity and submergence stresses considering different morphological parameters.

The submerged plants are very sensitive to salinity, particularly at the early growth stages (Barrett-Lennard 2002). Waterlogging interrupts plant growth in two ways, directly by reducing the physiological activities and indirectly by decreasing the availability of essential nutrients with reduced aeration around the root zone whereas salt stress affects plant growth by enhancing the osmotic potential of the soil solution as well as by depleting the soil structure (Singh 2017). The results of our study revealed that the growth and development of rice seedlings in all genotypes are severely affected under combined stress of salinity and submergence (Table 2) however, some genotypes namely *ACM-18, ACM-35, RC-251, ACM-11, ACM-23,* and *ACM-4* displayed their ability to minimize combined stress-induced toxicity and maintain the higher value of growth parameters viz., higher live leaves (%), high root and shoot length, and high plant biomass production under stressed conditions in compared to other genotypes (Tabe 3). The ability of roots to uptake water with nutrients from the soil environment is depleted under salinity stress which may also disarrange many important physiological and biochemical processes in plants such as photosynthesis, redox homeostasis, and toxic ion assimilation in plant cells (Motos et al. 2017). Moreover, when salinized plants expose to waterlogging conditions, normal root function get damaged and the selectivity for K^+ over Na^+ is declined (Barrett-Lennard 2003), and thus the concentrations of Na^+ and Cl^- considerably increased in the shoot of plants (Marcar et al. 2002; Araki 2006). When root parts become injured, shoot growth is impeded due to the less uptake of essential nutrients like K^+, Ca^{2+} Mg^{2+}, etc. through symplastic xylem loading in the root (Läuchli and Grattan 2007). In the present investigation, the root length, and shoot length was reduced in all genotypes with the increasing of salinity level under submergence condition (Table 5). In line with our results, several other researchers also manifested the negative effects of combined salinity and submergence stress with lower root and shoot growth in tomato (*Solanum lycopersicum* L.) (Horchani et al. 2010), barley (*Hordeum vulgare* L.) (Zeng et al. 2013) and rice (*Oryza sativa* L.) (Prusty et al. 2018). On the contrast, the genotypes *viz., ACM-18, ACM-35,* and *RC-251* showed the highest root and shoot length under salt stress coupled with waterlogging condition even at 10 days in the late vegetative stage whereas susceptible *ACM-23, ACM-5,* and *Binadhan-7* could not withstand combined salinity and submergence stress and thereby had lowest growth of root and shoot (Table 4). The higher root and shoot growth of the tolerant genotypes can be explained by the ability to maintain sufficient root aeration with the adaptation of morpho-physiological mechanisms under salt-submergence stress (Colmer et al. 2014). Moreover, tolerant genotypes might consume excessive photo-assimilates and stored carbohydrates for rapid elongation of shoots by cell division and cell elongation as well as by photosynthetic fixation of $CO_2$when faced submergence (Anandan et al. 2015; Jackson and Ram 2003). Singh et al. (2001) also observed maximum root length in tolerant genotypes compared to sensitive one's along with less adverse effects on root volume and porosity in tolerant genotypes under submergence stress. On the other hand, the leaves of the susceptible genotypes usually senesced and depleted and recovered more slowly because of slower shoot elongation and lower leaf formation under submergence in saline water (Singh et al. 2014a). However, shoot growth usually demonstrated more susceptibility than root growth in both saline and submergence situations (Omisun et al. 2018; Fukao et al. 2019). The toxicity of salt stress occurs primarily in the aged leaves because Na^+ and Cl^- accumulate in the transpiring leaves for long-time leading toxicity on leaves which ultimately reduces leaf live (%) of plants (Amirjani 2011). Besides, the salinized plant faced pervaded sunlight during submergence causing the reduction of the leaf chlorophyll content which sometimes causes the death of many leaves (Afrin et al. 2018). The results of this study revealed that the leaf live (%) was significantly declined in rice seedlings under combined stressed conditions compared to control condition plants but identified highly tolerant genotypes namely *ACM-3, ACM-35,* and *RC-251* minimized the salt-submergence induced toxicity and therefore, exhibited maximum live leaf (%) (Table 4), indicating that those genotypes could adopt faster recovery from stress-induced metabolic changes and might have the mechanism to maintain required photosynthesis for the synthesis of leaf chlorophyll content during combined submergence and salinity stress (Ella and Ismail 2006). On the other hand, sensitive genotypes viz., *ACM-5, ACM-6, and ACM-16* exhibited the higher reduction of leaf live (%) when faced salinity stress in waterlogging condition (Table 5). This is mainly because of continuous loss of oxygen in root atmosphere which exerts an adverse effect on respiration and photosynthesis of plants causes withering and death of active leaves (Yadav et al. 2018). Furthermore, the rapid degradation of leaf chlorophyll in sensitive genotypes under water reflected higher levels of leaf chlorosis as well as leaf senescence (Bui et al. 2019). Due to the reduction of the number of live leaves under stress conditions, the supply of carbohydrates and growth hormones to meristematic tissues badly impeded with the unusual photosynthetic process which ultimately decelerates the plant biomass production (Munns and Tester 2008). In the current study, the exposure of rice seedlings to com-

bined salt and submergence stress caused the significant reduction of shoot, and root biomasses which might be due to the inhibition of root and shoot growth (Table 5) as also previously observed in other plant species such as shrubby sea blight (*Suaeda salsa*), and birdsfoot trefoil (*Lotus corniculatus*) under combined salinity and waterlogging stress (Teakle et al. 2016; Song et al. 2011). The recorded plant biomass retrenchment in most of the genotypes probably because of conjunction of salt-induced osmotic stress and oxygen-deficient environment due to submergence in plant cells (Shani and Ben-Gal, 2005). Moreover, submergence stress considerably obstructs the generation of tiller number and other agronomic traits that collectively can reduce the fresh and dry weight of the plant (Afrin et al. 2018). Notably, the dry matter reduction was relatively higher in sensitive genotypes viz., *ACM-5, ACM-16, ACM-26*, and *ACM-29* under combined stressed conditions (Table 5), as also reported by Tatar et al. (2010), Kano-Nakata et al. (2011), and Talat et al. (2013) in rice (*Oryza sativa* L.) and wheat (*Triticum aestivum* L) under salt stress or submergence stress. The maximum reduction of leaves and root dry weights of the sensitive genotypes might be due to the rapid death and decay of tissues with confined underwater photosynthesis in submergence stress situations (Winkel et al. 2013). On the contrast, tolerant genotypes namely *ACM-35, RC-251, ACM-4, ACM-23, and ACM-3* demonstrated the higher plant fresh and dry matter production even when exposed to combined salinity and submergence stress conditions (Table 4). The higher accumulation of dry matter in tolerant genotypes against combined stress might be due to the increase in culm dry matter content rather than leaf area or total leaf dry weight (Sarkar and Das 2003; Yin et al. 2010). Besides, the multiple stress-tolerant rice genotypes might adopt morpho-physiological mechanisms such as salt exclusion, salt reabsorption, root-shoot translocation, and leaf-to-leaf compartmentation through which they can exclude the accumulation of excessive salt on leaves in submerged conditions to maintain the normal cell metabolism and consequently plant achieve higher biomass production (Chen et al. 2018).

Several approaches exist for sorting out salt or submergence stress-tolerant genotypes such as standard evaluation score (SES) which is extensively used (Kranto et al. 2016). In the present study, the modified SES scoring system was employed to categorize the rice genotypes for salt-submergence tolerance at the late vegetative stage and there was a significant variation found in the mean tolerance score among the rice genotypes in terms of different growth parameters under combined stressed situation (Fig. 1; Table 3). This finding was in line with Ali et al. (2014) and Nishanth et al. (2017) who observed the substantial disparity in injury score among the rice germplasm grown under salinity and submergence conditions in a separate experiment. In our study, rice seedlings exposed to 10 days of complete submergence in saline solution demonstrated several injury symptoms such as rolling and drying of leaves, brownish of leaf tip and stunted plant growth. However, tolerant genotypes *ACM-18, ACM-35*and *RC-251* considerably lessened the salt-submergence commenced visual toxicity symptoms and thereby exhibited a maximum value of growth attributes with lowest mean tolerance score (<2.5) (Fig. 1; Table 3) when combined stress is imposed. These genotypes might adopt a combination of anatomical, morpho-physiological, and metabolic strategies such as the formation of higher aerenchyma tissue in the nodal region, higher shoot elongation, restriction of chlorophyll degradation, less utilization of storage carbohydrates, more adventitious roots generation, the regulation of ion uptake, exclusion of excessive salt in plant parts and the increased activity of antioxidant defense system to withstand the hazardous effect of combined salinity and waterlogging stress conditions (Barrett-Lennard 2003; Carter et al. 2006; Yadav et al. 2018). On the other hand, some genotypes viz., *ACM-5, ACM-8, ACM-10,* and *Binadhan-7* displayed the maximum mean tolerance score with the greater reduction of morphological parameters in stressed conditions and therefore, these genotypes were depicted as stress-sensitive genotypes (Fig. 1; Table 3). Bharathkumar et al. (2015) and Afrin et al. (2018) also successfully separated the rice genotypes for salt-submergence tolerance based on the injury score under salinity and waterlogging stress in previous experiments. The findings of cluster analysis and PCA classification of rice genotypes produced similar results with the results obtained from the categorization of genotypes based on mean tolerance score in this investigation (Fig. 1 and 2). Ward's minimum-variance cluster analysis is the most frequently used exoteric scheme that can group genotypes from the diverse origin based on their similarities (Ravikiran et al. 2018). Besides, PCA can also classify the genotypes of similar categories together compared to dissimilar genotypes (Khatun et al. 2015; Kim et al. 2013). Furthermore, genotype versus variable biplot also can explore the strength and weaknesses of genotypes in a stress situation, which is fundamental for the selection of tolerant genotypes (Yan and Kang 2003). In the present study, both heatmap and PCA analysis clearly distinguished the tolerant rice genotypes from the sensitive genotypes considering the reduction (%) of growth attributes under salt-submergence stress (Fig. 1 and 2), similar with the findings of Sorkheh et al. (2012). In hierarchical cluster analysis, the highly tolerant genotypes viz., *ACM-4, ACM-35,* and *RC-251* were grouped in the same cluster (C) and similarly, these genotypes were also found in the right lower side together in the PCA biplot (Fig. 1

and 2). Those genotypes demonstrated normal growth and development when exposed to combined stress and had a higher value of growth traits in comparison with other genotypes (Fig. 3). The rice genotypes showing both salinity and waterlogging tolerance may be due to the adaptation of similar physiological mechanisms and co-expression of the related genes under stress conditions. On the other hand, sensitive genotypes (*ACM-5, ACM-8, ACM-10,* and *Binadhan-7*) also found in the same group both in PCA and cluster analysis which demonstrated the higher growth attributes reduction under stressed situation (Fig. 2 and 3; Table 5). The results of our investigation were also inconsistent with Rasel et al. (2020) and Chunthaburee et al. (2016) who successfully differentiated rice cultivars into distinct groups by PCA and cluster analysis in terms of salt tolerance considering agronomic traits. Moreover, several other researchers also previously used clustering and PCA analysis as useful tools for the classification of rice (*Oryza sativa* L.), wheat (*Triticum aestivum* L.) and corn (*Zea mays* L.) cultivars into different tolerance levels considering morpho-physiological traits under different stress conditions for instance salinity, submergence, drought etc. (Cha-um et al. 2012; Wijewardana et al. 2016; Siddiqui et al. 2017).

Correlation analysis is a novel method for exploring the relationships between the parameters and their principal components in phenotypic screening of genotypes under stress conditions (Dehbalaei et al. 2013; Sun et al. 2013). In the present study, morphological attributes such as LL (%), RL, RFW, RDW, and SFW showed the highest negative correlation and association with mean tolerance score under combined stress situation (Table 6) reflecting that tolerant genotype (having lower mean tolerance score) exhibited a higher value of those growth attributes in stressed condition, similar with the findings of Rasel et al. (2018). Thus, these traits might be used as the best descriptors to evaluate the tolerance level of rice genotypes as well as to find out the tolerant genotypes at the seedling stage under combined salinity and waterlogging stress in comparison to other growth parameters. Ali et al. (2014) also found the strongest and significant correlations between shoot length, and plant biomass with SES at the seedling stage of rice plants and used these traits as important selection criteria to find out salt-tolerant rice genotypes. Similarly, the genetic analysis also showed that the growth parameters viz., LL, RL, RFW, RDW, and SFW had the highest value for PCV (%), GCV (%), heritability (%), and genetic advance (Table 9) indicating that the phenotypic expression of these traits are less influenced by environment and therefore, selection can be done by using these traits for the identification of rice genotypes that can tolerate combined salinity and waterlogging stress condition simultaneously and the higher value of these traits would facilitate better scope for the improvement of rice genotypes against multiple stress.

Conclusion

A large variability was observed among the rice genotypes for all growth traits under combined salinity and waterlogging stress. Several parameters such as leaf live (%), root length, root fresh weight, shoot fresh weight, and root dry weight exhibited a strong and negative correlation with mean tolerance score reflecting their importance as useful indicators for the selection of tolerant rice genotypes in combined stress salinity and submergence. Rice seedlings showed the reduction of morphological parameters due to the interactive effects of salinity and waterlogging. However, some genotypes namely *ACM-18,* and *ACM-35* significantly minimized the stress-induced reduction of growth attributes likewise tolerant check *RC-251* and therefore, those genotypes were depicted as highly tolerant. The results of clustering and PCA also revealed those genotypes in the same group. Besides, *ACM-11, ACM-23,* and *ACM-14* also performed very well and demonstrated the higher value in agro-morphological assays under stress situations. Therefore, the genotypes viz., *ACM-18, ACM-35, ACM-11, ACM-23,* and *ACM-14* could be used as a potential donor of *Saltol* and *Sub1* gene as well as in marker-assisted backcrossing for the development of salt-submergence tolerant high-yielding rice variety.

Acknowledgements

This research was supported by the Ministry of Science and Technology, Bangladesh. The authors gratefully acknowledge Bangladesh Institute of Nuclear Agriculture (BINA), Mymensingh, Bangladesh for providing laboratory facilities throughout the experimental work.

References

Abedin MH, Al-Mamun MA, Mia MAB, Karim MA (2019) Evaluation of submergence tolerance in landrace rice cultivars by various growth and yield parameters. J Crop Sci Biotechnol 22:335-344.

Afrin W, Nafis MH, Hossain MA, Islam MM, Hossain MA (2018) Responses of rice (*Oryza sativa* L.) genotypes to different levels of submergence. Compt Rend Biol 341:85-96.

Ahmed MF, Haider MZ (2014) Impact of salinity on rice production in the south-west region of Bangladesh. Environ Sci: An Indian J 9:135-141.

Alexandratos N, Jelle B (2012) World agriculture towards

2030/2050: the 2012 revision. FAO Agricultural Development Economics Division. Food and Agriculture Organization of the United Nations. www.fao.org/economic/esa.

Ali MN, Yeasmin L, Gantait S, Goswami R, Chakraborty S (2014) Screening of rice landraces for salinity tolerance at seedling stage through morphological and molecular markers. Physiol Mol Biol Plant 20:411-423.

Ali S, Gautam RK, Mahajan R, Krishnamurthy SL, Sharma SK, Singh RK, Ismail AM (2013) Stress indices and selectable traits in *saltol QTL* introgressed rice genotypes for reproductive stage tolerance to sodicity and salinity stresses. Field Crop Res 154:65-73.

Amirjani MR (2011) Effect of salt stress on growth, sugar content, pigment and enzyme activities in rice. Int J Bot 7:73-81.

Anandana A, Pradhan SK, Das SK, Behera L, Sangeetha G (2015) Differential responses of rice genotypes and physiological mechanism under prolonged deep water flooding. Field Crop Res 172:153-163.

Araki H (2006) Water uptake of soybean (*Glycine max* L. Merr.) during exposure to O_2 deficiency and field level CO_2 concentration in the root zone. Field Crop Res 96:98-105.

Barrett-Lennard E (2002) Restoration of saline land through revegetation. Agric Water Manag 53:213-226.

Barrett-Lennard E (2003) The interaction between waterlogging and salinity in higher plants: causes, consequences and implications. Plant Soil 253:35-54.

BharathKumar S, Pragnya PJ, Jitendra K, Archana B, Niharika M, Nupur N, Sulagna S, Soumya, M, Durga PM, Reddy JN (2015) Rice landraces with genetic variations for salinity tolerance and their association with submergence tolerance. Int J Genet 7:177-179.

Boling AA, Bouman BAM, Tuong TP, Murty MVR, Jatmiko SY (2007) Modelling the effect of groundwater depth on yield-increasing interventions in rainfed lowland rice in central Java, Indonesia. Agric Syst 92:115-139.

Bui LT, Ella ES, Dionisio-Sese ML, Ismail AM (2019) Morpho-physiological changes in roots of rice seedling upon submergence. Rice Sci 26:167-177.

Carter JL, Colmer TD, Veneklaas EJ (2006) Variable tolerance of wetland tree species to combined salinity and waterlogging is related to regulation of ion uptake and production of organic solutes. New Phytol 169:123-134

CGIAR (2016) The global staple. http://ricepedia.org/rice-asfood/the-global-staple-rice-consumers.

Chartzoulakis KS (2005) Salinity and olive: growth, salt tolerance, photosynthesis and yield. Agric Water Manag 78:108-121.

Cha-um S, Chuencharoen S, Mongkolsiriwatana C (2012) Screening sugarcane (*Saccharum* sp.) genotypes for salt tolerance using multivariate cluster analysis. Plant Cell Tissue Organ Cult 110:23-33.

Chen M, Yang Z, Liu J, Zhu T, Wei X, Fan H, Wang B (2018) Adaptation mechanism of salt excluders under saline conditions and its applications. Int J Mol Sci 19:3668.

Chen Y, Zhou Y, Yin TF, Liu CX, Luo FL (2013) The invasive wetland plant *Alternanthera philoxeroides* shows a higher tolerance to waterlogging than its native congener *Alternanthera sessilis*. PLoS ONE 8:e81456.

Chunthaburee S, Dongsansuk A, Sanitchon J, Pattanagul W, Theerakulpisut P (2016) Physiological and biochemical parameters for evaluation and clustering of rice cultivars differing in salt tolerance at the seedling stage. Saudi J Biol Sci 23:467-477.

Colmer TD, ArmstrongW, Greenway H, Ismail AM, Kirk GJD, Atwell BJ (2014) Physiological mechanisms in flooding tolerance of rice: transient complete submergence and prolonged standing water. Prog Bot 75:255-307.

Colmer TD, Flowers TJ (2008) Flooding tolerance in halophytes. New Phytol 179:964-974.

Dehbalaei S, Farshadfar E, Farshadfar M (2013) Assessment of drought tolerance in bread wheat genotypes based on resistance/tolerance indices. Int J Agric Crop Sci 5:2352-2358.

Ella ES, Ismail AM (2006) Seedling nutrient status before submergence affects survival after submergence in rice. Crop Sci 46:1673-1681.

Evelin H, Kapoor R, Giri B (2009) Arbuscular mycorrhizal fungi in alleviation of salt stress: a review. Annals Bot 104:1263-1280.

Fukao T, Barrera-Figueroa BE, Juntawong P, Peña-Castro JM (2019) Submergence and waterlogging stress in plants: a review highlighting research opportunities and understudied aspects. Front Plant Sci 10:340.

Ghosh B, Md NA, Saikat G (2016) Response of rice under salinity stress: a review update. Rice Res: Open Access 4:167.

Gill MB, Zeng F, Shabala L, Zhang G, Min Yu, Demidchik V, Shabala S, Zhou M (2019) Identification of QTL related to ROS formation under hypoxia and their association with waterlogging and salt tolerance in barley. Int J Mol Sci 20:699.

Goswami S, Labar R, Paul A, Adak KM, Dey N (2015) Physio-biochemical and genetic exploration for submergence tolerance in rice (*Oryza sativa* L.) landraces with special references to *Sub*1 loci. Am J Plant Sci 6:1893-1904.

Hakim MA, Juraimi AS, Hanafi MM, Ismail MR, Rafii MY, Islam MM, Selamat A (2014) The effect of salinity on growth, ion accumulation and yield of rice varieties. J Anim Plant Sci 24:874-885.

Haque SA (2006) Salinity problems and crop production in coastal regions of Bangladesh. Pak J Bot 38:1359-1365.

Hatton TJ, Ruprecht J, George RJ (2003) Preclearing hydrology of the Western Australia wheat belt: target for the

future. Plant Soil 257:341-356.
Horchani F, Hajri R, Khayati H, Aschi-Smiti S (2010) Physiological responses of tomato plants to the combined effect of root hypoxia and NaCl salinity. J Phytol 2:36-46.
Hussain S, Jun-Hua Z, Chu Z, Lian-Feng Z, Xiao-Chuang C, Sheng-Miao Y, James AB, Ji-jie H, Qian-Yu J (2017) Effects of salt stress on rice growth and development characteristics and the regulating ways: a review. J Integr Agric 16:2357-2374.
Ismail AM, Singh U, Singh S, Dar MH, Mackill DJ (2013) The contribution of submergence-tolerant (*Sub1*) rice varieties to food security in flood-prone rainfed lowland areas in Asia. Field Crop Res 152:83-93.
Ismail AM, Thomson MJ, Vergara GV, Rahman MA, Singh RK, Gregoio GB, Mackill DJ (2010) Designing resilient rice varieties for coastal deltas using modern breeding tools. In Hoanh CT, Szuster BW, Suan-Pheng K, Ismail AM, Noble AD, Eds., Tropical Deltas and Coastal Zones: Food Production, Communities and Environment at the Land-water Interface CAB international. Oxfordshire, UK.
Jackson MB, Ram PC (2003) Physiological and molecular basis of susceptibility and tolerance of rice plants to complete submergence. Ann Bot 91:227-241.
Kano-Nakata M, Inukai Y, Wade LJ, Siopongco JDLC, Yamauchi A (2011) Root development, water uptake, and shoot dry matter production under water deficit conditions in two CSSLs of rice: functional roles of root plasticity. Plant Prod Sci 14:307-317.
Khatun MT, Hanafi MM, Yusop MR, Wong MY, Salleh FM, Ferdous J (2015) Genetic variation, heritability, and diversity analysis of upland rice (*Oryza sativa* L.) genotypes based on quantitative traits. Biomed Res Int 2015:290861
Kibria MG, Hossain M, Murata Y, Hoque MA (2017) Antioxidant defense mechanisms of salinity tolerance in rice genotypes. Rice Sci 24:155-162.
Kim JK, Park SY, Lim SH, Yeo Y, Cho HS, Ha SH (2013) Comparative metabolic profiling of pigmented rice (*Oryza sativa* L.) cultivars reveals primary metabolites are correlated with secondary metabolites. J Cereal Sci 57:14-20.
Kordrostami M, Rabiei M, Kumleh HH (2017) Biochemical, physiological and molecular evaluation of rice cultivars differing in salt tolerance at the seedling stage. Physiol Mol Biol Plant 23:529-544.
Kranto S, Chankaew S, Monkham T, Theerakulpisut P, Sanichon J (2016) Evaluation for salt tolerance in rice using multiple screening methods. J Agric Tech 18:1921-1931.
Kumar V, Singh A, Mithra SA, Krishnamurthy SL, Parida SK, Jain S, Khurana JP (2015) Genome-wide association mapping of salinity tolerance in rice (*Oryza sativa*). DNA Res 22:133-145.
Läuchli A, Grattan SR (2007) Plant Growth and Development Under Salinity Stress. Springer, Berlin, pp 1-32.
Marcar NE, Crawford DF, Saunders A, Matheson AC, Arnold RA (2002) Genetic variation among and within provenances and families of *Eucalyptus grandis* W. Hill and *E. globulus* Labill. subsp. *globulus* seedlings in response to salinity and waterlogging. Forest Ecol Manag 162:231-249.
Masutomi Y, Takahashi K, Harasawa H, Matsuoka Y (2009) Impact assessment of climate change on rice production in Asia in comprehensive consideration of process/parameter uncertainty in general circulation models. Agric Ecosys Environ 131:281-291.
Motos JRA, Ortuño MF, Vicente AB, Vivancos PD, Blanco MJS, Hernandez JA (2017) Plant responses to salt stress: adaptive mechanisms. Agronomy 7:18.
Munns R, Tester M (2008) Mechanisms of salinity tolerance. Annu Rev Plant Biol 59:651-681.
Neerja CN, Maghirang-Rodriguez R, Pamplona A, Collard BCY, Septiningsih EM, Vergara G, Sanchez D, Xu K, Ismail AM, Mackill DJ (2007) A marker-assisted backcross approach for developing submergence-tolerant rice cultivars. Theor Appl Genet 115:767-776.
Nicholls RJ, Wong PP, Burkett VR, Codignotto JO, Hay JE, McLean RF, Ragoonaden S, Woodroffe CD (2007) Coastal systems and low-lying areas. In Parry ML, Canziani OF, Palutikof JP, van der Linden PJ, Hanson CE, Eds., Climate Change 2007: Impacts, Adaptation, and Vulnerability. Contribution of working group II to the fourth assessment report of the intergovernmental panel on climate change. Cambridge University Press, Cambridge, pp 315–356.
Nishanth GK, Dushyanthakumar BM, Gangaprasad S, Gowda TH, Nataraju SP, Shashidhar HE (2017) Screening and genetic variability studies in submergence tolerance rice germplasm lines under flood prone lowlands of hill zone of Karnataka, India. Int J Curr Microbiol Appl Sci 6:1254-1260.
Omisun T, Sahoo S, Saha B, Panda SK (2018) Relative salinity tolerance of rice cultivars native to Northeast India: a physiological, biochemical and molecular perspective. Protoplasma 255:193-202.
Parihar P, Singh S, Singh R, Singh VP, Prasad SM (2015) Effect of salinity stress on plants and its tolerance strategies: a review. Environ Sci Pollut Res 22:4056-4075.
Prusty N, Pradhan B, Deepa Chattopadhyay K, Patra BC, Sarkar RK (2018) Novel rice (*Oryza sativa* L.) genotypes tolerant to combined effect of submergence and salt stress. Indian J Plant Genetic Res 31(3):260-269.
Rahman MM, Ahsan M (2001) Salinity constraints and agricultural productivity in coastal saline area of Bangladesh. Soil resources in Bangladesh: assessment and utilization. Proc Ann Workshop Soil Resource. pp 1-14.

Rahman MM, Jahan I, Al Noor MM, Tuzzohora MF, Sohag AAM, Raffi SA, Islam MM, Burritt D, Hossain MA (2020) Potential determinants of salinity tolerance in rice (*Oryza Sativa* L.) and modulation of tolerance by exogenous ascorbic acid application. J Phytol 12:86-98.

Rasel M, Arif MTU, Hossain MA, Sayed MD, Hassan L (2019) Discerning of rice landraces (*Oryza sativa* L.) for morpho-physiological, antioxidant enzyme activity, and molecular markers' responses to induced salt stress at the seedling stage. J Plant Growth Regul 38:1-19.

Rasel M, Hassan L, Hoque MIU, Saha SR (2018) Estimation of genetic variability, correlation and path coefficient analysis in local landraces of rice (*Oryza sativa* L.) for the improvement of salinity tolerance. J Bangladesh Agric Uni 16:41-46.

Rasel M, Tahjib-Ul-Arif M, Hossain MA, Hassan L, Farzana S, Brestic M (2020) Screening of Salt-tolerant rice landraces by seedling stage phenotyping and dissecting biochemical determinants of tolerance mechanism. J Plant Growth Regul 39:41-59.

Ravikiran RT, Krishnamurthy SL, Warraich AS, Sharma PC (2018) Diversity and haplotypes of rice genotypes for seedling stage salinity tolerance analyzed through morpho-physiological and SSR markers. Field Crop Res 220:10-18.

Rogers ME, Colmer TD, Nichols PGH, Hughes SJ, Frost K, Cornwall D, Miller SM, Craig AD (2011) Salinity and waterlogging tolerance amongst accessions of messina (*Melilotus siculus*). Crop Pasture Sci 62:225-235.

Sarkar RK, Das S (2003) Yield of rainfed lowland rice with medium water depth under anaerobic direct seeding and transplanting. Tropical Sci 43:192-198.

Shani U, Ben-Gal A (2005) Long-term response of grapevines to salinity: osmotic effects and ion toxicity. Am J Enol Vitic 56:148-154.

Shelley IJ, Takahashi-Nosaka M, Kano-Nakata M, Haque MS, Inukai Y (2016) Rice cultivation in Bangladesh: present scenario, problems, and prospects. J Int Cooper Agric Develop 14:20-29.

Siddiqui MN, Mostofa MG, Akter MM, Srivastava AK, Sayed MA, Hasan MS, Tran LSP (2017) Impact of salt-induced toxicity on growth and yield-potential of local wheat cultivars: oxidative stress and ion toxicity are among the major determinants of salt-tolerant capacity. Chemosphere 187:385-394.

Singh A (2015) Soil salinization and waterlogging: A threat to environment and agricultural sustainability. Ecol Indic 57:128.

Singh A (2017) Waterlogging and salinity management for sustainable irrigated agriculture. I: overview, implication, and plant response. J Irrig Drain Eng 143:04017035.

Singh HP, Singh BB, Ram PC (2001) Submergence tolerance of rainfed lowland rice: search for the physiological marker's traits. J Plant Physiol 158:883-889.

Singh S, Mackill DJ, Ismail AM (2014a) Physiological basis of tolerance to complete submergence in rice involves genetic factors in addition to the *SUB1* gene. AoB Plant 6:plu060.

Singh US, Dar MH, Singh S, Zaidi NW, Bari MA, Mackill DJ, Collard BCY, Singh VN, Singh, JP, Reddy JN, Singh RK, Ismail AM (2013) Field performance, dissemination, impact and tracking of submergence tolerant (Sub1) rice varieties in South Asia. SABRAO J Breed Genet 45:112-131.

Singh A (2014b) Conjunctive water use management through simulation-optimization modeling. Agric Water Manag 141:23-29.

Singh R, Flowers T (2010) The physiology and molecular biology of the effects of salinity on rice. In Mohammad Pessarakli, Eds,. Handbook of Plant and Crop Stress, CRC Press, USA, pp. 899-939

Song J, Shi G, Gao B, Fan H, Wang B (2011) Waterlogging and salinity effects on two *Suaeda salsa* populations. Physiol Plant 141:343-51.

Sorkheh K, Shiran B, Rouhi V, Khodambashi M, Sofo A (2012) Salt stress induction of some key antioxidant enzymes and metabolites in eight Iranian wild almond species. Acta Physiol Plant 34:203-213.

Sun J, Luo H, Fu J, Huang B (2013) Classification of genetic variation for drought tolerance in Tall Fescue using physiological traits and molecular markers. Crop Sci 53:647-54.

Sun L, Zhang J, Lu X, Zhang L, Zhang Y (2011) Evaluation to the antioxidant activity of total flavonoids extract from persimmon (*Diospyros kaki* L.) leaves. Food Chem Toxicol 49:2689-2696.

Talat A, Nawaz K, Hussian K, Bhatti KH, Siddiqi EH, Khalid A, Anwer S, Sharif MU (2013) Foliar application of proline for salt tolerance of two wheat (*Triticum aestivum* L.) cultivars. World Appl Sci J 22:547-554.

Tatar O, Brueck H, Gevrek MN, Asch F (2010) Physiological responses of two Turkish rice (*Oryza sativa* L.) varieties to salinity. Turkish J Agric Forest 34:451-459.

Teakle NL, Real D, Colmer TD (2006) Growth and ion relations in response to combined salinity and waterlogging in the perennial forage legumes *Lotus corniculatus* and *Lotus tenuis*. Plant Soil 289:369-383.

Wijewardana C, Henry WB, Hock MW, Reddy KR (2016) Growth and physiological trait variation among corn hybrids for cold tolerance. Can J Plant Sci 96:639-656.

Winkel A, Colmer TD, Ismail AM, Pedersen O (2013) Internal aeration of paddy field rice (*Oryza sativa*) during complete submergence importance of light and floodwater O_2. New Phytol 197:11931203.

Yadav V, Prasad S, Singh S, Verma OP (2018) Effect of submergence stress on yield and yield components of

various rice (*Oryza sativa* L.) genotypes with its mapping population. J Pharmacogn Phytochem 7:2386-2389.
Yan K, Shao H, Shao C, Chen P, Zhao S, Brestic M, Chen X (2013) Physiological adaptive mechanisms of plants grown in saline soil and implications for sustainable saline agriculture in coastal zone. Acta Physiol Plant 35:2867-2878.
Yan W, Kang MS (2003) GGE biplot analysis: a graphical tool for breeders, geneticists, and agronomists. CRC Press, Boca Raton (FL),
Yeo AR (1999) Predicting the interaction between the effects of salinity and climate change on crop plants. Sci Hortic 78:159-174.
Yin D, Chen S, Chen F, Guan Z, Fang W (2010) Morpho-anatomical and physiological responses of two *Dendranthema* species to waterlogging. Environ Exp Bot 68:122-130.
Zeng F, Shabala L, Zhou M, Zhang G, Shabala S (2013) Barley responses to combined waterlogging and salinity stress: separating effects of oxygen deprivation and elemental toxicity. Front Plant Sci 4:313.
Zeng Y, Zhang H, Li Z, Shen S, Sun J (2007) Evaluation of genetic diversity of rice landraces (*Oryza sativa* L.) in Yunnan, China. Breed Sci 57:91-99.

Acta Biologica Szegediensis

Volume 65(2):163-170, 2021
Acta Biologica Szegediensis
http://abs.bibl.u-szeged.hu/index.php/abs
DOI:10.14232/abs.2021.2.163-170

ARTICLE

Evaluation of the frost tolerance of Hungarian-bred walnut cultivars

Krisztina Szügyi-Bartha[1]*, Géza Bujdosó[1], Veronika Froemel-Hajnal[2], Sándor Szügyi[4], Éva Stefanovits-Bányai[3], László Szalay[2]

[1]Hungarian University of Agriculture and Life Sciences, Institute for Horticultural Sciences, Research Centre for Fruit Growing, Budapest
[2]Hungarian University of Agriculture and Life Sciences, Institute of Horticulture, Department of Pomology
[3]Hungarian University of Agriculture and Life Sciences, Institute of Food Science and Technology, Department of Food and Analytical Chemistry
[4] Private researcher

ABSTRACT At present very few walnut cultivars can be said to be cosmopolitan cultivars, grown widely in the walnut-producing countries of the world. Walnut (*Juglans regia* L.) has poor ecological adaptability, as its cultivation is greatly influenced by low temperatures during the winter dormancy period and in early spring. The breeding activities conducted in various countries are therefore of great significance. Choosing suitable locations for cultivation is of key importance if optimum yield stability is to be achieved. The introduction of foreign walnut cultivars regularly runs into problems if, despite their high yielding ability, they are unable to adapt to the Hungarian climate. In Hungary the most critical weather events for walnuts are the frequent frosts in early spring. Buds therefore need to burst late to avoid damage to the flowers. Many papers have dealt with the frost tolerance of stone fruit, but only limited information has been published on the frost tolerance of walnut. For the first time in Hungary, artificial freezing tests were performed in the present work to determine the frost tolerance of the cultivars available in Hungary. The results could be of service to Hungarian growers in choosing the most suitable cultivar. **Acta Biol Szeged 65(2):163-170 (2021)**

KEY WORDS
artificial freezing test
buds
Juglans regia
LT_{50} values
phenology

ARTICLE INFORMATION
Submitted
10 August 2021
Accepted
15 October 2021
***Corresponding author**
E-mail: kriszta.bartha9@gmail.com

Introduction

If walnut production is to be profitable, however, the growing site requirements must be fully met. As Hungary is situated close to the northern boundary of the walnut production area, walnuts are not cultivated for commercial purposes in more northerly countries. Winter cold and spring frosts are of great significance for cultivation in Hungary. The trees must receive satisfactory nutrition and the shoots must be fully matured if they are to survive frosts; this can be achieved by foliage protection in summer. It is characteristic of the Hungarian climate that several days of mild weather during January or February are frequently followed by sudden sharp temperature declines.

One of the most decisive factors in yield safety is the frequency of spring frosts, to which early blossoming cultivars are especially sensitive. Despite the considerable frost tolerance of walnut trees, early spring frosts may cause damage to young shoots (Hemery et al. 2010; Poirier et al. 2010). During the dormancy period the trees may endure temperatures as low as minus 25 or 28 °C with little damage (Szentiványi 1978), but studies made by Fady et al. (2003) indicated that early spring frosts may injure the apical buds, or in more severe cases, the ends of young shoots. A close correlation was detected between frost tolerance and origin (Guàrdia et al. 2013). Although differences in the frost tolerance of species and cultivars can be attributed to genetically inherited traits, frost tolerance is not a static phenomenon, but exhibits constant changes. Plants can protect themselves against frost in two ways: by avoidance or tolerance (Charrier et al. 2011). Avoidance means that the annual development cycle is synchronized with the critical environmental periods (Parmesan and Yohe 2003; Menzel et al. 2006), so that the overwintering organs are gradually cold hardened after the foliage has fallen. In autumn the dynamics of decreasing temperature and increasing frost tolerance can be observed for both deciduous and evergreen species (Greer et al. 2000; Luoranen et al. 2004). The dynamics of acclimatization is determined primarily by environ-

Table 1. Flowering dates of the female flowers of Hungarian walnut cultivars (Szentiványi 1980).

Flowering date of female flowers	Early	Mid-Early	Mid-Late	Late
Cultivar	None	Milotai 10	Alsószentiváni 117	Milotai kései
			Tiszacsécsi 83	Alsószentiváni kései
			Milotai bőtermő	
			Milotai intenzív	

mental factors between September and January, while from January onwards significant genotype effects have been observed in the time of budburst in connection with both tolerance and avoidance mechanisms (Charrier et al. 2001). Frost damage is one of the factors causing the greatest losses in walnut production (Xin and Browse 2000; Sanghera et al. 2011). The frost tolerance of the cultivars exhibited a close correlation with their flowering traits. The flowering time of the female flowers of Hungarian-bred cultivars is shown in Table 1.

The leafless period is often thought to be inactive, but in fact the trees need to actively modify their metabolism through cold acclimatization processes if they are to cope with winter frost effects (Charrier et al. 2018). The level of frost damage differs for different plant organs (Mahmodzahed and Imani 2011), the flowers being the most sensitive (Charrier et al. 2013).

Laboratory tests are required for the precise measurement of the frost tolerance of individual plant organs. The analysis of tissues after artificial freezing reveals the extent of damage caused by a given temperature. The LT_{50} index, or frost tolerance mean value, can then be calculated (Szalay 2001; Szalay et al. 2010, 2016, 2017). Frost tolerance must be tested on several occasions during the dormancy period in order to obtain a clear picture of the frost tolerance of each cultivar. Frost tolerance is an extremely complex phenomenon from both the physiological and genetic points of view, being the result of several independent processes. It is advisable to use a climate chamber to test winter hardiness. As the frost tolerance of the buds changes in the course of the winter, the temperature in the chamber must reflect that experienced in nature. Several temperatures should be applied at each testing date, at least three, if possible. The rate of chilling and the duration of the treatment are also important. The rate of temperature change should be 1-2 °C an hour, and experience has shown that the buds should be kept at the critical temperature for 3.5 - 4.0 hours (Szalay et al. 2016, 2017).

Materials and Methods

The experiments were performed between October and March in 2013–2014, 2014–2015 and 2015–2016. Ten to twelve one-year-old shoots measuring 50 cm in length were collected once a month from each cultivar in a large-scale non-irrigated plantation in its 20th year in Lengyeltóti, where the annual number of sunshine hours averaged 2098 hours, the annual mean temperature was 11.2 °C and the annual mean precipitation sum 550 mm. The soil was a chernozem (upper limit of plasticity, K_A = 38, pH 8, total lime content in the upper 60 cm soil layer 5%, humus content 1.9%). The height above sea level was 150–160 m, and the summer was long enough for the shoots to reach full maturity (Bujdosó et al. 2019).

The cultivars examined were the Hungarian-bred 'Alsószentiváni 117', 'Milotai 10' and 'Tiszacsécsi 83', all of which only produce nuts from terminal buds, and hybrids of the first two cultivars with 'Pedro': 'Milotai bőtermő' (high-yielding), 'Milotai kései' (late), 'Milotai intenzív' (intensive) and 'Alsószentiváni kései' (late). The Californian-bred 'Pedro' cultivar was used as the control. All the cultivars were grafted onto walnut sapling rootstocks.

The laboratory analyses were carried out in the Department of Pomology at Corvinus University of Budapest (now Fruit Production Department, Institute of Horticultural Sciences, Hungarian University of Agriculture and Life Sciences). The artificial freezing tests were carried out in Rumed 3301 climate chambers (Rubarth Apparate, Laatzen, Germany). At each testing date, three freezing temperatures were applied, chosen to represent the external temperatures. While the lowest temperature tested in October was -16 °C, in January a test temperature of -26 °C was applied to buds that had undergone hardening. The rate of cooling and warming was 2 °C an hour, and the shoots were maintained at the freezing temperature for 4 hours.

After the end of the treatment, the samples were kept at room temperature for 12 hours, after which the buds were cut open and the degree of frost damage was determined based on the discoloration of the tissues. Green tissues were regarded as healthy and brown tissues as frost damaged. The aim of the investigations was to determine the LT_{50} values, i.e. the temperature that caused 50% freezing damage to mixed buds of the given cultivar at the given time. The frost damage values recorded for the three

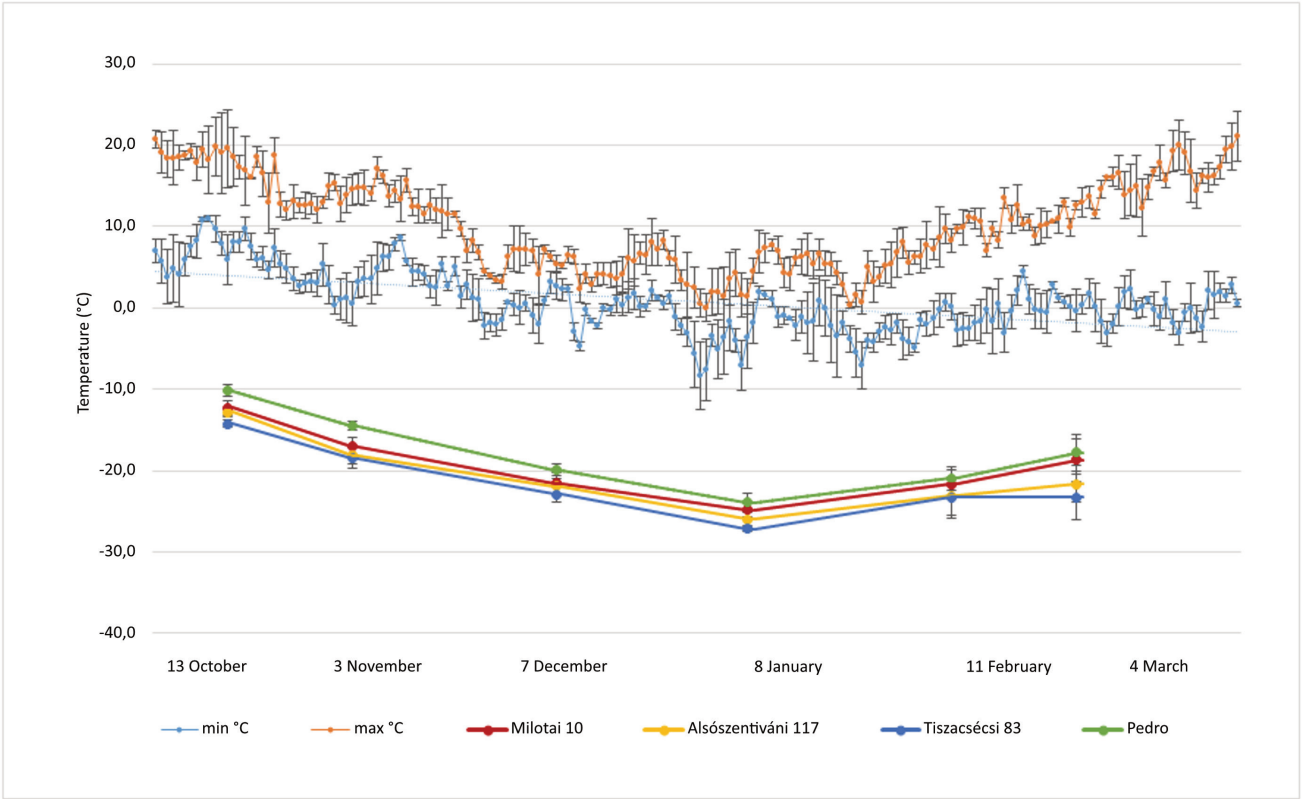

Figure 1. Frost tolerance mean values (mean and standard deviation) of the mixed buds of standard cultivars and the cultivar 'Pedro', and three-year means and standard deviations of daily maximum and minimum temperatures (upper part of the figure).

different freezing temperatures gave the frost tolerance profile of the given cultivar at the individual sampling dates, which could be approximated by a sigmoid graph where the section between 20 and 80% could be regarded as linear (Gu 1999). The LT_{50} values were then determined by linear regression from the results of artificial freezing. The IBM PASW Statistic 18 statistical program package was used for the statistical evaluation. The data were analyzed using the ANOVA model, while means were compared and significant differences determined with the help of Duncan's test at the 95% probability level. The SPSS 25.0 (Chicago, USA) program package was used for the statistical evaluation of the data.

Results

The results are illustrated in Figs. 1-3. As no significant differences were detected between the years, the results of the three years were averaged, and the mean values and standard deviation were used to determine the frost tolerance dynamics of the flower buds and differences between the cultivars. Fig. 4 demonstrates the homogeneous groups determined by means of analysis of variance, from which the frost sensitivity order was deduced. The frost tolerance of the generative organs of the walnut cultivars was characterized using the LT_{50} values obtained from the artificial freezing tests. The frost tolerance of the flower buds gradually developed in the first half of the winter. The hardening process had begun well before the first sampling date, as LT_{50} values of below -10 °C were generally recorded in mid-October. The initial stage of hardening occurs when the external temperature is still well above freezing point. By the time long-term frosts were experienced, the LT_{50} values of the flower buds approached -20 °C for some cultivars. The hardening process continued until January: the LT_{50} values were the lowest at the January sampling date in all the years. This was followed by the dehardening process, when the frost tolerance of the flower buds gradually declined, parallel with the gradual rise in the external temperature.

The frost tolerance of the three standard cultivars and 'Pedro' in the three years is illustrated in Fig. 1. Averaged over the three years, 'Pedro' was the most frost-sensitive and 'Tiszacsécsi 83' the most tolerant, the LT_{50} value of the latter being 4 °C lower on average in October than that of

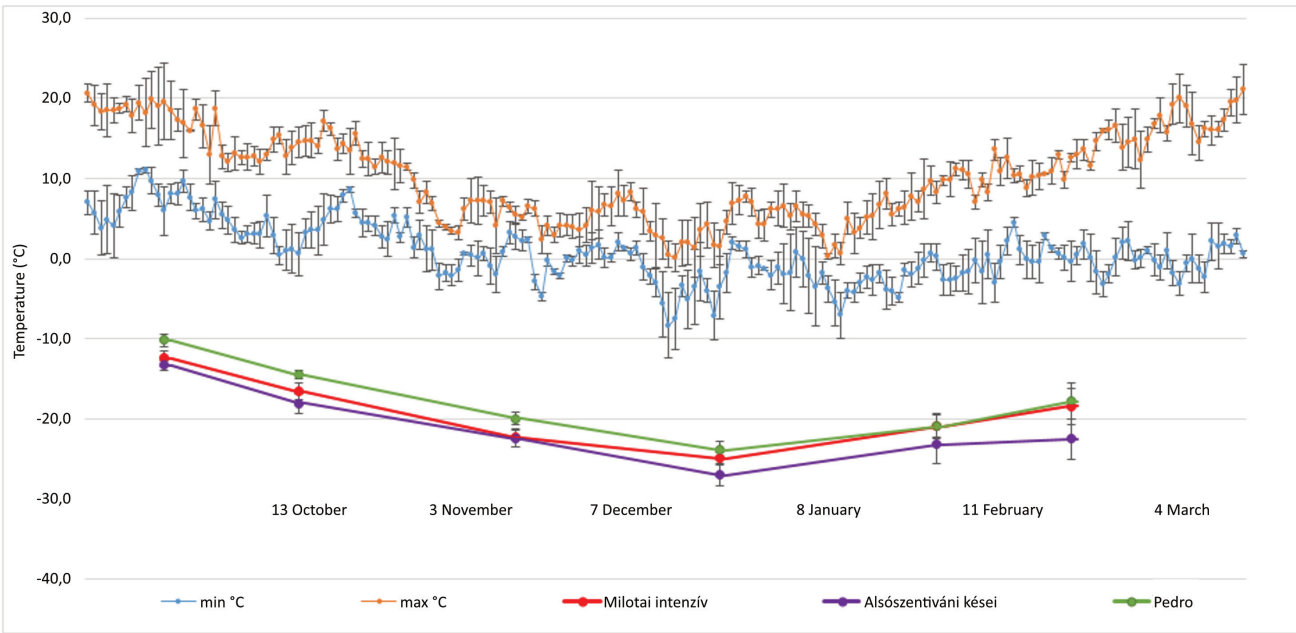

Figure 2. Frost tolerance mean values (mean and standard deviation) of the mixed buds of 'Alsószentiváni kései', 'Milotai intenzív' and 'Pedro', and three-year means and standard deviations of daily maximum and minimum temperatures (upper part of the figure).

'Pedro'. The average difference between the two cultivars was 3 °C in January and 5 °C in March. The maximum level of frost tolerance was recorded in January for all the cultivars, after which it gradually declined, with a continuous rise in the LT_{50} values. The frost tolerance of 'Milotai 10' was closer to that of 'Pedro', while that of 'Alsószentiváni 117' was almost the same as that of 'Tiszacsécsi 83'.

Fig. 2 gives a comparison of the frost tolerance of 'Milotai intenzív', 'Alsószentiváni kései' and 'Pedro', the first two of which are hybrids originating from a cross with 'Pedro' as pollinator. The results showed that the frost tolerance of 'Milotai intenzív' tended to be like that of 'Pedro', with lower values than that of the female parent 'Milotai 10'. Considerable differences were exhibited in the case of 'Alsószentiváni kései', particularly in January, February and March. In January the mixed buds of this genotype survived freezing at a temperature 2-3 °C lower than those of the other two genotypes on average, while in February and March the difference increased to 4-5 °C. The slower rise in LT_{50} values can be explained by the later budburst of this genotype.

Based on knowledge of the female flowering dates of the genotypes, a comparison was made of those in the medium late flowering group. Most of the genotypes included in the study belonged to this group, namely 'Milotai bőtermő', 'Milotai intenzív', Alsószentiváni 117', 'Tiszacsécsi 83' and 'Pedro' (Fig. 3). Genotypes in the same flowering groups could be expected to have similar levels of frost tolerance, which should be most evident at the March sampling date, shortly before budburst. Nevertheless, the results for individual genotypes could be clearly distinguished from each other, indicating that genetic traits other than the budburst date were also responsible for their winter hardiness. Even in January, the coldest month, 'Pedro' had the highest LT_{50} values, and the frost tolerance of 'Milotai intenzív' was closest to that of this cultivar, while 'Milotai bőtermő' was able to survive lower temperatures during the dormancy period than either of these genotypes. On the other hand, 'Alsószentiváni 117' and 'Tiszacsécsi 83' were both more frost-tolerant than the hybrids.

The flower buds of the genotypes were the most frost tolerant in January in all three dormancy periods. As the LT_{50} values of the individual genotypes did not differ significantly over the years, it was concluded that they had reached the maximum frost tolerance of which they were genetically capable, though tests need to be performed in further years to give convincing proof of this conclusion. The differences between the genotypes as regards the winter frost tolerance of the flower buds was analyzed for the January data. It can be seen in Fig. 4 that three homogeneous groups could be distinguished: 'Pedro' was frost-sensitive, 'Milotai kései', 'Milotai 10', 'Milotai bőtermő' and 'Mikotai intenzív' had medium frost tolerance, and 'Alsószentiváni 117', 'Alsószentiváni kései' and 'Tiszacsécsi 83' were frost-tolerant.

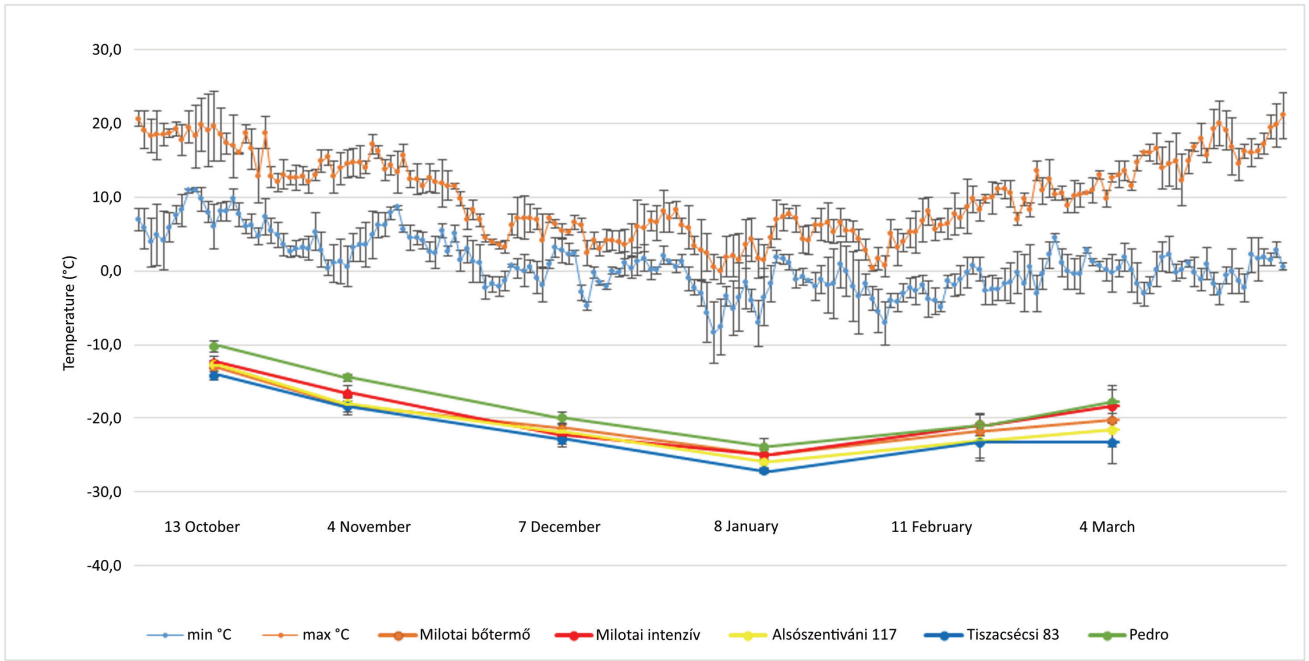

Figure 3. Frost tolerance mean values (mean and standard deviation) of the mixed buds of cultivars in the same flowering date groups, and three-year means and standard deviations of daily maximum and minimum temperatures (upper part of the figure).

Discussion

Frost damage in winter and spring often cause substantial yield losses in fruit and nut production. Among the overwintering organs of deciduous trees in the temperate zone, the generative organs (flower buds and mixed buds) are the most frost-sensitive during the dormancy period and suffer damage most frequently. The main emphasis has therefore always been placed on these organs in studies on the frost tolerance of different genotypes (Proebsting and Mills 1978; Faust 1989; Tromp 2005; Bartolini et al. 2006; Szalay et al. 2010; Salazar-Gutiérrez 2014). Under the same thermal conditions (including a constant mild temperature) walnut (*Juglans regia* L.) trees may exhibit diverse levels of frost tolerance (Charrier et al. 2013). In addition to genetic traits, frost tolerance is also influenced to a considerable extent by environmental factors, so the frost tolerance of individual genotypes may change as a function of the growing site and year (Pénzes and Szalay 2003; Szentiványi and Kállayné 2006). The general condition of the trees is a further influencing factor (Poirier et al. 2010). The most precise method for determining the frost tolerance of overwintering organs is the artificial freezing test (Pedryc 1999; Miranda et al. 2005; Szalay et al. 2010). In most cases LT_{50} values are used to determine frost tolerance (Lindén and Palonen 2000; Szalay et al. 2010; Ferguson et al. 2011; Salazar-Gutiérrez et al. 2014).

Walnut is not one of the most frost-sensitive fruit species in the temperate zone, as the overwintering organs are able to survive temperatures as low as -28-29 °C in December and January (Westwood 1993; Szentiványi and Kállayné 2006; Kállayné 2014). By comparison, the critical temperature is -25 °C for sweet cherry and -20 °C for peach during the winter dormancy period (Szewczuk et al. 2007). In Central Europe, including the Carpathian

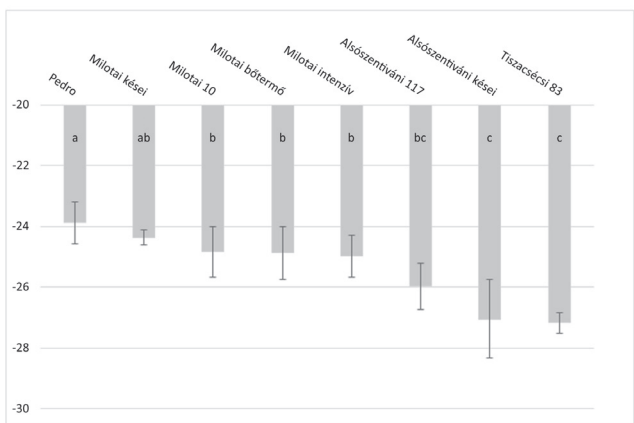

Figure 4. LT_{50} values of the flower buds of the tested cultivars averaged over three years, based on the data of freezing experiments in January. Different letters represent significant differences between cultivars at the LT_{50} value.

Basin, temperatures cold enough to damage walnut trees are rarely encountered in winter. In spring, however, after the buds burst, the young shoots and flower organs often sustain damage in these regions due to repeated spells of intense cold. For this reason, it is important for breeders to select cultivars with late budburst (Szentiványi and Kállayné 2006; Kállayné 2014). In order to achieve long-term yield safety, however, it is important to obtain knowledge on the frost tolerance of cultivated walnut genotypes during the winter dormancy period. For this reason, detailed investigations were begun on the winter frost tolerance of the cultivars selected or bred in Hungary that are grown most frequently in this country. The Californian-bred cultivar 'Pedro' was used as the control. A further incentive for this research was the fact that no detailed data are to be found either in the Hungarian or international literature on how the frost tolerance of the overwintering generative organs of walnut cultivars changes during the winter.

The LT_{50} values of the cultivars were determined on all the sampling dates during the dormancy period in all three years. Very similar results were obtained each year, so no significant year effect could be detected. The greatest frost tolerance was recorded for the cultivar 'Tiszacsécsi 83' during the years tested, while the most sensitive cultivar was the control genotype, 'Pedro'. The frost tolerance data for 'Alsószentiváni kései' were similar to those of 'Tiszacsécsi 83', while those of 'Milotai 10' were almost the same as those of 'Pedro'. Differences were observed between the hybrids, 'Milotai intenzív' being frost-sensitive, 'Milotai bőtermő' and 'Milotai kései' moderately frost-tolerant and 'Alsószentiváni 117' frost-tolerant. The flower buds were the most frost-tolerant in January. The values recorded in January were probably equivalent to the genetically programmed optimum frost tolerance levels, but this needs to be confirmed in further research. Charrier et al. (2011) observed a genotype effect between January and budburst, and during this period this played a greater role than the environmental effect.

The weather in the experimental years was characterized by slightly lower minimum temperatures in the first week of October, after which the temperature was like the long-term mean. The next substantial cold spell occurred in mid-December, which was followed by the second stage of hardening in the case of mixed buds. There was a further sudden intensive drop in temperature in mid-January, but by this time the mixed buds of walnut have reached maximum hardening, so frost tolerance means of -23.8 °C were measured on average even for the most frost-sensitive genotype. The gradual warming from January onwards was interrupted by very cold temperatures at dawn on one or two occasions, but as warming did not proceed at a rapid rate, these cold snaps were not a problem and the mixed buds retained their frost tolerance. By March the continuous rise in temperature led to higher LT_{50} values, but as the winter weather was similar at the experimental location in all three years, no significant year effect was detected. If the experiments were continued over a longer period, differences would probably be observed, as the effect of climatic factors on the frost tolerance of overwintering organs has been reported for a number of temperate fruit species (Faust 1989; Tromp 2005; Szalay et al. 2010). However, no relevant data on walnut are to be found in the literature.

It is difficult to compare the present results with earlier data, as those available were obtained at different locations for different cultivars. Based on the results obtained with various methods, however, it can be concluded that the frost tolerance of the overwintering organs constantly changes and that both genotypic and environmental factors play a role in hardening and dehardening processes, resulting in considerable differences between the cultivars (Aslamarz et al. 2010a; Aslamarz et al. 2010b; Charrier et al. 2013; Guàrdia et al. 2013; Charrier et al. 2018). The data recorded by Aslamarz et al. (2010a) in plantations in the neighborhood of Teheran showed 'Pedro' to be the most frost-tolerant of the cultivars, indicating that, under diverse climatic conditions, the same cultivar may give quite different results. This was confirmed in the present work, which was designed to provide information on the winter frost tolerance of walnut cultivars of importance for production in Hungary. Knowledge on the winter frost tolerance of cultivars is important for the determination of their suitability for cultivation at various growing sites, and is likely to become increasingly necessary in the light of climate change predictions, as alterations in climatic conditions will influence the developmental processes of cultivated plants and their levels of tolerance (Parmesan and Yohe 2003; Menzel et al. 2006).

References

Aslamarz AA, Vahdati K, Rahemi M (2010a) Supercooling and cold-hardiness of acclimated and deacclimated buds and stems of Persian walnut cultivars and selections. Hortic Sci 45(11):1662-1667.

Aslamarz AA, Vahdati K, Rahemi M (2010b) Cold-hardiness evaluation of Persian walnut by thermal analysis and freezing technique. VI International Walnut Symposium. Acta Hortic 861:269-272.

Bartolini S, Zanol G, Viti R (2006) The cold hardiness of flower buds in two apricot cultivars. Acta Hortic 701:141-146.

Bujdosó G, Gandev S, Izsépi F, Szügyi- Bartha K, Végvári Gy (2019) Detection and quantification of some phenolic

compounds in kernel of selected Hungarian and Bulgarian Persian walnut cultivars. Eur J Hortic Sci 84(2):85-90.
Charrier G, Bonhomme M, Lacointe A, Améglio T (2011) Are budburst dates, dormancy and cold acclimation in walnut trees (*Juglans regia* L.) under mainly genotypic or environmental control? Int J Biometeorol 55(6):763-774.
Charrier G, Poirier M, Bonhomme M, Lacointe A, Améglio T (2013) Frost hardiness in walnut trees (*Juglans regia* L.): How to link physiology and modelling? Tree Physiol 33(11):1229-1241.
Charrier G, Lacointe A, Améglio T (2018) Dynamic modeling of carbon metabolism during the dormant period accurately predicts the changes in frost hardiness in walnut trees *Juglans regia* L. Front Plant Sci 9:1746.
Fady B, Duccy F, Aleta N, Becquey J, Diaz Vazquez R, Fernandez Lopez F, Jay-Allemand C, Lefèvre F, Ninot A, Panetsos K, Paris P, Pisanelli A, Rumpf H (2003) Walnut demonstrates strong genetic variability for adaptive and wood quality traits in a network of juvenile field tests across Europe. New Forest 25:211-225.
Faust M (1989) Physiology of Temperate Zone Fruit Trees. John Wiley and Sons, New York. 338.
Ferguson JC, Tarara JM, Mills LJ, Grove GG, Keller M (2011) Dynamic thermal time model of cold hardiness for dormant grapevine buds. Ann Bot 107(3):389-396.
Greer DH, Robinson LA, Hall AJ, Klages K, Donnison H (2000) Frost hardening of *Pinus radiata* seedlings. Effect of temperature on relative growth rate, carbon balance and carbohydrate concentration. Tree Physiol 20:107-114.
Gu S (1999) Lethal temperature coefficient- a new parameter for interpretation of cold hardiness. J Hortic Sci Biotechnol 74(1):53-59.
Guàrdia M, Savé R, Díaz R, Vilanova A, Aletà N (2013) Genotype and environment: two factors related to autumn cold hardiness on Persian walnut (*Juglans regia L.*). Ann Forest Sci 70:791-800.
Hemery GE, Clark JR, Aldinger E, Claessens H, Malvolti ME, O'Connor E, Raftoyannis Y, Savill PS, Brus R (2010) Growing scattered broadleaved tree species in Europe in a changing climate: a review of risks and opportunities. Forestry 83:65-81.
Kállayné T (2014) Gyümölcsösök termőhelye. Mezőgazda Kiadó, Budapest. 248 [in Hungarian].
Lindén L, Palonen P (2000) Relating freeze-induced electrolyte leakage measurements to lethal temperature in red raspberry. J Amer Soc Hort Sci 125(4):429-435.
Luoranen J, Repo T, Lappi J (2004) Assessment of the frost hardiness of shoots of silver birch (*Betula pendula*) seedlings with and without controlled exposure to freezing. Can J Forest Res 34:1108-1118.
Mahmodzadeh O, Imani A (2011) Effect of some of anti-frost on morphology, anatomy and proline of selective almond cultivars flower buds. IJNRS 2:35-40.
Menzel A, Sparks TH, Estrella N, Koch E, Aasa A, Ahas R, Alm-Kübler K, Bissolli P, Braslavská O, Briede A, Chmielewski FM, Crepinsek Z, Curnel Y, Dahl Å, Defila C, Donnelly A, Filella Y, Jatczak K, Måge F, Mestre A, Nordli Ø, Peñuelas J, Pirinen P, Remišová V, Scheifinger H, Striz M, Susnik A, VanVliet AJH, Wielgolaski F-E, Zach S, Zust A (2006) European phenological response to climate change matches the warming pattern. Global Change Biol 12:1969-1976.
Miranda C, Santesteban LG, Royo JB (2005) Variability in the relationship between frost temperature and injury level for some cultivated prunus species. Hortic Sci 40(2):357-361.
Parmesan C, Yohe G (2003) A globally coherent fingerprint of climate change impacts across natural systems. Nature 421:37-42.
Pedryc A, Korbuly J, Szabó Z (1999) Artificial frost treatment methods of stone fruits. Acta Hortic 488:377-380.
Poirier M, Lacointe A, Améglio T (2010) A semi-physiological model of cold hardening and dehardening in walnut stem. Tree Physiol 30(12):1555-1569.
Probesting EL Jr, Mills HH (1978) A synoptic analysis of peach and cherry flower bud hardiness. J Am Soc Hortic Sci 103(6):842-845.
Salazar-Gutiérrez MR, Chaves B, Anothai J, Whiting M, Hoogenboom G (2014) Variation in cold hardiness of sweet cherry flower buds through different phenological stages. Sci Hortic-Amsterdam 172:161-167.
Sanghera GS, Wani SH, Hussain W, Singh NB (2011) Engineering cold stress tolerance in crop plants. Curr Genom 12(1):30-43.
Surányi D, Molnár L (2011) A fajták téli és tavaszi fagytűrése. In Surányi D, Ed., A sárgabarack. Szent István Egyetemi Kiadó, Gödöllő. 303. [in Hungarian].
Szalay L (2001) Kajszi- és őszibarackfajták fagy- és téltűrése. PhD Thesis. Szent István Egyetem, Budapest. [in Hungarian].
Szalay L (2003) A kajszi ökológiai igényei. In Pénzes B, Szalay L, Eds., Kajszi. Mezőgazda Kiadó, Budapest. 43-50. [in Hungarian].
Szalay L, Timon B, Németh Sz, Papp J, Tóth M (2010) Hardening and dehardening of peach flower buds. Hortic Sci 45(5):761-765.
Szalay L, Ladányi M, Hajnal V, Pedryc A, Tóth M (2016) Changing of the flower bud frost hardiness in three Hungarian apricot cultivars. Hortic Sci (Prague) 43(3):134-141.
Szalay L, Molnár Á, Kovács Sz (2017) Frost hardiness of flower buds of three plum (*Prunus domestica* L.) cultivars. Sci Hortic-Amsterdam 214:228-232.
Szentiványi P (1978) A gesztenye- és diótermesztés délnyugat Dunántúlon, a fiatal gesztenye- és dióültetvények agrotechnikája. In Vig P, Ed., Újabb kutatási eredmények

a gyümölcstermesztésben. Gyümölcs- és Dísznövénytermesztési Kutató Intézet, Budapest. [in Hungarian].
Szentiványi P (1980) Dió. In Nyéki J, Ed., Gyümölcsfajták virágzásbiológiája és termékenyülése. Mezőgazdasági Kiadó, Budapest. 281-290. [in Hungarian].
Szentiványi P, Kállayné T (2006) Dió. Mezőgazda Kiadó, Budapest, 204. [in Hungarian].
Szewczuk A, Gudarowska E, Dereń D (2007) The estimation of frost damage of some peach and sweet cherry cultivars after winter 2005/2006. J Fruit Ornam Plant Res 15:55-63.
Tromp J (2005) Frost and plant hardiness. In Tromp J, Webster AD and Wertheim SJ, Eds., Fundamentals of Temperate Zone Tree Fruit Production. Backhuys Publishers, Leiden, The Netherlands. 74-83.
Westwood MN (1993) Dormancy and plant hardiness. In Temperate-Zone Pomology: Physiology and Culture. 3rd Ed, Timber Press, Portland, Oregon. 382-419.
Xin Z, Browse J (2000) Cold comfort farm: the acclimation of plants to freezing temperatures. Plant Cell Environ (23):893-902.

Acta Biologica Szegediensis

Volume 65(2):171-184, 2021
Acta Biologica Szegediensis
http://abs.bibl.u-szeged.hu/index.php/abs

DOI:10.14232/abs.2021.2.171-184

ARTICLE

Biomass production, water use efficiency and nutritional value parameters of sorghum (*Sorghum bicolor* L.) genotypes as affected by seed hydro-priming and transplanting

Isaac Mirahki[1], Mohammad Reza Ardakani[1]*, Farid Golzardi[2]*, Farzad Paknejad[1], Ali Mahrokh[2]

[1]Department of Agronomy, Karaj Branch, Islamic Azad University, Karaj, Iran
[2]Seed and Plant Improvement Institute, Agricultural Research, Education and Extension Organization (AREEO), Karaj, Iran

ABSTRACT To investigate hydropriming and transplanting effect on biomass and nutritional content of forage sorghum, a two-year field experiment was conducted in the semiarid condition of Iran. Experimental factor consisted of planting dates (July-1st, July-11th, July-23rd, August-1st) in the main plot and the factorial combination of planting methods (direct planting, hydropriming, transplanting) with cultivars (*Speedfeed* and *Pegah*) in the subplot. Planting date postponement from 1st of July to 10th of July, 23rd of July, and 1st of August, respectively, caused 16.1, 32.5 and 47.2% reduction in dry matter yield (DMY) and 7.4, 20.2, and 35.1% reduction in water use efficiency of DMY production (WUE_{DMY}). Hydropriming and transplanting produced 23.6 and 22.4% more DMY, 24.5 and 21.8% more WUE_{DMY}, 24 and 16.3% more crude protein yield, 22.7 and 20.9% more digestible dry matter (DDM) yield, and 22.2 and 20.1% more metabolic energy (ME) yield, compared to the direct planting. Hydropriming compared to direct planting caused 29% increase in plant growth rate and utilized growing season more productively than transplanting for DMY production. Conclusively, hydropriming and transplanting compensated for delay in planting through enhancing and accelerating germination and plant development but, applying hydropriming on *Speedfeed* and planting in July-1st caused the highest DMY, WUE_{DMY} and the yield of nutritive parameters.

Acta Biol Szeged 65(2):171-184 (2021)

KEY WORDS
digestible organic matter
protein, metabolic energy
seed hydropriming
Sorghum bicolor L.

ARTICLE INFORMATION
Submitted
30 May 2021
Accepted
19 August 2021
***Corresponding author**
E-mail: mreza.ardakani@gmail.com
faridgolzardi@gmail.com

Introduction

Extreme heat (Biswas 2020), limited water and soil resources (Elamin et al. 2019), continuous global population growth (Amouzou et al. 2019), and climate change and its subsequences (Michelon et al. 2020) organizes a set of threatening factors toward agricultural sustainability and food production in arid and semiarid regions (Biswas 2020). On this approach, the second cropping strategy could substantially supply the growing food demands and protect the food safety (Velten et al. 2015; Martin et al. 2017). Thus, the selected forage species must produce an adequate quantitative and qualitative yield in a short period, be adaptable to withstand high temperature and drought conditions (Martin et al. 2017) and allelopathic residue (Costa et al. 2020). Studies in arid and semiarid regions introduced sorghum as a promising option to provide the required forage (Michelon et al. 2020) during different growing seasons and water availabilities.

Abbreviations

$D1_{PD}$: Planting date 1st of July; $D2_{PD}$: Planting date 10th of July; $D3_{PD}$: Planting date 23rd of July; $D4_{PD}$: Planting date 1st of August; D_{PM}: Direct seed planting method; H_{PM}: Hydroprimed seed planting method; T_{PM}: Transplant planting method; S_{CV}: *Speedfeed* cultivar; P_{CV}: *Pegah* cultivar; DMY: Dry matter yield; NDF: Neutral detergent fiber; ADF: Acid detergent fiber; CP: Crude protein; CPY: Crude protein yield; Hem: Hemicelluloses; DDM: Digestible dry matter; DDMY: Digestible dry matter yield; RFV: Relative feed value; WSC: Water soluble carbohydrates; ME: Metabolic energy; MEY: Metabolic energy yield; DOM: Digestible organic matter.

Sorghum is an annual, low-cost crop with a large size canopy that specialized to grow during warm seasons in the warm regions; it can produce the same biomass as corn by consuming less water (Bhattaraia 2020) in areas with a short growing season (Naoura et al. 2019). Late, uneven, and slow germination in the early stages of growth is the main issue in sorghum cultivation (Bajwa et al. 2018). After harvesting winter crops, it takes time to prepare the soil and seedbed for second cultivation (Junnyor et al. 2015). Delay in planting affects the synchronicity of plant growth stages with environmental conditions, which shortens the growing season, overshadows the vegetative and reproductive phases, and ultimately reduces forage yield (Junnyor et al. 2015; Zandonadi et al. 2017). Seed-hydropriming is a physiological method and because of its considerable effect on seed germination, crop establishment, and growth rate, could get widely used to increase the growing season productivity (Zida et al. 2018; Bajwa et al. 2018; Jatana et al. 2020; Kukal and Irmak 2020). In hydropriming, before sowing, the controlled seed-soaking in water starts primitive germination phases without bud sprouting (Forti et al. 2020). This method reduces the average germination duration (Chen et al. 2021); increases the germination percentage (Zida et al. 2018), seedling establishment and growth (Bajwa et al. 2018), fastens the flowering and maturity and ultimately increases the yield (Zida et al. 2018) in a wide range of environmental conditions (Jatana et al. 2020). Transplanting, as another method that increases the grain and forage yield of sorghum, has been reported from India, Japan, Mali, Cameroon, Chad, Nigeria, and Senegal (Jo et al. 2016; Biswas 2020). Transplanting compared to the conventional planting method significantly increased the established seedling rate (Rattin et al. 2015); caused the proper plant population per hectare (Biswas 2020); maximized the absorbed light and optimum leaf area index and the light use efficiency (Jo et al. 2016; Biswas 2020); improved the productivity of growing season (Jo et al. 2016), seed, and pesticides (Rattin et al. 2015); decreased the days till flowering, weed population and damage (Mapfumo et al. 2013), disease and pest population; increased the grain and biomass yield per capita (Biswas 2020). Therefore, cultivating the forage sorghum by employing planting methods that accelerates the germination and improves the plant establishment for compensating the reprieved planting while increasing the water use efficiency seems unavoidable to attain, maintain, and develop agricultural sustainability. The main objectives of this study are to (i) evaluate the singular and multiple effects of experimental factors on biomass yield, quality, and yield of nutritional components of forage sorghum; (ii) assessing the regression model variation of DMY production based on the obtained GDD under the effect of each experimental factors; (iii) study the correlation coefficient among quantitative and qualitative traits as well as the results of regression analysis with dry matter yield; (iv) specifying an approved PD, PM and, CV for different scenario based on the accessible facilities, growth season and required forage quantity and quality.

Materials and methods

Experimental site

A two-year field experiment was conducted at the Seed and Plant Improvement Institute, Agricultural Research, Education and Extension Organization (AREEO), Karaj, Iran (35°48'N, 50°57'W, altitude 1312.5 m) during the 2017 (Y1) and 2018 (Y2) growing seasons. The area categorized as a semiarid climate with an average annual precipitation of 251 mm, an annual average temperature of 13.5 °C, an annual average soil temperature of 14.5 °C, and a total annual class "A" pan evaporation of 2184 mm. The meteorological data obtained from the Synoptic Meteorology Station, located beside the experimental farm, are shown in Fig. 1. The experiments were carried out on clay-loam soil in which the average field capacity of the root zone was 23%. Before planting, soil samples were taken from the top 30 cm of soil to test its background nutritional level. Some of the physicochemical properties of the soil of the experimental site are presented in Table 1.

Experimental design and cultural practices

The experiment was arranged as a three-replicated split plot-factorial design with four levels of planting dates (PD) as the main factor consisted of $D1_{PD}$ (planting date 1st of July), $D2_{PD}$ (planting date 10th of July), $D3_{PD}$ (planting date 23rd of July), $D4_{PD}$ (planting date 1st of August) and three planting methods (PM) including the D_{PM} (direct planting), H_{PM} (hydroprimed seeds) and T_{PM} (transplant-

Table 1. Physicochemical properties of the top soil (0 - 30 cm) at the experimental site.

Year	N (%)	$CaCO_3$ (%)	P (mg kg^{-1})	K (mg kg^{-1})	Zn (mg kg^{-1})	Cu (mg kg^{-1})	Mn (mg kg^{-1})	Fe (mg kg^{-1})	OM (%)	EC (ds/m)	pH	FC	CEW (%)	AW (%)	Clay (%)	Silt (%)	Sand (%)	Soil texture
2017	0.06	10	12.6	256	0.32	1.47	12.7	5.02	0.58	2.22	7.24	34	11	23	27	49	24	Clay loam
2018	0.05	9	12.1	248	0.29	1.44	18.6	4.89	0.56	2.2	7.24	32	10	21	28	46	26	Clay loam

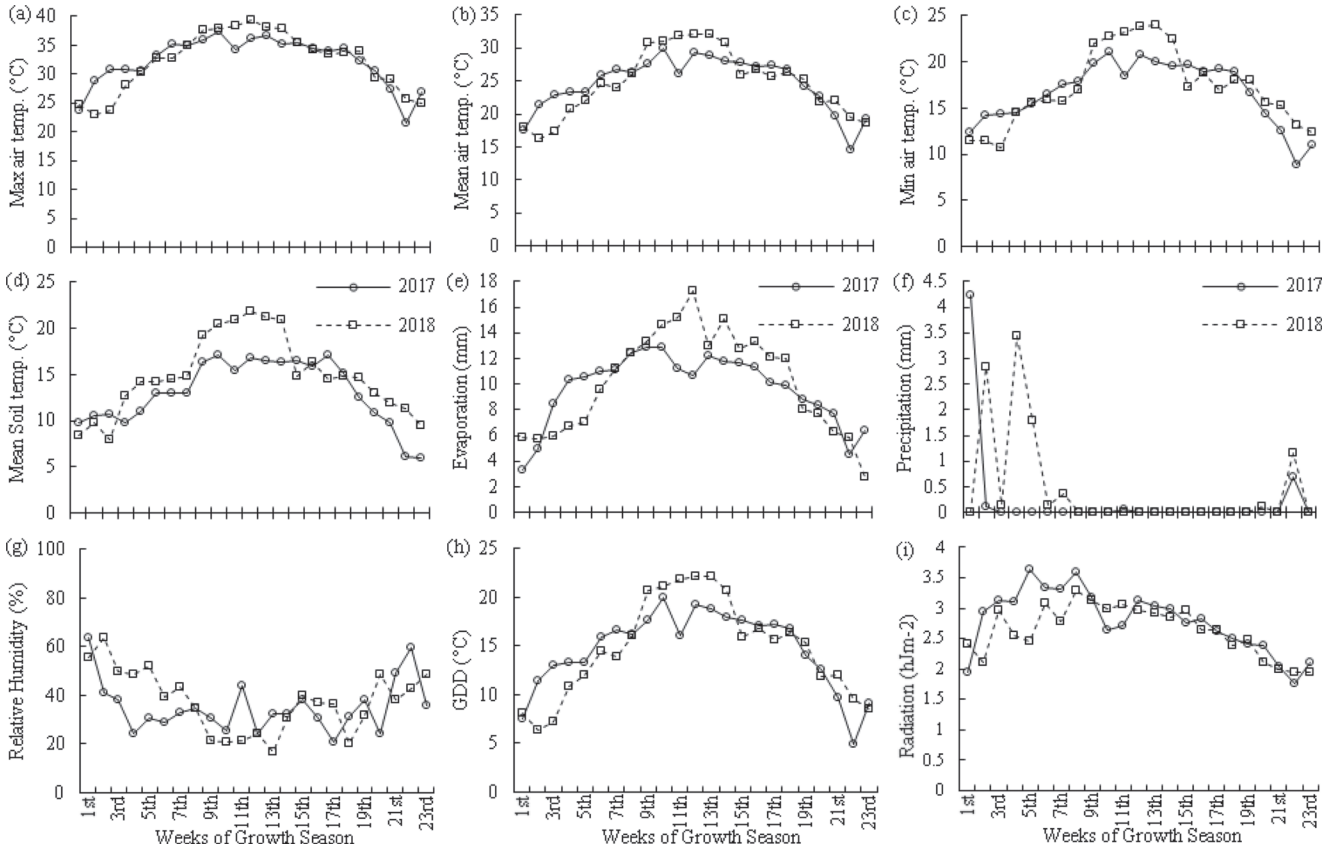

Figure 1. Weekly ombrothermic diagram of growth season for second cultivation during 2017 and 2018 from Karaj (agriculture) synoptic station, Iran. (a) Weekly average of maximum air temperature (°C). (b) Weekly average of air's mean temperature (°C). (c) Weekly average of minimum air temperature (°C). (d) Weekly average of soil's mean temperature (°C). (e) Weekly average of evaporation (mm). (f) Weekly average of precipitation (mm). (g) Weekly average of relative humidity (%). (h) Weekly average of growth degree day for sorghum growth (°C). (i) Weekly average of radiation (hJm^{-2})

ing) were factorially combined with two cultivars (CV) including S_{CV} (*Speedfeed*) and P_{CV} (*Pegah*) as subplots (collectively 24 treatments). S_{CV} is an Australian-originated and improved, multi-cut hybrid forage sorghum with high-yield potential that typically each 60 to 70 days produces one cut. Currently, S_{CV} is the most known forage sorghum cultivar in Iran that has been cultivated for fresh, dry, and direct grazing purposes. P_{CV} (LFS56×Early Orange) is a mid-late open-pollinated (OP) forage sorghum cultivar that each 75 to 90 days produces one cut forage sorghum with fresh, dry, and silage purposes (Golzardi et al. 2019). The seedbed preparation operation in 2017 (Y1) and 2018 (Y2) was included moldboard plow, cultivator, harrow, leveler, furrower, and dividing into three blocks. Each block contained four main plots, and each main plot consisted of 6 subplots. Each subplot consisted of four rows with 6 m length, and the interval between rows and plants considered 60 and 8 cm spacing (208000 plant ha^{-1}), respectively. To prevent the treatment interference between adjacent subplots and main plots and replications, there were 0.6, 1, and 2 m distances, respectively. Based on soil test results (Fig. 3) and both cultivar's requirements, before planting 250 and 100 kg ha^{-1} ammonium-phosphate and urea, respectively, and in the V6 stage, 100 kg ha^{-1} urea was applied. Weed control performed by applying 5 l ha^{-1} Eradikan as pre-planting and 1.5 l ha^{-1} MCPA + 2,4-D as post-emergence in the V6 stage. In the V10 and V12phases, pest control executed by applying 2 l ha^{-1} from the Diazinon source. To applying the H_{PM} treatment, seeds submerged in pure water for 6 h so that the water level was 2 cm above the seed surface, and then with fan-made airflow dried for 24 h at room temperature (close to 25 °C) (Zida et al. 2018). Young and Atokple (2003) reported the 20 days after planting (while seedlings have 2 to 3 leaves) as the suitable time for transferring the seedlings to the field. Thus, 20 days before planting dates, the seeds were planted in the (marked with each treatment information) 72 cells trays filled with a mixture of 60% field soil, 20% fine sand, and 20% rotted manure. After complete emergence of

Table 2. General linear model (GLM) sources, levels of statistical significance in traits.

Components		DMY	DDMY	CPY	MEY	WUE_{DMY}
			(t ha^{-1})		(Gcal ha^{-1})	(kg ha^{-1})
Years	2017	19.1 b	11.3 b	1.83	38.3	5.64
	2018	24.4 a	14.4 a	2.28	48.2	6.96
p Val.		0.0449	0.0437	0.0504	0.0504	0.4858
LSD		5.04	2.96	ns	ns	ns
Planting dates	$D1_{PD}$	28.6 a	16.7 a	2.56 a	55.9 a	7.47 a
	$D2_{PD}$	24.0 b	14.1 b	2.24 b	47.6 b	6.92 b
	$D3_{PD}$	19.3 c	11.5 c	1.90 c	38.6 c	5.96 c
	$D4_{PD}$	15.1 d	9.1 d	1.51 d	30.8 d	4.85 d
p Val.		0.0011	0.0006	0.0006	0.0005	0.0003
LSD		2.28	1.03	0.15	3.28	0.30
Planting methods	D_{PM}	18.1 b	10.8 b	1.75 c	36.6 b	5.42 b
	H_{PM}	23.7 a	14.0 a	2.30 a	47.1 a	6.91 a
	T_{PM}	23.4 a	13.7 a	2.10 b	45.9 a	6.58 a
p Val.		0.0239	0.0215	0.0061	0.0147	0.0273
LSD		2.97	1.59	0.13	4.27	0.80
Cultivars	S_{CV}	23.1	13.3	2.13	44.2	6.69
	P_{CV}	20.4	12.4	1.97	42.2	5.92
p Val.		0.1444	0.2228	0.0569	0.2491	0.1186
LSD		ns	ns	ns	ns	ns

$D1_{PD}$, $D2_{PD}$, $D3_{PD}$, $D4_{PD}$ represent 1st of July, 10th of July, 23rd of July and 1st of August planting dates, respectively. D_{PM}, H_{PM}, and T_{PM} represent Direct, Hydroprime, and Transplant planting methods, respectively. S_{CV} and P_{CV} represent *Speedfeed* and *Pegah* cultivars, respectively. DMY: Dry Matter Yield; DDMY: Digestible Dry Matter Yield; CPY: Crude Protein Yield; MEY: Metabolic Energy Yield; WUE_{DMY}: Water Use Efficiency of Dry Matter production. Means in the same column followed by different letters differ significantly at $P<0.05$.

primary leaves in the nursery, seedlings sprayed with 20-20-20 NPK fertilizer (1×1000^{-1} concentration) and humic acid (0.75×1000^{-1} concentration). Also, the double concentrated solution repeated one week later. Due to the farm's suitable weather and to reduce the transference stress on transplants, the nursery placed nearby the experimental section, and to prevent pest damage, the transplant trays were placed under a frame and covered with a net. To provide the most suitable soil conditions in terms of temperature and moisture, immediately (right after planting), first, and 48 h later, second irrigation was applied. Pressured strip drip (16 mm type strips with 10 cm dropper distance), water mass counter, and shut-off valves formed the distribution, measurement, and control components of the irrigation system, respectively. Calculating the amount of evapotranspiration in different growth stages, based on the following equation, determined the consumed water volume:

$$\text{Equation (1): } ETc = ETo \times Kc$$

Where, ETc is the sorghum evapotranspiration, ETo is the reference-crop evapotranspiration and calculated from the Penman-Monteith method, and Kc is the sorghum crop coefficient (Allen et al. 1998; FAO 2012).

Measurements and data analysis

To eliminate marginal factors, two sidelines and 50 cm from the north-side and south-side of all lines in each subplot were eliminated. Each sub plot was divided into two separate sections: "Section A", which consisted of the 4.5 m^2 of the two main lines and assigned to measuring the final biomass yield parameters. To achieve the highest biomass yield multi-cut principle was employed. Harvesting S_{CV} and P_{CV} before flowering threatens the livestock's health with prussic acid, but by starting the flowering phase, the amount of anti-nutritional compound reduces to the safe balance (Amirsadeghi et al. 2019). "Section B", which consisted of the other remained 4.5 m^2 of the two main lines, was addressed to sampling during the growth season for regression analysis purpose. Collecting data for regression analysis purposes for the T_{PM} treated plants started at each planting date (before planting in the field), and in the ten days paste the samplings carried out until harvesting. To ground a similar situation for all PMs and also to be able to compare them at the same days after planting (e.g., in 10, 20), the D_{PM} and H_{PM} sample collection started 20 days (the same duration of nursery for T_{PM}) after planting in the field. Likewise, the measured amount of the GDD received by the T_{PM} treated plants added to the total GDD. Water use efficiency of dry matter production (WUE_{DMY}) calculated by using the following equation:

$$\text{Equation (2): } WUE_{DMY} = DMY/WU$$

Where, DMY is dry matter yield (kg ha^{-1}), WU is the water used for irrigation (m^{-3}).

In each stage of sampling for regression analysis, five plants were fully cut from above the ground. Before and after drying the samples in a forced ventilation oven at 70 °C for 72 h, the weights were recorded. The final harvest was carried out at the beginning of the flowering; after recording the fresh weight to assess the produced biomass and nutritional factors, the 1 kg fully packed samples in the 4 kg paper bags were dried in the forced-air oven at 70 °C for 72 h.

Laboratory analysis

The taken samples pulverized, milled, sifted (through 0.2 mm sieve), and scanned by using the near-infrared reflectance spectroscopy (NIRS, Informatics Perten 8600 Feed Analyzer) with 6-20 wavelengths ranging from 500 to 2400 nm to determining the NDF (neutral detergent fiber), ADF (acid detergent fiber), WSC (water soluble carbohydrates. The CP (crude protein) was measured

by the Kjeldahl method. The gas production method (in vitro) was appointed to extract the data of the metabolic energy (ME) and digestible organic matter (DOM) contents. Three 200 mg dry forage samples were incubated in the sifted rumen fluid (obtained from the Moghani sheep breed) and buffer mixture in 100 ml ceiled glass syringes (Menke and Steingass 1988; Kaplan et al. 2019) in the 39 ± 0.5 °C temperature. Also, three syringes (filled with only the rumen fluid and buffer mixture) were used as the control to determine the correction factor for gas production. Eventually, after 24 hours based on the produced gas data and following equations, the ME (MJ kg^{-1}) and OMD (g kg^{-1}) were computed (Menke et al. 1979; Blümmel et al. 1997):

Equation (3): ME = 2.2 + 0.136 x GP + 0.057 x CP
Equation (4): OMD = 14.88 + 0.889 x GP + 0.45 x CP + 0.0651 x CA

Where, GP is 24-hour net gas production (mL/200 mg), CP is crude protein, CA is crude ash contents

The rest of the traits calculated by using the following formulas:

Equation (5): Hemicellulose = NDF - ADF
Equation (6): DDM = 88.9 – (0.779 x ADF)
Equation (7): RFV = DDM x DMI x 0.775

Where, DDM is Digestible dry matter, DMI is Dray matter intake.

Statistical analysis

Ascertainment from the homogeneity of variance obtained by employing the Bartlett test (Bartlett 1937). Thereafter, the combined data analyzed by general linear model (GLM) SAS procedures (SAS Institute 2003). The least significant differences (LSD) test was used to separate levels of GLM sources. The effect of factors considered significant at *P*-values ≤ 0.05 in the F-test. Interactions in the levels of 0.05 and 0.01 of significance used for the means comparisons. The correlation amongst traits and the results of regression analysis recruited to maximize interpretation accuracy.

Regression analysis

The regression model with the highest coefficient of determination (R^2), least RMSE and components considered the desired model (Anfinrud et al. 2013). Afterward, the results showed the ability of linear regression to model the DMY production at *P*-values ≤ 0.05 level of significance for all PDs, PMs, and CVs.

Results

Yield parameters

The DMY was substantially (*P*<0.01) affected by PD (Table 2). Simultaneously with delay in planting date from $D1_{PD}$ to $D2_{PD}$, $D3_{PD}$ and $D4_{PD}$, respectively: the DMY was 16.1, 32.5 and 47.2% reduced (Table 2); the a-factor (line slope) or the growth rate was 2.8, 7.1 and 15.7% descended; the b-factor (line intercept) was 0.3, 5.8 and 20.1% increased; the adjusted R^2 was 1.1, 3.2 and 7.4% decreased (Table 8, Fig. 3). The DMY was considerably (*P*<0.05) influenced by PM (Table 2). Employing H_{PM} instead of D_{PM} resulted in 23.6% elevation in DMY (Table 2); 29% increase in a-factor and 6.6% in the adjusted R^2; the RMSE value 23.94% reduced (Table 8, Fig. 3). Contrary to H_{PM}, applying the T_{PM} instead of D_{PM} caused 8% reduction in a-factor (line slope) and 1.8% inflation in RMSE value (Table 8, Fig. 3). S_{CV}, in comparison with P_{CV}, showed 9.7% higher growth rate (a-factor), 4.2% less line intercept, 27.5% less RMSE value, and 4.1% higher adjusted-R^2 (Table 8, Fig. 3). The dual interaction of PD×PM was significantly (*P*<0.01) affected the DMY production (Table 4). T_{PM} in $D1_{PD}$ generated the most harvested DMY, and D_{PM} in $D4_{PD}$ produced the least DMY (Table 4). Interestingly, H_{PM} in $D2_{PD}$ produced the same DMY as T_{PM} but, in $D3_{PD}$ and $D4_{PD}$ significantly produced more DMY (Table 4). Likewise, the dual interaction of PM×CV was highly (*P* <0.05) affected the DMY production (Table 6). Applying H_{PM} and T_{PM} on S_{CV} produced the most, and applying D_{PM} on P_{CV} generated the least DMY. DDMY was significantly affected by PD (*P*<0.01) and PM (*P*<0.05) (Table 2). Planting date postponement from $D1_{PD}$ to $D2_{PD}$, $D3_{PD}$, and $D4_{PD}$, respectively, caused 15.6, 31.1, and 45.5 % reduction in the DDMY (Table 2). H_{PM} and T_{PM} compared to D_{PM} caused 22.9 and 21.2 % elevation in DDMY production (Table 2). Also, DDMY significantly (*P*<0.05) affected by dual interaction of PD×PM (Table 4). T_{PM} in $D1_{PD}$ produced the most, and D_{PM} in $D4_{PD}$ produced the least DDMY (Table 4). H_{PM} in $D2_{PD}$, $D3_{PD}$, and $D4_{PD}$ considerably (*P*<0.05) produced more DDMY than T_{PM} (Table 4). Also, the dual interaction of PD×CV notably (*P*<0.05) affected DDMY (Table 5). In $D1_{PD}$, the S_{CV} produced the highest DDMY, and in $D4_{PD}$, both CVs produced the least DDMY (Table 5). The dual interaction of PM×CV significantly (*P*<0.05) affected DDMY production (Table 6) that with applying the H_{PM} on S_{CV} highest and with applying D_{PM} on P_{CV} least DDMY was generated. CPY and MEY were considerably affected by PD (*P*<0.01) and PM (*P*<0.05) (Table 2). Delay in PD from $D1_{PD}$ to $D2_{PD}$, $D3_{PD}$, and $D4_{PD}$, respectively, resulted in 12.5, 25.8, and 41% reduction in the produced CPY and 14.8, 30.9, and 44.9% reduction in MEY production (Table 2). Also, H_{PM}, compared to D_{PM} and T_{PM}, made 23.9 and 8.7% more CPY (Table 2). H_{PM} and T_{PM}

Table 3. General linear model (GLM) sources, levels of statistical significance in quality traits.

Components		ME	NDF	ADF	Hem	CP	WSC	DDM	DOM	RFV
		(Mcal kg^{-1})				(g kg^{-1})				(Gcal ha^{-1})
Years	2017	2.02 a	591 b	377 b	214	97.0	96 b	595 a	625 a	93.8 a
	2018	2.00 b	597 a	383 a	215	95.0	107 a	591 b	620 b	92.2 b
p Val.		0.0069	0.0103	0.0089	0.9271	0.0527	0.0345	0.0087	0.0091	0.0002
LSD		0.01	3.73	3.46	ns	2.02	9.97	2.69	2.76	.36
Planting dates	$D1_{PD}$	1.96 c	607 a	391 a	216	90.0 d	107 a	584 c	613 c	89.6 d
	$D2_{PD}$	1.99 bc	599 b	384 ab	215	93.6 c	104 ab	590 bc	619 bc	91.6 c
	$D3_{PD}$	2.02 ab	592 c	377 b	215	99.1 b	100 bc	595 b	625 b	93.8 b
	$D4_{PD}$	2.06 a	579 d	367 c	212	101.2 a	96 c	603 a	632 a	97.0 a
p Val.		0.0153	0.0004	0.0132	0.4194	0.0002	0.0120	0.0136	0.0145	0.0023
LSD		0.04	3.25	9.33	ns	1.09	4.44	7.36	7.65	1.58
Planting methods	D_{PM}	2.04 a	585 c	373 b	212 c	98.4 a	97	599 a	628 a	95.4 a
	H_{PM}	2.00 b	596 b	381 a	215 b	98.6 a	105	592 b	621 b	92.7 b
	T_{PM}	1.98 b	603 a	386 a	217 a	90.9 b	103	588 b	617 b	90.9 b
p Val.		0.0225	0.0092	0.0236	0.0088	0.0236	0.0744	0.0213	0.0223	0.0171
LSD		0.02	5.39	6.21	1.48	4.14	ns	4.66	4.86	1.80
Cultivars	S_{CV}	1.93 b	607	398 a	209	93.6	97 b	579 b	607 b	88.7 b
	P_{CV}	2.08 a	582	361 b	220	98.3	107 a	608 a	637 a	97.3 a
p Val.		0.0129	0.0662	0.0112	0.1004	0.1755	0.0111	0.0119	0.0105	0.0290
LSD		0.04	ns	8.29	ns	ns	2.29	6.88	6.18	4.94

$D1_{PD}$, $D2_{PD}$, $D3_{PD}$, $D4_{PD}$ represent 1st of July, 10th of July, 23rd of July and 1st of August planting dates, respectively. D_{PM}, H_{PM}, and T_{PM} represent Direct, Hydroprime, and Transplant planting methods, respectively. S_{CV} and P_{CV} represent Speedfeed and Pegah cultivars, respectively. ME: Metabolic Energy; NDF: Neutral Detergent Fiber; ADF: Acid Detergent Fiber; Hem: Hemicelluloses; CP: Crude Protein; WSC: Water Soluble Carbohydrates; DDM: Digestible Dry Matter; DOM: Digestible Organic Matter; RFV: Relative Feed Value. Means in the same column followed by different letters differ significantly at $P<0.05$.

compared to D_{PM}, produced 22.3 and 20.3% more MEY, respectively (Table 2). PD×PM interaction effect on MEY was significant ($P<0.01$) (Table 4). T_{PM} in $D1_{PD}$ produced the highest, and D_{PM} in $D4_{PD}$ generated the least MEY; but, with delay in PD H_{PM}, significantly produced more MEY than other PMs (Table 4). PD×CV interaction had a significant effect ($P<0.05$) on CPY (Table 5). In $D1_{PD}$ and $D2_{PD}$, the S_{CV} produced more CPY than P_{CV}, but in $D3_{PD}$ and $D4_{PD}$, the difference between cultivars was insufficient (Table 5). PM×CV interaction also was significant ($P<0.05$) on CPY production that with applying H_{PM} on S_{CV} highest and with D_{PM} on both CVs, the least MEY was generated (Table 6).

Quality traits

NDF content was significantly ($P<0.05$) affected by PD and PM. In $D4_{PD}$, using the D_{PM}, caused the least content of NDF (Table 3). Interaction of PD×PM had a considerable ($P<0.01$) effect on NDF content (Table 4). T_{PM} and H_{PM} in $D1_{PD}$ produced forage with the highest NDF content (Table 4). With the delay in PD substantial difference in NDF production between T_{PM} and H_{PM} occurred; in such a way that T_{PM} in $D2_{PD}$, $D3_{PD}$ and $D4_{PD}$, respectively, produced 0.66, 1.66 and 1.87% more NDF than H_{PM}. Also, must note that in $D4_{PD}$, the existed significant difference between H_{PM} and D_{PM} in the prior PDs faded away and both treatments placed in the lowest statistical grouping (Table 4).

ADF content was significantly ($P<0.05$) influenced by PD, PM, and CV (Table 3). In $D1_{PD}$ compared to $D3_{PD}$ and $D4_{PD}$, respectively, 3.6 and 6.1 % more ADF produced. Applying H_{PM} and T_{PM} compared to D_{PM} produced 2.1 and 3.4 % more ADF content (Table 3). S_{CV} compared to P_{CV} produced 9.3% more ADF (Table 3). Hem content was significantly ($P<0.01$) affected by PM. T_{PM} made 2.3 and 0.9% more Hem content than H_{PM} and T_{PM}, respectively. CP content was notably affected by PD ($P<0.01$) and PM ($P<0.05$) (Table 3). Delay in PD from $D1_{PD}$ to $D2_{PD}$, $D3_{PD}$, and $D4_{PD}$ respectively caused 4, 10.1, and 12.4% elevation in the CP content of forage (Table 3). H_{PM} and D_{PM} compared to T_{PM} respectively, produced 7.8 and 7.6% more CP content (Table 3). WSC content of forage was significantly ($P<0.05$) affected by PD (Table 3). In $D1_{PD}$ compared to $D3_{PD}$ and $D4_{PD}$, forage was produced with 6.5 and 10.3% more WSC (Table 3). The interaction effect of PD×CV on WSC content was considerable ($P<0.05$) (Table 5). In $D1_{PD}$ and $D2_{PD}$, P_{CV} produced forage with the highest WSC content; except in $D4_{PD}$ in all other PDs, the difference between S_{CV} and P_{CV} was notable ($P<0.05$) (Table 5). DDM and DOM content in forage were significantly ($P<0.05$) affected by PD, PM, and CV factors (Table 3). $D4_{PD}$ compared to

Table 4. Effect of planting dates and planting methods on traits.

Planting dates	Planting methods	DMY	DDMY	CPY	MEY	WUE_{DMY}	ME	NDF	ADF	Hem	CP	WSC	DDM	DOM	RFV
			(t ha^{-1})		(Gcal ha^{-1})	(kg ha^{-1})	(Mcal kg-1)				(g kg^{-1})				(Gcal ha^{-1})
1st of July	D_{PM}	24.3 d	14.4 e	2.25	48.2 e	6.57 c	2.00	594 d	382	212	93	103	592	621	92.8 e
	H_{PM}	30.2 b	17.6 b	2.76	58.8 b	7.93 a	1.94	613 a	396	218	92	109	581	610	88.3 h
	T_{PM}	31.4 a	18.2 a	2.67	60.8 a	7.92 a	1.94	615 a	396	219	85	110	581	609	87.8 h
11th of July	D_{PM}	20.5 f	12.3 g	1.94	41.4 g	6.08 d	2.03	589 e	375	213	95	101	597	626	94.3 cd
	H_{PM}	25.9 c	15.3 c	2.47	51.1 c	7.46 b	1.98	603 c	386	217	96	106	588	617	91.0 f
	T_{PM}	25.7 c	14.9 d	2.31	50.2 d	7.24 b	1.96	607 b	391	216	90	105	584	613	89.6 g
23rd of July	D_{PM}	15.6 h	9.3 i	1.53	31.8 i	4.95 f	2.05	581 f	369	213	99	96	602	631	96.6 b
	H_{PM}	21.5 e	12.8 f	2.20	42.8 f	6.65 c	2.01	592 d	379	213	104	103	594	623	93.3 de
	T_{PM}	20.8 f	12.4 g	1.96	41.3 g	6.28 d	1.99	602 c	383	219	95	101	590	620	91.3 f
1st of August	D_{PM}	12.3 i	7.3 j	1.30	25.2 j	4.07 g	2.06	574 g	366	209	107	89	604	634	97.9 a
	H_{PM}	17.3 g	10.6 h	1.78	35.9 h	5.59 e	2.08	576 g	363	213	103	102	606	636	98.1 a
	T_{PM}	15.6 h	9.3 i	1.44	31.4 i	4.88 f	2.04	587 e	373	214	94	96	598	627	95.0 c
p Val.		0.0022	0.0004	0.0723	<0.0001	0.0151	0.1163	0.0019	0.1483	0.5858	0.2252	0.1738	0.1401	0.1586	0.0118
LSD		0.74	0.30	ns	0.77	0.22	ns	3.43	ns	ns	ns	ns	ns	ns	1.28

D_{PM}, H_{PM}, T_{PM} represents direct hydroprimed and transplante planting method, respectively. DMY: Dry Matter Yield; DDMY: Digestible Dry Matter Yield; CPY: Crude Protein Yield; MEY: Metabolic Energy Yield; WUE_{DMY}: Water Use Efficiency of Dry Matter production; ME: Metabolic Energy; NDF: Neutral Detergent Fiber; ADF: Acid Detergent Fiber; Hem: Hemicelluloses; CP: Crude Protein; WSC: Water Soluble Carbohydrates; DDM: Digestible Dry Matter; DOM: Digestible Organic Matter; RFV: Relative Feed Value. Means in the same column followed by different letters differ significantly at $P<0.05$.

$D3_{PD}$, $D2_{PD}$, and $D1_{PD}$, respectively, produced forage with 1.3, 2.2, and 3.2% more DDM content and 1.1, 2.1, and 3% more DOM (Table 3). D_{PM}, in comparison with T_{PM} and H_{PM} respectively, produced forage with 1.8 and 1.2% more DDM and 1.8 and 1.1% more OMD (Table 3). P_{CV} produced forage with 4.8% more DDM and 4.7% more DOM content than S_{CV} (Table 3). ME content significantly ($P<0.05$) affected by PD, PM, and CV. The ME content in $D4_{PD}$ was respectively 3.4 and 4.9% higher than the amount that produced in $D3_{PD}$ and $D4_{PD}$. D_{PM} generated 2 and 2.9% more ME than H_{PM} and T_{PM}, respectively. P_{CV} generated forage with 7.2% more ME than S_{CV}.

The forage RFV was significantly affected by PD ($P<0.01$), PM ($P<0.05$), and CV ($P<0.05$) (Table 3). The produced forage in $D4_{PD}$ compared to $D3_{PD}$, $D2_{PD}$, and $D1_{PD}$ respectively had 3.3, 5.6, and 7.6% more RFV (Table 3). D_{PM} compared to T_{PM}, and H_{PM} respectively, had 4.7 and 2.8% more RFV. P_{CV} produced forage with 8.8% more RFV than S_{CV} (Table 3).

Table 5. Effect of planting dates and cultivars on traits.

Planting dates	Planting methods	DMY	DDMY	CPY	MEY	WUE_{DMY}	ME	NDF	ADF	Hem	CP	WSC	DDM	DOM	RFV
			(t ha^{-1})		(Gcal ha^{-1})	(kg ha^{-1})	(Mcal kg-1)				(g kg^{-1})				(Gcal ha^{-1})
1st of July	S_{CV}	30.4	17.2 a	2.67 a	56.9	7.92 a	1.88	621	412	209	89	98.9 bc	568	597	85.1
	P_{CV}	26.8	16.3 b	2.45 b	54.9	7.03 b	2.05	593	370	223	91	115.7 a	601	630	94.2
11th of July	S_{CV}	26.2	15.1 c	2.42 b	49.9	7.58 a	1.91	611	404	207	93	95.7 c	575	603	87.4
	P_{CV}	21.8	13.2 d	2.06 c	45.2	6.28 c	2.07	588	365	223	94	112.2 a	605	634	95.8
23rd of July	S_{CV}	20.6	11.9 e	1.99 cd	39.7	6.34 c	1.94	603	395	208	97	95.5 c	581	610	89.7
	P_{CV}	18.0	11.1 f	1.80 d	37.5	5.57 d	2.09	580	359	222	101	104.3 b	610	639	97.8
1st of August	S_{CV}	15.2	9.0 g	1.44 e	30.3	4.91 e	2.00	593	383	211	96	96.1 c	591	620	92.7
	P_{CV}	14.9	9.1 g	1.57 e	31.3	4.79 e	2.12	565	352	213	107	95.3 c	615	644	101.3
p Val.		0. 0569	0.0408	0.0407	0.1151	0.0321	0.1040	0.3009	0.0963	0.1256	0.0665	0.0173	0.0875	0.0980	0.3844
LSD		ns	0.77	0.20	ns	0.44	ns	ns	ns	ns	ns	5.90	ns	ns	ns

S_{CV} and P_{CV} represent Speedfeed and Pegah cultivars, respectively. DMY: Dry Matter Yield; DDMY: Digestible Dry Matter Yield; CPY: Crude Protein Yield; MEY: Metabolic Energy Yield; WUE_{DMY}: Water Use Efficiency of Dry Matter production; ME: Metabolic Energy; NDF: Neutral Detergent Fiber; ADF: Acid Detergent Fiber; Hem: Hemicelluloses; CP: Crude Protein; WSC: Water Soluble Carbohydrates; DDM, Digestible Dry Matter; DOM, Digestible Organic Matter; RFV, Relative Feed Value. Means in the same column followed by different letters differ significantly at $P<0.05$.

Table 6. Effect of planting methods and cultivars on traits.

Planting dates	Planting methods	DMY	DDMY	CPY	MEY	WUE_{DMY}	ME	NDF	ADF	Hem	CP	WSC	DDM	DOM	RFV
			(t ha^{-1})		(Gcal ha^{-1})	(kg ha^{-1})	(Mcal kg-1)				(g kg^{-1})				(Gcal ha^{-1})
D_{PM}	S_{CV}	19.0 c	11.0 d	1.81	37.0 d	5.65 e	1.97	596	390	207	97	93	585	614	91.4
	P_{CV}	17.3 d	10.6 e	1.70	36.3 d	5.18 f	2.10	573	356	217	100	101	612	641	99.4
H_{PM}	S_{CV}	25.5 a	14.7 a	2.39	48.7 a	7.42 a	1.93	610	400	210	95	99	577	606	88.2
	P_{CV}	22.0 b	13.4 c	2.22	45.6 c	6.40 c	2.08	582	362	220	102	111	607	636	97.1
T_{PM}	S_{CV}	24.9 a	14.2 b	2.19	47.0 b	6.99 b	1.90	615	405	210	89	97	573	602	86.6
	P_{CV}	21.8 b	13.2 c	2.00	44.8 c	6.17 d	2.06	590	366	224	93	109	604	633	95.3
p Val.		0.0292	0.0222	0.5232	0.0296	0.0027	0.4608	0.2441	0.5341	0.5772	0.4033	0.2427	0.5184	0.5245	0.5984
LSD		0.72	0.27	ns	0.92	0.06	ns	ns	ns	ns	ns	ns	ns	ns	ns

D_{PM}, H_{PM}, T_{PM} represents direct hydroprimed and transplante planting method, respectively. S_{CV} and P_{CV} represent Speedfeed and Pegah cultivars, respectively. DMY: Dry Matter Yield; DDMY: Digestible Dry Matter Yield; CPY: Crude Protein Yield; MEY: Metabolic Energy Yield; WUE_{DMY}: Water Use Efficiency of Dry Matter production; ME: Metabolic Energy; NDF: Neutral Detergent Fiber; ADF: Acid Detergent Fiber; Hem: Hemicelluloses; CP: Crude Protein; WSC: Water Soluble Carbohydrates; DDM: Digestible Dry Matter; DOM: Digestible Organic Matter; RFV: Relative Feed Value. Means in the same column followed by different letters differ significantly at $P<0.05$.

Water use efficiency

The WUE_{DMY} was considerably affected by PD ($P<0.01$) and PM ($P<0.05$) (Table 2). PD postponement from $D1_{PD}$ to $D2_{PD}$, $D3_{PD}$, and $D4_{PD}$, respectively, caused 7.4, 20.2, and 35.1% reduction. Employing H_{PM} and T_{PM} instead of D_{PM} caused 27.5 and 21.4% elevation in water usage productivity. Dual interaction of PD×PM considerably ($P<0.05$) affected WUE_{DMY} (Table 4). H_{PM} and T_{PM} in $D1_{PD}$ generated the highest, and the D_{PM} in $D4_{PD}$ caused the least WUE_{DMY}. By delay in PD, the WUE_{DMY} of same PMs were significantly decreased, and simultaneously, H_{PM} notably used water more productively than T_{PM} in $D3_{PD}$ and $D4_{PD}$. Also, interaction of PD×CV meaningfully ($P<0.05$) affected WUE_{DMY}. In $D1_{PD}$ and $D2_{PD}$, S_{CV} generated the highest WUE_{DMY}, and only in $D4_{PD}$ the difference between S_{CV} and P_{CV} was insignificant. Interaction of PM×CV notably affected WUE_{DMY}. Highest productivity in water usage was generated by applying H_{PM} on S_{CV} and the least WUE_{DMY} caused by D_{PM} of P_{CV}.

Correlations

Correlation test amongst traits showed that contrary to significantly ($P<0.01$) negative correlation of DMY with CP (60%), DDM (57%), and ME (57%), DMY was positively

Table 7. Correlation coefficient among quantitative and qualitative parameters.

Traits	DMY	WUE_{DMY}	NDF	ADF	CP	Hem	WSC	DDM	RFV	ME	DOM	CPY	DDMY	MEY
DMY	1													
WUEDMY	0.75**	1												
NDF	0.70**	0.48**	1											
ADF	0.57**	0.37**	0.87**	1										
CP	-0.60**	-0.40**	-0.66**	-0.54**	1									
Hem	0.05	0.07	-0.05	-0.52**	-0.05	1								
WSC	0.26**	-0.05	-0.08	-0.21**	-0.03	0.30**	1							
DDM	-0.57**	-0.37**	-0.87**	-0.99**	0.54**	0.53**	0.21*	1						
RFV	-0.65**	-0.44**	-0.97**	-0.96**	0.63**	0.28**	0.14	0.96**	1					
ME	-0.57**	-0.37**	-0.87**	-0.99**	0.54**	0.53**	0.21*	0.99 **	0.96**	1				
DOM	-0.57**	-0.37**	-0.87**	-0.99**	0.54**	0.53**	0.21*	0.99**	0.96**	0.99**	1			
CPY	0.97**	0.75**	0.61**	0.49**	-0.41**	0.06	0.30**	-0.50**	-0.54**	-0.50**	-0.50**	1		
DDMY	0.99**	0.75**	0.65**	0.49**	-0.58**	0.12	0.30**	-0.50**	-0.59**	-0.50**	-0.50**	0.97**	1	
MEY	0.98**	0.76**	0.61**	0.44**	-0.57**	0.15	0.32**	-0.45**	-0.55**	-0.45**	-0.45**	0.97**	0.99**	1

DMY: Dry Matter Yield; WUE_{DMY}, Water Use Efficiency for Dry Matter Production; NDF, Neutral Detergent Fiber; ADF, Acid Detergent Fiber; CP, Crude Protein; CPY, Crude Protein Yield; Hem, Hemicelluloses; DDM, Digestible Dry matter; DDMY, Digestible Dry Matter Yield; RFV, Relative Feed Value; WSC, Water Soluble Carbohydrates; ME, Metabolic Energy; MEY, Metabolic Energy Yield; DOM, Digestible Organic Matter.
* and ** indicate significant at $P \leq 0.05$ and $P \leq 0.01$, respectively.

Table 8. The linear regression models and their components for dry matter yield (independent variable) production of different treatments as affected by changes in GDD (dependent variable) during growth seasons. Suitable regression equation for 24 treatments: DMY= ax + b; where a = line slope; b = intercept value; R^2= coefficient of determination; Adj-R^2= adjusted coefficient of determination; RMSE= root mean square of errors

Components			a	b	R^2	Adj-R^2	RMSE	p Val.
$D1_{PD}$	D_{PM}	S_C	0.0191	-10.418	0.9795	0.9775	1.4483	<0.0001
		P_C	0.0195	-12.960	0.9314	0.9245	2.7686	<0.0001
	H_{PM}	S_C	0.0243	-10.501	0.9815	0.9797	1.7459	<0.0001
		P_C	0.0217	-12.235	0.9764	0.9741	1.7648	<0.0001
	T_{PM}	S_C	0.0207	-10.053	0.9821	0.9803	1.7734	<0.0001
		P_C	0.0178	-10.868	0.9408	0.9349	2.8287	<0.0001
$D2_{PD}$	D_{PM}	S_C	0.0194	-10.990	0.9702	0.9669	1.4872	<0.0001
		P_C	0.0182	-11.461	0.9153	0.9059	2.4189	<0.0001
	H_{PM}	S_C	0.0257	-11.838	0.9893	0.9881	1.1722	<0.0001
		P_C	0.0214	-12.199	0.9548	0.9498	2.0359	<0.0001
	T_{PM}	S_C	0.0191	-10.646	0.9683	0.9648	1.9107	<0.0001
		P_C	0.0158	-9.7184	0.9368	0.9298	2.2701	<0.0001
$D3_{PD}$	D_{PM}	S_C	0.0186	-10.500	0.9257	0.9164	1.9098	<0.0001
		P_C	0.0168	-9.9055	0.8792	0.8641	2.2503	<0.0001
	H_{PM}	S_C	0.0242	-11.391	0.9903	0.9891	0.8683	<0.0001
		P_C	0.0223	-11.907	0.9544	0.9487	1.7630	<0.0001
	T_{PM}	S_C	0.0176	-10.104	0.9618	0.9570	1.6751	<0.0001
		P_C	0.0149	-9.3567	0.9187	0.9085	2.1252	<0.0001
$D4_{PD}$	D_{PM}	S_C	0.0171	-8.9442	0.8864	0.8702	1.8875	0.0002
		P_C	0.0149	-7.9432	0.8478	0.8261	1.9406	0.0004
	H_{PM}	S_C	0.0226	-9.8810	0.9818	0.9792	0.9483	<0.0001
		P_C	0.0230	-11.396	0.9291	0.9190	1.9557	<0.0001
	T_{PM}	S_C	0.0127	-7.4861	0.8756	0.8578	1.9891	0.0002
		P_C	0.0135	-7.9237	0.9041	0.8904	1.8322	<0.0001

(*P*<0.01) correlated with CPY (97%), DDMY (99%), and MEY. Also, DMY was positively (*P*<0.01) correlated with WUE_{DMY} (75%), NDF (70%), ADF (57%), WSC (26%), and was negatively (*P*<0.01) correlated with RFV (65%) and DOM (57%). NDF was negatively (*P*<0.01) correlated with CP (66%), DDM (87%), RFV (97%), ME (87%) and DOM (87%). Also, ADF had notably (*P*<0.01) negative correlation with CP (53%), Hem (52%), WSC (21%), DDM (99%), RFV (96%), ME (99%) and DOM (99%). RFV had significantly (*P*<0.01) positive correlation with CP (63%), Hem (28%), DDM (96%), ME (96%) and DOM (96%) (Table 7). The correlation amongst the components of the regression illustrated the significantly (*P*<0.01) positive correlation of DMY with line slope (53%) and Adj-R^2 (78%). Although DMY was negatively correlated (*P*<0.01) with line intercept (50%) (Table 9).

Table 9 Correlation coefficient amongst the results of regression analysis with dry matter yield.

	DMY	A	B	Adj-R^2	RMSE
DMY	1				
A	0.53**	1			
B	-0.50*	-0.73**	1		
Adj-R^2	0.78**	0.76**	-0.61**	1	
RMSE	-0.05	-0.50*	-0.03	-0.51*	1

DMY, Dray matter yield; a, line slope; b, intercept value; Adj-R^2, adjusted coefficient of determination; RMSE, root mean square of errors.
* and ** indicate significant at P ≤ 0.05 and P ≤ 0.01, respectively.

Discussion

Yield parameters

Biomass yield production is the core objective in forage cultivation practices (Nematpour et al. 2020). In addition to the GLM and regression analysis, Figure 2 also exhibits the trend of DMY production influenced by variation in PD. The reductions in DMY influenced by delay in PD probably occurred due to (1) the changes in light parameters that affected the ERF protein activity which leads to various physiological reactions and the DMY productions in sorghum (Mathur et al. 2020), and (2) reductions in the adequacy of required environmental characteristics especially GDD for maximum DMY production (Hassan et al. 2020). Figure 2 illustrates the elevation of line-slope in both simulated and produced DMY under the changes in PMs. Figure 2 shows contrary to the equal acquired GDD for both H_{PM} and D_{PM}, but H_{PM} used growth season's ambient factors (specifically GDD) more productive, which lead to more DMY production in all PDs; likewise illustrated the H_{PM}'s ability in producing the same DMY as the T_{PM}, despite the less available GDD in $D1_{PD}$. This result, alongside the produced DMY under further lagged PD ($D2_{PD}$, $D3_{PD}$, and $D4_{PD}$), emphasized the higher productivity of H_{PM} over T_{PM} and D_{PM} in using the available adequate growing season for DMY production. Probably this difference between H_{PM} and T_{PM} occurred because of the Gramineae species sensitivity towards the removal of primary roots (Biswas 2020) during the transference of seedling to the field, which is the prevalent obstacle for transplanting (Lee et al. 2019). Figure 2 shows that in each specific PM and PD, the CV affected the slope and intercept of regression models. Blunt angled lines with more intercepts defined by researchers as the slower crop growth rate and less harvested DMY (Tagarakis et al. 2017). These results assist in clarification of the role of suitable cultivar, planting method, and planting date in maximizing the harvested forage sorghum DMY in a second cropping system. A high-quality forage characterizes by a high level of DDM.

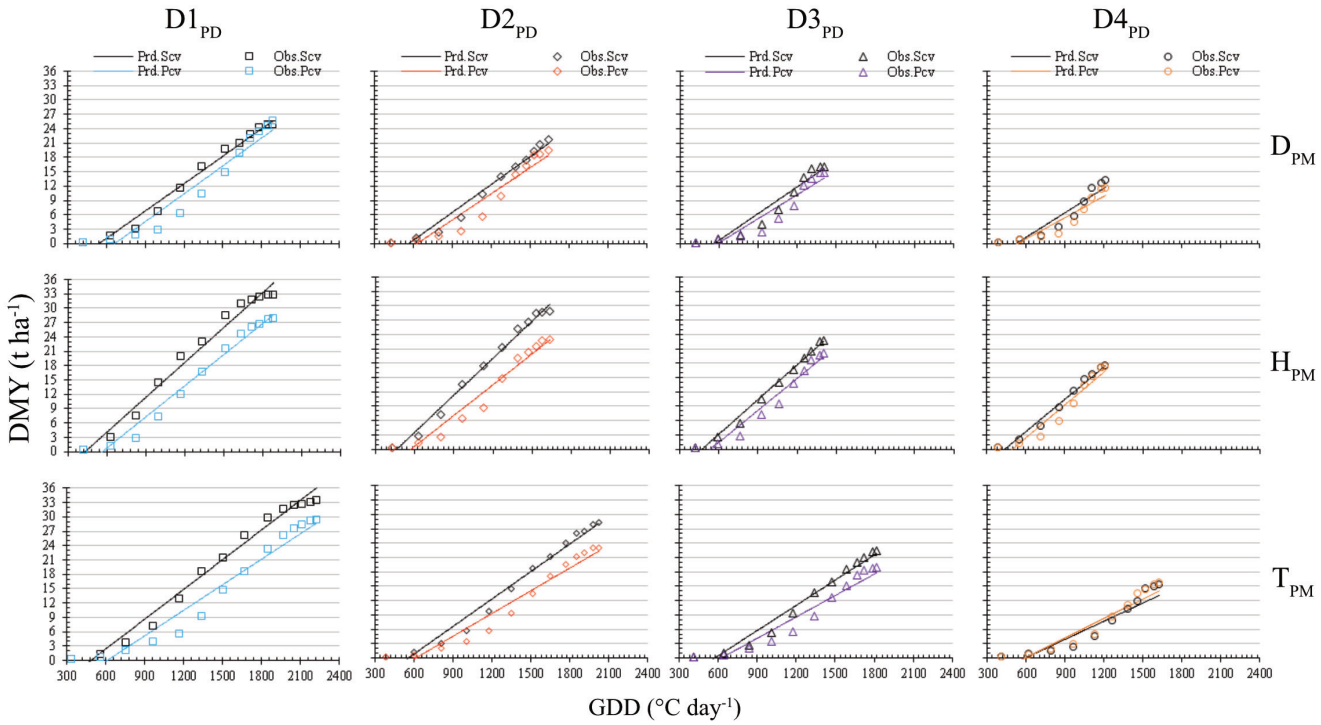

Figure 2. Regression relationship of observed (Obs) and predicted (Prd) dry matter yield (DMY) versus cumulated growth degree day (GDD) during 1st of July ($D1_{PD}$), 11th of July ($D2_{PD}$), 23rd of July ($D3_{PD}$) and 1st of August ($D4_{PD}$) planting dates of Speedfeed (S_{CV}) and Pegah (P_{CV}) cultivars under hydroprimed seeds (H_{PM}), transplanting (T_{PM}) and conventional planting methods (D_{PM}).

Probably hence, $D1_{PD}$ provided a longer growing season (Hassan et al. 2019) highest DDMY recorded, and with delay in PD, the DDMY significantly decreased. Likely, hence $D1_{PD}$ supplied the required duration to compensate for the transplant transference stress (Biswas 2020), T_{PM} produced the highest DDMY. But delay in PD and growth season reduction eliminated the supremacy of T_{PM} (Rattin et al. 2015), and subsequently, in $D2_{PD}$, $D3_{PD}$, and $D4_{PD}$, it was H_{PM} that significantly produced more DDMY (Chen et al. 2021).

Jahanzad et al. (2013) recognized CP as one of the most critical parameters in determining the forage quality. Zanonadi et al. (2017) identified the minimum air temperature and the mean soil temperature as the key environmental factors for sorghum growth and yield production. Therefore, probably reduction in mentioned factors because of the delay in PD was the main reason in CPY and MEY production reduction (Table 2). Zida et al. (2018) explained the hydropriming role in DMY enhancement via crop growth rate acceleration through activating the seed's enzymes prior to sowing. Thus, probably more CPY and MEY were harvested due to the significant effect of H_{PM} on DMY production. On the other hand, Lee et al. (2019) addressed the sowing date as one of the key factors to adjust the plant's growth requirement with suitable ambient characteristics for maximum yield production. Thus, the lag of PD reduced the required environmental competency and affected the CPY and MEY production in $D4_{PD}$ compared to the $D1_{PD}$. Jahanzad et al. (2013) reported the S_{CV} dominance over P_{CV} in growth rate and total protein yield production.

Quality parameters

Lyons et al. (2019a) reported the significant effect of sowing times on the DMY. Chen et al. (2021) and Ibrahim et al. (2020) respectively reported the considerable effect of hydropriming and transplanting effects on DMY. Jahanzad et al. (2013) reported a significant positive correlation between DMY and NDF. Probably hence, amongst the PDs, the highest DMY was obtained in $D1_{PD}$ (due to the most fitted synchronicity between plant growth stages and environmental condition), T_{PM} and H_{PM} also, facilitated and accelerated the plant growth, highest NDF content obtained. But, growing season reduction in $D2_{PD}$, $D3_{PD}$ and $D4_{PD}$, the T_{PM} continued to produce higher NDF compared to the H_{PM}. Probably the 20 days more growth season in the nursery stage was the reason for these distinctions. Bhattarai et al. (2017) and Hassan et al. (2020) recognized the effect of soil and air temperature as the determinative factors in germination and yield production in forage sorghum cultivation. Hence Nematpour et al. (2020) reported the positive correlation

between ADF and DMY, and probably hereupon, in $D1_{PD}$, the ambiance condition for growth and development was more desirable, these results recorded. Hassan et al. (2019) reported asynchronous growth season and plant development phases would reduce the potential for DMY production. Probably, the PD postponement by lowering the environmental suitability affected the plant development and caused the considerable reduction in DMY, and hence the direct positive correlation between ADF and DMY was in progress, the forage produced with less ADF content. Chen et al. (2021) and Lee et al. (2019) respectively stated the significant effect of H_{PM} and T_{PM} on DMY; accordingly, more ADF content produced by H_{PM} and T_{PM} compared to D_{PM}. Jahanzad et al. (2013), in addition to positive correlation of NDF and DMY, also reported the higher ADF content of S_{CV} compared to the P_{CV}. The content of CP in forage represents the actual quantity of true protein or amino acid that absorbed by the animal (Das et al. 2014). The elevation in average air temperature optimizes the plant development throughout supplying the ambient requirements for sorghum growth (Lyons et al. 2019a, b). Premier growth rate reduces nitrogen absorption, which eventually compromises the protein production in forage sorghum (Kukal and Irmak 2018). The D_{PM} compared to the H_{PM} and T_{PM} reduced the line slope and increased the line intercept of the regression models (which represents the growth rate) (Figure 2). Therefore, probably more time for absorbing nitrogen and more time for producing proteins that resulted in more CP content production. Lyons et al. (2019b) and Kukal and Irmak (2018) reported higher temperature increases the growth rate and reduces the N absorption and the content of CP. In all likelihood, hence delay in PD reduced the growth rate because of the reduction in mean and minimum air temperature and also the average soil temperature, suitable situation to produce more CP content in $D4_{PD}$ compared to the prior PDs provided. Jahanzad et al. (2013) reported a lower growth rate of P_{CV} compared to S_{CV}. Figure 2 clarifies the blunter line angle and higher line intercept of P_{CV} included treatments compared to the S_{CV} ones; likely, according to this results, P_{CV} was able to produce higher CP than S_{CV}. The forage that is abundant in WSC provides the required sugar for a successful silage process (fermentation) and also supplies the animal needs to energy for high productive digestion. Forage with a high volume of WSC is a promising feedstock to produce bioethanol at the industrial level. Probably hence in $D1_{PD}$, the ambient factors like minimum air temperature and the mean soil temperature stimulated the effect of long days on photosynthesis, subsequently, the level of WSC was higher than other PDs. Nematpour et al. (2020) reported forages that planted at the later dates produced higher net energy content for lactation. Probably suitable environmental condition in $D1_{PD}$ and $D2_{PD}$ alongside the genetic property of P_{CV} induced WSC production. These results are in agreement with the report from Jahanzad et al. (2013).

Kaplan et al. (2019) reported the negative correlation between DMY with OMD. RFV in forage plays the determinative role in portion selection of a specific forage in the ration for feedstock (Tang et al. 2018). RFV and NDF content constantly have a considerable negative correlation (Imoro 2020). Probably because of the desirable ambient condition in $D4_{PD}$ for forage production with less indigestible content like lignin was the main reason for forage production with most DDM, OMD, ME content, and RFV (Kaplan et al. 2019; Hassan et al. 2019). Nematpour et al. (2020) reported a positive correlation between NDF and ADF with growth rate; since D_{PM} caused the growth rate with a blunter angle (Fig. 2) than H_{PM} and T_{PM}, thus, highest content of DDM, DOM, ME content, and RFV generated by D_{PM}. Jahanzad et al. (2013) reported lower NDF and ADF content of P_{CV} compared to the S_{CV}.

Water use efficiency

Globally, 70% of freshwater usage is dedicated to agricultural activities (Michelon et al. 2020). The most restricting factor of farming in arid and semiarid regions are supplying the required water and increasing the "Water Use Efficiency" in production systems (Hao et al. 2014; Teixeira et al. 2017; Bhattaraia et al. 2020). Hassan et al. (2019) reported the unsynchronized growth stage and ambient factors reduce the resource usage productivity. Thus, delay in planting that significantly reduced harvested DMY conclusively caused a notable reduction in WUE_{DMY}. Michelon et al. (2020) acknowledged priming as one of the strategies to increase water usage productivity. Jahanzad et al. (2013) reported the advantage of S_{CV} over P_{CV} in yield production. Thus, probably by applying H_{PM} on S_{CV}, the germination and seedling establishment enhanced, and the plant development rate elevated, which resulted in considerably higher WUE_{DMY} than D_{PM} and even T_{PM}.

Correlation

According to the correlation results between water use efficiency and nutritional parameters with DMY, factors like early planting dates (Hassan et al. 2019), advanced planting methods (H_{PM}, and T_{PM}) (Mapfumo et al. 2013; Pinheiro et al. 2018; Bajwa et al. 2018; Zida et al. 2018; Ibrahim et al. 2020), and early cultivars (Jahanzad et al. 2013; Tirfessa et al. 2020; Hasan et al. 2020; Bhattarai et al. 2020) that significantly increases the DMY production, empowers the forage production systems to generate forage with an acceptable yield of nutritional components and water use efficiency. Based upon the results of cor-

relation among the results of regression analysis with DMY (Table 8), it could be a valid interpretation that with avoiding the delay in PD, using the conventional PM, and utilizing the P_{CV} that reduces the a-coefficient and elevates the b-factor, maximize the probability to reach the most DMY.

Conclusion

The inevitable effect of global warming added to the naturally restricted water and soil resources, population growth, and historic low livelihood state in arid and semiarid regions are the most threatening factors toward the sustainability of resources, agricultural practices, and food safety. A second cropping system by cultivating the water shortage-resistant species under developed planting methods could be worthwhile to introduce another alternative to attain, maintain, and develop the production sustainability and food safety in these regions. The holdup of planting in a second cropping system due to various factors could improvise planting date and consequently yield production. The results showed that in Y2, while the temporal factors increased yield of both S_{CV} and P_{CV} elevated. Studied planting methods revealed the significant elevation in quantity and nutritional traits. Also, the H_{PM} and T_{PM} were able to compensate for the delay in planting dates through accelerating the germination, facilitating the seedling establishment, and advancing the plant development. Conclusively results asserted that the preparedness for executing the H_{PM} process on S_{CV} would produce a hefty forage yield with an acceptable range of quality.

Author contribution statement

IM Collected data (field and lab works), data analysis, writing the article. FG performed the research concept and design, statistical analysis, writing the article. MRA performed the research concept and design, field works, writing the article, critical revision of the article, final approval of article. FP performed the research concept and design, lab works, writing the article. AM contributed lab works and writing the article. No funding was received for conducting this study.

References

Allen RG, Pereira LS, Raes D, Smith M (1998) Crop evapotranspiration-guidelines for computing crop water requirements. FAO Irrigat Drain 56:26-40.

Amirsadeghi M, Gholami H, Fazaeli H, Kochaki A (2019) Investigation of prussic acid and nitrate concentration in eighteen varieties of forage sorghum. Anim Sci J 121:205-218.

Amouzou KA, Lamers JPA, Naab JB, Borgemeister C, Vlek PLG, Becker M (2019) Climate change impact on water and nitrogen-use efficiencies and yields of maize and sorghum in the northern Benin dry savanna West Africa. Field Crops Res 235:4-117.

Anfinrud R, Cihacek L, Johnson BL, Ji Y, Berti MT (2013) Sorghum and kenaf biomass yield and quality response to nitrogen fertilization in the Northern Great Plains of the USA. Ind Crop Prod 50:159-165.

Bajwa AA, Farooq M, Nawaz A (2018) Seed priming with sorghum extracts and benzyl aminopurine improves the tolerance against salt stress in wheat (*Triticum aestivum* L.) Physiol Mol Biol Plants 24:239-249.

Bartlett MS (1937) Properties of sufficiency and statistical tests. Proceed Royal Stat Soc Ser A 160:268-282.

Bhattarai B, Singh S, West CP, Ritchie GL, Trostle CL (2020) Water depletion pattern and water use efficiency of forage sorghum pearl millet and corn under water limiting condition. Agric Water Manag 238:106-206.

Biswas S (2020) Prospects and constraints of transplanted maize wheat sorghum and pearl millet: A review. IJECC 10:24-43.

Blümmel M, Makkar HPS, Chisanga G, Mtimuni J, Becker K (1997) The prediction of dry matter intake of temperate and tropical roughages from in vitro digestibility/gas-production data, and the dry matter intake and in vitro digestibility of African roughages in relation to ruminant live weight gain. Anim Feed Sci Tech 69:131-141.

Chen X, Zhang R, Xing Y, Jiang B, Li B, Xu X, Zhou Y (2021) The efficacy of different seed priming agents for promoting sorghum germination under salt stress. PLoS ONE 16(1):e0245505.

Costa TD, Giacobbo CL, Galo L, Forte CT, Dmis R, Tironi SP (2020) Management of soil cover and its influence on phytosociology physiology and fig production. Com Sci 11:32-36.

Das LK, Kundu SS, Kumar D, Datt C (2014) The evaluation of metabolizable protein content of some indigenous feedstuffs used in ruminant nutrition. Veter World 7:57-261.

Elamin HE, Mohamed AE, Abdeldaim AM (2019) Impact of climate change on crop water requirements for Abu-Sabeen forage sorghum (*Sorghum bicolor* L.) and alfalfa (*Medicago sativ*a L.) in Khartoum State, Sudan. J Agric Eng 5:36-40.

FAO (2012) 'Crop evapotranspiration—guidelines for computing crop water requirements ' Natural Resources Management and Environment Department. FAO.

Forti C, Shankar A, Singh A, Balestrazzi A, Prasad V, Macovei A (2020) Hydropriming and biopriming improve

Medicago truncatul seed germination and upregulate DNA repair and antioxidant genes. Genes 11:242.
Golzardi F, Nazari Sh, Rahjoo V (2019) Sorghum Cultivation. ETKA Publication [In Persian].
Hassan MU, Chattha MU, Barbanti L, Chattha MB, Mahmood A, Khan I, Nawaz M (2019) Combined cultivar and harvest time to enhance biomass and methane yield in sorghum under warm dry conditions in Pakistan. Ind Crops Prod 132:84-91.
Hassan MU, Chattha MU, Khan I, Chattha MB, Barbanti L, Aamer M, Iqbal MM, Nawaz M, Mahmood A, Ali A, Aslam MT (2020) Heat stress in cultivated plants: nature impact mechanisms and mitigation strategies - A review. Plant Biosys 155(2):211-234.
Ibrahim MEH, Ali AYA, Zhou G, Elsidding AMI, Zhu G, Nimir NEA, Ahmad I (2020) Biochar application affects forage sorghum under salinity stress. Chil J Agric Res 80:3.
Jahanzad E, Jorat M, Moghadam H, Sadeghpour A, Chaichi MR, Dashtaki M (2013) Response of a new and a commonly grown forage sorghum cultivar to limited irrigation and planting density. Agric Water Manag 117:62-69.
Jatana BS, Ram H, Gupta N (2020) Application of seed and foliar priming strategies to improve the growth and productivity of late sown wheat (*Triticum aestivum* L.). Cereal Res Commun 48:383-390.
Jo SM, Jung KY, Kang HW, Choi YD, Lee JS, Jeon SH (2016) Effect of seedling age on growth and yield at transplanting of sorghum (*Sorghum bicolor* L. Moench). Korean J Crop Sci 61:50-56.
Junnyor WSG, Severiano EDC, Da-Silva AG, Goncalves WG, Andrade R, Martins BRR, Custodio GD (2015) Sweet sorghum performance affected by soil compaction and sowing time as a second crop in the Brazilian Cerrado. Rev Bras Cien Solo 39:1744-1754.
Kaplan M, Kara K, Unlukara A, Kale H, Buyukkilic Beyzi S, Varol IS, Kizilsimsek M, Kamalak A (2019) Water deficit and nitrogen affects yield and feed value of sorghum sudangrass silage. Agric Water Manag 218:30-36.
Kukal MS, Irmak S (2018) US agro-climate in 20th century: growing degree days first and last frost growing season length and impacts on crop yields. Sci Rep 8:6977.
Kukal MS, Irmak S (2020) Evidence of arithmetical uncertainty in estimation of light and water use efficiency. Sustainability 12(6):2271.
Lee HJ, Young HJ, Lee SS, Paradipta DHV, Han OK, Ku JH, Min HG, Oh JS, Kim SC (2019) Effect of the sowing and harvesting dates on the agronomic characteristics and feed value of corn and sorghum×sorghum hybrid in Youngnam Mountain area. J Korean Soc Grassl Forage Sci 39:53-60.
Lyons SE, Ketterings QM, Godwin GS, Cherney DJ, Cherney JH, Amburgh MEV, Meisinger JJ, Kilcer TF (2019a) Optimal harvest timing for brown midrib forage sorghum yield, nutritive value, and ration performance. J Dairy Sci 102:8.
Lyons SE, Ketterings QM, Godwin GS, Cherney JH, Cherney DJ, Meisinger JJ, Kilcer TF (2019b) Double-cropping with forage sorghum and forage triticale in New York. Agron J 111:3374-3382.
Mapfumo S, Chiduza C, Young EM, Murungu FS, Nyamudeza P (2013) Effect of cultivar seedling age and leaf clipping on establishment growth and yield of pearl millet (*Pennisetum glaucum*) and sorghum (*Sorghum bicolor*) transplants. South Afric J Plant Soil 24:202-208.
Martin NP, Russelle MP, Powell JM, Sniffen CJ, Smith SI, Tricarico JM, Grantll RJ (2017) Invited review: Sustainable forage and grain crop production for the US dairy industry. J Dairy Sci 100:1-16.
Mathur S, Priyadarshini SS, Singh V, Vashisht I, Jung KH, Sharma R, Sharma MK (2020) Comprehensive phylogenomic analysis of ERF genes in sorghum provides clues to the evolution of gene functions and redundancy among gene family members. Biotech 10:139.
Menke KH, Raab L, Salewski A, Steingass H, Fritz D, Schneider W (1979) The estimation of the digestibility and metabolizable energy content of ruminant feeding stuffs from the gas production when they are incubated with rumen liquor in vitro. J Agr Sci 93:217-222.
Menke KH, Steingass H, (1988) Estimation of the energetic feed value obtained from chemical analysis and in vitro gas production using rumen fluid. Anim Res Dev 28:47-55.
Michelon N, Pennisi G, Ohn Myint N, Orsini F, Gianquinto G (2020) Strategies for improved water use efficiency (WUE) of field-grown lettuce (*Lactuca sativa* L.) under a semi-arid climate. Agronomy 10:668.
Naoura G, Sawadogo N, Atchozou EA, Emendack Y, Hassan MA, Reoungal D, Amos DN, Djirabye N, Tabo R, Laza H (2019) Assessment of agro-morphological variability of dry-season sorghum cultivars in Chad as novel sources of drought tolerance. Sci Rep 9:19581.
Nematpour A, Eshghizadeh HA, Zahedi M, Ghorbani GR (2020) Millet forage yield and silage quality as affected by water and nitrogen application at different sowing dates. Grass Forage Sci 75:169-180.
Pinheiro CL, Araujo HTN, de-Brito SF, Maia MDS, Viana JDS, Filho SM (2018) Seed priming and tolerance to salt and water stress in divergent grain sorghum genotypes. Am J Plant Sci 9:606-616.
Rattin J, Valinote JP, Gonzalo R, Di-Benedetto A (2015) Transplant and change in plant density improve sweet maize (*Zea mays* L.) yield. Am J Exp Agric 5:336-351.
SAS Institute (2003) SAS/STAT User's Guide Version 9.1. SAS Institute Cary NC.
Tagarakis AC, Ketterings QM, Lyons S, Godwin G (2017)

Proximal Sensing to Estimate Yield of Brown Midrib Forage Sorghum. Agronomy J 109:107-114.

Tirfessa A, McLean G, Mace E, Oosterom EV, Jordan D, Hammer G (2020) Differences in temperature response of phenological development among diverse Ethiopian sorghum genotypes are linked to racial grouping and agroecological adaptation. Crop Sci 60:977-990.

Velten S, Leventon J, Jager N, Newig J (2015) What is sustainable agriculture? A systematic Review. Sustainability 7:7833-7865.

Young EM, Atokple IDK, (2003) Transplanting sorghum and millet as a means of increasing food security in upper east region of Ghana project (R7341) Centre for Arid Zone Studies University of Wales Bangor Gwynedd. UK LL57 2UW.

Zandonadi CHS, Albuquerque CJB, Freitas RS, Paula ADM, Clemente MA (2017) Agronomic characteristics and macronutrient export of grain sorghum hybrids from different sowing dates. Ciênc Agrotec 41:7-14.

Zida PE, Neya BJ, Stockholm MS, Jenson MS, Soalla WR, Sereme P, Lund OS (2018) Increasing sorghum yields by seed treatment with an aqueous extract of the plant *Eclipta alba* may involve a dual mechanism of hydropriming and suppression of fungal pathogens. J Crop Prot 107:48-55.

Acta Biologica Szegediensis

Volume 65(2):185-198, 2021
Acta Biologica Szegediensis
http://abs.bibl.u-szeged.hu/index.php/abs

DOI:10.14232/abs.2021.2.185-198

ARTICLE

Diversity and distribution of wild mushrooms in different forest areas of Bankura district, WB, India

Arindam Ganguly[1], Susmita Nad[1], Krishanu Singha[2], Rituparna Pathak[1], Palash Hazra[1], Pritha Singha[1], Priti Dhua[1], Pradeep Kumar Das Mohapatra[3], Asish Mandal[4]*

[1]Department of Microbiology, Bankura Sammilani College, Bankura-722102, West Bengal, India
[2]Department of Microbiology, Vidyasagar University, Midnapore-721102, W. B., India
[3]Department of Microbiology, Raiganj University, Raiganj-733134, Uttar Dinajpur, W. B., India
[4]P. G. Department of Botany, Ramananda College, Bishnupur, Bankura-722122, W. B., India

ABSTRACT Mushrooms are macroscopic fruit bodies of fungi; one of the most diverse groups of living organisms distributed all over the world. In recent past, they have gained significant scientific attention for their profound nutraceutical potentiality. The objective of the present study was to explore the diversity and ecological distribution of mushrooms in different forest areas of Bankura district. The study area includes intermittent dense forest and flood plains from middle-east to eastern part of Bankura district. However, this area received very little attention from a conservation perspective, and there is no such documentation on mushrooms of this area. The survey was conducted from August 2019 to October 2020 including vivid field surveys in the forest depots. The study has revealed a total of 53 identified mushroom species belonging to 40 genera and 30 families. The study has also identified 25 edible, 18 inedible and 15 medicinally potential mushrooms. The genus *Russula* and the family *Russulaceae* dominates the myco-population. The finding shows that this region is rich in macrofungal diversity complicatedly linked to the functioning of the local ecosystem. The present study opens new possibilities regarding the exploration and utilization of wild mushrooms in India.
Acta Biol Szeged 65(2):185-198 (2021)

KEY WORDS
bioactive compound
mushroom diversity
nutritional value
therapeutic potentiality

ARTICLE INFORMATION
Submitted
20 August 2021
Accepted
28 December 2021
***Corresponding author**
E-mail: mandalasish71@gmail.com

Introduction

Fungi are one of the most diverse groups of organisms on earth. They are eukaryotic heterotrophs that obtain their energy by absorption of nutrients. The large visible fructification of the underground mycelia of macro-fungi is known as 'Mushrooms'. They mainly belong to the phylum Basidiomycota and Ascomycota with observable spore bearing structure. Mushrooms are abundant in nature and they are the first known fungi. Wild edible mushrooms have been collected and consumed by people from the very early stage of civilization, even when people didn't know about its nutritive value.

Macrofungi varies widely in their habitats. The species diversity of mushrooms is directly related to the habitat. They are found on soil (terrestrial), dead leaves (folicolous), wood (lignicolous) or dung and decomposing organic materials (coprophilous). Macrofungi, based on their nutrition, can be categorized into three groups: saprophytes, parasites, and symbiotic (Kinge et al. 2017). Mushrooms predominantly grow during rainy season in forests and can be epigeous or hypogeous. They vary mostly in shape, size and colour. Some of them are edible whereas some are proven to be poisonous. The various environmental factors that affect the growth of mushrooms are temperature, humidity, light and the substrate over which they grow. All the species of mushrooms shows remarkable diversity in their morphological characteristics.

Mushrooms contain high amounts of nutritious compounds including vitamins, proteins, minerals, fiber and trace elements. Edible mushrooms have been considered to be an ideal food for obese persons due to high fibre, low fat and low starch content. They are considered as "poor man's protein" because of their high nutrient content (Singha et al. 2017b). Chang and Buswell (1996) coined the term 'mushroom nutraceuticals' to describe those compounds that have considerable potentiality as dietary supplements, used for the enhancement of health and prevention of various human diseases.

Mushrooms are seasonal fungi, which earn additional ecological significance. They appear in between reaching a highest point of development with the diverse niches in the forest ecosystem. Their habitat and climate are the

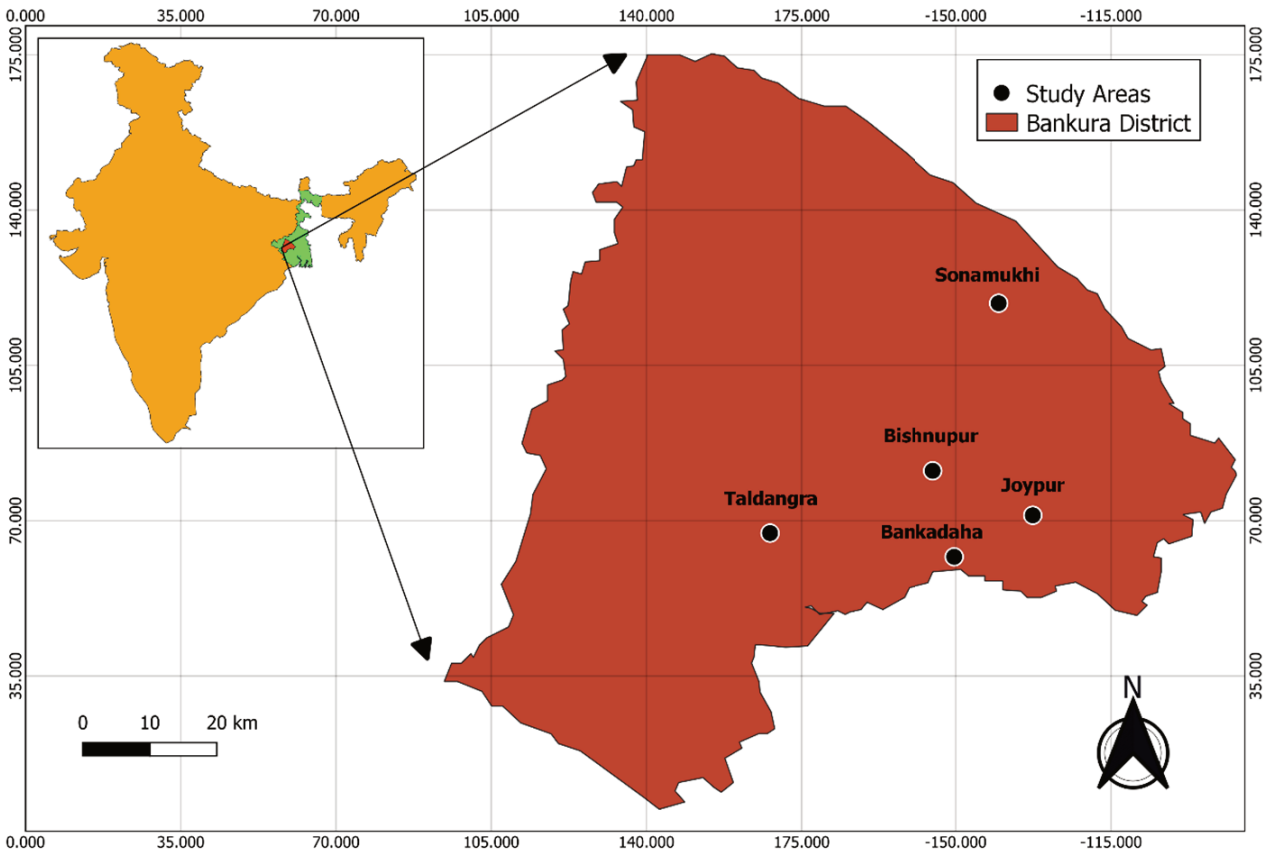

Figure 1. Study location and map of Bankura forest areas.

major factors that indicate their biodiversity. Fungi also play an important role as decomposers. They breakdown plant components like lignin and cellulose and thus are particularly important in woody-ecosystems. They also degrade surface waste and release nitrogen back into the soil in the form of ammonium nitrate, an important nutrient that plants need for their survival. Mushrooms are also known to produce several bioactive compounds that have therapeutic uses. However, they protect themselves from deleterious effect of plant phenolic tannins by producing a hydrolytic enzyme, called tannase that form gallic acid and glucose (Das Mohapatra et al. 2020). It is often been noticed that local people who consume the mushroom *Astraeus hygrometricus* (*Kurkure chhatu*) on regular basis enjoy several health benefits (Dutta and Acharya 2014). This mushroom possesses antitumor, anti-Leishmanial, anti-Candidal, antioxidant and immune-modulatory activity (Biswas et al. 2017).

Macrofungal diversity is an integral component of the global diversity. Diverse abundance of macrofungal species is a helpful indicators to interpret the current status of the ecosystem. Most healthy forest ecosystem contains at least 45% mycorrhizal fungi (Arnolds 1988). Native people living in nearby forest areas relate to the wild mushrooms in respect to their socio-economic lifestyles by means of both food ingredients as well as small business elements. Chang and Miles (2004) reported that out of 14000 known mushroom species, there were nearby 7000 well-studied species that possesses varying degree of edibility. Among them, only 200 species were experimentally cultured; 100 were economically cultivated, 60 were commercially cultivated and about 10 species have gained industrial importance.

The total recorded mushrooms in India are approximately 850 species (Deshmukh 2004). The collection and scientific study of mushrooms in India has started during 19th century (Kaul et al. 2002). Butler and Bisby (1931) published the first list on Indian fungi which was further revised by Vasudeva (1960). Purkayastha and Chandra (1985) published the first comprehensive account of Indian edible mushrooms and their cultivation technology.

India has an ancient history of using mushrooms as food, medicine, minerals and drugs. It has become a centre of herbal therapy (Nad et al. 2021). However, such kind

of studies is very rare in West Bengal. Dutta and Acharya (2014) obtained 31 edible and 3 medicinally important macrofungi that were used by local and indigenous communities in eight districts of West Bengal. Das et al. (2015) reported 16 wild edible mushrooms with ethno-medical value from tropical dry deciduous forest of Eastern *Chota Nagpur* plateau. Deshmukh et al. (2006) reported that, around 40 species found from all over India were lethal. Singha et al. (2017b) explored the nutritional and antibacterial potentiality of some wild edible mushrooms from Gurguripal Eco-forest, Paschim Medinipur, West Bengal, India. Thus, the studies on mushroom diversity are often significant and contribute to the knowledge of the ecosystem of a forest.

The forest region of Bankura district is one of the enriched forest areas of West Bengal. The district possesses dense forest dominated by Sal (*Shorea robusta*). Other trees found in the forests include *Azadirachta indica* (Neem), *Dillenia indica* (Chalta), *Syzygium cumini* (Jam) (Basu et al. 2013). A higher proportion of mycorrhizal fungi is generally correlated with a region that contain better conserved forests (Pradhan et al. 2016). Bankura is surrounded with low-lying alluvial-laterite soil (Das and Paul 2015) with an average annual rainfall of 1329 mm (Majumder and Patra 1993). Overall, the biogeological environment provide favourable climatic zone for fungal growth. However, there is no valid documentation on diversity of mushrooms in this area till date. Hence, the present study is focused on the diversity and distribution of mushrooms in Bishnupur and adjacent forest areas of Bankura district, West Bengal.

Materials and Methods

Study area

Five major forest areas namely Bishnupur (23°04′48″N, 87°19′12″E; Altitude 59 m), Joypur (23°02′N, 87°27′E; Alt.74 m), Sonamukhi (23°18′11.5848″N, 87°24′56.4948″E; Alt. 66 m), Taldangra (23°01′1.092″N, 87°06′29.3688″E; Alt. 74 m), and Bankadaha (22°58′03.64″N 87°21′05.43″E; Alt. 74 m) of Bankura district were selected as the study area (Fig. 1). These forest areas have a tropical climate with dry and rainy season (annual average rainfall: 11000-15000 mm), dominated by 'Sal' trees with a laterite and alluvial type soil. The average temperature of this locations ranges between 20-30 °C during rainy season. The field study was conducted from August 2019 to October 2020 to obtain the maximum outcome.

Collection of samples

Opportunistic sampling method was being performed and conspicuous specimens were collected precisely from the study area (Mueller et al. 2004). After finding a colony or a single species of mushroom, the fruiting bodies were collected with the help of knife. Their habitat conditions and occurrence frequency were recorded. The samples were photographed (Nikon D5300 camera), both in their natural habitats and with the reference of a scale or coin, for identification. The samples were then taken in a container, labelled and kept for further study.

Identification of the specimens

The collected samples were examined in laboratory by observing the formation of the cap, arrangements of the gills, presence of pores on the under surface of the fruit bodies or not, presence of stipe and volva or not, the type of the surface (smooth or rough), etc. Then according to their characteristics, they were then identified with the help of standard literatures (Pradhan et al. 2010; Pushpa and Purushothama 2012; Acharya and Pradhan 2017).

Preservation of the specimens

All the samples were preserved immediately in liquid preservative (25:5:70 ml rectified alcohol + formalin + distilled water) for further studies (Hawksworth et al. 1995).

Data analysis

The frequency of occurrence for each species was calculated by following formula as suggested by Aung et al. (2008).

$$\frac{\text{Occurrence frequency of species A}}{\text{Total number of all species}} \times 100$$

Simpson Index of Diversity was calculated as suggested by Simpson (1949).

Simpson Index of Diversity =1-D; where,

$$D = \frac{\Sigma n\,(n-1)}{N\,(N-1)}\text{; where,}$$

n = total number of organisms of a particular species
N = total number of organisms of all species

Shannon diversity index for mushroom was calculated as suggested by Margalef (2008).

$$H = -\Sigma\,(n/N)\log(n/N)\text{; where,}$$

H = diversity index
N = total number of individuals of all the species
n = total number of individuals of a particular species

Considering the values of diversity index, the evenness of the mushrooms was calculated according to Pielou (1996).

$$e = H/\log S;\ \text{where,}$$

e = evenness
H = Shannon index
S = the number of species

Menhinick's index of species richness was calculated as suggested by Menhinick (1964).

$$D = s/\sqrt{N};\ \text{where, D = species richness}$$

s = the number of different species
N = total number of individuals

Results

The study areas were spread over the central eastern part of Bankura district (Agro Climatic Zone), marked by flood plains and interfluves. The climate of the study area is tropical, slightly warm and humid with average annual rainfall of 1400 mm. The mean temperature is around 33 °C. Relative humidity during the study time was found around 80%. From this point of view, the study areas possess a good geographical environment for the growth of mushrooms.

In the span of survey, a total number of 53 species were identified, among which 29 specimens were identified up to species level. Majority of the identified mushrooms (96.07%) belongs to Basidiomycota (51 specimens), where only 2 species belong to Ascomycota. All the identified mushrooms are distributed in diverse group of 40 genera belonging to 30 families (Table 1). The family/ genus ratio of 0.75 and genus/ species ratio of 0.75 suggest the presence of comparatively high familial and generic diversity in the region.

The study revealed that members of *Russulaceae* (12%) grow predominantly in the study area, followed by *Agaricaceae* (10%), *Polyporaceae* (10%), *Ganodermataceae* (6%) and *Psathyrellaceae* (6%) as shown in Fig. 2. Among the two species of Ascomycota, one was *Xylaria* sp. belonging to the family *Xylariaceae* and the other was *Daldinia concentrica* from the family *Hypoxylaceae.*

Most diverse specimens were obtained from the family *Russulaceae* which was found to be the most dominant in overall survey. As per sampling areas, *Polyporaceae* and *Russulaceae* in Bishnupur (16.66% each) and Bankadaha (13.33% each), *Agaricaceae* in Taldangra (36.36%), *Marasmiaceae*, *Agaricaceae* and *Psathyrellaceae* in Sonamukhi (10% each) and *Russulaceae* in Joypur (27.27%) were found most frequently. *Marasmius*, *Polyporus* and *Ganoderma* were the most common genera in all five study areas.

Mushrooms were found to be largely saprophytic (30 specimen), whereas rest of them were mycorrhizal (17 specimen) and parasitic (6 specimen) in the present study (Fig. 3). Ectomycorrhizal specimens were notable in the overall survey as it is one type of reflexion of the forest health. *Russulaceae*, *Lyophyllaceae*, *Sclerodermataceae* and *Hydnangiaceae*; the common ectomycorrhizal families were found to be predominant in the study area. The most common mycorrhizal species were *Russula rosea*, *Russula nobilis*, *Scleroderma citrinum* and *Laccaria laccata*. On the other hand, *Pleurotus ostreatus* and *Russula cyanoxantha* were identified as rare species from this area. Some species like *Aleuria aurantia*, *Daldinia concentrica*, *Coprinus logopus*, *Podoscypha venustula*, *Cyathus striatus*, *Coprinus logopus* mostly fruited upon decaying logs and organic matters. However, this occasional sighting at the base of diseased and/or infected trees indicate their facultative parasitic nature. Majority of mushroom were found to grow on soil (25 specimen) and wood (23 specimen), rest were found to grow on leaf (2 specimen) and decaying organic materials (3 specimen) (Fig. 4).

Through interaction with the local people living nearby the study areas, it was revealed that 25 species were edible, 15 species have medicinal importance and rest are inedible (18 species) and with unknown significance (10 species) (Fig. 5). Moreover, the mushroom species *Termitomyces heimii*, *Russula cyanoxantha*, *Agaricus* sp., *Auricularia* sp., *Calocybe indica*, *Tremella fuciformis* were found to be potential food sources for local livelihood. It also contributes to local economy. On the other hand, some poisonous fungi like *Coprinus logopus*, *Amanita* sp., *Lepiota* sp., *Conocybe* sp. were also found in the forest regions of Bankura. Among the medicinally important mushrooms, *Ganoderma lucidum*, *Auricularia* sp., *Ganoderma applanatum* were traditionally used by local physicians for the treatment of diabetes, hyper cholesterol, muscle pain and flu, respectively.

Mushroom richness and abundance in different forest areas

There are several factors through which biological diversity of a species can be quantified. Among them, the two major factors are species richness and species abundance. In the present study, mushrooms collected from five forest areas namely Sonamukhi, Bishnupur, Bankadaha, Joypur and Taldangra were analysed for mushroom diversity. Species diversity richness and abundance of mushrooms in forest areas of Bankura district were analysed thoroughly (Table 2).

The forest area of Sonamukhi had 20 species of mushrooms belonging to 18 genera and 17 families. A family/

Table 1. Mushroom diversity, habitat, significance, and mode of nutrition in forest areas of Bankura District, West Bengal, India.

Family	Scientific name	Observed frequency	Site of collection	Habitat	Significance	Mode of nutrition	Common/ Local name
Agaricaceae	*Agaricus campestris*	1	Taldangra	Soil	Edible & medicinally important	Saprophytic	Field or Meadow mushroom
	Lepiota sp.	5	Taldangra	Soil	Inedible	Saprophytic	––
	Leucocoprinus birnbaumii	1	Sonamukhi	Soil	Inedible (poisonous)	Saprophytic	Flowerpot parasol
	Leucocoprinus sp.	13	Taldangra, Sonamukhi	Decaying matter	Inedible	Saprophytic/ Mycorrhizal	––
	Lycoperdon pyriforme	1	Taldangra	Soil	Edible	Saprophytic	Pear shaped puffball
Amanitaceae	*Amanita* sp.	6	Bankadaha, Bishnupur	Soil	Inedible	Saprophytic/ Mycorrhizal	––
Auriculariaceae	*Auricularia* sp.	6	Bankadaha, Sonamukhi	Wood	Edible & medicinally important	Saprophytic	Wood ear/ jelly ear
Bolbitiaceae	*Conocybe* sp.	2	Bishnupur	Soil	Unknown	Saprophytic	––
Boletaceae	*Boletus* sp.	14	Joypur	Soil	Edible	Mycorrhizal	––
	Tylophilus sp.	2	Bishnupur	Soil	Edible	Mycorrhizal	Bitter bolete
Bondarzewiaceae	*Amylosporus* sp.	4	Bankadaha	Wood	Unknown	Saprophytic	––
Clavariaceae	*Clavaria* sp.	38	Bishnupur	Soil	Edible	Saprophytic	Fairy fingers
Clavulinaceae	*Clavulina cristata*	6	Sonamukhi, Bankadaha	Soil	Edible	Saprophytic	White coral fungus
Crepidotaceae	*Crepidotus* sp.	15	Bankadaha	Wood	Inedible	Saprophytic	Jelly crep
Dacrymycelaceae	*Dacryopinax spathularia*	7	Bankadaha	Wood	Edible	Saprophytic	Jelly fungus
Diplocystaceae	*Astraeus* sp.	1	Sonamukhi	Soil	Edible & medicinally important	Mycorrhizal	––
Fomitopsidaceae	*Daedalea quercina*	3	Sonamukhi	Wood	Inedible & medicinally important	Saprophytic	Oak mazegill
Ganodermataceae	*Ganoderma lucidum*	7	Taldangra, Joypur	Wood	Inedible & medicinally important	Parasitic	Lingzhi or Reishi mushroom
	Ganoderma applanatum	2	Sonamukhi, Bankadaha	Wood	Edible & medicinally important	Parasitic	Artist's conk/ bear bread
	Ganoderma sp.	2	Bishnupur	Wood	Unknown	Parasite	Conks
Hydnangiaceae	*Laccaria laccata*	3	Sonamukhi	Wood	Edible & medicinally important	Mycorrhizal	Waxy Laccaria
Hypoxylaceae	*Daldinia concentrica*	7	Bankadaha, Bishnupur	Organic matter	Inedible	Saprophytic	Cramp balls/ coal fungus/ Kath chhatu
Lyophyllaceae	*Calocybe indica*	7	Taldangra	Soil	Edible	Mycorrhizal	Doodh chhatu/milky mushroom
	Termitomyces heimii	22	Joypur, Bishnupur	Soil	Edible	Terricolous-saprotrophic	Sib chhatu/ Sikh chhatu
Marasmiaceae	*Marasmius vladimirii*	9	Sonamukhi	Soil	Unknown	Saprophytic	––
	Marasmius sp.	103	Bankadaha, Bishnupur, Taldangra, Sonamukhi, Joypur	Wood/ leaf/soil	Unknown	Saprophytic	––
Meripilaceae	*Grifola frondosa*	4	Joypur, Bishnupur	Soil	Edible & medicinally important	Parasitic	Hen of the woods
	Rigidoporus lineatus	1	Taldangra	Wood	Edible	Parasitic	––
Meruliaceae	*Podoscypha vensustula*	1	Sonamukhi	Leaf	Unknown	Saprophytic/ Parasitic	Bracket fungi
Nidulariaceae	*Cyathus striatus*	7	Sonamukhi	Organic matter	Inedible	Saprophytic	Fluted bird's nest
Phallaceae	*Phallus indusiatus*	1	Sonamukhi	Soil	Edible	Mycorrhizal	Basket Chhatu
Pleurotaceae	*Pleurotus ostreatus*	2	Taldangra	Wood	Edible & medicinally important	Saprophytic	Pearl oyster mushroom
	Pleurotus sp.	12	Bishnupur, Sonamukhi	Wood	Edible	Saprophytic	Oyster mushroom

Table 1. Continued.

Family	Scientific name	Observed frequency	Site of collection	Habitat	Significance	Mode of nutrition	Common/ Local name
Polyporaceae	*Coriolopsis occidentalis*	7	Bankadaha	Wood	Unknown	Saprophytic	––
	Coriolopsis sp.	5	Bishnupur	Wood	Unknown	Saprophytic	––
	Polyporus sp.	6	Bishnupur, Bankadaha, Joypur	Wood	Edible	Saprophytic	Spring polypore
	Pycnoporus cinnabarinus	3	Sonamukhi	Wood	Inedible	Saprophytic	Cinnabar polypore
	Pycnoporus sp.	5	Bishnupur, Taldangra	Wood	Inedible	Saprophytic	Cinnabar-red polypore
Psathyrellaceae	*Coprinus lagopus*	1	Sonamukhi	Organic matter	Edible & medicinally important	Saprophytic	Hare's foot inkcap
	Cystoagaricus sp.	1	Sonamukhi	Soil	Inedible	Saprophytic	––
	Coprinopsis sp.	1	Bishnupur	Soil	Inedible	Saprophytic	Ink cap
Pyronemataceae	*Aleureia aurantia*	12	Bankadaha	Wood	Edible	Saprophytic	Orange peel fungus
Russulaceae	*Lactarius* sp.	6	Bankadaha Sonamukhi	Soil	Edible	Mycorrhizal	Milkcaps
	Russula cyanoxantha	3	Bankadaha, Bishnupur	Soil	Edible & medicinally important	Mycorrhizal	The sickener or vomiting/ jam patra
	Russula emetica	2	Bishnupur	Soil	Inedible	Mycorrhizal	Beechwood sickener/ murgi oat
	Russula nobilis	1	Joypur	Soil	Inedible	Mycorrhizal	Beechwood sickener
	Russula rosea	2	Joypur	Soil	Edible	Mycorrhizal	Rosy russula
	Russula sp.	4	Joypur, Bishnupur	Soil	Unknown	Mycorrhizal	Charcoal burner
Schizophyllaceae	*Schizophyllum commune*	24	Taldangra	Wood	Edible & medicinally important	Mycorrhizal	Pakha chhatu
	Schizophyllum sp.	23	Bishnupur, Bankadaha	Wood	Inedible & medicinally important	Mycorrhizal	Split gill mushroom
Sclerodermataceae	*Scleroderma citrinum*	8	Joypur	Soil	Inedible	Mycorrhizal	Common earthball
Tremellaceae	*Tremella fuciformis*	7	Sonamukhi	Wood	Edible & medicinally important	Saprophytic	Snow fungus
Xylariaceae	*Xylaria* sp.	160	Sonamukhi, Joypur	Wood	Inedible & medicinally important	Saprophytic	Dead man's finger

Table 2. Species diversity richness and abundance of mushrooms in forest areas of Bankura District, West Bengal, India.

	Sonamukhi	Bishnupur	Bankadaha	Joypur	Taldangra
No. of families	17	14	13	8	8
No. of genera	18	16	15	9	11
Family/ genus ratio	0.94	0.88	0.87	0.89	0.73
No. of species (s)	20	18	15	11	11
Genus/ species ratio	0.9	0.89	1.0	0.82	1.0
Total number of individuals (N)	185	114	86	142	69
Simpson diversity index (1-D)	0.2763	0.1532	0.0949	0.2998	0.1914
Shannon diversity index (H)	0.83	1.11	1.25	0.74	1.03
Richness (S)	1.47	1.69	1.62	0.92	1.32
Evenness (e)	0.83	1.81	2.06	1.52	1.82

genus ratio of 0.94 and genus/ species ratio of 0.90 suggest the presence of higher familial and generic diversity in the area. Out of 20 species in Sonamukhi, *Pycnoporus cinnabarinus*, *Tremella fuciformis*, *Marasmius vladimirii*, *Leucocoprinus birnbaumii*, *Cyathus striatus*, *Podoscypha venustula*, *Daedalea quercina*, *Laccaria laccata*, *Coprinus logopus*, *Phallus indusiatus*, *Cystoagaricus* sp. and *Astraeus* sp. were collected only at this site. The Simpson and Shannon's diversity index were found to be 0.2763 and 0.83 respectively; evenness was found to be 0.83 and species richness was

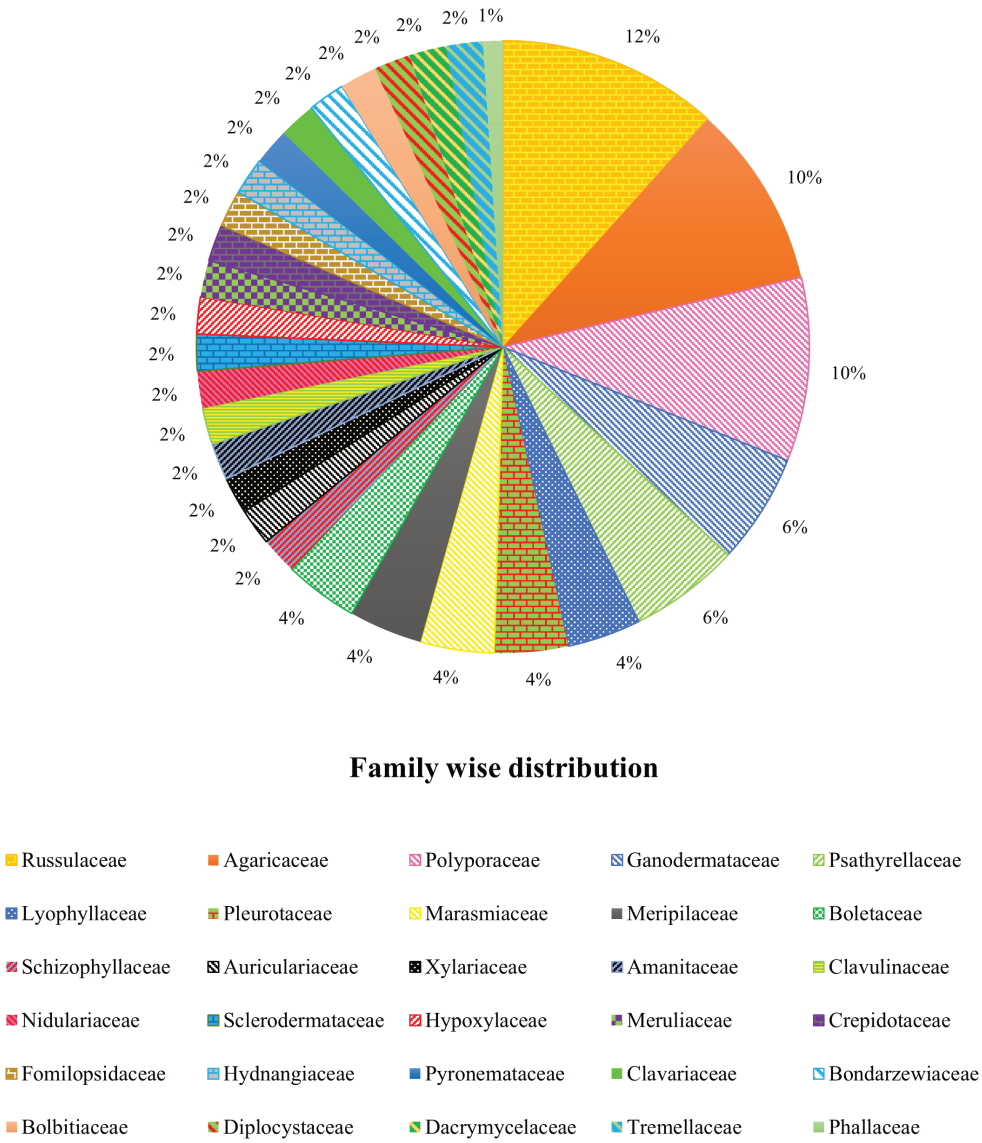

Figure 2. Diversity of mushrooms in forest areas of Bankura District, West Bengal, India.

found to be 1.47. Though the species richness is more in this collection area, but species evenness is comparatively less. Hence, the mushroom diversity was found to be less, may be due to the interference of anthropogenic activities.

The forest area of Bishnupur had 18 species of mushrooms belonging to 16 genera and 14 families. A family/ genus ratio of 0.88 and genus/ species ratio of 0.89 suggest the presence of higher familial and generic diversity in the area. Out of 18 species in Bishnupur, *Russula emetica*, *Conocybe* sp., *Coprinopsis* sp., *Tylophilus* sp. and *Clavaria* sp. were exclusively collected only at this site. This implies more diverse mushroom population. This increased diversity of mushrooms may be due to less interference of human activities and more availability of degradable organic materials.

The forest area of Bankadaha had 15 species of mushrooms belonging to 15 genera and 13 families. A family/ genus ratio of 0.87 and genus/ species ratio of 1.0 suggest the presence of higher familial and highest generic diversity in the area. Out of 15 species in Bankadaha, *Coriolopsis occidentalis*, *Aleuria aurantia*, *Dacryopinax spathularia*, *Crepidotus* sp. and *Amylosporus* sp. were obtained only at this site. The Simpson and Shannon's diversity index were found to be 0.0949 and 1.25, respectively; evenness was found to be 2.060, which was highest among all study areas and species richness was found to be 1.62. The diversity index found less in this collection area. This may be due to the reduced availability of

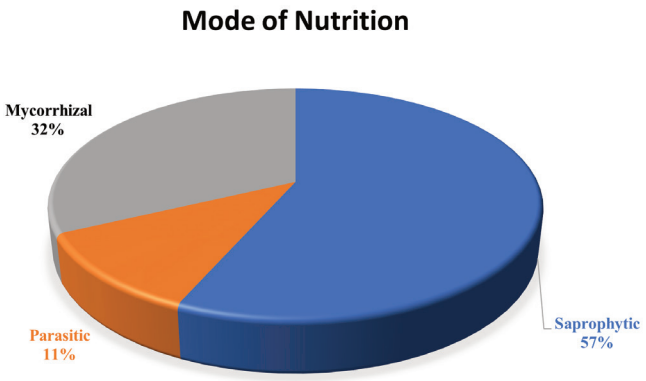

Figure 3. Distribution of mushrooms based on ecological mode of nutrition.

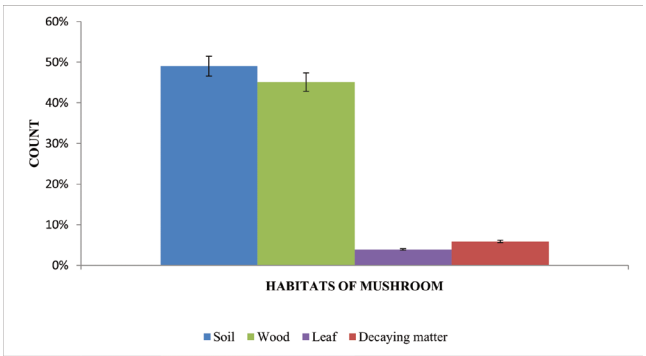

Figure 4. Distribution of mushrooms based on habitat of specimens.

degradable organic matter.

The forest area of Joypur had 11 species of mushrooms belonging to 9 genera and 8 families. A family/ genus ratio of 0.89 and genus/ species ratio of 0.82 suggest the presence of higher familial and generic diversity in the area. Out of 11 species in Joypur, *Scleroderma citrinum*, *Russula nobilis*, *Russula rosea* and *Boletus* sp. were collected only at this site. The Simpson and Shannon's diversity index were found to be 0.2998 and 0.74, respectively; evenness was found to be 1.524 and species richness was found to be 0.92. Though the evenness was more species were found as lowest among all collection areas. This infers to the increased human activity in the forest.

The forest area of Taldangra had 11 species of mushrooms belonging to 11 genera and 8 families. A family/ genus ratio of 0.73 and genus/ species ratio of 1.0 suggest the presence of moderately higher familial and highest generic diversity in the area. Out of 11 species in Taldangra, *Agaricus campestris*, *Calocybe indica*, *Lepiota* sp., *Lycoperdon pyriforme* and *Rigidoporus lineatus* were collected only at this site. The Simpson and Shannon's diversity index were found to be 0.1914 and 1.03 respectively; evenness was found to be 1.82 and species richness was found to be 1.324. The diversity index reflects the decreasing population of mushroom in this collection area due to less availability of organic matter in soil and drastic air pollution of anthropogenic origin.

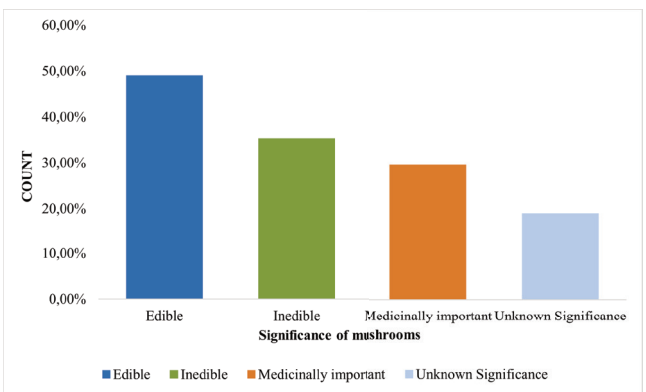

Figure 5. Distribution of mushrooms based on significance of specimens.

Discussion

Mushrooms play a major role in natural and managed ecosystems as ectomycorrhizal fungi. Some fruit bodies of mushrooms from different forest areas of Bankura District are depicted in Fig. 6. They become an important factor for reforestation programme worldwide (Wongchalee and Pukahute 2012). There are several ecological factors, such as geographic location, temperature, relative humidity; light and surrounding flora which greatly influence the growth and development of macrofungi (Kumar et al. 2013). Therefore, the myco-diversity along with the eco-climatic factors of an area is important in a forest community. Here in the study this is focussed in the natural forests of Bankura district, West Bengal.

The overall result shows that human activity and surrounding environment plays a significant role in the population of mushrooms. Less human interference, climatic condition, vegetation and availability of degradable materials in higher amount helps a greater number of litter decomposing and wood rooting mushrooms to colonise. Plant litter mainly grows in the dense forest where the atmosphere contains favourable moisture. It increases the fertility of soil. Thus, it becomes clear that the diversity of mushroom indicates the quality of the ecosystem.

Mushrooms have enormous significance as food material for human and other animals. A wide number of mushrooms are considered to have medicinal importance. The local tribal people also have informed about their

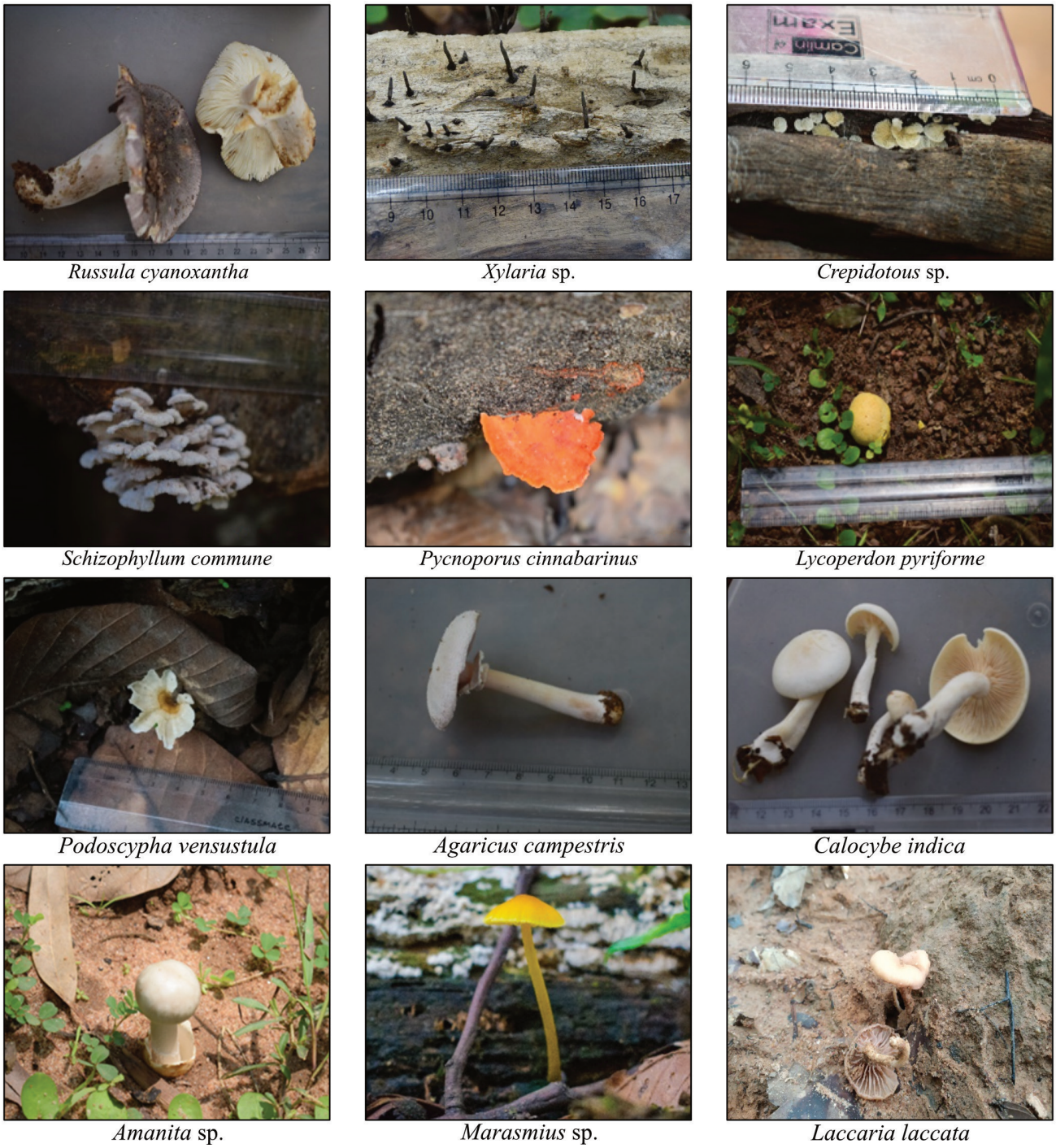

Figure 6(A). Some fruit bodies of mushrooms from the forest areas of Bankura District, West Bengal, India.

habit of consumption of mushrooms for the treatment of several ailments. Further literature study was then performed on the obtained mushrooms.

There is an important aspect regarding the local study on mushroom as they have medicinal importance. 12 obtained genera were medically important. *Ganoderma lucidum,* collected from both Taldangra and Joypur, shows anti-HIV, anti-tumor, anti-cancerous and anti-HSV activities. It is also cytotoxic to hepatoma cells. It is effective against atherosclerosis and type-2 diabetes (Sagar et al.

Figure 6(B). Some fruit bodies of mushrooms from the forest areas of Bankura District, West Bengal, India.

2007). Murrill (1905) found *G. lucidum* for the first time in 1905. *Ganoderma applanatum*, collected from Sonamukhi and Bankadaha, is antagonist to both Gram positive and Gram-negative bacteria. It produces D-glucans which activate the immune response of the host (Nomura et al. 1994). It also shows activity against influenza virus type A. It is useful in the treatment of pain (Sagar et al. 2007). *Russula cyanoxantha*, collected from Bankadaha, may have high phenolic concentration for which it shows great antioxidant and antimicrobial activity (Ribeiro et al. 2008,

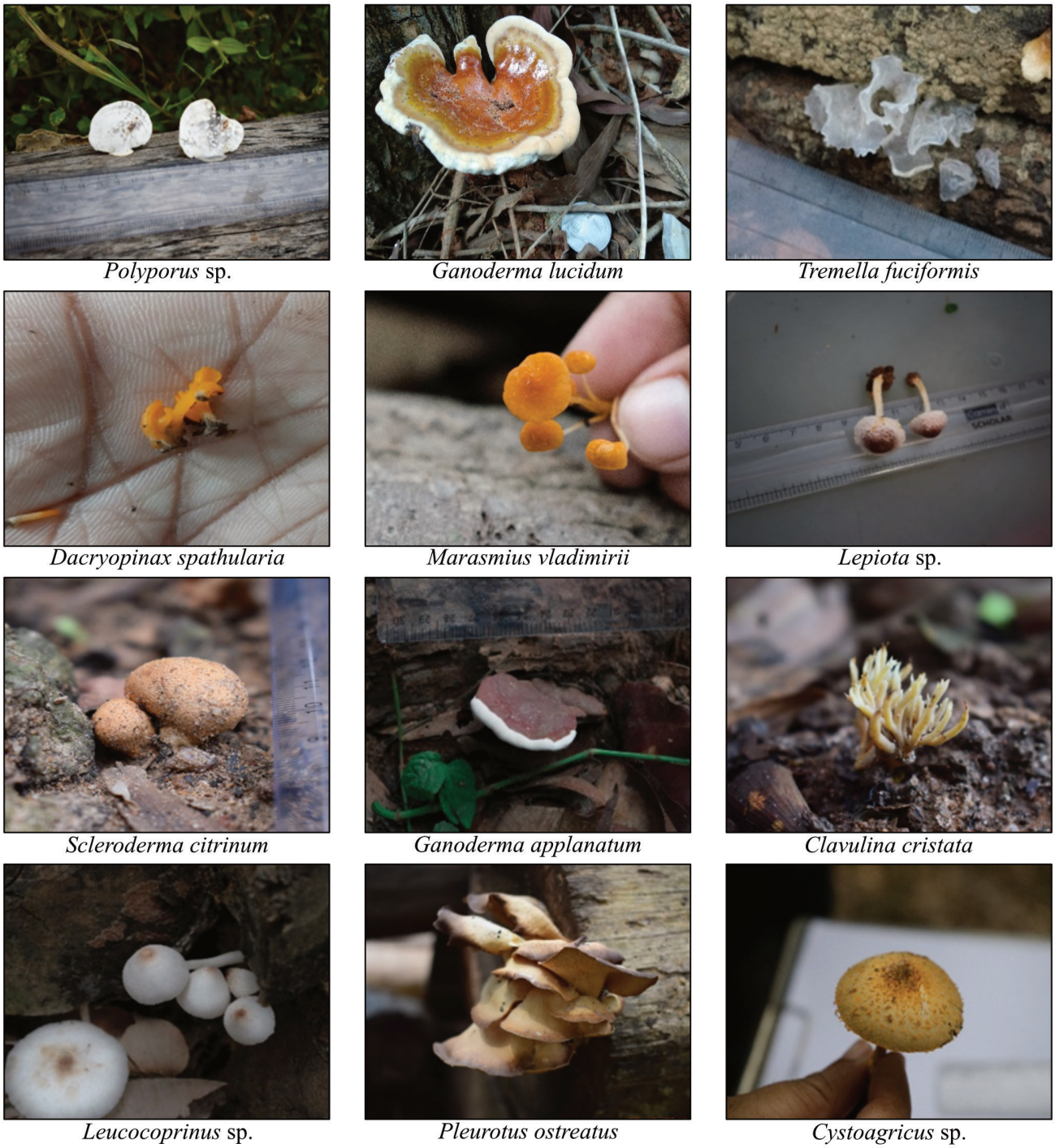

Figure 6(C). Some fruit bodies of mushrooms from the forest areas of Bankura District, West Bengal, India.

Kosanić and Ranković 2016). *Tremella fuciformis*, collected from Sonamukhi, is well known for its remarkable anti-aging, anti-wrinkle and nutraceutical properties. It also shows anti-tumor, anti-decrepitude and anti- thrombus activities (Zhang et al. 2007). *Auricularia* sp., collected from Bankadaha and Sonamukhi, have high antioxidative properties along with hyperglycaemia, immunomodulating, anti-inflammatory and anti-radiative bioactivity. It also lowers hyper-cholesterol and maintains blood sugar level (Zhang et al. 2007). *Astraeus* sp., collected from *Bishnupur,*

contains polysaccharide which increases macrophage stimulation (Mallick et al. 2007). *Laccaria laccata*, collected from Sonamukhi, acts as an effective biocatalyst in organic media (Rahi and Malik 2016). *Pleurotus ostreatus*, collected from Taldangra, has the potentiality to neutralize HIV through degradation of viral genetic material (Nomura et al. 1994). It shows bioactivity against hyperglycaemia, atherosclerotic and tumor patients (Sagar et al. 2007). It has also been reported for its hypocholesterolaemia and hypolipidemic properties (Wasser and Weis 1999). *Coprinus logopus*, collected from Sonamukhi, is reported to inhibit the growth of sarcoma 180 and Ehrlich Solid cancer by 100% and 90%, respectively, and is also effective against Gram-positive and Gram-negative bacteria (Coletto and Striano 2000). *Schizophyllum commune*, collected from Taldangra, is pharmacologically very important as it produces polysaccharide, schizophyllan (β-D-glucan), which shows anti-cancer activity in xenography and anti-tumoral activity in clinical practice (Ooi and Liu 2000). *Xylaria* sp., collected from Joypur and Sonamukhi had been proved as a valuable source of bioactive compounds such as chemokine receptor (CCR5) antagonist 19, 20-epoxycytochalasin Q (Ramesh et al. 2014). *Daedalea quercina*, collected from Sonamukhi forest, is capable of producing an anti-inflammatory compound named quercinol (Gebhardt et al. 2007).

The previous studies also indicated potential therapeutic and immunostimulatory role of wild mushrooms. Pushpa and Purushothama (2012) recorded 90 species in 46 genera belonging to 19 families in and around Bangalore, Karnataka and the Simpson and Shannon diversity index were found to be 0.8 and 1.24 respectively. Altogether 98 macrofungal species representing 72 genera belonging to 47 families were recorded in the Eastern Himalayan ecosystem and the Simpson and Shannon biodiversity index was found ranging from 0.07-0.86 and 0.16-2.13 respectively (Pradhan et al. 2016). Earlier, Pradhan et al. (2010) summarised the role of Wild Edible Mushrooms (WEMs) in the *Santal* livelihood in lateritic region of West Bengal and recorded 21 species of WEMs from the villages as well as Sal forests. In 2013, a case study of macrofungal diversity and habitat specificity of lateritic regions of West Bengal revealed 122 species, belonging to 11 orders, 29 families and 70 genera (Pradhan et al. 2013). Dutta et al. (2013) studied the macrofungal diversity and ecology of the mangrove ecosystem in the Indian part of *Sundarbans* and recorded 59 species over 25 families. A total number of 71 species in 41 genera belonging to 24 families were recorded in *Gurguripal* eco-forest of *Paschim Medinipur*, West Bengal and the Simpson and Shannon biodiversity index was found to be 0.92 and 2.206 respectively (Singha et al. 2017a). Chakraborty (2019) recorded a total number of 82 macrofungal species in 60 genera belonging to 30 families in 12 orders from the locality of 8 blocks of *Dakshin Dinajpur* district of West Bengal.

At the time of survey, some species may lack fruit bodies or have a sporulating strategy that is disproportional to their underground abundance (Baptista et al. 2010). This is the reason why the study conducted for a span of limited durations has a propensity for reflecting inadequate diversity profiles. Therefore, long term observation in specific time interval is required for betterment and adding to the current understanding of structure of regional mushroom assembles and species diversity (Straatsma and Krisai-Greilhuber 2003). The present study revealed the rich diversity of macrofungal population in the study area. The moderate rainfall in the study area supported a rich flora. However, the medicinal and edible properties of maximum mushrooms were mostly unknown to the local people. More studies are required to explore the cryptogamic mushrooms in the forest region of Bankura District.

Conclusion

The present study is the first systematic study of mushrooms distributed in the forest areas of Bankura District. There was no documentation on any ethno-mycological diversity of mushrooms till date. This is an important first step towards producing a checklist of mushrooms in this territory. However, the list of macrofungi in this study provides baseline information needed for the assessment of changes in biological diversity of mushroom.

The importance of mushrooms is not only in the ecosystem dynamics but also in human nutrition and health. Hence, it increases the need for the conservation of these non-timber forest product resources. Overall, the present study has revealed rich macrofungal diversity.

However, there are several mushrooms whose economic importance still unknown. Future investigation is needed in different seasons as well as in other different forest regions. It will result the identification of new exotic species of mushroom-flora, which will represent a complete overview on the mushroom flora of different forest areas of Bankura.

Acknowledgement

The authors are thankful to all forest offices (Bishnupur, Joypur, Sonamukhi, Taldangra and Bankadaha) for granting permission to carry out this research work on wild mushrooms.

References

Acharya K, Pradhan P (2017) Common Wild Mushrooms of West Bengal: (1-121, i-vi). West Bengal Biodiversity Board, Kolkata.

Arnolds E (1988) The changing macromycete flora in the Netherlands. Trans Brit Mycol Soc 90:391-406.

Aung OM, Soytong K, Hyde KD (2008) Diversity of entomopathogenic fungi in rainforests of Chiang Mai Province. Thailand. Fung Diver 30:15-22.

Baptista P, Martins A, Tavares RM, Lino-Neto T (2010) Diversity and fruiting pattern of macrofungi associated with chestnut (*Castanea sativa*) in the Trás-os-Montes region (Northwest Portugal). Fungal Ecol 3(1):9-19.

Basu PS, Banerjee A, Palit D (2013) Assessment of diversity and resource potential of non-timber forest product (NTFP) in selected sites of Bishnupur forest division of Bankura district, West Bengal, India. N Y Sci J 6:46-53.

Biswas G, Nandi S, Kuila D, Acharya K (2017) A comprehensive review on food and medicinal prospects of *Astraeus hygrometricus*. Phcog J 9(6):799-806.

Butler EJ, Bisby GR (1931) The Fungi of India, Scientific monograph. Indian Council of Agricultural Research 18:1-233.

Chakraborty TK (2019) Macrofungi of Dakshin Dinajpur of West Bengal, India. NeBio 10(2):66-76.

Chang ST, Buswell A (1996) Mushroom nutraceuticals. World J Microbiol Biotechnol 12(5):473-476.

Chang ST, Miles PG (2004) Mushrooms: cultivation, nutritional value, medicinal effect and environmental impact, CRC Press, United States.

Coletto MAB, Striano B (2000) Antibiotic activity in basidiomycetes. XIII. Antibiotic activity of mycelia and cultural filtrates. Allionia 37:253-255.

Das Mohapatra PK, Biswas I, Mondal KC, Pati BR (2020) Concomitant yield optimization of tannase and gallic acid by *Bacillus licheniformis* KBR6 through submerged fermentation: An industrial approach. Acta Biol Szeged 64(2):151-158

Das K, Paul PK (2015) Soil moisture retrieval model by using RISAT-1, C-band data in tropical dry and sub-humid zone of Bankura district of India. Egypt J Remote Sens Space Sci 18(2):297-310.

Das SK, Mandal A, Dutta AK, Das D, Paul R, Saha A, Sengupta S, Gupta S, Halder S (2015) Identification of wild edible mushrooms from tropical dry deciduous forest of Eastern Chota Nagpur Plateau, West Bengal, India. Proc Natl Acad Sci India Sect B Biol Sci 85(1):219-232.

Deshmukh SK (2004) Biodiversity of tropical Basidiomycetes as sources of novel secondary metabolites. Microbiology and Biotechnology for Sustainable Development. CBS Publishers and Distributors, New Delhi, 121-140.

Deshmukh SK, Natarajan K, Verekar SA (2006) Poisonous and hallucinogenic mushrooms of India. Int J Med Mushrooms 8(3):251-262.

Dutta AK, Acharya K (2014) Traditional and ethno-medical knowledge of mushrooms in West Bengal, India. Asian J Pharm Clin Res 7:36-41.

Dutta AK, Pradhan P, Basu SK, Acharya K (2013) Macrofungal diversity and ecology of the mangrove ecosystem in the Indian part of Sundarbans. Biodiversity 14(4):196-206.

Gebhardt P, Dornberger K, Gollmick FA, Gräfe U, Härtl A, Görls H, Schlegel B, Hertweck C (2007) Quercinol, an anti-inflammatory chromene from the wood-rotting fungus *Daedalea quercina* (Oak Mazegill). Bioorg Med Chem Lett 17(9):2558-2560.

Hawksworth DL, Kirk PM, Sutton BC, Pegler DN (1995) Ainsworth and Bisby's Dictionary of the Fungi, 8th Ed., IMI CAB International, Wallingford, Oxon, U.K. 616.

Kaul TN, Watling R, Frankland JC, Anisworth AM, Isaac S, Robinson CH (2002) Conservation of mycodiversity in India: An appraisal. Tropical Mycology (CABI Publishing). 1:131-147.

Kinge TR, Apalah NA, Nji TM, Acha AN, Mih AM (2017) Species richness and traditional knowledge of macrofungi (mushrooms) in the Awing Forest Reserve and Communities, Northwest Region, Cameroon. J Mycol 2017(1):1-9.

Kosanić M, Ranković B (2016) Bioactivity of edible mushrooms. Zbornik radova 2. / XXI savetovanje o biotehnologiji sa međunarodnim učešćem 21(24):645-650.

Kumar R, Tapwal A, Pandey S, Borah RK, Borah D, Borgohain J (2013) Macro-fungal diversity and nutrient content of some edible mushrooms of Nagaland, India. Nusantara Biosci 5(1):1-7.

Majumder S, Patra S (1993) Prospects of dryland farming in West Bengal: A case study in Bankura district. Indian J Agric Econ 48:246-254.

Mallick SK, Bhutia SK, Maiti TK (2007) Macrophage stimulation by polysaccharides isolated from barometer earthstar mushroom, *Astraeus hygrometricus* (Pers.) Morgan (Gasteromycetideae). Int J Med Mushrooms 11(3):237-248.

Margalef R (2008) Correspondence between the classic types of lakes and the structural and dynamic properties of their populations: With 1 figure and 2 tables in the text. Verh Int Ver Theor Angew Limnol 15(1):169-170.

Menhinick EF (1964) A comparison of some species-individuals diversity indices applied to samples of field insects. Ecology 45:859-861.

Mueller GM, Bills GF, Foster MS (2004) Recommended protocols for sampling macrofungi. Elsevier Academic Press, Burlington.169-172.

Murrill WA (1905) Tomophagus for dendrophagus. Tor-

reya 5:197.
Nad S, Mandal A, Das Mohapatra PK, Ganguly A (2021) Herbal drug: A natural bioactive formulation & its scope against viral diseases. In Sinha D, Ed., Handbook of Agriculture & Plant Sciences. ABS Books Publisher, New Delhi, India. 187-230.
Nomura H, Inokuchi N, Kobayashi H, Koyama T, Iwama M, Ohgi K, Irie M (1994) Purification and primary structure of a new guanylic acid specific ribonuclease from *Pleurotus ostreatus*. J Biochem 116(1):26-33.
Ooi VEC, Liu F (2000) Immunomodulation and anti-cancer activity of polysaccharide-protein complexes. Curr Med Chem 7(7):715-729.
Pielou EC (1996) The measurement of diversity in different types of biological collections. J Theor Biol 13:131-144.
Pradhan P, Banerjee S, Roy A, Acharya K (2010) Role of wild edible mushrooms in the Santal livelihood in lateritic region of West Bengal. J Bot Soc Bengal 64(1):61-65.
Pradhan P, Dutta AK, Paloi S, Roy A, Acharya K (2016) Diversity and distribution of macrofungi in the Eastern Himalayan ecosystem. Eurasia J Biosci 10(1):1-12.
Pradhan P, Dutta AK, Roy A, Basu SK, Acharya K (2013) Macrofungal diversity and habitat specificity: a case study. Biodiversity 14(3):147-161.
Purkayastha RP, Chandra A (1985) Manual of Indian Edible Mushrooms. Today and Tomorrows Printers and Publishers, New Delhi. 192-194.
Pushpa H, Purushothama KB (2012) Biodiversity of mushrooms in and around Bangalore (Karnataka), India. Am Eurasian J Agric Environ Sci 12(6):750-759.
Rahi DK, Malik D (2016) Diversity of mushrooms and their metabolites of nutraceutical and therapeutic significance. J Mycol 1-18.
Ramesh V, Karunakaran C, Rajendran A (2014) Optimization of submerged culture conditions for mycelial biomass production with enhanced antibacterial activity of the medicinal macro fungus *Xylaria* sp. strain R006 against drug resistant bacterial pathogens. Curr Res Environ Appl Mycol 4(1):88-98.
Ribeiro B, Lopes R, Andrade PB, Seabra RM, Gonçalves RF, Baptista P, Quelhas I (2008) Comparative study of phytochemicals and antioxidant potential of wild edible mushroom caps and stipes. Food Chem 110(1):47-56.
Sagar A, Gautan C, Sehgal AK (2007) Studies on some medicinal mushrooms of Himachal Pradesh. Indian J Mushrooms 25:8-14.
Simpson EH (1949) Measurement of diversity. Nature 163:688.
Singha K, Banerjee A, Pati BR, Das Mohapatra PK (2017a) Eco-diversity, productivity and distribution frequency of mushrooms in Gurguripal Eco-Forest, Paschim Medinipur, West Bengal, India. Curr Res Environ Appl Mycol 7:8-18.
Singha K, Pati BR, Mondal KC, Das Mohapatra PK (2017b) Study of nutritional and antibacterial potential of some wild edible mushrooms from Gurguripal Ecoforest, West Bengal, India. Indian J Biotechnol 16:222-227.
Straatsma G, Krisai-Greilhuber I (2003) Assemblage structure, species richness, abundance, and distribution of fungal fruit bodies in a seven-year plot-based survey near Vienna. Mycol Res 107(5):632-640.
Vasudeva RS (1960) The Fungi of India (revised). Indian J Agric Sci, ICAR, New Delhi. 255.
Wasser SP, Weis AL (1999) Medicinal properties of substances occurring in higher Basidiomycetes mushrooms: current perspectives. Int J Med Mushrooms 1(1):31-62.
Wongchalee P, Pukahute C (2012) Diversity of mushrooms in Dry Dipterocarp forest at Phuphan National Park, Sakon Nakhon Province. Nat Sci 4:1153-1160.
Zhang M, Cui SW, Cheung PCK, Wang Q (2007) Antitumor polysaccharides from mushrooms: A review on their isolation process, structural characteristics and antitumor activity. Trends Food Sci Tech 18(1):4-19.

Acta Biologica Szegediensis

Volume 65(2):199-209, 2021
Acta Biologica Szegediensis
http://abs.bibl.u-szeged.hu/index.php/abs
DOI:10.14232/abs.2021.2.199-209

ARTICLE

Diversity of arbuscular mycorrhizal fungi in the rhizosphere of saffron (*Crocus sativus*) plants along with age of plantation in Taliouine region in Morocco

Samah Ourras[1], Soumaya EL Gabardi[1], Ismail El Aymani[1], Najoua Mouden[2], Mohamed Chliyeh[1], Karima Selmaoui[1], Soukaina Msairi[3], Rachid Benkirane[1], Cherkaoui El Modafar[4], Amina Ouazzani Touhami[1], Allal Douira[1]*

[1]Laboratory of Plant, Animal and Agro-Industry Productions, Botany, Biotechnology and Plant Protection Team, Faculty of Sciences, Ibn Tofail University, Kenitra, Morocco
[2]Laboratory of Molecular Chemistry and Environmental Molecules, Multidisciplinary Faculty of Nador-Mohammed 1er University Oujda, Morocco
[3]National Agency of Medicinal and Aromatic Plants, Taounate, Morocco
[4]Center of Agrobiotechnology, Research Unit labelled CNRST (URL-CNRST05), Faculty of Sciences and Techniques Guéliz, Cadi Ayyad University, Marrakech, Morocco

ABSTRACT Saffron cultivation is a viable alternative for marginal areas where low soil fertility and water availability severely limit the cultivation of other crops with higher water and input requirments. Under these conditions, arbuscular mycorrhizal fungi (AMF) are an essential alternative for maintaining fertility and water conservation, stimulating growth, and providing plant protection against soil-borne diseases. The aim of this work is to highlight the diversity of the arbuscular mycorrhizal fungi communities associated with saffron roots in plantations of different ages (two, four and ten years old) in the region of Taliouine (Morocco). The highest number of endomycorrhizal spores was recorded in the rhizosphere of saffron plants harvested at the level of plots that have carried saffron for two years (138.66/100 g soil), while the lowest number was observed in the rhizosphere of plants of plots that are occupied for 10 years by saffron. All collected spores from plots under study represent 17 morphotypes belonging to 5 genera: *Glomus* (7 species), *Acaulospora* (7 species), *Rhizophagus* (one species), *Densicitata* (one species), and *Funneliformis* (one species).

KEY WORDS
diversity
duration of soil exploitation
endomycorrhizae
Morocco
saffron

ARTICLE INFORMATION
Submitted
29 November 2021
Accepted
19 January 2022
***Corresponding author**
E-mail: douiraallal@hotmail.com

Introduction

Saffron (*Crocus sativus* L.) is a very special crop that produces a valuable spice. It is the most expensive spice worldwide. In Morocco, the saffron sector represents a major issue for this local product in both social and economic terms. This sector is a promising way that may help to reduce inequalities in income in saffron areas as Taliouine and Taznakht. However, due to some ancestral cultural practices applied at the level of saffron fields, the lack of information about the behavior of the plant viz-a-viz the environment and the scarce knowledge of the potentialities of the local cultivated crop may constitute a handicap to the sector development.

Among many biotic and abiotic factors that disturb the growth and the yield of saffron plants, the ecological degradation of saffron fields related to plantation age turns out to be the most important (El Aymani et al. 2019). Generally, in Morocco, the cultivation of *C. sativus* L. is carried out in areas with low soil fertility, harboring rhizospheric microorganisms, such as endomycorrhizae that are supposed to be essential for plant growth and ecosystem functioning. Great saffron productivity would be achieved since the agricultural practices applied in field-grown saffron maintain the population of these microorganisms at a suitable level (Onguene 2000). Indeed, numerous studies have reported that soil fertility and productivity are highly correlated with the biological activity of soil microorganisms. The development of plants depends on the interactions they have with the surrounding environment, especially with soil microorganisms. Their importance in natural and semi-natural ecosystems (Sylvia et al. 1992) is to improve the absorption of water and nutrients such as phosphorus, nitrogen, and micronutrients, thereby improving plant growth and resistance to biotic and abiotic stresses (Goussous and Mohammad 2009; Lone et al. 2015).

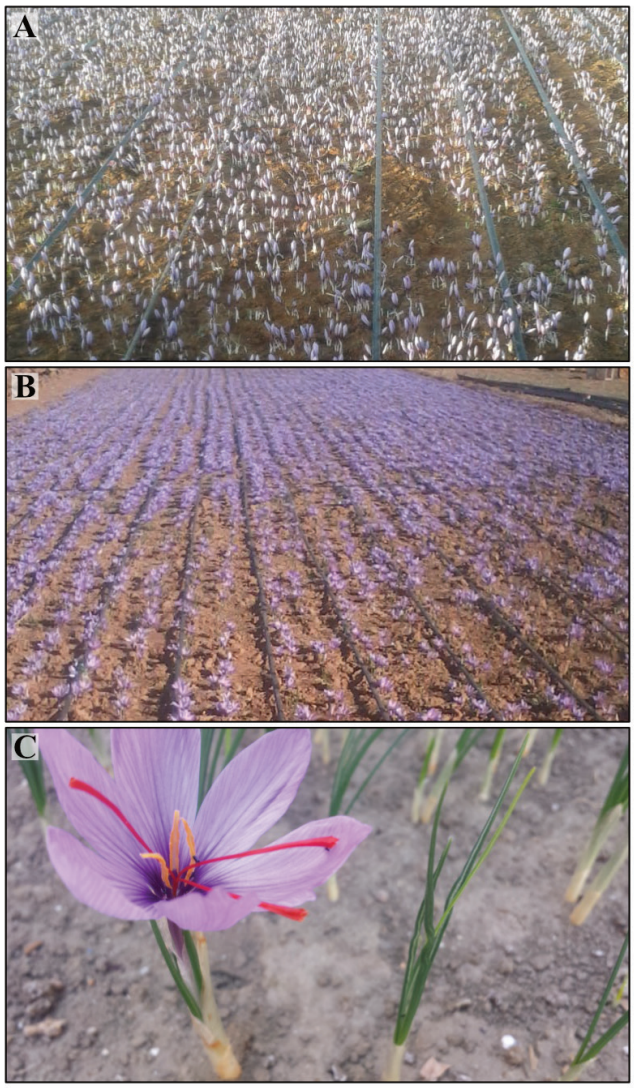

Figure 1. The fields of saffron in bloom. (A): Plot of 2 years of land use of saffron. (B): Plot of 4 years of land use of saffron. (C): Saffron plant at flowering stage or blooming and unflowering saffron plants.

Exploiting the beneficial effects of endomycorrhizae requires an appropriate knowledge regarding the diversity of arbuscular mycorrhizal fungi in areas of saffron crop in Morocco. The most exhaustive possible highlighting of this diversity needs the recruitment of more sites and samples of saffron plant rhizosphere for analysis. In this context, the present study ensures the continuation of the works already undertaken by El Aymani et al. (2019) and Chamkhi et al. (2018, 2019). Therefore, the aim was to assess the effect of the age of saffron plantations on the diversity of the populations of arbuscular mycorrhizal fungi. Such studies are expected to provide a broad overview of AMF communities existing at the rhizosphere level upon agronomic practices and should with time also lead to the selection of the best endomycorrhizal species colonizing the roots of saffron plants.

Materials and methods

Prospecting and sampling

The samples of rhizospheric soil and fine roots of saffron plants were collected in October 2020 from 15 different plots of saffron belonging to the Taliouine area (Morocco). Three lots of plots were selected, each one is characterized by the number of years (2, 4 or 10) of land use by saffron cultivation (Fig. 1). Soil samples were taken from the rhizosphere of plants from a depth of 0-25 cm. Very fine roots, likely to be mycorrhized and easily observable under the microscope, were also collected with the soil in sterilized polythene bags. Each lot of plots was represented by three composite samples after the samplings were homogenized.

Root clearing and staining

The roots were cleaned from soil particles by thorough rinsing with tap water in a sieve. Then only the smallest fine roots were selected. According to the lightening technique described by Philips and Hayman (1970), roots were cut into fragments of approximately 1 to 2 cm and placed in vials containing 10 ml of 10% potassium hydroxide solution. These flasks were then placed in a water bath at 90 °C for 15 min. The root fragments were then bleached by adding a few drops of H_2O_2 to the KOH solution. After 15 min, the fragments were rinsed with distilled water and then stained with a solution of cresyl blue (0.05%) for 15 min.

Assessment of AMF colonization

Evaluation of the mycorrhizal parameters was performed by observing thirty root fragments of about 1 cm, randomly chosen to quantify the mycorrhizae (Amir and Renard 2003; Kormanik and McGraw 1982). These fragments were mounted parallel in groups of 10 to 15 in a drop of glycerine water (8%) between blade and coverslip (Kormanik and McGraw 1982). Each fragment was thoroughly checked over its entire length, at magnifications of 100× and 400×.

The frequency and levels of arbuscules and vesicles of AMF within the root bark were measured by assigning a mycorrhizal index ranging from 0 to 5 (Derkowska et al. 2008): 0: absence; 1: traces; 2: less than 10%; 3: from 11 to 50%; 4: from 51 to 90%; 5: more than 91%.

Frequency of mycorrhization (F%):

$$F\% = 100 \times (N - n0) / N$$

Table 1. Parameters of mycorhization of saffron plant roots in studied sites.

Parameters of mycorhization	Site 2	Site 4	Site 10
Frequency (%)	95.20	88,23	60.40
Intensity of mycorrhization (%)	38.85	31.60	18.32
Arbuscules (%)	36.50	35.80	19.40
Number of spores/100 g soil	138.66	96, 00	71,00

where N is the number of fragments observed and n0 is the number of non-mycorrhizal fragments.

Intensity of mycorrhization (M%):

$$M\% = (95\ n5+70\ n4+30\ n3+5\ n2+n1) / N$$

Where n is the number of affected fragments of the index 0, 1, 2, 3, 4 or 5

Arbuscular content (A%):

$$A\% = (100\ mA3 + 50\ mA2 + 10\ mA1) / 100$$

where mA3, mA2 and mA1 are assigned with the notes A3, A2 and A1, respectively, with mA3 = (95 n5 A3 + 70 n4 A3 + 30 n3 A3 + 5 n2 A3+ n1 A3) / N, as the same for A1, A2.

In this formula, n5A3 represents the number of fragments noted with A3; n4A3 the number of fragments rated 4 with A3; etc.

A0: no arbuscules; A1: few arbuscules (10%); A2: moderately abundant arbuscules (50%); A3: very abundant arbuscules (100%).

Extraction of spores

The spores were extracted from 100 g of each rhizospheric soil sample using the humid sifting technique (Gerdemann and Nicolson 1963), then centrifuged in a sucrose solution (Daniels and Skipper 1982, as modified by Brundrett et al. 1996). After centrifugation (2000 rpm for 4 min), the supernatant was discarded, and a viscosity gradient was created by adding a solution of 50% sucrose into each centrifuge tube. After centrifugation at 5000 rpm for 10 min, the supernatant was poured onto sieve of 2 mm- 50 µm mesh screen. The resulting substrate was rinsed with distilled water to remove sucrose and recovered in an Erlenmeyer flask.

This content was observed with a binocular magnifying glass, by successive samples of small quantities. These aliquots were reversed on filter paper placed in a Petri dish and then observed using a binocular loupe. Microscopic observations of spores were made in a few drops of polyvinyl-lactic acid-glycerol (PVLG) and checked at magnifications of 100x and 400x. A preliminary identification at the genus level was made based on the criteria proposed by Ferrer and Herrera (1981), Berch and Koske (1986), Schenck and Smith (1982), Hall (1987), Schenck and Perez (1987), Morton and Benny (1990), Walker et al. (1982), Dalpé (1995), Pérez and Peroza (2013), Pérez et al. (2012), Monroy et al. (2013), Rodríguez-Morelos et al. (2014), Rajeshkumar et al. (2015), Błaszkowski et al. (2018), and information available in different databases.

Statistical analysis

The statistical treatment of results focused on the analysis of variance to a single criterion of classification (ANOVA).

Results

Study of the diversity of arbuscular mycorrhizal fungi (AMF) in the rhizosphere of *C. sativus* showed that overall roots of saffron plants were mycorrhized and showed the existence of typical structures of mycorrhizae including arbuscules, intra- and extracellular hyphae and spores (Fig. 1, 2, 3 and 4).

As shown in Table 1, the average frequencies of mycorrhization rate, which reflect the inoculum pressure or propagule rate infecting surrounding medium, varied among sites. Thus, the maximum frequency value was 95.20% at site 2 occupied during 2 years by saffron, while the lowest frequency value was 60.40% noted at the site exploited for 10 years. The highest mean percent mycorrhizal root colonization intensity expressing the percent of mycorrhizal root cortex attained 38.85% in roots of saffron plants growing in 2-year-old plantation, while in those from the 10-year-old plantation, the value was 18.32%. The arbuscular content of root at aged plantation site (10 years) was 19.4% and increased to 35.50% and 36.50% at plantation sites operated from four years and six years, respectively, whereas the vesicles were not found (Table 1).

The maximum spore richness (138.66/100 g soil) was observed at plantation site exploited for 2 years, followed by the 4-year-old plantation (96 spores/100 g soil) while the site operated for 10 years contained only 71 spores/100 g soil (Table 1).

Based on morphological criteria of spores (shape, colour, mean size, wall, surface) and hyphal size, 12, 10 and 7 morphotypes of arbuscular mycorrhizal fungi were distinguished in plots occupied along 2, 4 and 10 years by saffron, respectively (Tables 2 and 3; Figs. 1 and 2). The species *Acaulospora mellea*, *Glomus macrocarpum*, *Glomus versiforme* and *Rhizophagus intraradices* were common in three plots. *Acaulospora laevis* and *Densicitata nigra*

Table 2. Occurrence of mycorrhizal species in saffron plantation sites.

Mycorrhizal species	Ages of saffron plantation		
	10 years	4 years	2 years
Acaulospora mellea	+	+	+
Acaulospora foveta	+	+	-
Acaulospora laevis	-	+	+
Acaulospora scorbiculata	-	-	+
Acaulospora sp. 1	+	-	+
Acaulospora sp. 2		-	+
Acaulospora sp. 3	-	-	-
Glomus macrocarpum	+	+	+
Glomus microcarpum	+	-	+
Glomus versiforme	+	+	+
Glomus lamellosum	-	+	-
Glomus deserticola	-	+	-
Glomus sp. 1	-	-	+
Glomus sp. 2	-	+	-
Rhizophagus intraradices	+	+	+
Funneliformis geosporum	-	-	+
Densicitata nigra	-	+	+

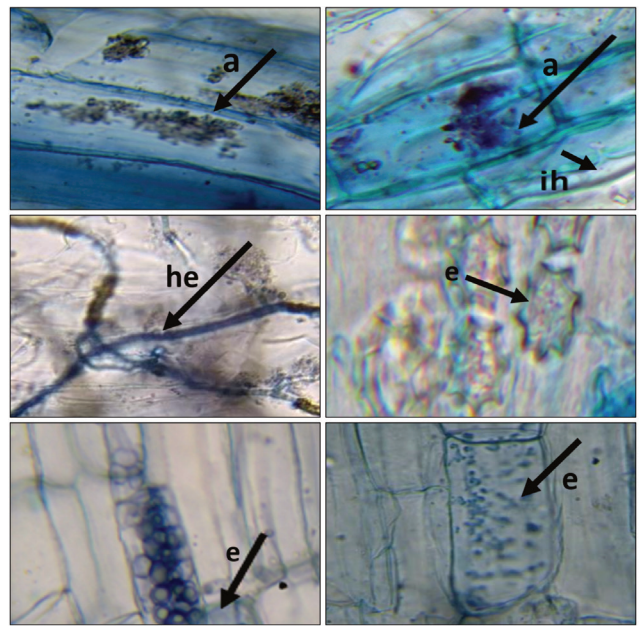

Figure 2. Crocus sativus roots with arbuscular mycorrhizal structures: arbuscles (a); intraductal hyphae (ih); external hyphae (he) and endophytes (e). (G. x 400).

were frequent in 2- and 4-year-old saffron plantations. *Glomus microcarpum* was reported in 2- and 10-year-old saffron plots.

These results show that the optimum of all mycorrhization parameters such as mycorrhization frequency and intensity, number of arbuscules and spores, as well as species richness of arbuscular mycorrhizal fungi was found at the site exploited by saffron for 2 years.

Discussion

Mophological examination of saffron under light microscope revealed the presence of AMF structures among the examined roots which showed different colonization levels. This suggests that *C. sativus* is a mycrotrophic species. In addition, the values of mycorrhization frequency and intensity and the arbuscular contents strongly differ versus age of the saffron plantation. The same observation was fulfilled for spore richness which appeared to be dependent on the age of the plantation. In agreement with our results, El Aymani et al. (2019) reported a smallest richness and mean number of spores in the rhizosphere of saffron plants from 10-year-old plantation with 27 spores/100 g soil and the highest density level at a 4-year-old site (45 spores/100 g soil). Conversely, in the same region, Chamkhi et al. (2019) signaled that the density of AMF spores in Taliouine saffron soils is significantly affected by the plantation age, it is higher in the soil of the oldest saffron plantation (169.33 spores/100 g soil). But these authors did not mention any significant effect of planting or fertilization methods on the density of AMF spores.

The increase of spore density with field age has been mentioned in the literature (Burni et al. 2011; Birhane et al. 2017). These authors related this to increasing soil organic matter and water capacity retention over time. Johnson et al. (1991) found a positive correlation between increased organic matter fraction including elements like carbon and azote and diversity of Glomales spores. Talbi et al. (2016) pointed out that each mycotrophic species may favor the proliferation and dominance of one or many species of endomycorrhizal fungi. The variation often observed can be related to the physicochemical and microbiological properties of the soil (Anderson et al. 1984; Johnson et al. 1991; Houngnandan et al. 2009), to the microclimate fluctuation (Koske 1987; Dalpé et al. 1989), to the vegetation coverage; (Benjamin et al. 1989) and the sampling season (Gemma et al.1989; Bouamri et al. 2006).

The composite endomycorrhizal inoculum containing 26 species monitored in the rhizosphere of olive plants by Semane et al. (2018) for 30 and 42 months revealed a distinct evolution of the initial inoculum numbers of species which were not able to sporulate versus time, while others, viz. four species of *Glomus* (*G. clarum*, *G. intraradices*, *G. mossea* and *G. versiforme*) have been able to maintain a stable sporulation rate in the rhizosphere

Table3. Morphological characteristics of endomycorrhizal species isolated from rhizospheric soil of different aged saffron plantations (2, 4 and 10 years).

Species	Shape of spores	Color of spores	Mean spore size (µm)	Wall surface	Hyphal length (µm)
Glomus microcarpum	Globular	brown	102.36	Granular	-
Acaulospora foveata	Globular	brown	112.36	Granular	-
Acaulospora sp. 1	Ovale	brown	104.2	Smooth	-
Acaulospora mellea	Ovale	yellow brown	115.36	Granular	-
Acaulospora laevis	Globular	brown	102.7	Granular	-
Glomus versiforme	Ovale	brown	104.2	Granular	-
Rhizophagus intraradices	Globular	yellow	91.1	Granular	-
Glomus macrocarpum	Ovale	brown	102.37	Smooth	-
Glomus deserticola	Globular	black	113.51	Granular	-
Densicitata nigra	Globular	brown	86.37	Smooth	-
Glomus sp. 1	Globular	brown	122.37	Granular	-
Glomus lamellosum	Globular	brown	114.14	Granular	-
Funneliformis geosporum	Globular	yellow brown	102.36	Smooth	-
Acaulospora scorbiculata	Globular	yellow	106.18	Smooth	-
Glomus sp. 2	Globular	brown	107.9	Smooth	25.6
Acaulospora sp. 2	Globular	yellow brown	128.36	Granular	-
Acaulospora sp. 3	Globular	brown	124.2	Granular	-

of olive plants. Yang et al. (2010) reported that AMF soil community evolved in the function of environmental conditions and better-adapted AM fungi appeared to replace less-adapted AM fungi as environmental conditions changed.

Studies on AMF linked to the roots and rhizosphere of *C. sativus* plants in saffron-producing countries are still rare. Lone et al. (2016) signaled that the early studies on the AM-saffron fungal association focused on the seasonal variation of spore density in the rhizosphere of saffron plants in Iran (Kianmehr 1981). Zare Maivan and Nakhaei (2000) noted the dominance of *Acaulospora morrowiae* and *Glomus coronatum* among endomycorrhizal species associated with the rhizosphere of three saffron cultivars that grow in the Irano-Turani climatic region. Mohebi-Anabat et al. (2015) found three species belonging to the *Glomus* genus in northeastern Iran (*G. aggregatum*, *G. mosseae* and *G. etunicatum*). In the present paper, the AMF richness of saffron plant rhizosphere in the Taliouine zone was reflected by a total of 17 species making up *Acaulospora mellea*, *A. laevis*, *A. scorbiculata*, *A.* sp. 1, *A.* sp. 2, *Glomus macrocarpum*, *G. microcarpum*, *G.* sp. 1., *G. versiforme*, *Rhizophagus intraradices*, *Funneliformis geosporum*, *A. foveata*, *G.* sp. 2, *G. deserticola*, *G. lamellosum*, *Densicitata nigra* and *Acaulospora* sp. 2. The highest number was 12 species recovered from the rhizosphere of saffron plants originating from 2-year-occupied plots against 7 species in 10-year-occupied plots. The species *A. mellea*, *G. macrocarpum*, *G. versiforme* and *Rhizophagus intraradices* were most common at three lots of plots exploited by saffron for 2, 4 and 10 years, while the most predominant species in saffron-grown fields of 2 and 4 years were *A. laevis* and *Densicitata nigra*. Saffron plots operated for 2 and 10 years shared *G. microcarpum*. There is a difference in the composition and the species richness of the AM fungal community of saffron plants within the same sampling region in comparison with the research work of Chamhki et al. (2019), who reported the occurrence of 10 AMF species in the soil of saffron grown fiels in Taliouine, viz *Glomus tenebrosum*, *G. reticulatum*, *Septoglomus deserticola*, *Sclerocystis taiwanensis*, *Rhizoglomus aggregatum*, *R. intraradices*, *Funneliformis coronatus, Enterophospora infrequens*, *Acaulospora* sp. and *Funneliformis* sp. with the predominance of Glomeraceae family species.

In 5 sites of the same zone, El Aymani et al. (2019) noted the presence of diversified AMF community making up 36 identified species. According to these authors, this diversity varied among sites and increased in the site in four successive years of exploitation by saffron (24 species), which registered the highest Shannon diversity index (H' = 2.82). A regression Shannon index was noted at the sites of six or ten years of occupation by saffron.

According to Fuji et al. (1991), saffron is among the plants that are recognized as strong allelopathic plants. Variations in the AMF population structure among studied plots are likely related to the accumulation of allelopathic substances in the soil. Indeed, Pellissier and Trosset (1989) have reported the negative effect of *Molinia caerulea* on AMF. Afzal et al. (2000) demonstrated that aqueous shoot extracts of *Imperata cylindrica*, an allelopathic herb, reduced

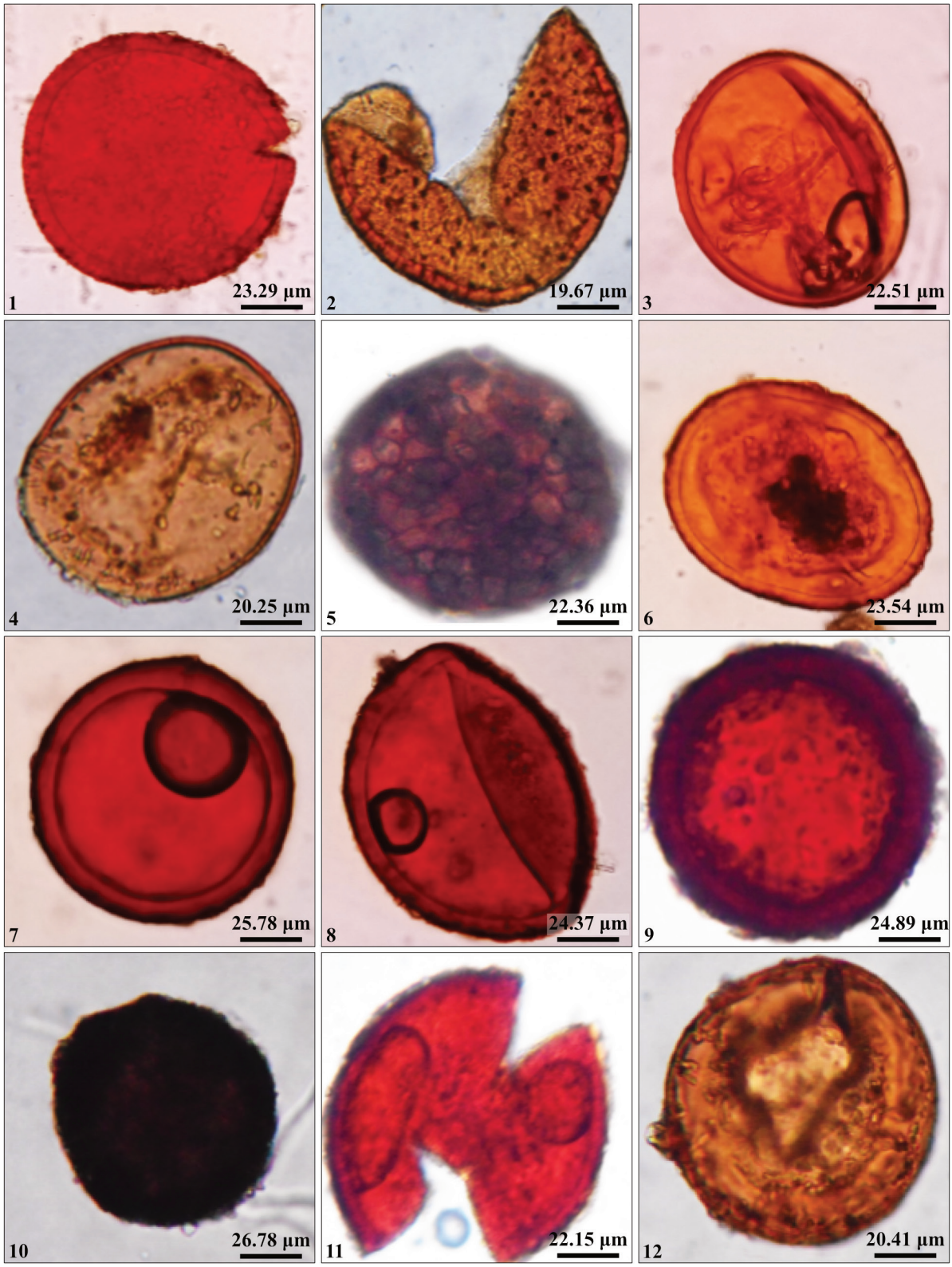

Figure 3. Morphology of some AMF species recovered from the rhizospheric soil of saffron plantations. (1): *Glomus microcarpum*; (2): *Acaulospora foveata*; (3): *Acaulospora* sp. 1; (4): *Acaulospora mellea*; (5): *Acaulospora laevis*; (6): *Glomus versiforme*; (7): *Rhizophagus intraradices*; (8): *Glomus macrocarpum*; (9): *Glomus deserticola*; (10): *Densicitata nigra*; (11): *Glomus* sp. 1; (12): *Glomus lamellosum*.

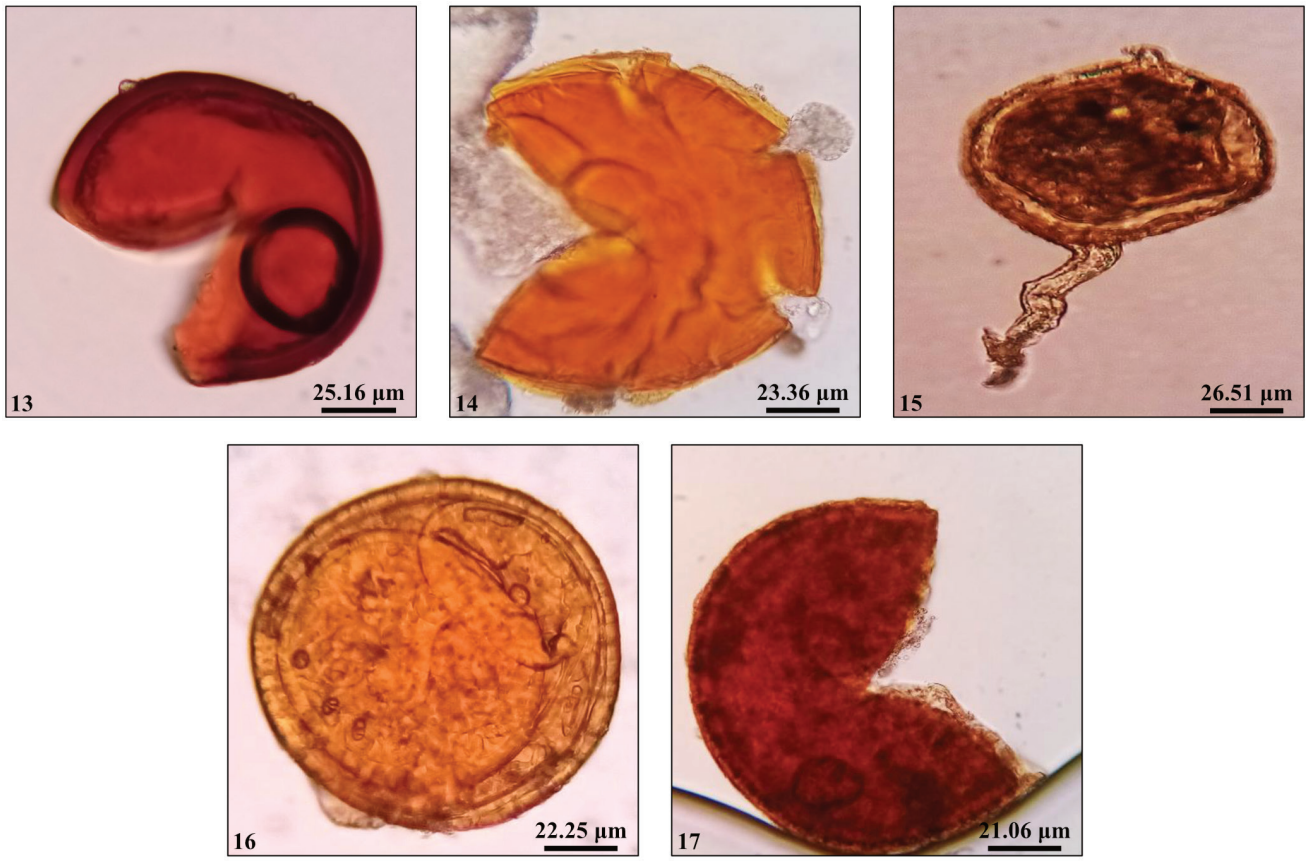

Figure 4: Morphology of some AMF species recovered from the rhizospheric soil of saffron plantations. (13): *Funneliformis geosporum*; (14): *Acaulospora scorbiculata*; (15): *Glomus* sp. 2; (16): *Acaulospora* sp. 2; (17): *Acaulospora* sp. 3.

root endomycorrhizal colonization in *Vigna radiata* (L.) Wlczek and *Phaseolus vulgaris*.

The influence of cultural practices on the populations of rhizospheric microorganisms of saffron plants is not yet well known. Jalali (1962) stated that after one period of cultivation, saffron cannot be cultivated in the same soil. Other researchers found that the continuous saffron cultivation induces some undesirable changes in soil chemical and physical properties (Khozaei et al. 2015). These changes can play an important role in decreasing the saffron yields even after 6 years of cultivation (Khozaei et al. 2015). Azizi Zohan and Sepaskhah (2002) affirmed that the unsuccessful saffron cultivation after one cultivation period can be due to allelopathic effects or accumulation of special salts in the root zone. Qarai and Beiji (1995) noted that the yield decreases with the age of the saffron fields, afterwards the plot becomes unsuitable for cultivation. Following these authors, the probable reason for this diminution can be a change in physicochemical and biochemical properties of soil or the major change in the population of soil microorganisms. Sharif and Moawad (2006) noted that the diversity of AMF species in agricultural systems is highly affected by the types of input. For instance, the effect of the tissue extract of one plant species on the growth or reproduction of another species has been observed in numerous cases (Hoseini and Rizvi 2003; Jadhav et al. 1997; Kobayashi 2004). Jansa et al. (2014) have found that soil properties such as pH, soil fertility and texture, as well as site geography, especially the altitude strongly affected AMF community profiles.

The VA mycorhizae receive increasing attention during the last decades for their potential role in improving agricultural yield of economic crops (Mosse and Hayman 1971; Powell and Daniel 1978; Powell 1979; Kormanik et al. 1982; Fontana 1985; Strullu 1990). Indeed, these fungi are essential components of soil-plant systems (Smith and Read 2008; Van Der Heijden et al. (1998), they improved phosphorus assimilation, micronutrients (Bürkert and Robson 1994) and azote (Barea et al. 1991). They improved water nutrition and provided a greater tolerance to abiotic constraints to different host plants (Smith and Read 2008; Campagnac et al. 2010; Miransari 2010), like drought (Dalpé 2005; Gianinazzi et al. 2010; Pozo et al. 2013), organic pollutants and heavy metals (Joner

and Leyval 2001). The potential of AMF as biocontrol agents has also been proved for various root infections (Khaosaad et al. 2007; Fiorilli et al. 2011). The optimization of the symbiotic potential of the endomycorrhizal species taking place in the studied sites deems necessary to improve the productivity of the saffron culture and reduce the damage caused by fungal telluric pathogens. These symbionts will be able to increase the agronomic efficiency of phosphates and the resistance of the plants to different types of biotic and abiotic stresses. In this sense, it is very important to give a great importance to the multiplication and the production of a composite endomycorrhizal inoculum based on all the met species that will serve for the treatment of the corms of saffron destined to the culture. Indeed, according to Deirdre et al. (2009), arbuscular mycorrhizal fungi represent one of the key groups to ensure sustainable productivity of this agricultural system.

Through this study we can confirm the diversity of indigenous AMF community associated with saffron plants grown in Taliouine, the primary area of saffron production in Morocco and to underline the variation of AMF community structure versus age of saffron plantation. Therefore, it is time to explore the efficacy of different AMF species and identify the most effective association for developing a composite endomycorrhizal inoculum as a more suitable and environmentally acceptable alternative enabling to preserve, improve yield and protect saffron plants from telluric bio-agressors. It also may help to formulate, based on this inoculum, a biostimulant and biofungicide used in new agricultural practices for a sustainable agriculture less dependent on chemical inputs.

Acknowledgments

This study was conducted under the research project of the 2nd PMA 2020/11, entitled 'Elaboration d'un produit biofertilisant et biopesticide, à base de champignons endophytes, adapté à la protection et l'amélioration de la productivité du safran au Maroc' financed by 'Agence Nationale des Plantes Médicinales et Aromatique' et l'Université Ibn Tofail, Kénitra, Morocco'.

References

Afzal B, Bajwa R, Javaid A (2000) Allelopathy and VA mycorrhiza VII: Cultivation of *Vigna radiata* and *Phaseolus vulgaris* under allelopathic stress caused by *Imperata cylindrica*. Pak J Biol Sci 3(11):1926-1928.

Amir H, Renard A (2003) Etude microbiologique générale de quelques sols de forêts sclérophylles de Nouvelle-Calédonies: Statuts des mycorhizes à arbuscules. PCFS-UNC CP 54:22.

Anderson RC, Liberta AE, Dickman LA (1984) Interaction of vascular plants and vesicular-arbuscular mycorrhizal fungi across a soil moisture-nutrient gradient. Oecologia 64:111-117.

El Aymani I, Qostal S, Mouden N, Selmaoui K, Touhami AO, Benkirane R, Douira A (2019) Fungi associated with saffron (*Crocus sativus*) in Morocco. Plant Cell Biotechnol Mol Biol 20:1180-1188.

Azizi Zohan A, Sepaskhah AR (2002) The effect of leaching on soil improving and recultivation of saffron. Iran Seventh Congress of Agronomy, Karaj. p. 228. [In Persian]

Barea JM, Azcon Aguilar C, Azcon R (1991) The role of vesicular-arbuscular mycorrhizae in improving plant N acquisition from soil as assessed with ^{15}N. IAEA-SM 313/67 Ed. Stable Isotopes in Plant Nutrition. Soil Fertility and Environmental Studies. International Atomic Energy Agency, Vienna. 209-216.

Benjamin P, Anderson RC, Liberta AE (1989) Vesicular-arbuscular mycorrhizal ecology of little bluestem across a prairie-forest gradient. Can J Bot 67:2678-2685.

Berch SM, Koske RE (1986) *Glomus pansihalos*, a new species in the Endogonaceae, Zygomycetes. Mycologia 78(5):832-836.

Birhane E, Gebremedihin KM, Tadesse T, Hailemariam M, Solomon N (2017) Exclosures restored the density and root colonization of arbuscular mycorrhizal fungi in Tigray, Northern Ethiopia. Ecol Process 6:33.

Błaszkowski J, Kozłowska A, Niezgoda P, Goto BT, Dalpé Y (2018) A new genus, *Oehlia* with *Oehlia diaphana* comb. nov. and an emended description of *Rhizoglomus vesiculiferum* comb. nov. in the Glomeromycotina. Nova Hedwigia 107(3-4):501-518.

Bouamri B, Dalpé Y, Serrhini MN, Bennani A (2006) Arbuscular mycorrhizal fungi species associated with rhizosphere of *Phoenix dactylifera* L. in Morocco. Afr J Biotech 5(6):510-516.

Brundrett M, Bougher N, Dell B, Grove T, Malajczuk N (1996) Working with mycorrhizas in forestry and agriculture. Vol. 32. Australian Centre for International Agricultural Research, Canberra. p. 374.

Bürkert B, Robson A (1994) 65Zn uptake in subterranean clover (*Trifolium subterraneum* L) by 3 vesicular-arbuscular mycorrhizal fungi in a root-free sandy soil. Soil Biol Biochem 26:1117-1124

Burni T, Hussain F, Sharief M (2011) Arbuscular mycorrhizal fungi (AMF) associated with the rhizosphere of *Mentha arvensis* l., and *M. longifolia* Huds. Pak J Bot 43:3013-3019.

Campagnac E, Sahraoui ALH, Debiane D, Fontaine J, Laruelle F, Garçon G, Grandmougin-Ferjani A (2010) Arbuscular mycorrhiza partially protect chicory roots

against oxidative stress induced by two fungicides, fenpropimorph and fenhexamid. Mycorrhiza 20(3):167-178.
Chamkhi I, Sbabou L, Aurag J (2018) Endophytic fungi isolated from *Crocus sativus* L. (saffron) as a source of bioactive secondary metabolites. Pharmacog J 10(6):1143-1148.
Chamkhi I, Abbas Y, Tarmoun K, Aurag J, Sbabou L (2019) Morphological and molecular characterization of arbuscular mycorrhizal fungal communities inhabiting the roots and the soil of saffron (*Crocus sativus* L.) under different agricultural management practices. Arch Agron Soil Sci 65(8):1035-1048.
Dalpé Y (1995) Systématique des endomycorhizes à arbuscules, de la mycopaléntologie à la biochimie. Orbis Press 1-20.
Dalpé Y (2005) Les mycorhizes: un outil de protection des plantesmais non unepanacée. Phytoprotection 86(1):53-59.
Dalpé Y (1989) Ericoid mycorrhizal fungi in the Myxotrichaceae and Gymnoascaceae. New Phytol 113:523-527.
Daniels GW, Skipper HD (1982) Methods for the recovery and quantitative estimation of propagules from soil. In Schenck NC, Ed., Methods and Principles of Mycorrhizal Research. American Phytopathological Society, Saint Paul, MN. pp. 29-35.
Deirdre CR, Killham K, Bending GD, Baggs E, Weih M, Hodge (2009) Mycorrhizas and biomass crops: opportunities for future sustainable development. Trends Plant Sci 14:542-549.
Derkowska E, SasPaszt L, Sumorok B, Szwonek E, Głuszek S (2008) The influence of mycorrhization and organic mulches on mycorrhizal frequency in apple and strawberry roots. J Fruit Ornam Plant Res 16:227-242.
Ferrer RL, Herrera RA (1981) El género *Gigaspora* Gerdemann et Trappe (Endogonaceae) en Cuba. Rev Jardín Bot Nac Habana 1:43-66.
Fiorilli V, Catoni M, Francia D, Cardinale F, Lanfranco L (2011) The arbuscular mycorrhizal symbiosis reduces disease severity in tomato plants infected by *Botrytis cinerea*. J Plant Pathol 93:237-242.
Fontana A (1985) Vesicular arbuscular mycorrhizas of *Ginkgo biloba* L. in natural and controlled conditions. New Phytol 99(3):441-447.
Fuji Y, Furukawa M, Hayakawa Y, Sugawara K, Shibuya T (1991) Survey of Japanese medicinal plants for the detection of allelopathic properties. Weed Res 36:36-42.
Gemma JN, Koske RE, Carreiro M (1989) Seasonal dynamics of selected species of VA mycorrhizal fungi in a sand dune. Mycol Res 92:317-321.
Gerdemann JW, Nicolson TH (1963) Spores of mycorrhizal *Endogone* species extracted from soil by wet sieving and decanting. Trans Br Mycol Soc 46:235-244.
Gianinazzi S, Gollotte A, Binet MN, van Tuinen D, Redecker D, Wipf D (2010) Agroecology: the key role of arbuscular mycorrhizas in ecosystem services. Mycorrhiza 20(8):519-530.
Goussous SJ, Mohammad MJ (2009) Comparative effect of two arbuscular mycorrhizae and N and P fertilizers on growth and nutrient uptake of onions. Int J Agric Biol 11(4):463-467.
Hall IR (1987) A review of VA mycorrhizal growth responses in pastures. Angew Bot 61:127-134.
Houngnandan P, Yemadje RG, Kane A, Boeckx P, Van Cleemput O (2009) Les Glomales indigenes de la forêt Claire à Isoberlinia doka (Craib et Stapf) à Wari-Maro au centre du Bénin. Tropicultura 27(2):83-87.
Hoseini M, Rizvi SJH (2003) Une etude préliminaire sur le rôle possible de l'allélopathiedans le safran (*Crocus sativus* L.) Troisième Symposium National sur le Safran. Iran. pp 133-138.
Jadhav PS, Mulic NG, Chavan PD (1997) Effets allélopathiques d'Ipomoeacarnea spp. Fistulosasur la croissance du blé, du riz, du sorgho et du haricot rouge. Allelopathy J 4:345-348.
Jalali AK (1962) Saffron in Kashmir. Prajna-Banaras Hindu Univ J 7:205-211.
Jansa J, Erb A, Oberholzer HR, Šmilauer P, Egli S (2014) Soil and geography are more important determinants of indigenous arbuscular mycorrhizal communities than management practices in Swiss agricultural soils. Mol Ecol 23:2118-2135.
Johnson NC, Zak DR, Tilman D, Pfleger FL (1991) Dynamics of vesicular-arbuscular mycorrhizae during old field succession. Oecologia 86(3):349-358.
Joner E, Leyval C (2001) Time-course of heavy metal uptake in maize and clover as affected by root density and different mycorrhizal inoculation regimes. Biol Fertil Soils 33(5):351-357.
Khaosaad T, Garcia-Garrido JM, Steinkellner S, Vierheilig H (2007) Take-all disease is systemically reduced in roots of mycorrhizal barley plants. Soil Biol Biochem 39(3):727-734.
Khozaei M, Kamgarhaghighi AA, Sepaskhah A, Karimian NA (2015) The effect of 10-year continuous saffron cultivation on physical and chemical properties of soil. Iran Agricult Res 34(1):46-55.
Kianmehr H (1981) Vesicular-arbuscular mycorrhizal spore population and infectivity of saffron (*Crocus sativus*) in Iran. New Phytol 88:79-82.
Kobayashi K (2004) Facteurs affectant l'activité phytotoxique des substances alléliques dans le sol. Weed Bio. Manag 4:17.
Kormanik PP, McGraw AC (1982) Quantification of vesicular-arbuscular mycorrhizae in plant roots. In Schenck NC, Ed., Methods and Principles of Mycorrhizal Research. The American Phytopathological Society, St Paul, Minnesota. pp 37-45.

Kormanik PP, Schultz RC, Bryan WC (1982) The influence of vesicular-arbuscular mycorrhizae on the growth and development of eight hardwood tree species. Forest Sci 28(3):531-539.

Koske RE (1987) Distribution of VA mycorrhizal fungi along a latitudinal temperature gradient. Mycologia 79:55-68.

Lone R, Shuab R, Malla NA, Gautam AK, Koul KK (2016) Beneficial effects of arbuscular mycorrhizal fungi on underground modified stem propagule plants. J New Biol Rep 5:41-51.

Lone R, Shuab R, Wani KA, Ganaie MA, Tiwari AK, Koul KK (2015) Mycorrhizal influence on metabolites, indigestible oligosaccharides, mineral nutrition and phytochemical constituents in onion (*Allium cepa* L.) plant. Sci Horticult 193:55-61.

Miransari M (2010) Contribution of arbuscular mycorrhizal symbiosis to plant growth under different types of soil stress. Plant Biol 12(4):563-569.

Mohebi-Anabat M, Riahi H, Zanganeh S, Sadeghnezhad E (2015) Effects of arbuscular mycorrhizal inoculation on the growth, photosynthetic pigments and soluble sugar of *Crocus sativus* (saffron) in autoclaved soil. Int J Agron Agric Res 6:296-304.

Monroy LHJ, Salamanca SCR, Cano C, Moreno-Conn LM, Orduz-Rodríguez JO (2013) Influencia de lascoberturas en cultivos de cítricossobre los hongos formadores de micorrizas arbusculares en Oxisoles del piedemontellanero colombiano. Corp Cienc Tecnol Agropecu 14:53-65.

Morton JB, Benny GL (1990) Revised classification of arbuscularmycorrhizal fungi (Zygomycetes): a new order, Glomales, two new suborders, Glomineae and Gigasporineae, and two new families, Acaulosporaceae and Gigasporaceae, with an emendation of Glomaceae. Mycotaxon 37:471-491.

Mosse B, Hayman DS (1971) Plant growth responses to vesicular-arbuscular mycorrhiza: II. In unsterilized field soils. New Phytol 70(1):29-34.

Onguene NA (2000) Diversity and dynamics of mycorrhizal associations in tropical rain forests with different disturbance regimes in South Cameroon. Tropenbos Cameroon Series 3. University of Wageningen, Wageningen, The Netherlands.

Pellissier F, Trosset L (1989) Effect of phytotoxic solutions on the respiration of mycorrhizal and non mycorrhizal spruce roots (*Picea abies* L Karst) Ann Sci For 46(Suppl):731s-733s.

Pérez A, Peroza V (2013) Micorrizas arbusculares asociadas al pastoangleton (*Dichathium aristatum* Benth) en fincas ganaderas del municipio de Tolú, Sucre-Colombia. Rev MVZ Córdoba 18(1):3362-3369.

Pérez F, Castillo-Guevara C, Galindo-Flores G, Cuautle M, Estrada-Torres A (2012) Effect of gut passage by two highland rodents on spore activity and mycorrhiza formation of two species of ectomycorrhizal fungi (*Laccaria trichodermophora* and *Suillus tomentosus*). Botany 90(11):1084-1092.

Phillips JM, Hayman DS (1970) Improved procedures for clearing roots and staining parasitic and vesicular-arbuscular mycorrhizal fungi for rapid assessment of infection. Trans Br Mycol Soc 55:158-161.

Powell CL (1979) Spread of mycorrhizal fungi through soil. New Zealand Jf Agric Res 22(2):335-339.

Powell CL, Daniel J (1978) Mycorrhizal fungi stimulate uptake of soluble and insoluble phosphate fertilizer from a phosphate-deficient soil. New Phytol 80(2):351-358.

Pozo MJ, Jung SC, Martínez-Medina A, López-Ráez JA, Azcón-Aguilar C, Barea JM (2013) Root allies: arbuscular mycorrhizal fungi help plants to cope with biotic stresses. In Aroca R, Ed., Symbiotic Endophytes. Soil Biology. Vol 37. Springer, Berlin, Heidelberg. pp 289-307.

Qarai H, Beigi M (1995) The study of changes in physico-chemical and mineralogical properties of soil under saffron cultivation in Estahban. Report of Research, Department of Iran Scientific and Industrial Research, Shiraz. pp 37.

Rajeshkumar PP, Thomas GV, Gupta A, Gopal M (2015) Diversity, richness and degree of colonization of arbuscular mycorrhizal fungi in coconut cultivated along with intercrops in high productive zone of Kerala, India. Symbiosis. 65:125-141.

Rodríguez-Morelos VH, Soto-Estrada A, Pérez-Moreno J, Franco-Ramírez A, Díaz-Rivera P (2014) Arbuscular mycorrhizal fungi associated with the rhizosphere of seedlings and mature trees of *Swietenia macrophylla* (Magnoliophyta: Meliaceae) in Los Tuxtlas, Veracruz, Mexico. Rev Chil Hist Nat 87(1):1-10.

Schenck NC, Smith OS (1982) Additional new and unreported species of mycorrhizal fungi (Endogonaceae) from Florida. Mycologia 74(1):77-92.

Schenck NC, Perez Y (1987). Manual for the Identification of VA Mycorrhizal Fungi. Synergetic Publication, Gainsville, USA.

Semane F, Chliyeh M, Kachkouch W, Touati J, Selmaoui K, Touhami AO, Douira A (2018) Follow-up of a composite endomycorrhizal inoculum in the rhizosphere of olive plants, analysis after 42 months of culture. Ann Res Rev Biol 22(2):1-18.

Sharif M, Moawad AM (2006) Arbuscular mycorrhizal incidence and infectivity of crops in North West frontier province of Pakistan World J Agric Sci 2:123-132.

Smith SE, Read DJ (2008) Mineral nutrition, toxic element accumulation and water relations of arbuscular mycorrhizal plants. Mycorhiz Symb 3:145-148.

Strullu DG (1990) Les mycorhizes des arbresetplantescultivées. Collection TEC & DOC, Lavoisier, Paris. pp 250.

Sylvia DM, Williams SE (1992) Vesicular-arbuscular nycor-

rhizae and environmental stresses. In Bethlenfalvay GJ, Linderman RG, Eds, Mycorrhizae in Sustainable Agriculture. American Society of Agronomy, Madison, Wisconsin, USA. 101-123.

Talbi Z, Chliyeh M, Mouria B, El Asri A, AitAguil F, Ouazzani Touhami A, Douira A (2016) Effect of double inoculation with endomycorrhizae and *Trichoderma harzianum* on the growth of carob plants. IJAPBC 5(1):44-58.

Van Der Heijden MG, Klironomos JN, Ursic M, Moutoglis P, Streitwolf-Engel R, Boller T, Sanders IR (1998) Mycorrhizal fungal diversity determines plant biodiversity, ecosystem variability and productivity. Nature 396(6706):69-72.

Walker C, Mize CW, McNabb Jr, HS (1982) Populations of endogonaceous fungi at two locations in central Iowa. Can J Bot 60(12):2518-2529.

Yang C, Hamel C, Schellenberg MP, Perez JC, Berbara RL (2010) Diversity and functionality of arbuscular mycorrhizal fungi in three plant communities in semiarid grasslands National Park, Canada. Microb Ecol 59:724-733.

Zare Maivan H, Nakhaei A (2000) Mycorrhizal symbiosis of saffron (*Crocus sativus*) with two Glominae fungal species. Pajouhesh-Va-Sazandegi 13(3 (48)):80-83.

Acta Biologica Szegediensis

Volume 65(2):211-220, 2021
Acta Biologica Szegediensis
http://abs.bibl.u-szeged.hu/index.php/abs
DOI:10.14232/abs.2021.2.211-220

ARTICLE

Chemical analyses of two plant essential oils and their effects on functional response of *Habrobracon hebetor* Say to *Sitotroga cerealella* Olivier larvae

Mehdi Heidarian[1]*, Seyed-Mohammad Masoumi[1], Mohammad Asadi[2]

[1] Department of Biology, Faculty of Science, Razi University, Kermanshah, Iran
[2] Department of Plant Protection, Faculty of Agriculture and Natural Resources, University of Mohaghegh Ardabili, Ardabil, Iran

ABSTRACT *Salvia officinalis* L. and *Glycyrrhiza glabra* L. are two valuable medicinal plants from Kermanshah province in Iran. In this study, chemical analyses of their essential oils were performed by gas chromatography-mass spectrometry and the effects investigated on functional response of *Habrobracon hebetor* Say on larval stage of *Sitotroga cerealella* Olivier. Accordingly, emerged females of *H. hebetor* were treated by LC_{30} of the isolated essential oils for 24 h. Then, six wasps were accidentally selected and introduced to densities of host larvae for 24 h. The results showed that naphthalene, decahydro-4a-methyl and alpha-thujone were dominant compounds in both essential oils, respectively. Holling model (1959) by using regression analyses confirmed functional response type III in the control wasps and type II in both essential oils treatments. The highest and lowest attack rates were observed in the control wasps (0.0443 ± 0.00278 h^{-1}) and *S. officinalis* treatment (0.0349 ± 0.00257 h^{-1}), respectively. Moreover, the treated wasps by *G. glabra* essential oil showed shorter handling time than *S. officinalis* treatment (0.4497 ± 0.0373 h versus 0.5196 ± 0.0589 h). Accordingly, *G. glabra* due to lower negative effects on the functional response of *H. hebetor* was more compatible than *S. officinalis* for their combination in integrated pest management schedules.
Acta Biol Szeged 65(2):211-220 (2021)

KEY WORDS
analysis
ectoparasitoid
functional response
stored pest
volatile compound

ARTICLE INFORMATION
Submitted
01 September 2021
Accepted
18 October 2021
***Corresponding author**
E-mail: mft.heidarian@gmail.com

Introduction

Salvia officinalis L. (sage, also called as garden sage, common sage, or culinary sage) (Fig. 1A) is an important medicinal plant belonging to family Lamiaceae (Labiatae). This species is a perennial and shrubby plant with evergreen stems and large, elongated, and entire leaves. The height of the plant is about 50 to 80 cm and its young stems are dark green that covered with dense gray hairs (Asadi et al. 2018). This plant is native to the Mediterranean regions; but, grows in most parts of the world and is also cultivated as an ornamental plant. *S. officinalis* needs heat and dry conditions during growing season and it is cultivated in some provinces of Iran that have mentioned conditions. *Glycyrrhiza glabra* L. (Liquorice or Licorice) (Fig. 1B) is an important medicinal plant with many secondary metabolites which many features of them is remained unknown (Duan et al. 2016; Esmaeili et al. 2019). This species is a perennial plant that has adapted with mesophyte and xerophyte habitats during its evolutionary period. It is native for southern Europe, northern Africa, and temperate regions of Asia; but is found in abundance in many parts of Iran, especially in western half (Ghahreman and Attar 1999). According to Bao and Larsen (2010), *G. glabra* is considered as the most important species in genus *Glycyrrhiza* and family Fabaceae (Leguminosae) which has been widely used as an important medicinal plant.

Habrobracon hebetor Say (Fig. 2) is a minute wasp from family Braconidae that is an ectoparasitoid agent of moth caterpillars. This wasp feed quickly, aided by their gut enzymes which quickly destroy blood proteins in hosts larvae; this increases value of the species as an effective biological control agent (Salvador and Consoli 2008). Mass rearing projects of *H. hebetor* are frequently performed on the larval stage of *Sitotroga cerealella* Olivier and the other laboratory hosts in different commercial insectariums from Iran (Abedi et al. 2012; Mahdavi and Saber 2013). Angoumois grain moth (*S. cerealella*) is an important species of family Gelechiidae, commonly referred as the rice grain moth. It is most commonly associated as a pest of field and stored cereal grains. They burrow within the kernel grains of crop plants and rendering

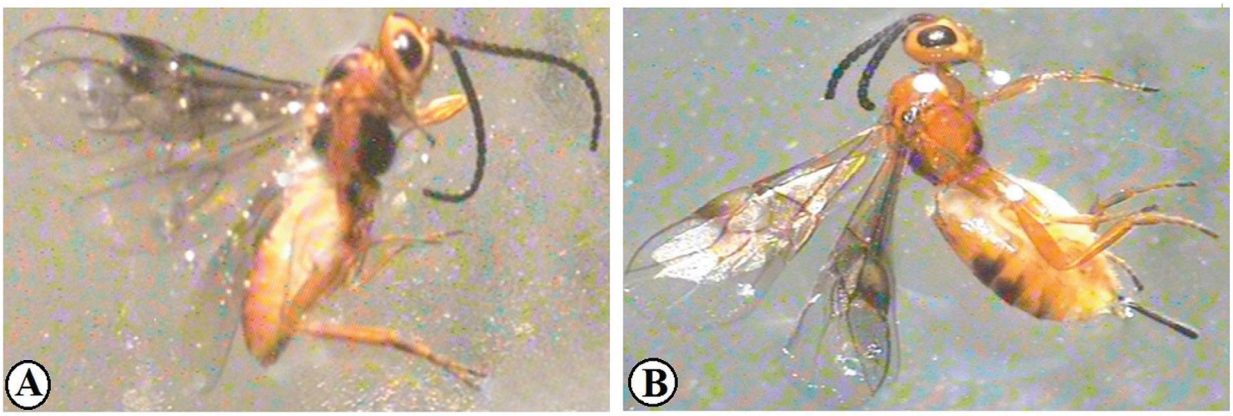

Figure 2. Adult male (A) and female (B) wasps of *H. hebetor*.

them unusable for human consumption. By laying eggs between the grains and hatching in later time during the processing, transportation, or storage stages; this moth can be transported to households or countries presently free of infestations. Thus, constant protection against this important pest is required for grain up untill consumption time (Throne and Weaver 2013). To date, *H. hebetor* parasitoid wasp has been released for effective control of *Helicoverpa armigera* (Hübner), *Sesamia cretica* Lederer, and *Ostrinia nubilalis* (Hübner) in agricultural crops of Iran (Baker and Fabrick 2000).

Essential oils are volatile materials in different plant species that contain terpenes, terpenoids, aromatic, and non-aromatic compounds. Identifying these compounds and understanding their roles are very important issues in plant science (Isman 2000; Isman et al. 2008). Essential oils, also known as the plant secondary metabolites, are mainly abundant in Myrtaceae, Lauraceae, Lamiaceae, and Asteraceae families due to their contact, fumigation, repellent, and anti-feeding effects. These compounds are one of the main components in defense mechanisms of various plants against herbivores during many centuries ago (Bakkali et al. 2008; Rafiee-Dastjerdi et al. 2013; Asadi et al. 2018, 2019). In terms of isolation method, the aromatic products from distillation process that are separated by volatile mechanisms are called the essential oil (Asadi et al. 2019). Research on these compounds has shown that the essential oils are used in different aspects due to their fumigant and medicinal effects. These compounds are different in each plant species and also in each geographical areas; therefore, it is not possible to expect same compounds in one plant species from different regions; although, there may be similarities between their compounds.

Biological control or biocontrol is one of main methods in integrated pest management (IPM). Functional response is the intake rate of a consumer as a function of food density or the amount of food available in a given ecotope (Baker and Fabrick 2000; Moezipour et al. 2008; Salvador and Consoli 2008). Following Holling (1959), functional responses are generally classified into three types, which are called Holling's type I, II, and III (Carneiro et al. 2010; Asadi et al. 2018). Totally, functional response type I has linear shape. In functional response type II, number of hosts attacked by each natural enemy reach to fix rate and most of the biocontrol agents show this type. Also, the functional response type III has sigmoid shape that is a preferred type or response about the natural enemies (Holling 1959; Hassell 1978).

Predators and parasitoids as important biocontrol agents commonly could be combined with compatible pesticides or botanical compounds (plant extracts and essential oils). To date, there are few information about the effects of these compounds on the functional response of *H. hebetor* to its hosts (Rafiee-Dastjerdi et al. 2009; Abedi et al. 2012; Mahdavi and Saber 2013; Mahdavi et al. 2013; Faal Mohammad-Ali et al. 2015; Jarrahi and Safavi 2015; Rashidi et al. 2018; Asadi et al. 2018, 2021). Due to great importance of functional response in population dynamics of plant pests by their natural enemies, the main idea for performing of this research was to determining safe botanical compounds on this important biocontrol agent for their efficient combination in IPM schedules.

Material and Methods

Identification of plant species

Identification of medicinal plants species collected from their natural habitats in Kermanshah province from Iran was done by sending complete samples to Razi University Herbarium (RUHK), Herbarium code: 2905 and 2906,

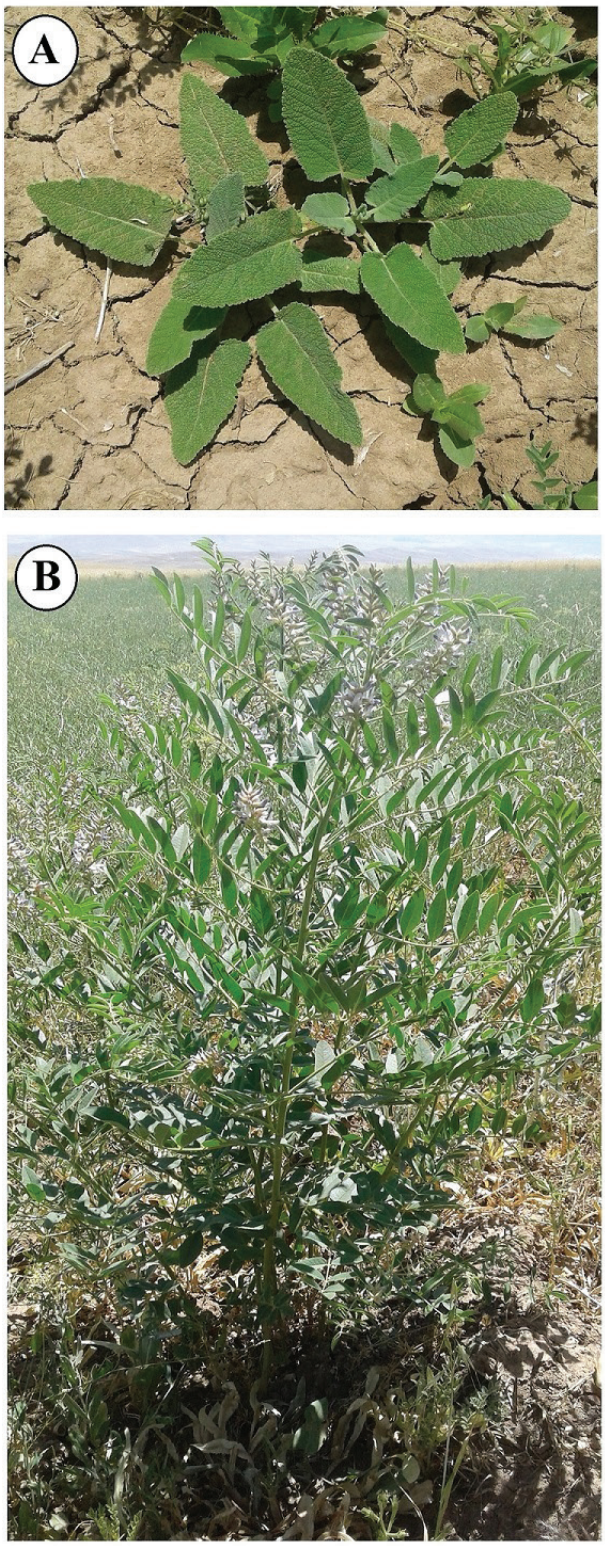

Figure 1. Mature plants of *S. officinalis* and *G. glabra* that collected from their natural habitats.

respectively; Kermanshah, Iran.

Isolation process of essential oil

After drying the plant specimens in shade (temperature about 25 °C), they were transferred to laboratory and their essential oils were gradually isolated. For this, aerial parts of the plants that have the highest content of volatile compounds were pulverized. Then, 50 g of the plant powder was mixed with 500 ml of distilled water in 1 liter balloon of Clevenger apparatus (Asadi et al. 2018). When the balloon heats up, volatile compounds are transferred to top of the tube and then cooled by condenser. After three hours, the essential oil was separated as a pale green layer on the water. The essential oil content of two medicinal plants was sufficient for these experiments and in each mentioned process approximately 0.5 ml was isolated. In order to remove water and purify the isolated essential oils, sodium sulfate (Na_2SO_4) was used (Asadi et al. 2019). Finally, the purified essential oils were stored in special glasses (5 ml) covered with aluminum tape in refrigerator (temperature about 4 °C) until GC-MS analyses and their usage in the experiments (Negahban et al. 2007; Shiva Parsia and Valizadegan 2015; Asadi et al. 2018).

Gas chromatography-mass spectrometry (GC-MS)

Chemical compounds in the purified essential oils of *S. officinalis* and *G. glabra* were identified by using a gas chromatographic device equipped with a split-splitless inlet (SSI) connected to mass spectrometer (GC-MS, Agilent 7980, USA). This device was available in the central laboratory, Islamic Azad University, Science and Research Branch, Tehran, Iran. The MS was equipped with EI ionization system and a four-coupled single analyzer (SQA) (Agilent, USA). To achieve the highest sensitivity in the detector, there was a triple detector (EMP) type that had very little noise and drift. After injecting of the essential oils by Hamilton syringe into the device, different compounds were gradually detected based on their molar mass at different times (run time). Based of the analyses by GC-MS, different compounds were explored according to their peak number, run time, and area.

Rearing of the host (S. ceralella)

Initial population of *S. cerealella* was gotten from a private insectarium (registered name: Jalilian) in Eslamabad-e Gharb city located in Kermanshah province (Iran), during 2019. The population was reared on wheat seed and maintained under the laboratory conditions including 25 ± 1 °C, 65 ± 5% relative humidity, and a photoperiod of 16:8 (L:D) h (Naseri et al. 2017).

Rearing of the parasitoid wasp (H. hebetor)

Females of *H. hebetor* were gotten from a private insecta-

Table 1. Fifteen dominant compounds in *S. officinalis* essential oil.

Compound number	Compound name	Run time (min)	Area%
1	Alpha-thujone	8.904	24.22
2	Bicyclo [2.2.1] heptan-2-one	9.865	15.51
3	1, 8-cineole 2-oxabicyclo	7.250	10.00
4	Thujone bicyclo [3.1.0] hexan-3	9.110	6.20
5	Veridiflorol	24.330	4.47
6	1-naphthalene propanol	31.786	4.10
7	1s-alpha-pinene	5.408	3.52
8	Camphene bicyclo [2.2.1] heptan	5.688	3.17
9	Alpha-humulene	20.416	2.65
10	Iron, monocarbonyl-(1, 3-butadien)	37.828	1.67
11	Borneol	10.369	1.65
12	Caryophyllene	19.341	1.60
13	12-oxabicyclo [9.1.0] dodeca-3	24.765	1.30
14	3, 6-dioxa-2, 4, 5, 7-tetrasilaoctan	38.034	1.13
15	1-naphthaleneethanol	37.565	1.09

rium (registered name: Jalilian) in Eslamabad-e Gharb city (Kermanshah province located in west of Iran), during 2019. The obtained wasps were urgently transferred to the growth chamber and reared on the last larval stage of *S. cerealella* as its laboratory host in 25 ± 1 °C, 65 ± 5% relative humidity, and a photoperiod of 16:8 (L:D) h. Honey solution (produced in Mahram factory, Iran) was used as food for the adult parasitoid during the mentioned processes (Rafiee-Dastjerdi et al. 2009; Abedi et al. 2012).

Bioassays experiments

For study the fumigant toxicity of two isolated essential oils on the young female wasps of *H. hebetor*; different concentrations of them (8.5, 17.8, 38, 79.45, and 166.5 µL/L air for *S. officinalis* and 8.9, 21.9, 54.95, 134.9, and 333.5 µL/L air for *G. glabra*) that showed the mortality rate between 20% and 80% were put on filter papers (1 × 1 cm) in 80 ml glass Petri dishes by using of sampler. The distilled water was used on the control wasps. Then, 20 female wasps of *H. hebetor* were introduced to each Petri dish and then the Petri dishes were immediately covered with parafilm tape to prevent of essential oil exit. For feeding of the parasitoids, the honey solution was used on a piece of white paper in each unit. Each concentration was assayed in four replications and after 24 h; numbers of dead wasps were carefully recorded (Shiva Parsia and Valizadegan 2015).

Functional response experiments

LC_{30} of each essential oil (6.657 and 6.754 µL/L air, respectively) was used as the lowest lethal concentration for the functional response experiments. For this, 100 mated females of *H. hebetor* were firstly treated by LC_{30} of selected essential oils on filter papers (1 × 1 cm) by using of sampler in 10 cm Petri dishes for 24 h. All stages were done for on control wasps with the distilled water. After 24 h, six treated wasps were randomly selected and separately transferred to the Petri dishes contained the different densities including 2, 4, 8, 16, 32, and 64 of *S. cerealella* larvae in a growth chamber that was set at 25 ± 1 °C, 65 ± 5 % relative humidity, and a photoperiod of 16:8 (L:D)h for 24 h. The honey solution was supplied as food source for the parasitoids. The experiments were designed in eight replication for the control wasps and each essential oil treatment and the numbers of paralyzed larvae were recorded after 24 h.

Functional response model

Model of Holling (1959) was used about the functional response of *H. hebetor* on variable densities of *S. cerealella* larvae which given as follows:

$$Na = aT_t N_0 / (1+ aT_h N_0)$$

The components of above equation are:

N_a= Number of attacked larvae
N_0= Different densities of *S. cerealella* larvae
T_t = Total time of experiments (24h)
a= Attack rate
T_h= Handling time

Simpler form of the above equation is:

$$a = (d + bN_0) / (1+ CN_0)$$

Table 2. Twenty dominant compounds in *G. glabra* essential oil.

Compound number	Compound name	Run time (min)	Area%
1	Naphthalene, decahydro-4a-methyl	25.578	15.62
2	2, 6-octadiene-1-ol, 3, 7-dimethyl	24.702	6.96
3	Butanoic acid, 3, 7-dimethyl-2	23.587	5.79
4	Lavandulyl acetate	18.294	4.93
5	3-hexene-1-ol, benzoate	23.890	3.45
6	Nerolidol 1, 6, 10-dodecatrien	23.735	3.22
7	Geranyl tiglate	27.037	3.04
8	Geranyl propionate 2, 6-octadiene	21.137	2.59
9	Geranyl benzoate	31.151	2.55
10	(e)-2-formyl-6-methyl-3-(1-propylen)	24.805	2.24
11	Benzyl benzoate benzoic acid	28.473	2.14
12	1, 6, 10-dodecatrien-3-ol	25.091	2.12
13	Naphthalene, 1, 2, 3, 4, 4a, 5, 6, 8a	25.337	2.09
14	2-naphthalenemethanol	25.967	1.98
15	Propanoic acid, 2-methyl	22.242	1.82
16	Hinesol	25.664	1.57
17	(-)-endo-2, 6-dimethyl-6-(4-methyl)	19.890	1.46
18	Neryl propionate 2, 6-octadiene	28.193	1.34
19	Beta-eudesmol 2-naphthalene	25.898	1.28
20	1h-cycloprop [e] azulene, decahydro	20.926	1.02

In this status; "b", "c" and "d" are model constants (Hassell 1978; Juliano 1993).

Statistical analysis

Logistic and non-linear regression models by using of SAS ver. 9.1 software were used to determine the functional response type and estimation of its parameters (attack rate and handling time), under essential oils treatments and in the control wasps, respectively (SAS Institute 2002).

Results

Chemical analysis of the essential oils

The GC-MS results showed that *S. officinalis* essential oils contained 93 chemical compounds with a total run time of 38.230 min. Among the identified compounds based on the exit analysis by detector device, fifteen compounds were occupied more than 1% of area and make up 82.28 % of total sum of areas in the essential oil (Table 1). Also, alpha-thujone (8.904 min - 24.22%) was the highest compound in this essential oil. Moreover, *G. glabra* essential oil contain 239 different chemical compounds with total run time of 38.469 min. As shown in Table 2, among the identified compounds, 20 compounds accounted more than 1% of sum of areas and mentioned as dominant compounds. By comparing of area in each compound to sum of areas, it was found that naphthalene, decahydro-4a-methyl (25.578 min -15.62 %) had the highest areae in this essential oil. These data were explored from the file produced by the chromatographic device.

Bioassay

The obtained LC_{30}, LC_{50}, and LC_{90} values for *S. officinalis* and *G. glabra* essential oils against the females of *H. hebetor* are shown in Table 3. The adult bioassays indicated that acute toxicity of *S. officinalis* essential oil on *H. hebetor* was higher than *G. glabra* essential oil.

Functional response type

Models of logistic regressions by linear (P_1) and non-linear parameters indicated functional response type in

Table 3. Acute toxicity of two plant essential oils on the female wasps of *H. hebetor*.

Essential oil	n	Slope ± E	LC30 µL/L air (95% CL)	LC50 µL/L air (95% CL)	LC90 µL/L air (95% CL)	Chi-Square
S. officinalis	480	1.564 ± 0.177	6.657 (4.181 - 9.159)	14.405 (10.744 – 18.083)	95.025 (70.572 – 145.715)	10.07
G. glabra	480	1.123 ± 0.134	6.754 (3.564 – 10.370)	19.792 (13.475 – 26.667)	273.871 (176.772 – 527.283)	8.99

Table 4. Functional response parameters in *H. hebetor* wasps were exposed to LC_{30} of two essential oils.

Treatments	Coefficient	Estimate	Stansard Error	Chi-Square	P-value
Control	P_0 (Constant)	1.2962	0.5316	5.95	0.0148
	P_1 (Linear)	0.0554	0.0813	0.46	0.4958
	P_2 (Quadratic)	-0.00292	0.00306	0.91	0.3406
	P_3 (Cubic)	0.00002	0.00003	0.81	0.3668
S. officinalis	P_0 (Constant)	1.5690	0.4790	10.73	0.0011
	P_1 (Linear)	-0.1267	0.0701	3.27	0.0707
	P_2 (Quadratic)	0.00410	0.00260	2.48	0.1151
	P_3 (Cubic)	-0.00004	0.00002	2.58	0.1082
G. glabra	P_0 (Constant)	1.6326	0.5021	9.85	0.0017
	P_1 (Linear)	-0.0248	0.0767	0.10	0.7469
	P_2 (Quadratic)	-0.00078	0.00285	0.07	0.7846
	P_3 (Cubic)	0.00001	0.00002	0.17	0.6828

the control and each essential oil treatment. If P_1 value be equal or more than 1, the response is type III and if be lower than 1 is type II (Table 4). According to the results, the functional response type III (P1 ≥ 0) in the control and type II (P1 < 0) in *S. officinalis* and *G. glabra* essential oils were determined, respectively (Fig. 3).

Functional response parameters

Estimation results of the attack rate, handling time, and theoretical maximum attack rate values for the treated wasps of *H. hebetor* by two isolated essential oils and the control are given in Table 5. Accordingly, the highest and lowest attack rates were obtained in the control wasps (0.0443 ± 0.00278 h^{-1}) and *S. officinalis* (0.0349 ± 0.00257 h^{-1}) treatment, respectively. The descending order of attack rate values was observed in the control, *G. glabra*, and *S. officinalis* treatments, respectively. In addition, the treated wasps by *G. glabra* essential oil showed shorter handling time than *S. officinalis* (0.4497 ± 0.0373 h versus 0.5196 ± 0.0589 h). Moreover, the respective ascending order of handling time values was observed in the control, *G. glabra*, and *S. officinalis* treatments. The highest and lowest values for theoretical maximum attack rate based on the obtained T/T_h (total time / handling time) were observed in the control and *S. officinalis* essential oil (62.19 versus 46.19), respectively. In addition, the respective descending order for this parameter was determined in the control, *G. glabra*, and *S. officinalis* treatments.

Discussion

Medicinal plants are god-given natural resources in each region and study of their chemical properties is very important. Due to high importance of *S. officinalis* and *G. glabra*, various researches have been done on these valuable plants over the world. There are good studies on the extract of these plants; but, we will abandon them. In addition, there are some studies on their essential oils that we will review them and explain differences or similarities with our results. Totally, the effects of essential oils on the functional response of *H. hebetor* and the other natural enemies could be considered as a useful tool for predicting the success of this useful agents in IPM schedules, especially on stored pest, *S. cerealella*.

Studies about the acute toxicity of different essential oils on *H. hebetor* is very limit (Seyyedi et al.

Table 5. Logistic regression analysis from *S. cerealella* larvae that parasitized by *H. hebetor* wasp.

Treatment	Functional response type	Attack rate (h^{-1}) a ± SE (Lower - Upper)	Handling time (h) T_h ± SE (Lower - Upper)	Theoretical maximum attack rate (T_{toal} / $T_{handling}$)	Correlation coefficient (R^2)
Control	III	0.0443 ± 0.00278 (0.0387 - 0.0449)	0.3859 ± 0.0317 (0.3221 - 0.4498)	62.19	0.96
S. officinalis	II	0.0349 ± 0.00257 (0.0343 - 0.0446)	0.5196 ± 0.0589 (0.4012 - 0.6381)	46.19	0.95
G. glabra	II	0.0364 ± 0.00340 (0.0296 - 0.0433)	0.4497 ± 0.0373 (0.3747 - 0.5247)	53.36	0.95

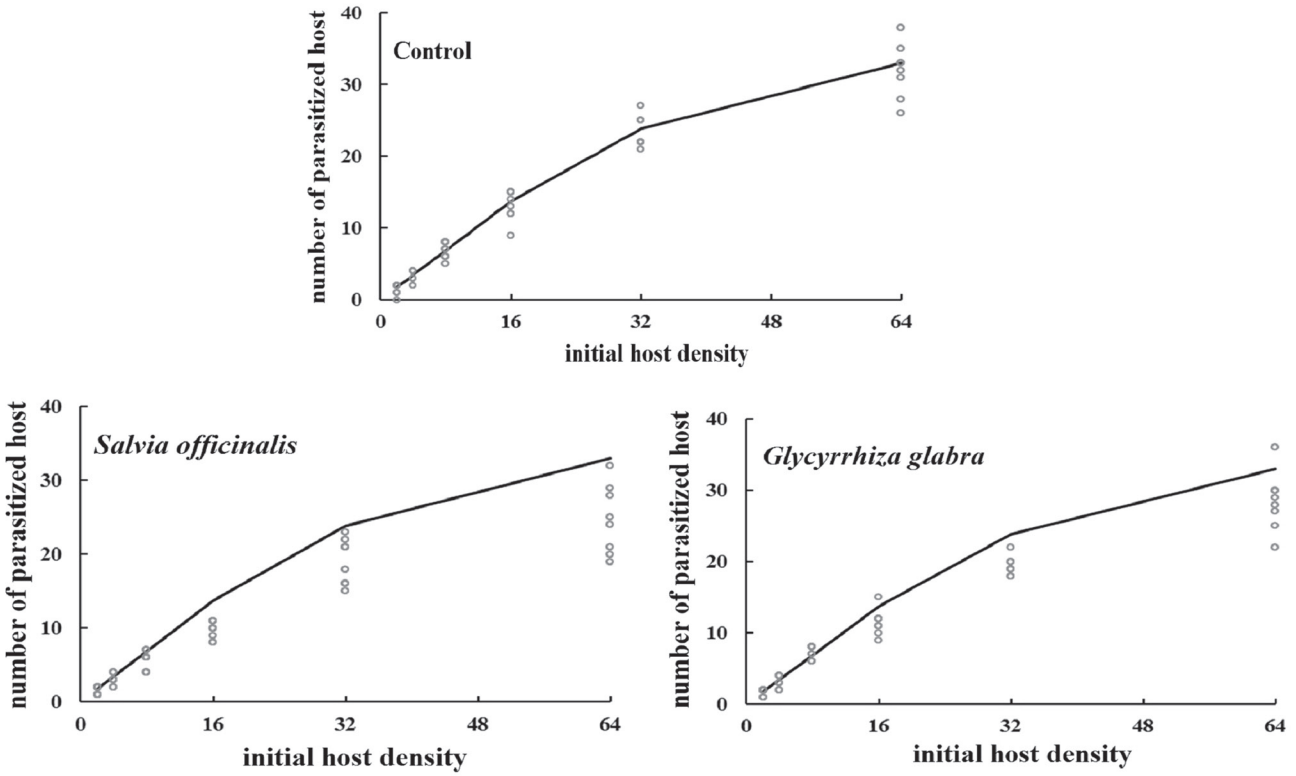

Figure 3. Curves of functional response from females of *H. hebetor* that treated by LC_{30} of selected essential oils and the control wasps to different densities of *S. cereaella* larvae.

2011; Hashemi et al. 2014; Ahmadpour 2017; Asadi et al. 2018, 2019). In our study, the tested essential oils showed different acute toxicity on the females of *H. hebetor* that extremely are similar to the results of Seyyedi et al. (2011), who studied the effects of *Ferula gummosa* L. essential oil on *H. hebetor* and concluded that the mortality was increased during 24h. Moreover, Hashemi et al. (2014) concluded that *Ferula assafoetida* L. essential oil had high toxicity on *H. hebetor*. Furthermore, Ahmadpour (2017) concluded that among *Ocimum basilicam* L., *Achillea millefolium* L., *Foeniculum vulgare* Mill., and *Zataria multiflora* Boiss, the essential oil of *F. vulgare* showed higher mortality compared with the others. Asadi et al. (2018, 2019) concluded that acute toxicity of *Rosmarinus officinalis* L. essential oil on the female wasps of *H. hebetor* was higher than the other essential oils including *Allium sativum* L., *Piper nigrum* L., *Salvia officinalis* L., and *Glycyrrhiza glabra* L. Also, *G. glabra* essential oil had the lowest acute toxicity in their research that is completely similar to our results.

In our research, alpha-thujone and naphthalene decahydro-4a-methyl were main components in *S. officinalis* and *G. glabra* essential oils, respectively. These compounds are volatile and aromatic with high toxicity on the female wasps of *H. hebetor*. These compounds have active molecules that make fumigant and contact effects and could be considered as natural insecticides against the insect pests especially in enclosed environments (Yazdgerdian et al. 2015). Accordingly, these essential oils and the other botanical compounds also can have negative effects on the natural enemies especially on behavioural freatures such as functional response that must be seriously considered (Croft 1990; Mahdavi and Saber 2013; Jarrahi and Safavi 2015). The results also showed that the attack rate values in treated wasps of *H. hebetor* by LC_{30} of the essential oils was lower than the control; but, the handling time values were higher. This subject indicated that these essential oils negatively have affected these important parameters in *H. hebetor*; because, when handling time increase the attack rate naturally decrease and this is a negative effect of each compound on a biocontrol agent.

There are limited research about the effects of essential oils on the functional response of *H. hebetor*; but, research on the insecticides effects are to some extent available. Asadi et al. (2018) concluded

that among *A. sativum*, *R. officinalis*, *P. nigrum*, *S. officinalis*, essential oil of *G. glabra* showed minimum negative effects on the functional response type and it's parameters in *H. hebetor*. Their results indicated that *G. glabra* essential oil can be recommended with *H. hebetor* in IPM that is similar with our results. Although, the studied host in their research was *Ephestia kuehniella* Zeller that is different with our host. Features of host directly could be effective on the natural enemies that this subject must be considered in related research on any natural enemy.

About the effects of pesticides on the functional response of this biocontrol agent, Rafiee-Dastjerdi et al. (2009) obtained the functional type II in *H. hebetor* on its laboratory host in the control and all insecticides treatments. Abedi et al. (2012) indicated that cypermethrin showed more adverse effects on this ectoparasitoid wasp compared with azadirachtin, methoxyfenozide, and pyridalil. In comparison, our results indicated that *S. officinalis* essential oil made higher negative effects on this biocontrol agent. Mahdavi and Saber (2013) concluded that malathion was compatible insecticide on the functional response of *H. hebetor* to *E. kuehniella* larvae compared with diazinon. But, our results showed that *G. glabra* were compatible. Mahdavi et al. (2013) studied the effects of abamectin, carbaryl, chlorpyrifos, and spinosad on the functional response of *H. hebetor* on adults treatment and reported functional response type III in all treatments; but, spinosad and abamectin were relatively compatible on the functional response parameters of this ectoparasitoid wasp. The dissimilarity of the results can belong to the type of host, laboratory conditions, quality of investigated wasps, type and mode of action of selected treatments, and their compatibility on *H. hebetor*.

Faal Mohammad-Ali et al. (2015) investigated the effects of chlorpyrifos and fenpropathrin on the functional response of *H. hebetor* in larval and pupl treatments and stated that the functional response of this parasitoid wasp in the control and all treatment were type III and the treatmenes have not any significant effects on the attack rate compared to the control; but, their effects on the handling time were significant. Different stages of *H. hebetor* have special features and their treatments could be made variable results. Jarrahi and Safavi (2015) concluded that Proteus® in pupal stage treatment made the highest handling time and lowest attack rate in *H. hebetor* compared to entomopathogenic fungus *Metarhizium anisopliae* sensu-lato and the control that their results were in agreement with our results about *S. offocinalis* treatment. The observed differences in results can belong to treated growth stage of *H. hebetor,* experimental conditions, colony quality of the parasitoid wasp, and type of examined treatments. Moreover, Rashidi et al. (2018) studied the effects of diazinon, phosalone, fipronil, and pyriproxifen on the functional response of *H. hebetor* on two lepidopteran host and concluded that the type of functional response in the treatments and control were similar; but, the attack rate and handling time negatively were affected by LC_{30} of mentioned insecticides that their results were in agreement with our results; although, in our research the type of functional response in all treatments were changed compared with the control. Asadi et al. (2021) studied the sublethal effects of chemical and botanical insecticides on the functional response of *H. hebetor* to larvae of *E. kuehniella* and stated that palizin and dayabon due to the lowest negative effects on *H. hebetor* were compatible insecticides for combination with this parasitoid wasp in IPM. In this study, we investigated the effects of two selected essential oils on the functional response in the ectoparasitoid wasp *H. hebetor* for second time. So far, the isolated essential oils from these medicinal plants have not been formulated as a commercial insecticide and we hope to find a way to formulate this natural compounds in future.

Acknowledgment

We wish to thank Mrs. Nashmieh Fathi the curator of Razi University Herbarium (RUHK) for her co-operation during this research.

References

Abedi Z, Saber M, Gharekhani G, Mehrvar A, Mahdavi V (2012) Effects of azadirachtin, cypermethrin, methoxyfenozide and pyridalil on functional response of *Habrobracon hebetor* Say (Hym.: Braconidae). J Plant Prot Res 52(3):353-358.

Ahmadpour R (2017) The effects of isolated essential oils from four medicinal plants on the ectoparasitoid wasp, *Habrobracon hebetor* Say under laboratory conditions. M.Sc. Thesis of Agriculture Entomology, University of Mohaghegh Ardabili, Ardabil, Iran. 75 pp.

Asadi M, Rafiee-Dastjerdi H, Nouri-Ganbalani G, Naseri B, Hassanpour M (2018) The effects of plant essential oils on the functional response of *Habrobracon hebetor* Say (Hymenoptera: Braconidae) to its host. ISJ 15:169-182.

Asadi M, Rafiee-Dastjerdi H, Nouri-Ganbalani G, Naseri B, Hassanpour M (2019) Insecticidal activity of the isolated essential oils from three medicinal plants on the biological control agent, *Habrobracon hebetor* Say (Hymenoptera: Braconidae). Acta Biol Szeged 63(1):63-68.

Asadi, M., Nouri-Ganbalani G, Rafiee-Dastjerdi H, Hassanpour M, Naseri B (2021) Comparative study about the sublethal effects of chemical and botanical insecticides on the functional response of *Habrobracon hebetor* Say (Hym.: Braconidae) to larvae of *Ephestia kuehniella* Zeller (Lep.: Pyralidae). Inter J Pest Manag, Published online, https://doi.org/10.1080/09670874.2020.1797231.

Bakkali F, Averbeck S, Averbeck D, Idomar M (2008) Biological effects of essential oils. Food Chem Toxic 46:446-475.

Baker JE, Fabrick JA (2000) Host hemolymph proteins and protein digestion in larval *Habrobracon hebetor* (Hym.: Braconidae). Insect Biochem Mol Bio 30(10):937-946.

Bao BJ, Larsen K (2010) Glycyrrhiza. In Wu ZY, Hong DY, Raven PH, Eds., Flora of China, Vol. 10. Science Press, Beijing. 509-511.

Carneiro TR, Fernandes OA, Cruz I, Bueno RCOF (2010) Functional response of *Telenomus remus* Nixon (Hymenoptera: Scelionidae) to *Spodoptera frugiperda* (Smith) (Lepidoptera: Noctuidae) eggs: effect of female age. Revista Brasil Entomol 54(4):692-696.

Croft BA (1990) Arthropod Biological Control Agents and Pesticides. John Wiley and Sons, New York, 723 p.

Duan L, Yang X, Liu PL, Johnson G, Wen J, Chang ZY (2016) A molecular phylogeny of Caraganeae (Leguminosae, Papilionoideae) reveals insights into new generic and infrageneric delimitations. Phytokey 70:111-137.

Esmaeili H, Karami A, Hadian J, Saharkhiz MJ, Ebrahimi SN (2019) Variation in the phytochemical contents and antioxidant activity of *Glycyrrhiza glabra* populations collected in Iran. Indust Crop Prod 137:248-259.

Faal Mohammad-Ali H, Allahyari H, Saber M (2015) Sublethal effect of chlorpyrifos and fenpropathrin on functional response of *Habrobracon hebetor* (Hym.: Braconidae). Arch Phytopath Plant Prot 48(4):288-296.

Ghahreman A, Attar F (1999) Biodiversity of plant species in Iran: the vegetation of Iran, plant species, red data of Iran, endemic species, rare species, species threatened by extinction. Central Herbarium of Tehran University, Faculty of Science.

Hashemi Z, Goldansaz H, Hosseini-Naveh V (2014) Effects of essential oil from *Ferula assafoetida* L. on biological parameters of the parasitoid wasp *Habrobracon hebetor* (Hym.: Braconidae) under laboratory conditions. Proceedings of the 21th Iranian Plant Protection Congress. 9-13 September, University of Urmia, Iran.

Hassell MP (1978) The dynamics of arthropod predator prey systems, monographs in population biology. Princeton University Press, Princeton.

Holling CS (1959) Some characteristics of simple types of predation and parasitism. Can Entomol 91(7):385-398.

Isman MB (2000) Plant essential oils for pest and disease management. Crop Prot 19:603-608.

Isman MB, Wilson JA, Bradbury F (2008) Insecticidal activities of commercial rosemary oil (*Rosmarinus officinalis*) against larvae of *Pseudaletia unipuncta* and *Trichoplusia ni* in relation to their chemical compositions. Pharm Biol 46(1-2):82-87.

Jarrahi A, Safavi SA (2015) Effects of pupal treatment with Proteus® and *Metarhizium anisopliae* sensu-lato on functional response of *Habrobracon hebetor* parasitizing *Helicoverpa armigera* in an enclosed experiment system. Biocontrol Sci Tech 26:206-216.

Juliano SA (1993) Nonlinear curve fitting: predation and functional response curves. In Scheiner SM, Gurevitch J, Eds., Design and Analysis of Ecological Experiments. Chapman and Hall, New York. 159-181.

Mahdavi V, Saber M (2013) Functional response of *Habrobracon hebetor* Say (Hymenoptera: Braconidae) to Mediterranean flour moth (*Anagastra kuehniella* Zeller) in response to pesticides. J Plant Prot Res 53:399-403.

Mahdavi V, Saber M, Rafiee-Dastjerdi H, Mehrvar A, Hassanpour M (2013) Efficacy of pesticides on the functional response on larval ectoparasitoid, *Habrobracon hebetor* Say (Hymenoptera: Braconidae). Arch Phytopath Plant Prot 46(7):841-848.

Moezipour M, Kafili M, Allahyari H (2008) Functional response of *Trichogramma brassicae* at different temperatures and relative humidities. Bullet Insect 61(2):245-250.

Naseri B, Abedi Z, Abdolmaleki A, Jafary-Jahed M, Borzoui E, Mansouri SM (2017) Fumigant toxicity and sublethal effects of *Artemisia khorassanica* and *Artemisia sieberi* on *Sitotroga cerealella* (Lepidoptera: Gelechiidae). J Insect Sci 17(5):100-108.

Negahban M, Moharramipour S, Sefidkon F (2007) Fumigant toxicity of essential oil from *Artemisia sieberi* Besser against three insects. J Stored Prod Res 43:123-128.

Rafiee-Dastjerdi H, Hejazi MJ, Nouri-Ganbalani G, Saber M (2009) Effects of some insecticides on functional response of ectoparasitoid, *Habrobracon hebetor* Say (Hymenoptera: Braconidae). J Entomol Soc Iran 6(3):161-166.

Rafiee-Dastjerdi H, Khorrami F, Razmjou J, Esmaielpour B, Golizadeh A, Hassanpour M (2013) The efficacy of some medicinal plant extracts and essential oils against potato tuber moth, *Phthorimaea operculella* (Zeller) (Lepidoptera: Gelechiidae). J Crop Prot 2(1):93-99.

Rashidi F, Nouri-Ganbalani G, Imani S (2018) Sublethal effects of some insecticides on functional response of *Habrobracon hebetor* (Hymenoptera: Braconidae) when reared on two lepidopteran hosts. J Econ Entomol 111(3):1104-1111.

Salvador G, Consoli LF (2008) Changes in the hemolymph and fat body metabolites of *Diatraea saccharalis* (Fabricius) (Lepidoptera: Crambidae) parasitized by *Cotesia flavipes* (Cameron) (Hymenoptera: Braconidae). Biol Cont 45(1):103-110.

SAS Institute (2002) The SAS System for Windows. SAS

Institute, Cary, NC. 58 p.
Seyyedi A (2011) Insecticidal effects of *Ferula gummosa* L. on *Ephestia kuehniella* Zeller and its parasitoid wasp *Habrobracon hebetor* Say. M.Sc. Thesis of Agriculture Entomology. University of Shahed, Tehran, Iran.100 pp.
Shiva Parsia A, Valizadegan O (2015) Fumigant toxicity and repellent effect of three Iranian eucalyptus species against the lesser grain beetle, *Rhyzopertha dominica* (F.) (Col.: Bostrychidae). J Entom Zool Stud 3(2):198-202.
Throne JE, Weaver DK (2013) Impact of temperature and relative humidity on life history parameters of adult *Sitotroga cerealella* (Lepidoptera: Gelechiidae). J Stored Prod Res 55:128-133.
Yazdgerdian AR, Akhtar Y, Isman MB (2015) Insecticidal effects of essential oils against woolly beech aphid, *Phyllaphis fagi* (Hemiptera: Aphididae) and rice weevil, *Sitophilus oryzae* (Coleoptera: Curculionidae). J Entomol Zool Stud 3(3):265-271.

Acta Biologica Szegediensis

Volume 65(2):221-232, 2021
Acta Biologica Szegediensis
http://abs.bibl.u-szeged.hu/index.php/abs
DOI:10.14232/abs.2021.2.221-232

ARTICLE

Influence of culture age on exopolymeric substances from common laboratory bacterial strains: a study on yield, profile and Cu(II) biosorption

Le Wei Chia and Adeline Su Yien Ting*

School of Science, Monash University Malaysia, Jalan Lagoon Selatan, 47500 Bandar Sunway, Selangor Darul Ehsan, Malaysia

ABSTRACT Extracellular polymeric substances (EPS) produced by laboratory strains *Bacillus cereus* and *Pseudomonas aeruginosa* were extracted from cultures incubated at various incubation periods (24, 48, 72, 96 and 120 h). At each sampling time, the EPS were analysed for yield, quality, functional groups present, and their efficacies in copper (Cu(II)) biosorption (using 30 and 50 ppm EPS). Results revealed that EPS yield was influenced by incubation period, with 48-h culture of *B. cereus* and 96-h culture of *P. aeruginosa* producing the highest yield of EPS at 8.30 mg and 6.95 mg, respectively. The EPS produced at various incubation periods have similar characteristics in solubility, quality and major functional groups (C-O, CH3, C=C, O-H) present. Efficacy of Cu(II) biosorption was influenced by the amount of EPS used and the EPS-metal incubation time. Although Cu(II) removal was higher for EPS from 24-h *B. cereus* (18.96%) and 48-h *P. aeruginosa* (19.19%) when 30 ppm was used, application of 50 ppm EPS demonstrated no distinct differences in amount of Cu(II) removed. This suggested that higher biomass of EPS used and longer EPS-metal incubation period, superseded the efficacy of EPS from various incubation periods. **Acta Biol Szeged 65(2):221-232 (2021)**

KEY WORDS
Bacillus cereus
exopolymeric substances
functional groups
metal removal
optimization
Pseudomonas aeruginosa

ARTICLE INFORMATION
Submitted
20 August 2021
Accepted
02 November 2021
***Corresponding author**
E-mail: adeline.ting@monash.edu
adelsuyien@yahoo.com

Introduction

Copper (Cu(II)) is one of the common inorganic metal cations that are extensively used in the manufacturing, electroplating and fertilizer industries (Sulaymon et al. 2013; Chen et al. 2018). By nature, Cu(II) is an essential metal required for physiological processes. However, high concentrations of Cu(II) in wastewater, can lead to toxicity, affecting living organisms and the environment. Prolonged exposure to high concentrations of Cu(II) can result in deleterious health implications affecting vital organs such as brain, heart, liver and kidney (Singh et al. 2011). The removal of Cu(II) from the environment is therefore pertinent to reduce hazards as Cu(II) cations are non-biodegradable and tend to accumulate in the environment. Several techniques have been adopted as approaches to remove Cu(II) from the environment. They include mostly physicochemical approaches such as chemical-metal precipitation, ion exchange, membrane filtration and adsorption (Cheah and Ting 2020). These approaches are useful, but are also costly and contributes to the generation of toxic sludge. As an alternative, bioremediation is investigated, in which biological agents are used to remove toxic metals from the environment. Bacteria, fungi and plants, are all capable of bioremediation via biosorption, biodegradation, bioaugmentation or bioflocculation.

In recent years, the application of biomolecules produced from microbes such as exopolymeric substances (EPS) has become an attractive alternative. The application of EPS eliminates the need to apply live microbial cells, addressing concerns of having microbial cell residues in the environment and potential transfer of resistance genes (Cheah and Ting 2020). EPS comprises of long chain polysaccharides and are naturally-produced by bacteria into the surrounding environment during bacterial growth, especially in response to stressful environmental conditions (Sivakumar et al. 2012; Ahmed et al. 2013; Cheah and Ting 2020). The typical composition of EPS includes macromolecules such as nucleic acids, proteins, lipids and carbohydrates (Sheng et al. 2010; Ozturk et al. 2014; Jia et al. 2017). These constituents contribute to the many functional groups present (e.g., carbonyl, carboxyl, hydroxyl, phosphoryl, sulfhydryl and amino groups) in the EPS, which assist in biosorption of metal cations (More et al. 2014; Crini and Lichtfouse 2018). While some of these EPS are well-known and used in various industries (i.e.,

xanthan, gellan, alginate, hyaluronan) (Messner 1997; De Philippis et al. 2011; Freitas et al. 2011); only scattered reports are available on microbial EPS for metal removal. For example, EPS from cyanobacteria have been found to be effective for the removal of Cu(II), Cr(III) and Ni(II) (Micheletti et al. 2007). Paniwichian et al. (2011) reported similar metal removal potential by EPS produced from *Rhodobium marinum* and *Rhodobacter sphaeroides,* which reduced levels of Cd(II), Cu(II), Pb(II) and Zn(II) from contaminated shrimp ponds. There is therefore a demand for more thorough investigations on EPS production, optimization of yield and quality, and their subsequent metal removal capacity.

The focus of this study is to investigate if EPS production is influenced by culture age. This is because EPS is organically produced by bacteria, and the EPS and possibly their constituents may differ depending on response of bacteria to incubation time, nutrient, and stress. To ascertain this, the influence of culture age on EPS production (yield), profile and subsequent Cu(II) removal efficacy, is determined. The influence of culture age encompasses the response of bacteria to incubation time as well as towards depletion of nutrients and build-up of toxic products (Brose and Eikeren 1990). As such, influence of culture age was the approach adopted in this study. The findings here would offer new understanding on the characteristics of the EPS from bacterial cultures of various incubation periods, and the integrity of their properties. It also outlines the consistency of the properties and quality of EPS to be used as an effective biomolecule for metal removal.

To achieve this, *Bacillus cereus* and *Pseudomonas aeruginosa* were selected as they are known to produce EPS. They also represent gram positive and gram negative bacteria, respectively. Both *B. cereus* and *P. aeruginosa* are laboratory strains, and has no prior exposure to metal stress or any other stress factors. The intention of using two laboratory strains are to eliminate pre-disposing factors that may induce EPS production other than under the typical controlled environment. The bacterial isolates were incubated at various incubation time to give rise to different culture ages, and the EPS produced was investigated for yield and quality (solubility, FTIR). The EPS produced were then studied (using different concentrations) for their efficacy for Cu(II) biosorption to remove Cu(II) from solutions.

Materials and Methods

Establishment of bacterial cultures

Two bacterial isolates, *Bacillus cereus* ATCC 14579 and *Pseudomonas aeruginosa* ATCC 10145 were selected as producers of EPS. Both isolates were from the Microbial Culture Collection, Microbiology Laboratory, School of Science, Monash University Malaysia. The bacterial isolates were cultured on Nutrient Agar (NA) (Merck 105450, Germany) and incubated for 24 h at 25 ± 2 °C and 35 ± 2 °C for *B. cereus* and *P. aeruginosa,* respectively, until use.

Bacterial growth and EPS production

Bacterial isolates were inoculated into 50 ml of Nutrient Broth (NB) (Merck 105443, Germany), and incubated with agitation (35 ± 2 °C, 100 rpm, 24 h) (Thermo Scientific, MaxQ 6000, USA). After incubation, the broth cultures were centrifuged at 4000 rpm (30 min, 25 ± 2 °C) (Thermo Scientific CL40R Centrifuge, USA) to obtain pellets (bacterial cells) (Chug et al. 2016). The pellets were weighed (fresh weight) (weighing balance, Ohaus® Pioneer™, USA) and the biomass recorded to represent bacterial growth. The supernatant was transferred into 250 ml flasks and three volumes of 95% ethanol (J. Kollin Chemical) were added. The mixture was incubated at 4 °C overnight to allow precipitation of EPS. After incubation, mixtures were centrifuged (4000 rpm, 45 min, 4 °C) and the supernatant discarded. The pellet (EPS) was mixed with double distilled water to dissolve the precipitate, followed by filtration using 0.45 μm membrane pore filters (Jet Biofil, China) to obtain cell-free EPS. The cell-free EPS was then lyophilized (freeze dryer Labconco Freezone 4.5, Missouri) to obtain powder-forms. The procedure was repeated to obtain EPS from both bacterial cultures incubated for 48, 72, 96 and 120 h.

Characterization of EPS

The physical properties of the lyophilized EPS was determined by characterizing based on colour and solubility in various solvents. The EPS was first weighed (Mettler Toledo, USA) and the colour of lyophilized EPS was assigned based on visual interpretation. The solubility of EPS was tested in distilled water and organic solvents, i.e. absolute ethanol (J. Kollin Chemical), ether (Friendemann Schmidt) and acetone (Friendemann Schmidt). Solubility test was performed by dissolving 0.5 mg EPS in 5 ml of the solvents (or distilled water). The procedure was repeated for EPS from both bacterial cultures incubated for 48, 72, 96 and 120 h.

The quality and purity of the EPS obtained was ascertained by detecting the presence/absence of DNA peaks. EPS (0.5 mg) was first mixed in 2 ml of distilled water, and the absorbance read within the range of 190-500 nm (UV-vis spectrophotometer, Perkin Elmer Lambda 365, USA). The absence of peaks within regions of 260 to 280 nm indicated absence of DNA in the EPS sample, suggesting high quality and purity of EPS (Lin et al. 2010; Liu et al. 2010). On the contrary, peaks detected at 260-280 nm regions would indicate contamination with DNA, concluding that EPS is of poor quality. The procedure was

repeated for EPS from both bacterial cultures incubated for 48, 72, 96 and 120 h.

The Fourier transformed infrared (FTIR) spectroscopy analysis was performed for EPS samples to determine the functional groups present on the EPS. EPS samples (0.5 mg) were analysed with the FTIR spectrometer (Perkin Elmer Spectrum Two, USA) with the spectrum measured at the resolution of 4 cm^{-1} in the range of 400-4000cm^{-1} (Chew and Ting 2016). The procedure was repeated for EPS from both bacterial cultures incubated for 48, 72, 96 and 120 h.

Cu(II) biosorption

The removal of Cu(II) by EPS was determined by first preparing the Cu(II) solution (10 ppm concentration) using Copper(II) nitrate trihydrate (Friendemann Schmidt) in 1000 ml of distilled water. The solution was then dispensed into 50 ml Falcon tubes (25 ml Cu(II) solution in each tube). The EPS (from 24-, 48-, 72-, 96-, 120-h culture) was then weighed (0.75 mg) and added into the Cu(II) solutions, to give a final concentration of 30 ppm of EPS for the treatment of 25 ml Cu(II) solution (Chug et al. 2016). The EPS-Cu(II) solution was incubated for 24 h, at room temperature (23 ± 2 °C), with agitation (120 rpm) (Lab Companion SI-600R, Korea). After incubation, the EPS-Cu(II) solutions were centrifuged (4000 rpm, room temperature, 45 min), and the supernatant collected while the pellet was discarded. The supernatant was subjected to Cu(II) analysis via Atomic Absorption Spectrometry (AAS) analysis using flame atomic absorption (Perkin Elmer AAnalyst 100, USA). The procedure was repeated for EPS-Cu(II) solutions incubated for 48 and 72 h. The removal of Cu(II) was recorded and calculated using Equation 1 (Eq.1), with C_0: initial concentration of Cu(II), and C_e: final Cu(II) concentration.

$$\% \text{ Cu(II) removal} = [(Co - Ce)/Co] \times 100\% \qquad \text{(Eq.1)}$$

A subsequent test was conducted using a higher concentration of EPS (50 ppm) and with longer EPS-Cu(II) solution incubation time (24, 48, 72, 96, and 120 h). For this test, 1.50 mg of EPS (from 24-, 48-, 72-, 96-, and 120-h culture) was added into 30 ml of 10 ppm Cu(II) solution to give rise to 50 ppm EPS for the test and incubated in similar conditions as described previously. At each sampling period (24, 48, 72, 96, and 120 h), aliquots were sampled and analysed for Cu(II) removal as previous.

Statistical analysis

Analysis for bacterial growth and EPS production was conducted using six replicates, while Cu(II) biosorption analyses were conducted in triplicates. Data was analysed using One Way Analysis of Variance (ANOVA) performed using SPSS Statistics version 21.0. Means were compared with Tukey's test ($p < 0.05$). Comparison between two variables were performed using T-test ($p < 0.05$).

Results and Discussion

Bacterial growth and EPS yield

The growth of *Bacillus cereus* was generally inferior to *Pseudomonas aeruginosa*, for all incubation periods (24-120 h) (Fig. 1). The growth of *B. cereus* was slower (184.83-449.66 mg) with highest biomass achieved at 120 h (449.66 mg). On the contrary, the biomass of *P. aeruginosa* was significantly higher than *B. cereus* (328.33-632.33 mg) for all incubation periods (Fig. 1), with highest biomass observed as early as 24 h (632.33 mg). It is presumed that both bacterial isolates achieved stationary phase by 96 h as there were no longer any significant increase in biomass thereafter (Fig. 1). Although 120-h culture of *B. cereus* and 24-h culture of *P. aeruginosa* had the highest biomass, keeping the cultures longer than 120 h may not necessary be beneficial. Bacteria will grow to a point where growth is then limited by the gradual depletion of nutrients and the possible build-up of toxic by-products (i.e. organic acids, carbon dioxide) (Brose and Eikeren 1990), which may have then inadvertently affected their growth in the later stages.

On the contrary, the production of EPS continued throughout the incubation period, suggesting that EPS production is possible exceeding beyond the optimum culture age of 120 h. Although maximum EPS yield was derived from 48-h culture for *B. cereus* (8.30 mg EPS) and 96-h culture for *P. aeruginosa* (6.95 mg EPS), there is an increasing trend in EPS production beyond the optimum culture age, more evidently for *P. aeruginosa* with 6.67 mg EPS recovered from 120-h culture (Fig. 1). For *B. cereus*, EPS production increased almost two-fold after 24 h, and subsequent 72-, 96- and 120-h cultures yield 7.81, 6.19 and 8.21 mg of EPS, respectively (Fig. 1). It is evident that cultures kept at prolonged incubation period beyond the optimum period, was able to sustain the production of high EPS yield.

When examined between growth and yield, 48-h culture of *B. cereus* appeared to produce more EPS (8.30 mg) despite the low biomass (184.83 mg). This gives a percentage of EPS production of 4.49% for B. cereus. In fact, *B. cereus* had lower biomass (poorer growth) (184.83-449.66 mg) compared to *P. aeruginosa* (328.33-632.33 mg), but the production of EPS by *B. cereus* was significantly higher than *P. aeruginosa*, especially from 48, 72 and 120-h cultures with 8.30, 7.81 and 8.21 mg of EPS obtained, respectively (Fig. 1). For *P. aeruginosa*, EPS production was highest from 96-h culture (6.945 mg) which had a

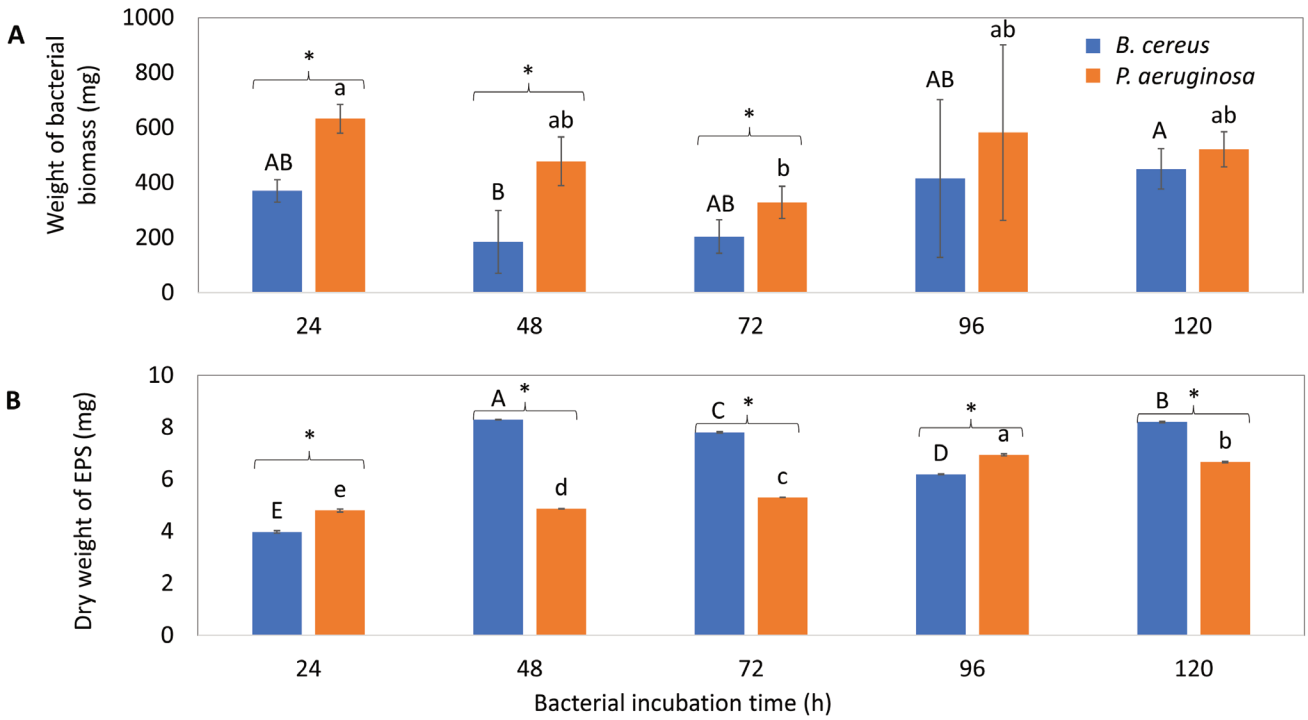

Figure 1. (a) Growth of *B. cereus* and *P. aeruginosa* expressed as weight of bacterial biomass (mg) from 24, 48, 72, 96 and 120 h cultures. (b) Production of exopolymeric substances (EPS, dry weight in mg) by 24, 48, 72, 96 and 120 h cultures of *B. cereus* and *P. aeruginosa*. Means with the same alphabets of the same caption are not significantly different (Tukey's Test, $p<0.05$). *indicates significant differences between the two bacteria as according to T-test ($p<0.05$). Bars indicate standard error.

corresponding biomass of 582 mg. This gives a percentage of EPS production of only 1.19%, This affirmed that *B. cereus* produced more EPS than *P. aeruginosa* although the growth of *B. cereus* was inferior to *P. aeruginosa*.

Clearly, EPS production differs in the two isolates tested. *B. cereus* have higher EPS production as early as 48 h incubation, suggesting EPS production is high during the early log (exponential) growth phase. On the contrary, *P. aeruginosa* produced more EPS at 96 h, coinciding with the stationary growth phase. The high EPS production during late log or stationary phase has been reported (Bragadeeswaran et al. 2011; Razack et al. 2011) and is associated with the various bacterial species and their response to limited nutrient conditions (Myszka and Czacyzk 2009) and release of EPS due to cell lysis (Zeng et al. 2016). Therefore, in some bacteria, growth is correlated to their production of EPS (Finore et al. 2014), whereas no correlation exists for others (Arunkumar et al. 2012). This study has shown that the two different bacteria responded to the incubation conditions differently which influenced growth. However, since EPS is typically produced at early or late log phase of growth between 48-96 h incubation, culture age does influence the EPS yield whereby older cultures (prolonged incubation) may produce high EPS yield irrespective of growth. The higher production of EPS by 48 and 96-h old cultures appeared typical for most bacteria (Kilic and Dönmez 2007; Sheetal and Gupte 2016).

Table 1. Properties (colour, solubility) of EPS produced from *Bacillus cereus* and *Pseudomonas aeruginosa*.

Physical properties	***Bacillus cereus***	***Pseudomonas aeruginosa***
Colour	Brown	Greyish white
Solubility in water	Yes	Yes
Solubility in absolute ethanol	No	No
Solubility in ether	No	No
Solubility in acetone	No	No

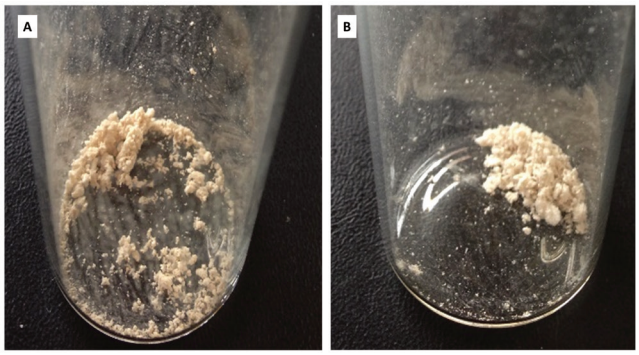

Figure 2. Lyophilized EPS produced by 120 h cultures of (a) *B. cereus* and (b) *P. aeruginosa*, bearing the distinct brownish and greyish white colours, respectively.

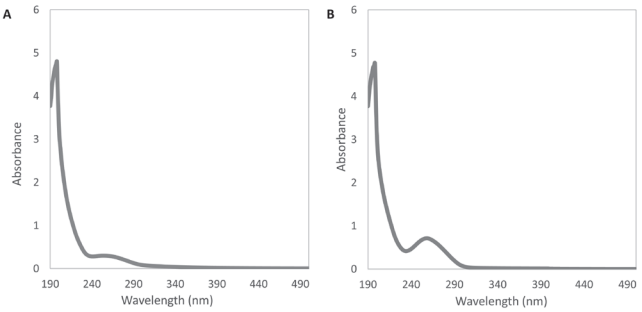

Figure 3. UV-Vis spectra of EPS derived from 24 h cultures of (a) *B. cereus* and (b) *P. aeruginosa*, measured within a wavelength of 190-500 nm.

Quality and purity of EPS yield

The quality of EPS produced from the various incubation periods was generally acceptable, as the integrity of physical properties was evident throughout. The colour of the EPS produced by *B. cereus* and *P. aeruginosa* were brown and white in colour, respectively (Fig. 2). EPS from both *B. cereus* and *P. aeruginosa* were soluble in water, but insoluble in the organic solvents (Table 1). The quality of EPS was consistent for all EPS sampled from all culture age of *B. cereus* and *P. aeruginosa* throughout the experiment.

The EPS produced by *B. cereus* and *P. aeruginosa* were considered pure, as no impurities (i.e. nucleic acids, proteins) were detected. Absence of peaks between 260 to 280 nm indicated absence of nucleic acids or proteins (Fig. 3). Minor shoulder peaks were however, detected at 190-210 nm and 250-260 nm. Peaks at 190-210 nm may be attributed to the n-σ* and/or π-π* transitions, associated with functional groups such as carboxyl, carbonyl or ester functional groups (Lin et al. 2010). Peaks at 250-260 nm wavelength may originate from the π-π* electron transitions of the aromatic and polyaromatic compounds (Liu et al. 2010; Lin et al. 2010). The EPS produced by both *B. cereus* and *P. aeruginosa* were concluded to have acceptable purity, and were not contaminated by nucleic acids or proteins, although aliphatic and aromatic compounds associated with the EPS were detected as inconspicuous shoulder peaks (Lin et al. 2010). This observation was consistent for all EPS derived from the various culture ages of *B. cereus* and *P. aeruginosa*.

The FTIR analysis showed that EPS from *B. cereus* and *P. aeruginosa* have similar spectral and major peak patterns, although the intensity of the peaks differed, especially within sections from wavenumber 500-1800 cm^{-1} (Fig. 4). In those regions, the peak widths for *B. cereus* were broader, whereas the peaks for *P. aeruginosa* were narrower. Broad strong bands of the O-H stretch was abundant in both bacteria (7) (3271.82-3258.98 cm^{-1}) (Fig. 4, Table 2 and 3). The primary functional groups detected were C-O stretching of alcohols (2) and carbonyl (3), alkanes (CH_3) (4,6), and C=C stretch of alkene compounds (5), each at their respective wavenumbers (Fig. 4; Table 2 and 3). These observations were consistent for all samples derived from EPS of *B. cereus* and *P. aeruginosa* of different culture age.

The FTIR spectra analysis confirmed the presence of polar and non-polar functional groups in EPS produced

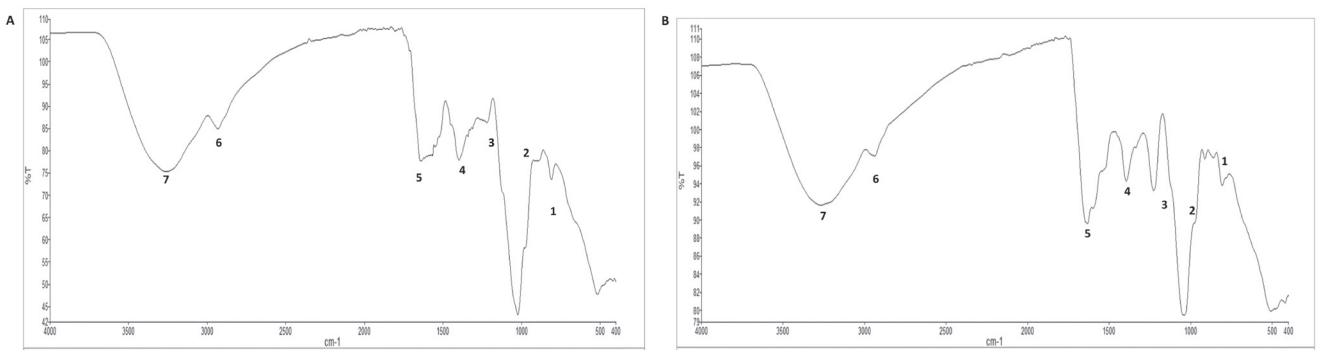

Figure 4. FTIR spectra of EPS derived from 24 h cultures of (a) *B. cereus* and (b) *P. aeruginosa*. Major peaks are labelled with numbers (i.e. 1-7), with corresponding functional groups listed in Table 2. and 3. for *B. cereus* and *P. aeruginosa*, respectively.

Table 2. Functional groups and their respective wavenumbers (cm^{-1}) detected from EPS samples produced by 24-h cultures of *Bacillus cereus*. Corresponding spectra peaks are in Figure 4.

No.	Wavenumber (cm^{-1})	Functional groups
1	810.78	C-Cl stretching of alkyl halides
2	1024.28	C-O stretching of alcohol
3	1220.45	C-O stretching of carbonyl; stretching vibration of C-O
4	1397.84	CH_3 (alkanes)
5	1636.28	C=C stretching of alkene compounds
6	2932.08	-CH_3 alkanes; symmetric and asymmetric CH_2- and CH_3- stretching vibrations
7	3258.98	O-H stretching of alcohol

by both gram-positive and gram-negative bacteria. The primary functional groups identified were alkyl halides, carbonyl, alcohol, alkane, and alkenes, which are negatively charged and capable of binding metal ions (Abraham and Le 1999; Wu et al. 2016). In this study, there were no distinct differences in major functional groups found in the EPS produced by *B. cereus* and *P. aeruginosa*. There were however, two peaks detected within 1210-1230 cm^{-1} (3) and 1630-1650 cm^{-1} (5) in *P. aeruginosa*, which had higher peak intensity than in *B. cereus* (Fig. 4). The intense peaks from EPS of *P. aeruginosa* correspond to phenol, amine and alkene, suggesting that more of the groups may be present in *P. aeruginosa* compared to *B. cereus*. FTIR analysis also revealed the presence of O-H stretching group (3000-3500 cm^{-1}), C-H stretching group (2930 cm^{-1}) and deviational vibration of C-H (1400-1200 cm^{-1}), which represent the polysaccharide constituent in the EPS (Ryder et al. 2007; Chen et al. 2017). This carbohydrate constituent (40-95% of the total composition of EPS) typically comprise of sugar molecules (e.g., hexose or uronic acids), homopolysaccharides, heteropolysaccharides, proteins and lipids (Messner 1997; Flemming and Wingender 2010; More et al. 2014; Gupta and Diwan 2017). Ionization of the functional groups releases the hydrogen ion, giving rise to negatively-charged groups that bind readily to metal cations (Wei et al. 2016; Gupta and Diwan 2017; Zhang et al. 2017). The differences in peak intensity were attributed to the gram positive and gram negative nature of the bacterial isolates, rather than to the culture age.

The quality and yield analyses indicated that both *B. cereus* and *P. aeruginosa* produced EPS of similar characteristics or properties throughout the experiment. EPS from both bacterial cultures, whether from 48, 72, 96 or 120-h cultures, all demonstrated similar characteristics and profile for quality (solubility, purity, functional groups). Older cultures may produce more EPS yield, given that it is within the late exponential or stationary phase of the bacteria growth cycle. This suggested that the EPS produced by both bacterial isolates has good integrity and consistency, although harvested from different culture ages.

Cu(II) biosorption by EPS

The initial Cu(II) removal test using 30 ppm EPS concentration for metal incubation from 24-72 h, indicated that a longer metal incubation time is required to benefit Cu(II) biosorption. The amount of Cu(II) removed was 2-3 fold higher when EPS-Cu(II) solution was incubated for 48 h and 72 h instead of 24 h (Fig. 5). This was evident for EPS derived from both *B. cereus* and *P. aeruginosa*. Application of EPS from *B. cereus* into EPS-Cu(II) solutions incubated for 48 h recorded 15.15 and 17.64% Cu(II) removal by EPS from 24- and 48-h cultures. The increasing trend

Table 2. Functional groups and their respective wavenumbers (cm^{-1}) detected from EPS samples produced by 24-h cultures of *Pseudomonas aeruginosa*. Corresponding spectra peaks are in Figure 4.

No.	Wavenumber (cm^{-1})	Functional groups
1	810.78	C-Cl stretching of alkyl halides
2	1041.40	C-O stretching of alcohol
3	1226.33	C-O stretching of carbonyl; stretching vibration of C-O
4	1394.91	CH_3 (alkanes)
5	1632.80	C=C stretching of alkene compounds
6	2939.45	-CH_3 alkanes; symmetric and asymmetric CH_2- and CH_3- stretching vibrations
7	3271.82	O-H stretching of alcohol

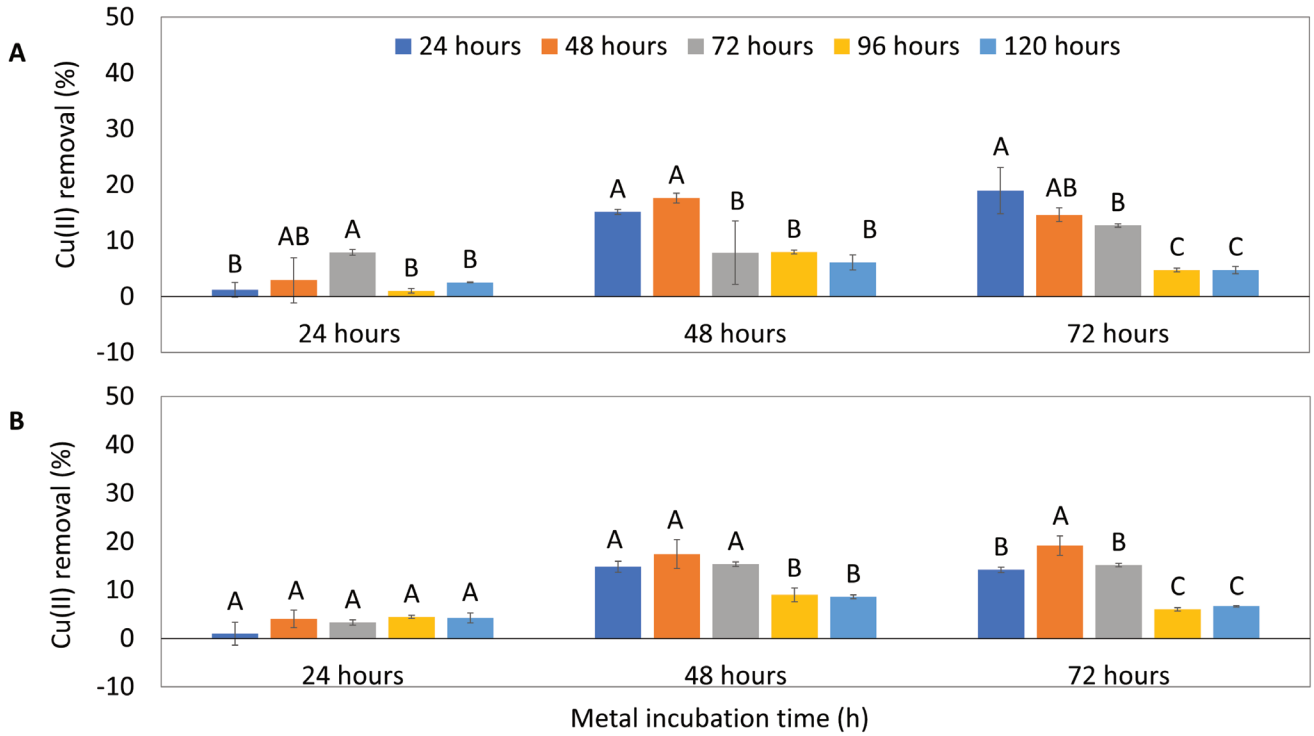

Figure 5. Cu(II) removal (%) by 30 ppm EPS produced by (a) *B. cereus* and (b) *P. aeruginosa* from 24, 48, 72, 96 and 120 h cultures. Cu(II) removal was assessed from EPS-Cu(II) incubation for 24, 48 and 72 h. Means with the same alphabets within a specific EPS-incubation period, are not significantly different (Tukey's Test, $p<0.05$). Bars indicate standard error.

continued with EPS-Cu(II) incubation for 72 h, in which 8.96%, 14.63% and 12.73% Cu(II) removal was achieved by EPS from 24-, 48- and 72-h cultures of *B. cereus*. These levels were higher than amount of Cu(II) removed when the EPS-Cu(II) solutions were incubated for 24 h. At 24 h of EPS-Cu(II) incubation, the highest Cu(II) removal was by EPS from 72-h cultures of *B. cereus* (7.92% Cu(II) removal) (Fig. 5).

Similarly, Cu(II) removal by EPS produced by *P. aeruginosa* were also higher when the EPS-Cu(II) solutions were incubated for 48 h and 72 h. At 48 h of EPS-Cu(II) incubation, Cu(II) removal was significantly higher by EPS derived from 24-, 48- and 72-h cultures, with 14.82%, 17.41% and 15.35% Cu(II) removal (Fig. 5). When EPS-Cu(II) solutions were incubated for 72 h, Cu(II) removal was relatively higher by EPS produced from 24-, 48- and 72-h cultures of *P. aeruginosa,* with 14.18%, 19.19% and 15.17% removal, respectively (Fig. 5). The EPS produced from 24-, 48- and 72-h cultures were therefore observed to have significantly higher Cu(II) removal potential than EPS produced from 96- and 120-h cultures (Fig. 5).

Comparing the efficacy of 30 ppm EPS from *B. cereus* and *P. aeruginosa*, the EPS produced by *P. aeruginosa* appeared to have significantly higher Cu(II) removal potential, particularly for EPS-Cu(II) solutions incubated for 48 and 72 h (Fig. 6). T-test analysis showed Cu(II) removal by EPS produced from 72-h (15.35%) and 120-h (8.60%) for EPS-Cu(II) incubation at 48 h, revealed significant differences. A more evident trend was observed for EPS-Cu(II) solutions incubated for 72 h. Cu(II) removal at this stage by EPS derived from 48-h (19.19%), 72-h (15.17%), 96-h (6.02%) and 120-h (6.67%) cultures of *P. aeruginosa* were significantly higher than EPS from *B. cereus* (Fig. 6). On the contrary, EPS from *B. cereus* removed only 7.84 (by 72-h culture) and 6.11% (by 120-h culture) of Cu(II) post EPS-Cu(II) incubation for 48 h. At 72 h of EPS-Cu(II) incubation, Cu(II) removal was only 14.63%, 12.73%, 4.75%, and 4.77%, by 48-, 72-, 96-, and 120-h cultures, respectively (Fig. 6). Interestingly, EPS from 72-h culture of *B. cereus* was more effective than *P. aeruginosa* for Cu(II) removal at 24 h EPS-Cu(II) incubation, with 7.92 compared to 3.31% of removal, respectively (Fig. 6).

The early indications here suggested that culture age may have influenced Cu(II) biosorption, with EPS from *B. cereus* and *P. aeruginosa* from specific culture age demonstrating more superior Cu(II) biosorption than others. This may be ascribed to the fact that EPS is organic and subtle variations in the EPS constituents may exist, particularly for EPS derived from a gram positive or gram negative bacteria. The production of EPS and their composition,

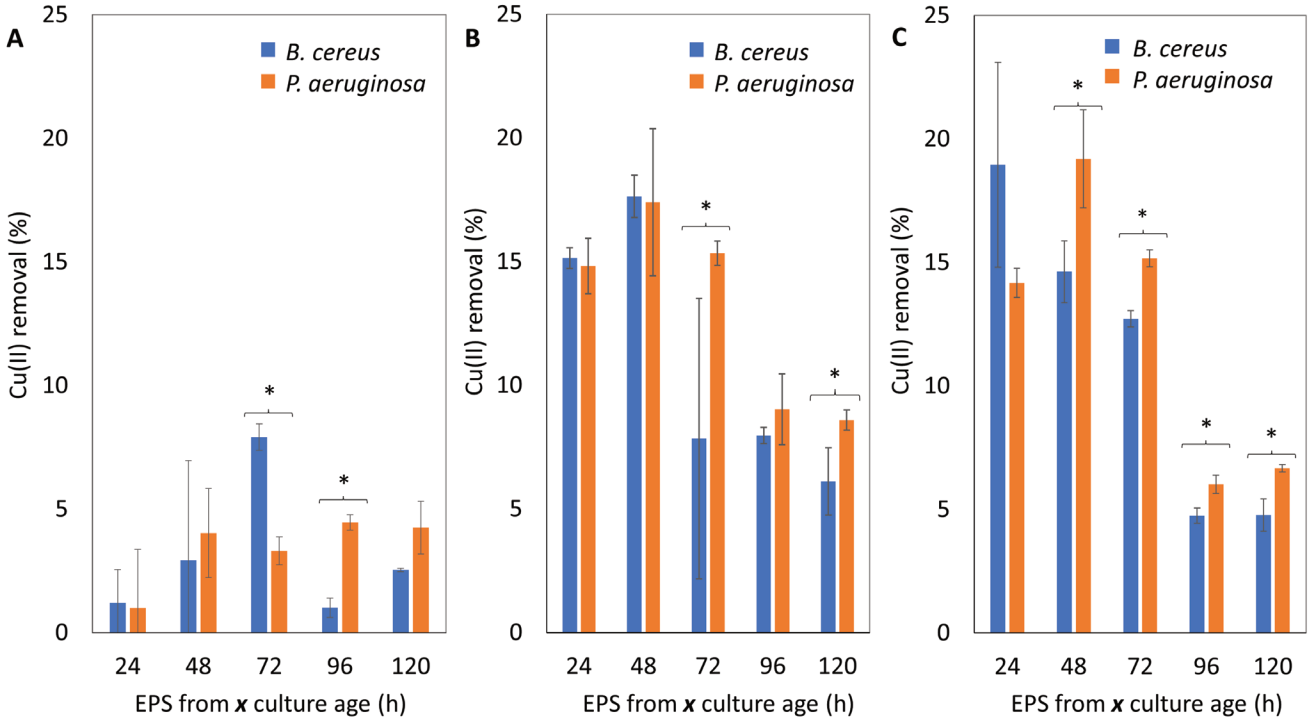

Figure 6. Comparison of Cu(II) removal (%) efficacy by EPS produced by *B. cereus* and *P. aeruginosa* from 24, 48, 72, 96 and 120 h cultures. Cu(II) removal was assessed using 30 ppm EPS incubated in EPS-Cu(II) solution for (a) 24, (b) 48 and (c) 72 h. *indicates significant differences between the two bacteria as according to T-test ($p<0.05$). Bars indicate standard error.

may have subtle differences in the carbohydrate and protein constituents, owing to their cell wall structures (Seltmann and Holst 2013). Gram-negative bacteria have an outer membrane that is rich in lipopolysaccharides, in addition to the thin inner layer of peptidoglycan. On the contrary, Gram-positive bacteria do not have an outer membrane; instead consists of several layers of peptidoglycan (Seltmann and Holst 2013). This may have influenced the composition in the EPS produced, thus influencing the metal adsorption capability of bacteria (Vu et al. 2009; More et al. 2014; Cheah and Ting 2020). This has also been shown in the FTIR results (in the earlier sections) in which peak intensity differs between *B. cereus* and *P. aeruginosa*. Nevertheless, there were no conclusive evidences on the significant influence of culture age on EPS and Cu(II) biosorption as EPS-Cu(II) incubation period and EPS concentration appeared to contribute to biosorption. As such, the EPS-Cu(II) incubation period

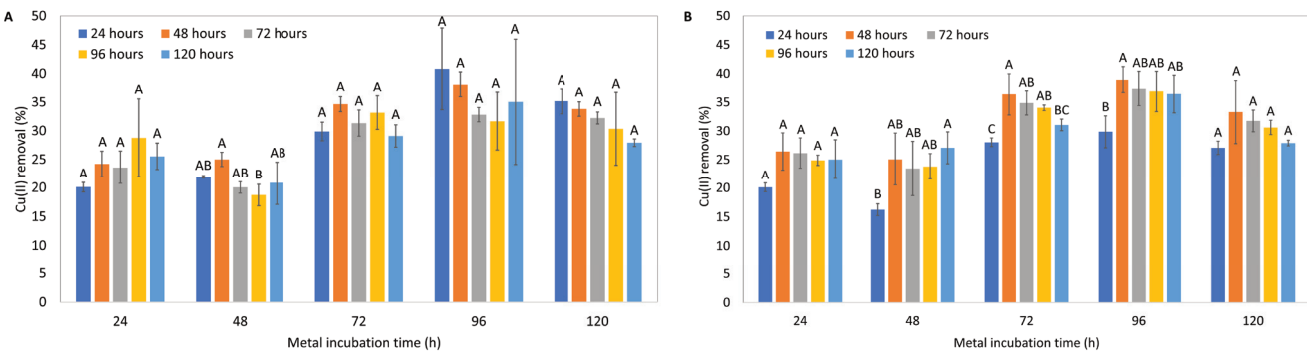

Figure 7. Cu(II) removal (%) by 50 ppm EPS produced by (a) *B. cereus* and (b) *P. aeruginosa* from 24, 48, 72, 96 and 120 h cultures. Cu(II) removal was assessed from EPS-Cu(II) incubation for 24, 48, 72, 96 and 120 h. Means with the same alphabets within a specific EPS-Cu(II) incubation period, are not significantly different (Tukey's Test, $p<0.05$). Bars indicate standard error.

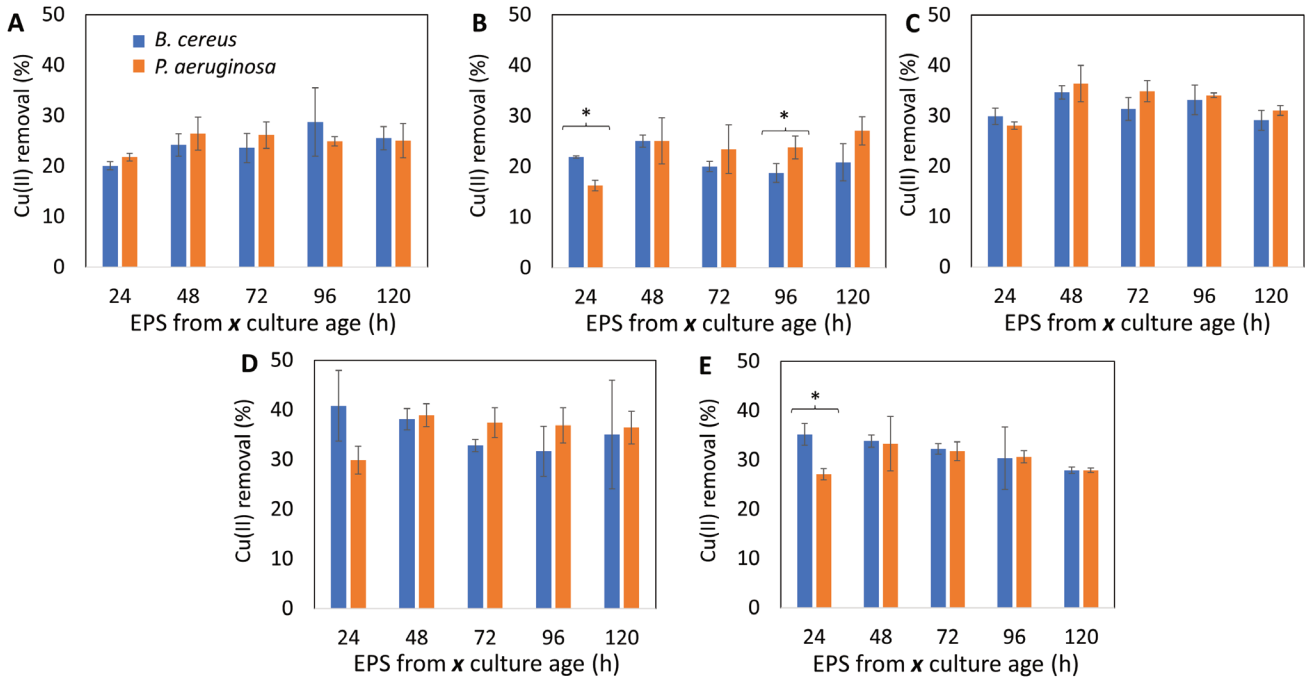

Figure 8. Comparison of Cu(II) removal (%) efficacy by EPS produced by *B. cereus* and *P. aeruginosa* from 24, 48, 72, 96 and 120 h cultures. Cu(II) removal was assessed using 50 ppm EPS incubated in EPS-Cu(II) solution for (a) 24, (b) 48, (c) 72 h, (d) 96, and (e) 120 h. *indicates significant differences between the two bacteria as according to T-test ($p<0.05$). Bars indicate standard error.

was prolonged and a higher concentration of EPS was used so that a clearer trend can be seen.

With higher concentration of EPS used (50 ppm) and prolonged incubation period beyond 72 h (to 96 and 120 h), higher amount of Cu(II) was removed (Fig. 7). As such, results here suggested that Cu(II) removal may now be independent of culture age, for both *B. cereus* and *P. aeruginosa*. When 50 ppm of EPS from *B. cereus* was used, the amount of Cu(II) removed by EPS from 24-, 48-, 72-, 96- and 120-h cultures were not significantly different, with the exception for EPS-Cu(II) incubated for 48 h (Fig. 7). With 48 h incubation, Cu(II) removal by EPS from 96-h culture (18.72%) was significantly lower than EPS derived from 48-h culture (25.03%) (Fig. 7). For *P. aeruginosa*, the EPS by 48- and 72-h cultures appeared to have an advantage in Cu(II) removal compared to 24-h cultures, particularly for EPS-Cu(II) incubations for 48, 72 and 96 h (Fig. 7). EPS from 24-h cultures of *P. aeruginosa* removed only 20.09%, 16.25%, 28.04%, 29.88%, and 27.08% of Cu(II) at 24, 48, 72, 96 and 120 h of EPS-Cu(II) incubation, respectively (Fig. 7). Clearly, with the higher amount of EPS used and prolonged EPS-Cu(II) incubation period, the Cu(II) removal efficacy has become less dependent on EPS derived from various culture ages of bacteria.

The efficacy of EPS from *B. cereus* was generally comparable to EPS from *P. aeruginosa* with the use of 50 ppm of EPS (based on T-test) (Fig. 8). Exceptions though, were observed for EPS from 24-h culture of *B. cereus*, which removed more Cu(II) when incubated for 48 (21.93%) and 120 h (35.18%) in EPS-Cu(II) solution, compared to *P. aeruginosa* (16.25 and 27.08%, respectively) (Fig. 8). On the contrary, EPS derived from 96-h cultures of *P. aeruginosa*, removed significantly higher Cu(II) when incubated in EPS-Cu(II) solution for 48 h, with 23.81% compared to 18.72% by EPS from *B. cereus* (Fig. 8). Notably, with a higher concentration of EPS used (50 ppm), the efficacy of Cu(II) removal is enhanced, and there were no longer significant discrepancies between the two EPS sources in removing Cu(II). Both *B. cereus* (gram positive) and *P. aeruginosa* (gram negative) were capable of producing EPS for Cu(II) removal. For *B. cereus*, the ability of EPS to remove Cu(II) conforms to reports of other *Bacillus* sp. in removing Cu(II), Pb(II) and Cd(II) (Shameer 2016). Similarly, gram negative bacteria are also known to produce EPS to remove metals. Ashruta et al. (2014) used EPS produced by a consortium of gram-negative bacteria, to effectively remove Zn(II), Pb(II), Cr(III), Ni(II), Cu(II) Cd(II) and Co(II). It is evident that Cu(II) removal by EPS is influenced significantly by the concentration of EPS used. It is anticipated that with increased concentrations of EPS used, Cu(II) removal would be enhanced by two to three-fold (Shameer 2016; Wei et al. 2016; Azzam and Tawfik 2015). In this study, the increase of Cu(II) removal

efficacy was observed when 50 ppm is used compared to 30 ppm. This is mainly attributed to having more available binding sites in EPS.

Observations here provided evidence that the influence of culture age on Cu(II) biosorption efficacy by EPS diminished with the use of higher EPS concentration (i.e. 50 ppm) and with prolonged EPS-Cu(II) incubation period. The age of the culture appeared to be more important when cells/biomass are used instead of EPS (Odokuma 2009). Although Pereira et al. (2009) suggested that composition of EPS produced by bacteria may have slight quantitative and qualitative differences attributed to age of culture, this was not clearly evident in this study. With prolonged incubation period, the influence of culture age diminished as EPS have more time to bind to the EPS (Kumar et al. 2009). This was demonstrated here whereby metal removal was enhanced two-fold (from < 20 to 40% removal efficacy) with incubation extended to 120 h. Nevertheless, metal binding may reach a saturation point where metal removal is gradually limited by the limited number of active binding sites (Pagnanelli et al. 2009).

Conclusions

To conclude, EPS produced from laboratory strains *B. cereus* and *P. aeruginosa* have potential use for Cu(II) removal. EPS production was higher in 48-h and 96-h cultures of *B. cereus* and *P. aeruginosa*, respectively, with acceptable quality and integrity across all culture ages. EPS produced from different culture ages also did not demonstrate varying metal removal capacity, especially when higher concentrations of EPS were used and with extended EPS-Cu(II) incubation time. There were also no clear distinctions between the efficacy of EPS produced from gram positive and gram-negative bacteria. This study revealed that culture age influenced the yield of EPS, but does not have a strong impact in determining the characteristics of the EPS (purity, solubility, functional groups) nor their Cu(II) biosorption efficacy.

Acknowledgements

The authors extend their gratitude to Monash University Malaysia for the facilities to conduct the study. Monash University Malaysia, through internal funding for academic research, was able to support the consumables and the facilities used in this study.

References

Abraham MH, Le J (1999) The correlation and prediction of the solubility of compounds in water using an amended solvation energy relationship. J Pharmac Sci 88(9):868-880.

Ahmed Z, Wang Y, Anjum N, Ahmad A, Khan ST (2013) Characterization of exopolysaccharide produced by *Lactobacillus kefiranofaciens* ZW3 isolated from Tibet kefir – Part II. Food Hydrocoll 30(1):343-350.

Arunkumar R, Vigneshwaran KPM, Vinothkumar AM (2012) Production and characterization of exopolysaccharides using *Lactobacillus sp.* isolated from milk and milk products. Int J Curr Res 4(12):103-107.

Ashruta G, Nanoty VD, Bhalekar UK (2014) Biosorption of heavy metals from aqueous solution using bacterial EPS. Int J Life Sci 2(4):373-377.

Azzam AM, Tawfik A (2015) Removal of heavy metals using bacterial bio-flocculants of *Bacillus* sp. and *Pseudomonas* sp. J Environ Eng Landsc Manag 23(4):288-294.

Bragadeeswaran S, Jeevapriya R, Prabhu K, Rani SS, Pritadharsini S, Balasubramanian T (2011) Exopolysaccharide production by *Bacillus cereus* GU812900, a fouling marine bacterium. Afr J Microbiol Res 5(24):4124-4132.

Brose DJ, Van Eikeren P (1990) A membrane-based method for removal of toxic ammonia from mammalian-cell culture. Appl Biochem Biotechnol 24:457-468.

Cheah C, Ting ASY (2020) Microbial exopolymeric substances for metal removal. In Inamuddin I, Ahamed MI, Lichtfouse E, Asiri AM, Eds., Methods for Bioremediation of Water and Wastewater Pollution. Environmental Chemistry for a Sustainable World, vol 51. Springer, Cham.

Chen SH, Cheow YL, Ng SL, Ting ASY (2018) Influence of dyes on metal removal: a study using live and dead cells of *Penicillium simplicissimum* in single-metal and dye-metal mixtures. Water Air Soil Pollut 229:271.

Chen SH, Ng SL, Cheow YL, Ting ASY (2017) A novel study based on adaptive metal tolerance behavior in fungi and SEM-EDX analysis. J Hazmat 334:132-141.

Chew SY, Ting ASY (2016) Biosorption behaviour of alginate-immobilized *Trichoderma asperellum, a* common microfungi in single- and multi-metal systems. Sep Sci Technol 51(5):743-748.

Crini G, Lichtfouse E (2018) Green Adsorbents for Pollutant Removal: Innovative Materials. Springer, France.

De Philippis R, Colica G, Micheletti E (2011) Exopolysaccharide-producing cyanobacteria in heavy metal removal from water: molecular basis and practical applicability of the biosorption process. Appl Microbiol Biotechnol 92(4):697.

Flemming HC, Wingender J (2010) The biofilm matrix. Nat Rev Microbiol 8(9):623-633.

Finore I, Donato PD, Mastascusa V, Nicolaus B, Poli A (2014) Fermentation technologies for the optimization of marine microbial exopolysaccharide production. Marine Drugs 12(5):3005-3024.

Freitas F, Alves VD, Reis MA (2011) Advances in bacterial exopolysaccharides: from production to biotechnological applications. Trends Biotechnol 29(8):388398.

Gupta P, Diwan B (2017) Bacterial exopolysaccharide mediated heavy metal removal: a review on biosynthesis, mechanism and remediation strategies. Biotechnol Rep 13(1):58-71.

Jia C, Li X, Zhang L, Francis D, Tai P, Gong Z, Liu W (2017) Extracellular polymeric substances from a fungus are more effective than those from a bacterium in polycyclic aromatic hydrocarbon biodegradation. Water Air Soil Pollut 228(6):195.

Kilic NK, Dönmez G (2007) Environmental conditions affecting exopolysaccharide production by *Pseudomonas aeruginosa, Micrococcus sp.*, and *Ochrobactrum sp.* J Haz Mater 154(1-3):1019-1024.

Kumar AV, Darwish NA, Hilal N (2009) Study of various parameters in the biosorption of heavy metals on activated sludge. World Appl Sci J 5(Special Issue for Environment):32-40.

Lin Y, de Kreuk M, van Loosdrecht MCM, Adin A (2010) Characterization of alginate like exopolysaccharides isolated from aerobic granular sludge in pilot-plant. Water Res 44(11):335-3364.

Liu C, Lu J, Liu Y, Wang F, Min X (2010) Isolation, structural characterization an immunological activity of an exopolysaccharide produced by *Bacillus licheniformis* 837-0-1. Biores Technol 101(14):5528-5533.

Messner P (1997) Bacterial glycoproteins. Glycoconj J 14(1):3-11.

More TT, Yadav JSS, Yan S, Tyagi RD, Surampalli RY (2014) Extracellular polymeric substances of bacteria and their potential environmental applications. J Environ Manag 144(1):1-25.

Micheletti E, Colica G, Viti C, Tamagnini P, De Philippis R (2007) Selectivity in the heavy metal removal by exopolysaccharide-producing cyanobacteria. J Appl Microbiol 105(1):88-94.

Myszka K, Czaczyk K (2009) Characterization of adhesive exopolysaccharide (EPS) produced by *Pseudomonas aeruginosa* under starvation conditions. Curr Microbiol 58:541-546.

Odokuma LO (2009) Effect of culture age and biomass concentration on heavy metal

uptake by three axenic bacterial cultures. Adv Natur Appl Sci 3(3):339.

Ozturk S, Aslim B, Suludere Z, Tan S (2014) Metal removal of cyanobacterial exopolysaccharides by uronic acid content and monosaccharide composition. Carbohyd Polymers 101(1):265-271.

Pagnanelli F, Mainelli S, Bornoroni L, Dionisis D, Toro L (2009) Mechanisms of heavy metal removal by activated sludge. Chemosphere 75(8):1028-1034.

Panwichian S, Kantachite D, Witayaweerasak B, Mallavarapu M (2011) Removal of heavy metals by exopolymeric substances produced by resistant purple nonsulfur bacteria isolated from contaminated shrimp ponds. Electron J Biotechnol 14(4):2.

Pereira S, Zille A, Micheletti E, Moradas-Ferreira P, Philippis RD, Tamagnini P (2009) Complexity of cyanobacterial exopolysaccharides: composition, structures, inducing factors and putative genes involved in their biosynthesis and assembly. FEMS Microbiol Rev 33:917-941.

Razack SA, Vijayagopal V, Viruthagiri T (2011) Production of exopolysaccharides by *P. aeruginosa*, *P. fluorescens* and *Bacillus* species. IUP J Biotechnol V(4):14-19.

Ryder C, Byrd M, Wozniak DJ (2007) Role of polysaccharides in *Pseudomonas aeruginosa* biofilm development. Curr Opin Microbiol 10(6):644-648.

Seltmann G, Holst O (2013) The Bacterial Cell Wall. Springer, Berlin, Heidelberg.

Singh R, Gautam N, Mishra A, Gupta R (2011) Heavy metals and living systems: An overview. Indian J Pharmacol 43(3):246-253.

Shameer S (2016) Biosorption of lead, copper and cadmium using the extracellular polysaccharides (EPS) of *Bacillus* sp., from solar salterns. 3 Biotech 6:194.

Sheetal S, Gupte A (2016) Production and characterization of exopolysaccharide by oil emulsifying bacteria. Int J Curr Microbiol Appl Sci 5(2):254-262.

Sheng GP, Yu HQ, Li XY (2010) Extracellular polymeric substances (EPS) of microbial aggregates in biological wastewater treatment systems: a review. Biotechnol Adv 28(6):882-894.

Sivakumar T, Narayani SS, Shankar T, Dhinakaran DI (2012) Applications of exopolysaccharide producing bacterium *Frateuria aurentia*. Asian Pac J Trop Biomed 1(3):1-7.

Sulaymon AH, Mohammed AA, Al-Musawi TJ (2013) Competitive biosorption of lead, cadmium, copper, and arsenic ions using algae. Environ Sci Pollut Res Int 20(5):3011-3023.

Vu B, Chen M, Crawford RJ, Ivanova EP (2009) Bacterial extracellular polysaccharides involved in biofilm formation. Molecules 14(7):25335-2554.

Wei W, Wang Q, Li A, Yang J, Ma F, Pi SS, Wu D (2016) Biosorption of Pb (II) from aqueous solution by extracellular polymeric substances extracted from *Klebsiella* sp. J1: Adsorption behavior and mechanism assessment. Sci Rep 6:31575.

Wu H, Wu Q, Wu G, Gu Q, Wei L (2016) Cd-Resistant strains of *B. cereus* S5 with endurance capacity and their capaci-

ties for cadmium removal from cadmium polluted water. PLoS ONE 11(4):e0151479.

Zeng J, Gao JM, Chen YP, Yan P, Dong Y, Shen Y, Guo JS, Zeng N, Zhang P (2016) Composition and aggregation of extracellular polymeric substances (EPS) in hyperhaline and municipal wastewater treatment plants. Sci Rep 6:26721.

Zhang X, Liu H, Ren J, Li J, Li X (2015) Fourier transform infrared spectroscopy quantitative analysis of SF6 partial discharge decomposition components. Spectrochim Acta Part A: Mol Biomol Spectroscop 136(Part B):884-889.

Zhang Z, Cai R, Zhang W, Fu W, Jiao N (2017) A novel exopolysaccharide with metal adsorption capacity produced by a marine bacterium *Alteromona*s sp. JL2810. Marine Drugs 15(6):175.

Acta Biologica Szegediensis

Volume 65(2):233-245, 2021
Acta Biologica Szegediensis
http://abs.bibl.u-szeged.hu/index.php/abs

DOI:10.14232/abs.2021.2.233-245

ARTICLE

Comprehensive review of *Mycobacterium ulcerans* and Buruli ulcer from a bioinformatics perspective – what have we learnt?

Saubashya Sur* and Biswajit Pal

Postgraduate Department of Botany, Life Sciences Block, Ramananda College, Bishnupur-722122, West Bengal, India

ABSTRACT *Mycobacterium ulcerans* is a non-tuberculous mycobacterium responsible for causing Buruli ulcer. This is a neglected tropical disease characterized by ulceration, necrotization and scarring of the soft tissues in human limbs. Pathogenesis of *M. ulcerans* is mediated by a cytotoxic and immunosuppressive compound called mycolactone. This steadily evolving mycobacteria has adapted itself with the aquatic insect ecosystem. Human communities in wetland ecosystems are prone to Buruli ulcer and several endemic regions have been identified. So far, there is no vaccine and surgery or prolonged treatment with antibiotic cocktail has been mandated to overcome resistance patterns. Application of bioinformatics tools in *M. ulcerans* and Buruli ulcer research during the post genomic era, has provided immense opportunities. In this review, we summarize the outcome of genome studies, comparative genomics, population genomics, genetic diversity analysis, phylogenetic studies and proteomics research pertaining to this disease. We also highlight the implications of in silico vaccine design and computational studies on natural products. Resultant findings are conducive for interpreting genome architecture, pathogenomic evolution and intraspecific divergence due to phylogeographic and virulence factors of *M. ulcerans*. Moreover, the outcome of population genomics studies in disease management, coupled with the efforts in discovering vaccine candidates and novel lead compounds, will enrich our understanding of Buruli ulcer.

Acta Biol Szeged 65(2):233-245 (2021)

KEY WORDS
bioinformatics
Buruli ulcer
infectious disease
Mycobacterium ulcerans
non-tuberculous mycobacteria

ARTICLE INFORMATION
Submitted
27 September 2021
Accepted
22 October 2021
***Corresponding author**
E-mail: saubashya@gmail.com

Introduction

The broadly diverse mycobacteria are known to exist in wide ranging environments like soil, water, dust etc. (Eddyani et al. 2008; Johansen et al. 2020). They have been divided into tuberculous and non-tuberculous mycobacteria (NTM) (Wolinsky 1992). Non-tuberculous mycobacteria (NTM) consist of more than 170 different species (Baldwin et al. 2019). While majority of them have a worldwide presence, some are endemic to certain geographical locations (Hoefsloot et al. 2013). NTM are responsible for a wide array of pulmonary, extrapulmonary and disseminated diseases affecting all organs (Baldwin et al. 2019; Johansen et al. 2020). NTM infections are increasing globally owing to a multitude of factors (Collins 1989; Faverio et al. 2016). Constrained diagnostic capabilities, coupled with high degree of antibiotic resistance and lack of vaccines has aggravated the problem (Ahmed et al. 2020).

First identified in 1947, *Mycobacterium ulcerans* is a pathogenic NTM responsible for causing Buruli ulcer (Yotsu et al. 2015). *M. ulcerans* is a fragile (Eddyani et al. 2008) environmental bacterial pathogen (Ohtsuka et al. 2014), that has an optimal growth temperature of 30-33°C (Hoxmeier 2014). It has been known to adapt to certain ecological niches (Stinear et al. 2007) and are transmitted by some aquatic insects, mosquitoes, mammals etc. (Stinear et al. 2004; Einarsdottir and Huygen 2011). Evidences show that *M. ulcerans* evolved one million years ago by diverging from the common ancestor shared by *Mycobacterium marinum* (Stinear et al. 2005). This was made possible by acquisition of a plasmid encoding mycolactone and reductive evolution (Demangel et al. 2009; Hoxmeier 2014). Mycolactone is responsible for the virulence of *M. ulcerans* (Liu et al. 2019). *M. ulcerans* infection results in tissue destruction of limbs owing to necrosis of the skin and soft tissues (Einarsdottir and Huygen 2011; O'Brien et al. 2019).

The World Health Organization (WHO) considers Buruli ulcer as a neglected tropical disease. It has been reported from 34 countries (Fig. 1), especially Ghana, Benin, Democratic Republic of Congo, Ivory Coast, Togo, French Guiana, Australia, China, Papua New Guinea, and Japan (Yotsu et al. 2015; Röltgen and Pluschke 2015, Simpson et al. 2019). People living near swamps, lakes

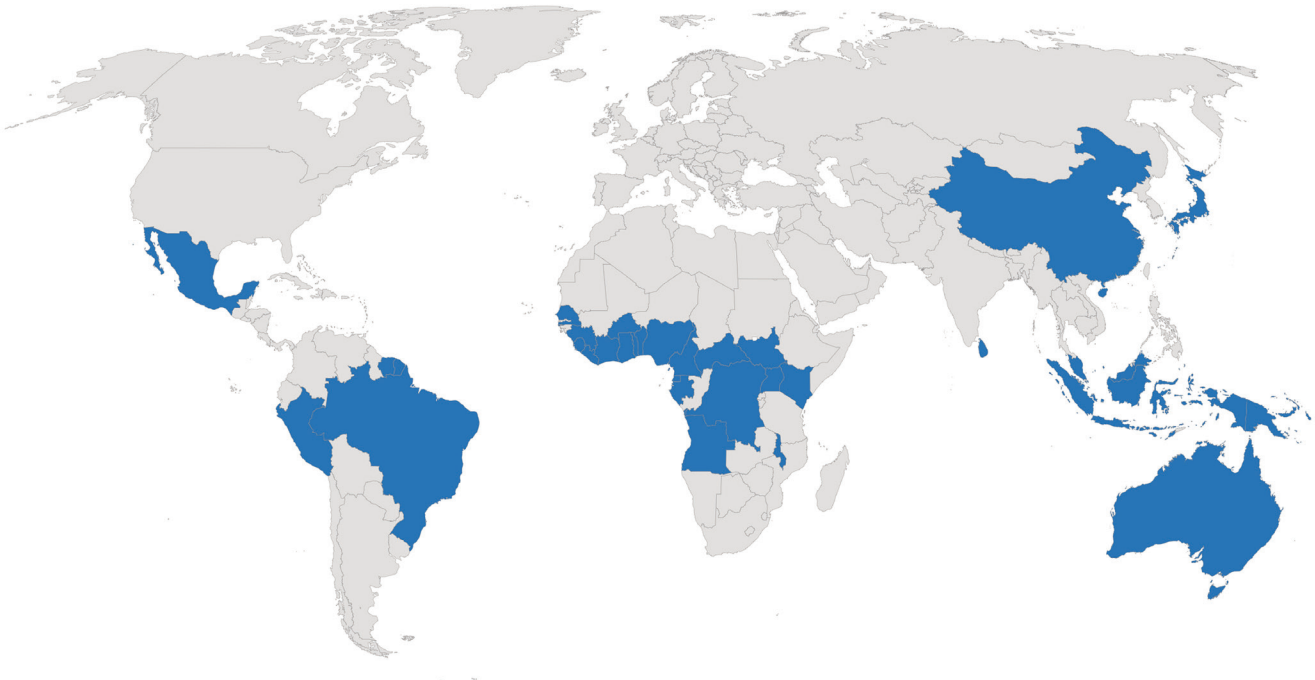

Figure 1. World map depicting countries with reported Buruli ulcer cases.

and rivers are more prone to infection (Brou et al. 2008; Einarsdottir and Huygen 2011). Changes in the ecosystem has been cited as a reason behind incidence of Buruli ulcer (Morris et al. 2014). Multiple lines of evidence have pointed out that amongst mycobacterial diseases, Buruli ulcer is the third common one after tuberculosis and leprosy (Van der Werf et al. 1999; Etuaful et al. 2005; Walsh et al. 2011). What starts as a painless nodule in the limbs, when left untreated progresses into severe ulceration and necrosis (Fig. 2) owing to the immunosuppression triggered by mycolactone (de Souza et al. 2012; Hall et al. 2014). Age, late diagnosis, and joint infections are some of the risk factors for Buruli ulcer severity (Tai et al. 2018). Immunization with BCG in a controlled setting offered small degree of protection (Smith et al. 1977). However, in the absence of suitable vaccine (Philips et al. 2014), surgery and combinatorial antibiotic treatment with rifampicin and streptomycin was recommended (Yotsu et al., 2015). In Japan, a regimen of rifampicin, levofloxacin and clarithromycin was followed (Sugawara et al. 2015). But numerous side-effects have been reported. Repurposed anti tuberculosis drugs proved to be ineffective against Buruli ulcer (Liu et al. 2018).

Explosion of genome projects in the last two decades, coupled with development of high-performance computational facilities and software have resulted in a wealth of information (Sur et al. 2010). This includes

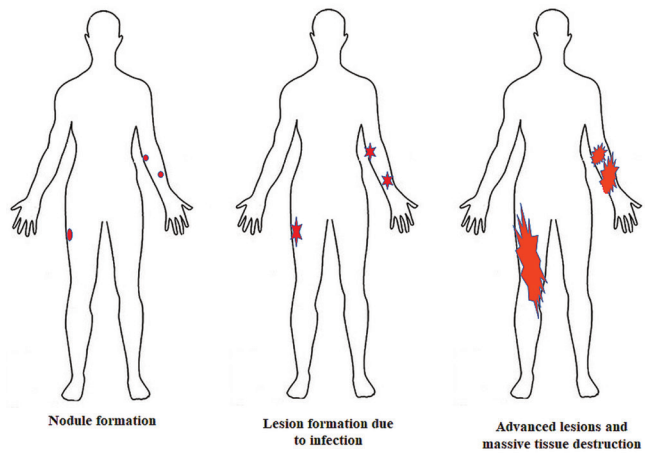

Figure 2. Buruli ulcer disease progression.

M. ulcerans as well. Here, we present a comprehensive review of the knowledge based on various bioinformatic analyses concerning *M. ulcerans* and Buruli ulcer. This is from the perspective of genomics and or comparative genomics, diversity, phylogenetic analyses, proteomics, vaccinomics, resistomics, etc. Additionally, we also comment on the opportunities of utilizing computational studies for controlling this pathogen.

Whole genome, comparative and population genomics research

Advances in molecular biology and genomics coupled with the publication of human genome in the early 21st century accelerated studies on whole genome. A necessity was felt to decode the huge deluge of information coming out from genome projects, aimed at enriching comparative genomics that could be applied to research on mycobacterial diseases (Zakham et al. 2011). While earlier genomic studies on identification of *M. ulcerans* concentrated on the use of 16SrRNA gene sequencing technology (Nakanaga et al. 2007), the whole genome sequencing of *M. ulcerans* Agy99 (Stinear et al. 2007) offered a new outlook into the biology of the pathogen. This was the first ever whole genome sequence of a *M. ulcerans* strain. It established the implication of reductive evolution and adaptation of the pathogen to specific niche (Stinear et al. 2007). Since 2007, several whole genome sequences of human pathogenic *M. ulcerans* strain Harvey, *M. ulcerans* subsp. *shinshuense* ATCC33728, *M. ulcerans* strain S4018, *M. ulcerans* strain CSURP7741, *M. ulcerans* strain SGL03, *M. ulcerans* strain P7741 etc. became available in the public domain. The genome sequence of *M. ulcerans* subsp. *shinshuense* ATCC33728 isolated from Japan and determined by 454 GS FLX Titanium technology, is made up of a 5.9 mb chromosome and a 166 kb plasmid (Yoshida et al. 2016). *M. ulcerans* strain S4018 isolated from a Buruli ulcer patient in Benin was sequenced on a MiSeq sequencer platform (Kambarev et al. 2017). *M. ulcerans* strain CSURP7741 isolated from French Guiana, was sequenced using a combinatorial approach of Nanopore and Illumina methods. It had some affinities with the frog pathogen *M. ulcerans* subsp. *lifandii* (Saad et al. 2019). Most of these genomes had a high GC content. *M. ulcerans* strain Harvey is the largest among human pathogenic *M. ulcerans,* having coding sequences more than 9000 coding sequences ((https://patricbrc.org/view/Taxonomy/2#view_tab=genomes&filter=and(keyword(Mycobacterium),keyword(ulcerans)). These genome sequences house valuable information that are crucial for understanding the phylogeny, pathophysiology, and lifestyle of this bacteria.

Over the years, comparative genomics research on different mycobacterial species have been the successful in providing valuable insights (Zakham et al. 2011). One such work focused on genes located within regions of difference accounting for 7% of *M. ulcerans* genome. The work demonstrated that gain of virulence plasmid along with deficiency of recognizable anti-virulence genes, catalyzed by IS2606 expansion. This armed the classical lineage with better capability with respect to virulence and transmissibility (Käser and Pluschke 2008). An extensive comparative genomics analyses from Benin using bioinformatic methods, resulted in the detection of 45 *M. ulcerans* specific proteins that could assist in the serodiagnosis of Buruli ulcer. This study underscored the importance of further research in generating antigenic repertoire of *M. ulcerans* (Pidot et al. 2010). That, *M. ulcerans* Agy99 showed affinity with *Mycobacterium leprae* Br4923, *Mycobacterium* sp. KMS and *Mycobacterium* sp. MCS was illustrated by a study with 14 mycobacterial genomes (Zakham et al. 2011). A comparison of whole genome sequences of thirty mycolactone producing mycobacteria and *M. marinum,* highlighted that *M. ulcerans* does not behave as a normal saprophyte. In all probability it had adapted itself to an aerobic and osmotically stable ecological niche that also protects it from light (Doig et al. 2012). Comparison of the *M. ulcerans* and *M. marinum* complex portrayed some fascinating aspects. The work highlighted mycolactone producing mycobacteria as a monophyletic group and stressed the importance to consider these bacteria as a single species i.e., *M. ulcerans* (Doig 2012). Moreover, the work also demonstrated the role of selective pressure and purifying selection in protein coding genes of *M. ulcerans.* Besides, the outcome also accentuated that speciation of *M. ulcerans* had no effect on codon translation (Doig 2012). Investigation of 21 mycobacterial genomes including *M. ulcerans* Agy99 divulged that although they differed in size, yet they had comparable high GC and low tRNA content. Besides, the ES1 locus extant in *Mycobacterium tuberculosis* and *M. marinum* was missing in *M. ulcerans* Agy99 (Zakham et al. 2012). A robust comparative genomics methodology was successful in detecting 424 essential genes from the genomes of *M. ulcerans* linked to carbohydrate and amino acid metabolism. Out of them, 236 were possible candidates for vaccine development. Furthermore, a number of enzymes associated with the cell wall, thiamine, histidine and protein biosynthesis pathways were also predicted to be prospective drug targets (Butt et al. 2012).

Increasing interest in mycobacterial comparative genomics prompted development of a user-friendly analysis platform named MycoCAP (Choo et al. 2015). This served as a suite for analyzing genomes from 55 *Mycobacterium* species including *M. ulcerans.* MycoCAP houses an assortment of web-based tools for searching, genome annotation, comparing genomes and virulence genes, determining phylogenetic relationships between mycobacterial strains and super classification. The developers of this trailblazing platform contemplate that, addition of newer genomes and their analysis will provide significant evolutionary insights (Choo et al. 2015).

The last decade also witnessed the use of whole genomes studies to figure out transmission and outbreak

of *M. ulcerans* in different countries. Research on whole genomes of *M. ulcerans* in clinical isolates from Ghana, Ivory Coast, Togo, Benin, and Nigeria, revealed widespread presence of the bacterium coupled with the existence of multiple genotypes in certain areas (Ablordey et al. 2015). The researchers opined that mobility of Buruli ulcer infected humans and livestock, from neighboring countries might have had contaminated the water bodies in different parts of Ghana. As a result, certain genotypes were introduced which later on transmitted among the population. This work stressed the need to undertake more whole genome surveys to understand the mechanism of genotype admixtures (Ablordey et al. 2015). Whole genome sequencing of isolates using NGS technologies from Benin and their comparison revealed incidence of exogenous Buruli ulcer reinfection (Eddyani et al. 2015). This incident demonstrated the importance of understanding transmission routes by targeted genome sequencing in Ouémé river valley. Another work based on whole genome amplification of crayfish samples in water bodies from Japan, illustrated seasonal emergence of *M. ulcerans* subsp. *shinshuense* (Luo et al. 2015). This study specified the link between contaminated water and incidence of Buruli ulcer.

Ever increasing number of mycobacterial genomes resulted in a plethora of information regarding cytochrome P450 monooxygenases (CYPs), a crucial enzyme for metabolic processes. Computational analysis of mycobacterial CYPs including those from *M. ulcerans* Agy99 demonstrated high diversity and their association with oxidation of steroids, fatty acids and terpenoids (Parvez et al. 2016). Human pathogenic mycobacteria have low count of CYPs which are crucial for lipid synthesis (Senate et al. 2019). Recently, a comparative study of CYPs from complete genomes of seven *M. ulcerans* strains provided insights into their lifestyle. Using CYPMiner software (Kweon et al. 2020) the study predicted 261 CYPs in the strains, classified into 35 and 38 families and subfamilies (Sur 2021). Although a few of them were diagnostic markers for some strains, there were 20 conserved families and subfamilies. While the flourishing family CYP140 was linked to mycolactone synthesis and pathogenesis, others were destined for lipid utilization. Interestingly, African strains showed similarities in their CYP profile (Sur 2021). Furthermore, the work revealed mutual association between CYP families and subfamilies.

Scientists have conducted population genomics studies applying bioinformatics methodologies, to ascertain the population structure and evolution of *M. ulcerans* in Africa. One such study using evolutionary trajectory and dynamics of *M. ulcerans* from Democratic Republic of Congo, Republic of Congo and Angola detected distinct sequence types. The research highlighted that a superior sublineage of *M. ulcerans* evolved in these countries and became endemic to hotspots in certain transmitted regions (Vandelannoote et al. 2019). This outcome once again pointed out the necessity for novel intervention-based health strategies, to disrupt transmission from localized outbreaks. Another study with whole genome sequences from clinical isolates in Melbourne, applying phylogeographic and Bayesian phylogenetic techniques divulged an interesting outcome. The investigation portrayed that *M. ulcerans* started migrating in eastern portion of Southeast Australia in the 1980's and gradually expanded to the western regions by increasing its population to a great extent (Buultjens et al. 2018). It once again emphasized the urgency to conduct environmental surveillance of pathogen mobility and have suitable interventional strategies in place to prevent migration and growth of endemic cases. It is clear from these sorts of research in Africa and Australia, that assessment of population structure and disease management based on comparative genomics data, is pivotal for controlling Buruli ulcer. In African countries and Australia with high burden of the disease, a localized assessment of *M. ulcerans* population using genomics (Vandelannoote et al. 2019a) can go a long way in treating Buruli ulcer.

Genomic diversity research based on computational techniques

Last decade of the 20th century witnessed a growing clamor for molecular typing of different strains of *M. ulcerans* from various parts of the globe (Jackson et al. 1995). Scientists were of the opinion that diversity studies would usher a new chapter for better understanding of Buruli ulcer epidemiology. Accessibility of genome sequence data of mycobacterial pathogens including *M. ulcerans,* signified the importance of studying genome polymorphisms to recognize pathogenic characteristics (Zhu et al. 2009). The necessity to have a database for mycobacterial genome polymorphisms gave birth to MyBASE. This user-friendly database accommodates information on genomic polymorphisms of different mycobacteria including *M. ulcerans*. It facilitates interpretation of diversity in pathogenicity, genome structure, evolution etc. (Zhu et al. 2009).

A single nucleotide polymorphism (SNP) profiling, using next-generation sequencing methodology from three strains of *M. ulcerans* demonstrated certain features (Qi et al. 2009). The Ghanaian isolate of *M. ulcerans* Agy99, when compared to a Japanese strain indicated 26564 SNPs in the latter. However, juxtaposition of *M. ulcerans* Agy99 with two other strains from Ghana revealed only 173 SNPs. This study illustrated that the Ghanaian clade

diverged from the Japanese strain 394-529 thousand years back, while two other Ghanaian subtypes diverged only 1000-3000 years back (Qi et al. 2009). One more study using high-throughput DNA sequencing data, of *M. ulcerans* genome isolates from Densu river basin of Ghana indicated sparse SNPs. Additional phylogenetic reconstruction analysis using SNP genotyping data divulged the ascendancy of a clonal complex and variants within it (Röltgen et al. 2010).

It was reported that multilocus sequence typing (MLST) based on housekeeping genes, of *M. ulcerans* isolates resulted in six contrasting genotypes from wide-ranging biogeographical regions of the world (Narh et al. 2014). Comparative DNA analysis between samples from water, soil, biofilms, and clinical samples, from Buruli ulcer patients in South Togo revealed similar *M. ulcerans* genetic profile (Maman et al. 2018). This study demonstrated riverine source of *M. ulcerans* infection in regions through which Haho and Zio rivers flow. MLST, short read DNA sequencing and SNP calling in a Japanese study, illustrated the difference between pigmented and non-pigmented colonies of *M. ulcerans* subsp. *shinshuense.* The pigmented and non-pigmented isolates differed only in 8 SNPs and 20 indels (Nakanaga et al. 2018). The latter was devoid of a large plasmid encoding regions for mycolatone biosynthesis, rendering it non-pathogenic in contrast to the former. Genome-wide association analysis of Buruli ulcer patients from Ouémé and plateau regions of Benin, revealed the role of lncRNAs and pathways linked to autophagy in the disease (Manry et al. 2019). These sort of genomic diversity studies using an assortment of computational techniques, enhanced our understanding of *M. ulcerans* regarding intraspecific divergence, geographical dissimilarities, virulence etc.

Research from Benin assessed bacterial diversity in skin lesions from individuals with Buruli ulcer. They performed a small-scale microbiome analysis using 16SrRNA sequencing, to gauge the composition of microbes from Buruli ulcer lesions, non Buruli ulcer lesions and skin samples of healthy persons (Leuvenhaege et al. 2017). The samples from Buruli ulcer lesions exhibited higher proportion of unassociated bacteria like *Bacteroides* and obligate anaerobes, in contrast to non Buruli ulcer lesions (Van Leuvenhaege et al. 2017). Since, skin microbiome is influenced by geography, genetics, climatic condition etc., its comparative study on a large scale should be used for estimating diversity in different populations (Nuhamunada et al. 2018). This work on Buruli ulcer lesions from Benin underlined that, additional microbiome-based analysis should be accompanied with standard microbiological studies.

In silico phylogenetics studies

Rapid improvement in "omics" data analysis and mycobacterial genomics research, has contributed to the understanding of evolutionary mechanisms (Bottai et al. 2014). One of the earliest works based on whole genome of *M. ulcerans* Agy99, indicated its evolution by lateral gene transfer and reductive evolution from *M. marinum* (Stinear et al. 2007). In fact, a number of factors viz., amassing 304 insertion sequence elements like IS2404 and IS2606, presence of 771 pseudogenes, genomic rearrangements, genome reduction, inability to tolerate sunlight, plasmid acquisition, mycolactone selective pressure and occurrence of foreign genes, contributed to its evolution and allowed it to colonize insects (Fig. 3a) by adapting to an arthropod ecosystem (Stinear et al. 2007). Moreover, the loss of ESX1 locus was also regarded as a survival strategy. Extensive comparative genomics analysis of insertions, deletions and genomic rearrangements from clinical isolates of *M. ulcerans* revealed that the microorganism evolved into five haplotypes (Käser et al. 2007). Two phylogeographically well-defined lineages were observed (Fig. 3a). The classical lineage underwent substantial genomic rearrangements and comprised of highly pathogenic genotypes concentrated mainly in Africa, Australia and Southeast Asia. They were over-represented by genes belonging to the PPE/PE families. On the other hand, the less pathogenic ancestral lineage housed environmental genotypes from China, South America and Mexico which showed similarity with *M. marinum* (Käser et al. 2007). There is strong evidence that, the classical and ancestral lineages diverged during the arrival of modern humans (Qi et al. 2009). However, the African isolates were not quite archaic and came into existence in the last 18,000 years (Stinear et al. 2000).

Some *in silico* analysis pointed out that, reductive evolution increased the pathogenic capacity of *M. ulcerans* by gaining a virulence plasmid pMUM001 (Demangel et al. 2009). Further comparative evolutionary genomic studies with two Ghanaian strains and one Japanese strain, demonstrated that the latter had an unstable genome compared to the former. Additionally, reductive evolutionary pressure was less among the Ghanaian strains (Qi et al. 2009). These were attributed to chromosomal rearrangements. Phylogenetic analysis of different mycobacterial species using 16SrRNA sequences, divulged the placement of *M. ulcerans* in a separate clade along with *M. marinum* (Zakham et al. 2012). A vast phylogenetic study with mycolactone producing mycobacteria including *M. ulcerans,* specified the role of pMUM plasmid housing genes for mycolactone biosynthesis to their advent (Doig et al. 2012). Add to this was the gain of cell wall associated genes and loss of cell wall antigens. This set

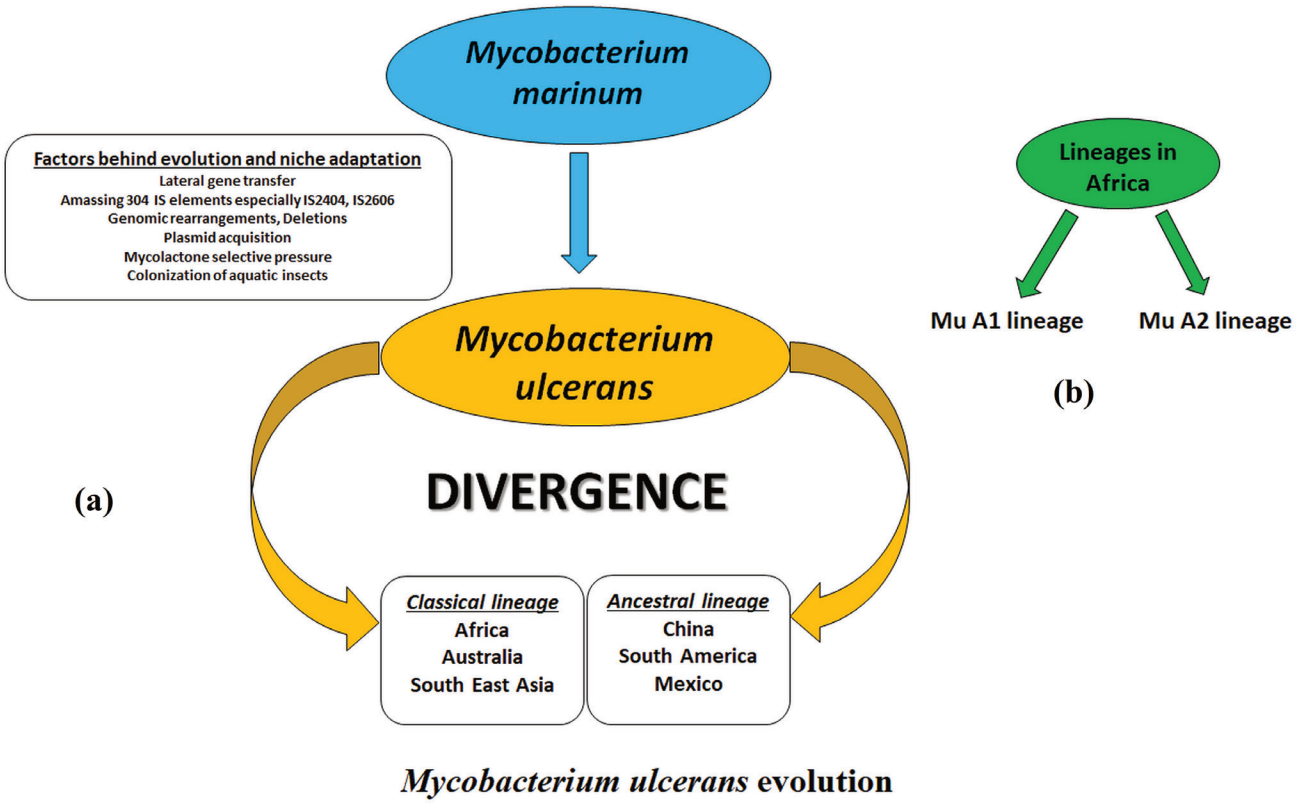

Figure 3. (a) Schematic depiction of the evolution of *Mycobacterium ulcerans* and its divergence into two major lineages (Stinear et al. 2007; Käser et al. 2007; Käser and Pluschke 2008). Note the factors responsible for evolution from *M. marinum* and niche adaptation. (b) Specific *M. ulcerans* lineages from Africa (Vandelannoote et al. 2017; Zingue et al. 2018).

off the process of cell wall remodeling that was crucial for the lifestyle of *M. ulcerans,* especially in its potential to form biofilms. Additional analysis of the mycolactone producing mycobacterial complex showed that, *M. ulcerans* were in all probability transferred between Africa and Australia not long ago. This was ascribed to genetic drift and deletion of some genes, linked to metabolism and respiration that were futile for adaptation to distinct ecological niches (Doig et al. 2012).

Phylogenetic analysis based on complete mycobacterial genomes, hypothesized occurrence of shared common mobile elements between *M. ulcerans* and *M. marinum* (Reva et al. 2015). Moreover, reticulate network analysis also supported the close relationship between these bacteria. Evolutionary reconstruction studies and Bayesian analysis of *M. ulcerans* from 11 endemic regions of Africa, identified two specific *M. ulcerans* lineages (Fig. 3b) housed in the continent (Vandelannoote et al. 2017). While the Mu_A1 lineage was from 68 BC, the Mu_A2 lineage was introduced by humans in 1800 AD (Zingue et al. 2018). The close relation of the latter with isolates from Papua New Guinea was attributed to anthropogenic activities.

One recent phylogenetic study with *M. ulcerans* from French Guiana and its comparison with global strains, utilizing core and accessory genomes threw up interesting facts. Five distinct lineages were identified by maximum likelihood phylogeny (Reynoud et al. 2019). Out of these, the L1.2 lineage was completely independent. The French Guinean strains were clustered together (Reynoud et al. 2019). Research using complex whole genome sequences of *M. ulcerans* from Australian counties, underscored the impact of microevolution. It was found that three *M. ulcerans* complex clones, were the reason behind uptick of cases in Southern Australian counties compared to non-endemic counties in rest of Australia (Saad et al. 2020).

The outcome of *M. ulcerans* phylogenetic studies accentuated the interplay of myriad factors including phylogeography and human activities, which were responsible for variation amongst lineages, pathogenic lifestyle, and adaptation to specific niches.

Proteomics of *M. ulcerans* and Buruli ulcer

Prokaryote research has reaped the benefit of rapid advances in the field of proteomics (Burley and Bonnano 2002). One of the pioneering computational proteome-based studies concerning *M. ulcerans,* was a comparative analysis of *Mycobacterium tuberculosis* strains and NTMs that included *M. ulcerans* Agy99 (Zakham et al. 2012). It used a BLAST matrix to perform genomic analysis of the predicted proteomes (Zakham et al. 2012). The work revealed low similarity between *M. tuberculosis* strains, *M. ulcerans* Agy99 and MAV complex. A classic investigation involving quantitative proteomics and transcript level analysis, highlighted the implication of culture conditions on the regulation of mycolactone toxin in *M. ulcerans* (Deshayes et al. 2013). Data from 2D gel electrophoresis and mass spectrometry analysis demonstrated that during pathogenesis and lesion formation, mycolactone altered the cytoskeleton and hindered collagen biosynthesis (Gama et al. 2014). It reiterated that mycolactone toxin was associated with reduction in collagen content in Buruli ulcer lesions. Another worker (Sarpong 2018) used high throughput mass spectrometry data to explore differentially expressed proteins from fast and slow healing Buruli ulcers. Highly expressed proteins viz., IFI30, PSME3, CD74, C4A linked to MHC class I, MHC class II and complement pathways showed better promise in healing Buruli ulcer (Sarpong 2018).

Vaccinomics research

The genome sequencing of a number of *M. ulcerans* strains opened up numerous possibilities for identifying potential vaccine candidates. Currently, there is no vaccine preventing Buruli ulcer (Mangas et al. 2020). A limited transient protection lasting for a year or so has been reported in individuals administered with *Mycobacterium bovis* BCG vaccine (Einarsdottir and Huygen 2011). Thus, development of a suitable vaccine is important for preventing *M. ulcerans* infections and Buruli ulcer severity. In the post genomic era, a study on mice revealed the efficacy of priming species specific Ag85A-DNA and homologous protein boosting, in eliciting strong Th1 immune responses against *M. ulcerans* infection (Tanghe et al. 2008). Efforts to develop inactivated vaccines, DNA/protein vaccines by targeting the mycolactone toxin, enzymes synthesizing mycolactones, mycobacterial proteins and *M. ulcerans* specific proteins demonstrated some degree of humoral and cellular responses (Huygen et al. 2009; Pidot et al. 2010; Einarsdottir and Huygen 2011). Comparative genomics methods were used for serological assessment of the antigens (Pidot et al. 2010). However, none of them were tested in clinical trials. The last decade saw increased interest in *in silico* identification of potential antigens and peptides for designing new vaccine candidates. Development of mycobacrvR package using reverse vaccinology and integrative immunoinformatic approach, served as a means for designing epitope-based vaccine candidates against mycobacterial diseases (Chaudhuri et al. 2014). This package used an assortment of 20 algorithms for determining adhesins with extracellular and surface localized characteristics (Chaudhuri et al. 2014). Analysis of the whole proteome of *M. ulcerans* Agy99 identified 36 adhesin and adhesin like proteins. Out of these, 26 potential vaccine candidates were identified by the enhanced reverse vaccinology method (Chaudhuri et al. 2014). Others attempted to develop a recombinant vaccine from *Mycobacterium marinum* against Buruli ulcer (Hart et al. 2016).

Mycobacterial secretory proteins have been the target of vaccine researchers since they are known to induce immune responses (Gcebe et al. 2016). There is evidence that the PE/PPE family of genes possess the capability to elicit Th1 response against tuberculosis (Bennan et al. 2017). Some workers studied the highly antigenic PE-PGRS family proteins from the whole proteome of *M. ulcerans* Agy99, to predict multi-epitope vaccine against it (Nain et al. 2020). They applied a robust integrated vaccinomics methodology (Fig. 4) by utilizing a wide array of algorithms. Initially, they selected 15 suitable epitopes which interacted with HLA binding alleles and demonstrated significant population coverage on a global coverage. This was followed by designing the vaccine chimera. The designed construct revealed antigenic, immunogenic, and non-allergenic characteristics. Docking and MD simulation studies demonstrated binding affinity with TLR2 receptor (Nain et al. 2020). Furthermore, *in silico* cloning, codon optimization and *in silico* immune response simulation analysis postulated that the vaccine construct is a suitable candidate for generating immune response against *M. ulcerans* Agy99 (Nain et al. 2020). Although, experimental studies are necessary to substantiate the findings.

In silico studies on antibiotic resistance and exploration of natural products as anti Buruli ulcer drugs

The World Health Organization (WHO) has approved the use of antibiotics for primary treatment of Buruli ulcer lesions (Omansen et al. 2019). Although there are some uncertainties surrounding antibiotic therapy, further treatments using surgery, physical therapy, analgesia, and community therapy are followed in many countries

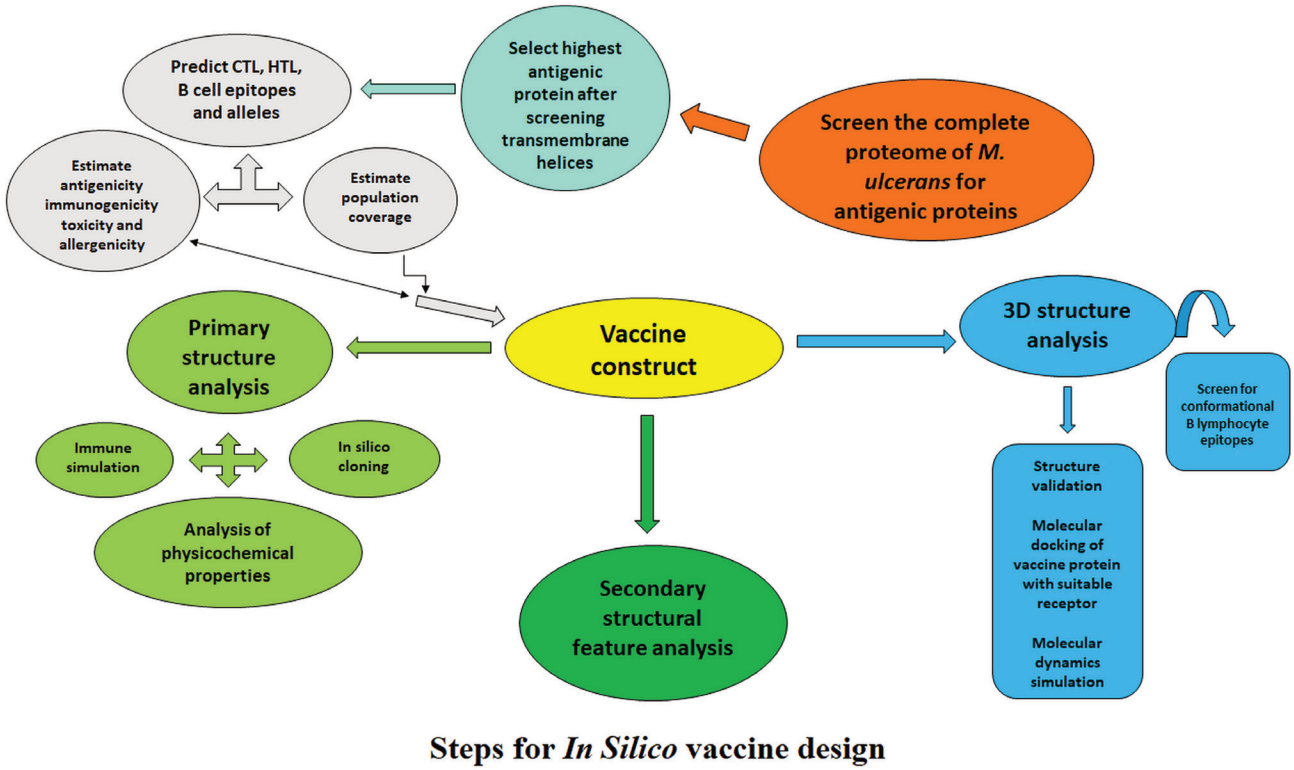

Figure 4. Schematic representation of the *in silico* vaccine design methodology (Nain et al. 2020). CTL = cytotoxic T-lymphocyte, HTL = helper T-lymphocyte.

(Omansen et al. 2019). In recent years, development of a number of bioinformatics tools and databases, opened up the possibility of exploring microbial whole genome sequencing data for investigating antibiotic resistance (Hendriksen et al. 2019). An *in silico* study highlighted the occurrence of 14 antibiotic resistance genes in *M. ulcerans* Agy99. Single mutation in *katG* and *pncA* genes were responsible for resistance to isoniazid and pyrazinamide drugs (Gupta et al. 2017). This rendered them useless against *M. ulcerans* Agy99. Additionally, this study predicted that, using a cocktail of antibiotics like rifampin, streptomycin, azithromycin, clarithromycin etc., probably assisted in overcoming the impact of mutation and may control Buruli ulcer (Gupta et al. 2017). Nonetheless, these sorts of studies should be expanded to other *M. ulcerans* strains as well.

The growing concern of antibiotic resistance, coupled with the lack of potent antibiotics against late stage Buruli ulcer has troubled the clinicians. Despite this, identification of suitable lead compounds that could act as anti Buruli ulcer drug in an *in silico* study from Ghana (Kwofie et al. 2018) showed promise. They screened isocitrate lyase from *M. ulcerans and* generated its three-dimensional structure using molecular modeling. After refinement, molecular dynamics simulation, and active site prediction, the structure was used for molecular docking with AutoDock (Kwofie et al. 2018). Virtual screening of the AfroDb for natural compounds, followed by docking resulted in 20 compounds showing reasonable affinity for isocitrate lyase. Further physicochemical analysis and ADMET testing narrowed upon ZINC38143792, ZINC95485880, and ZINC95486305 as best leads that could be suitable for experimental validation (Kwofie et al. 2018). These lead compounds known to possess inhibitory (Mujovo et al. 2008) and anti-bacterial properties (Kwofie et al. 2018) possibly restricted disease progression by neutralising isocitrate lyase.

Conclusion and future perspectives

Buruli ulcer caused by *M. ulcerans* is a neglected tropical disease. *M. ulcerans* has been understudied in comparison to other mycobacterial pathogens. The major burden of Buruli ulcer is often borne by the poor. This has resulted in socioeconomic problems. In the recent years, a deluge of information from *M. ulcerans* genome projects, coupled with state-of-the art research in comparative genomics,

population genomics, pathogen mobility/transmissibility, pathogen phylogeny, proteomics and designing vaccine candidates using *in silico* tools, has provided fantastic insights. This has revolutionized our understanding of Buruli ulcer. Phylogenetic and population genomics studies have illustrated the significance of incorporating microbial phylogeographic data in the analysis, since it highlighted information about strain origin, spread of the bacterium and migration of hosts. This has met with success in some regions of Africa and Australia wherein, early detection of active cases, surveillance and treatment resulted in reduced transmission and disease incidence (Vandelannoote et al. 2017, 2019). However, lot more needs to be done. Governments and international organizations should understand the necessity to finance Buruli ulcer research so as to improve disease control measures and minimize the burden. There is a need to have an international network of researchers with diverse expertise to foster technological innovations. This should be aimed at expanding high precision cost effective sequencing methodologies, advancing development of new tools/software, large scale targeted studies on genome variability/diversity in countries/regions with high prevalence, investigating the pattern of host microbiomes and identification of new vaccine candidates. Information from genomes could also be used to develop potent diagnostic and treatment regimens. Moreover, genome-based investigations should be increasingly conducted to understand insect vector-based transmission of Buruli ulcer. This is important since, *M. ulcerans* has crafted an ecological niche for itself in aquatic insects. Furthermore, there is a need to broaden newer genotyping strategies and boosting genomic diversity studies. Sequencing more genomes from different locations could aid such studies. Additionally, *in silico* techniques should be applied to understand the nature of pMUM plasmid and mechanism of mycolactone toxin immunosuppression (Einarsdottir and Huygen 2011). The information from such studies can aid in the development of effective vaccines and therapeutic drugs against *M. ulcerans,* using immunoinformatics and immunogenomics approaches. Pharmaceutical companies and biomedical industries should take initiatives to validate the vaccine constructs designed by robust *in silico* techniques. Computational studies on antimicrobial inhibitors and drug compounds from indigenous plants should be encouraged. This aspect of research is lacking. Clinicians and pharmaceutical scientists should assist bioinformaticians in this regard to combat the pathogen. The bottom line is to have a multidisciplinary effort in place, to better understand the epidemiological and transmission factors of this challenging and steadily evolving bacterium.

Acknowledgements

The authors express gratitude to Ramananda College, India. This work was partially carried out utilizing the grant support (Ref. No: 826/B/2020) to SS by Ramananda College. The authors also thank anonymous reviewers for their constructive comments.

References

Ablordey AS, Vandelannoote K, Frimpong IA, Ahortor EK, Amissah NA, Eddyani M, Durnez L, Portaels F, de Jong BC, Leirs H, Porter JL, Mangas KM, Lam MMC, Buultjens A, Seemann T, Tobias NJ, Stinear TP (2015) Whole genome comparisons suggest random distribution of *Mycobacterium ulcerans* genotypes in a Buruli ulcer endemic region of Ghana. PLoS Negl Trop Dis 9:e0003681.

Ahmed I, Tiberi S, Farooqi J, Jabeen K, Yeboah-Manu D, Migliori GB, Hasan R (2020) Non-tuberculous mycobacterial infections—a neglected and emerging problem. Int J Infect Dis 92S:S46-S50.

Baldwin SL, Larsen SE, Ordway D, Cassell G, Coler RN (2019) The complexities and challenges of preventing and treating nontuberculous mycobacterial diseases. PLoS Negl Trop Dis 13:e0007083.

Bottai D, Stinear TP, Supply P, Brosch R (2014) Mycobacterial pathogenomics and evolution. Microbiol Spectr 2:MGM2-0025-2013.

Brennan MJ (2017) The enigmatic PE/PPE multigene family of mycobacteria and tuberculosis vaccination. Infect Immun 85:e00969-16.

Brou T, Broutin H, Elguero E, Asse H, Guegan JF (2008) Landscape diversity related to Buruli ulcer disease in Côte d'Ivoire. PLoS Negl Trop Dis 2:e271.

Buultjens AH, Vandelannoote K, Meehan CJ, Eddyani M, de Jong BC, Fyfe JAM, Globan M, Tobias NJ, Porter JL, Tomita T, Tay EL, Seemann T, Howden BP, Johnson PDR, Stinear TP (2018) Comparative genomics shows that *Mycobacterium ulcerans* migration and expansion preceded the rise of Buruli ulcer in southeastern Australia. Appl Environ Microbiol 84:e02612-17.

Burley SK, Bonnano JB (2002) Structuring the universe of proteins. Ann Rev Genomics Hum Genet 3:243-262.

Butt AM, Nasrullah I, Tahir S, Tong Y (2012) Comparative genomics analysis of *Mycobacterium ulcerans* for the identification of putative essential genes and therapeutic candidates. PLoS ONE 7:e43080.

Chaudhuri R, Kulshrestha D, Raghunandan MV, Ramachandran S (2014) Integrative immunoinformatics for mycobacterial diseases in R platform. Syst Synth Biol

8:27-39.
Choo SW, Ang MY, Dutta A, Tan SY, Siow CC, Heydari H, Mutha NVR, Wee WY, Wong GH (2015) MycoCAP-*Mycobacterium* comparative analysis platform. Sci Rep 5:18227.
Collins FM (1989) Mycobacterial disease, immunosuppression, and acquired immunodeficiency syndrome. Clin Microbiol Rev 2:360–377.
Demangel C, Stinear T, Cole S (2009) Buruli ulcer: reductive evolution enhances pathogenicity of *Mycobacterium ulcerans*. Nat Rev Microbiol 7:50–60.
Deshayes C, Angala SK, Marion E, Brandli I, Babonneau J, Preisser L, Eyangoh S, Delneste Y, Legras P, De Chastellier C, Stinear TP, Jackson M, Marsollier L (2013) Regulation of mycolactone, the *Mycobacterium ulcerans* toxin, depends on nutrient source. PLoS Negl Trop Dis 7:e2502.
de Souza KD, Quaye C, Mosi L, Addo P, Boakye DA (2012) A quick and cost-effective method for the diagnosis of *Mycobacterium ulcerans* infection. BMC Infect 12:8.
Doig KD (2012) Comparative genomics of the *Mycobacterium ulcerans* and *Mycobacterium marinum* complex. MPhil Thesis, Melbourne University, Melbourne, Australia.
Doig KD, Holt KE, Fyfe JAM, Lavender CJ, Eddyani M, Portaels F, Yeboash-Manu D, Pluschke G, Seemann T, Stinear TP (2012) On the origin of *Mycobacterium ulcerans*, the causative agent of Buruli ulcer. BMC Genomics 13:258.
Eddyani M, De Jonckheere JF, Durnes L, Suykerbuyk P, Leirs H, Portaels F (2008) Occurrence of fee-living amoebae in communities of low and high endemicity for Buruli Ulcer in southern Benin. Appl Environ Microbiol 74:6547-6553.
Eddyani M, Vandelannoote K, Meehan CJ, Bhuju S, Porter JL, Aguiar J, Seemann T, Jarek M, Singh M, Portaels F, Stinear TP, de Jong BC (2015) A genomic approach to resolving relapse versus reinfection among four cases of Buruli Ulcer. PLoS Negl Trop Dis 9:e0004158.
Einarsdottir T, Huygen K (2011) Buruli ulcer. Human Vaccines 7:1198-1203.
Etuaful S, Carbonnelle B, Grosset J, Lucas S, Horsfield C, Phillips R, Evans M, Ofori-Adjei D, Klustse E, Owusu-Boateng J, Amedofu GK, Awuah P, Ampadu E, Amofah G, Asiedu K, Wansbrough-Jones M (2005) Efficacy of the combination rifampin-streptomycin in preventing growth of *Mycobacterium ulcerans* in early lesions of Buruli ulcer in humans. Antimicrob Agents Chemother 49:3182–3186.
Faverio P, Stainer A, Bonaiti G, Zucchetti SC, Simonetta E, Lapadula G, Marruchella A, Gori A, Blasi F, Codecasa L, Pesci A, Chalmers JD, Loebinger MR, Aliberti S (2016) Characterizing non-tuberculous mycobacteria infection in bronchiectasis. Int J Mol Sci 17:1913.
Gama JB, Ohlmeier S, Martins TG, Fraga AG, Sampaio-Marques B, Carvalho MA, Proença F, Silva MT, Pedrosa J, Ludovico P (2014) Proteomic analysis of the action of the *Mycobacterium ulcerans* toxin mycolactone: targeting host cells cytoskeleton and collagen. PLoS Negl Trop Dis 8:e3066.
Gcebe N, Michel A, Gey van Pittius NC and Rutten V (2016) Comparative genomics and proteomic analysis of four non-tuberculous *Mycobacterium* species and *Mycobacterium tuberculosis* complex: occurrence of shared immunogenic proteins. Front Microbiol 7:795.
Gupta SK, Drancourt M, Rolain JM (2017) In silico prediction of antibiotic resistance in *Mycobacterium ulcerans* Agy99 through whole genome sequence analysis. Am J Trop Med Hyg 97:810–814.
Hall BS, Hill K, McKenna M, Ogbechi J, High S, Willis AE, Simmonds RE (2014) The pathogenic mechanism of the *Mycobacterium ulcerans* virulence factor, mycolactone, depends on blockade of protein translocation into the ER. PLoS Pathog 10:e1004061.
Hart BE, Laura PH, Sunhee L (2016) Immunogenicity and protection conferred by a recombinant *Mycobacterium marinum v*accine against Buruli Ulcer. Trials Vaccinol 5:88–91.
Hendriksen RS, Bortolaia V, Tate H, Tyson GH, Aarestrup FM, McDermott PF (2019) Using genomics to track global antimicrobial resistance. Front Public Health 7:242.
Hoefsloot W, van Ingen J, Andrejak C, Angeby K, Bauriaud R, Bemer P, Beylis N, Boeree MJ, Cacho J, Chihota V, Chimara E, Churchyard G, Cias R, Daza R, Daley CL, Dekhuijzen PN, Domingo D, Drobniewski F, Esteban J, Fauville-Dufaux M, Folkvardsen DB, Gibbons N, Gómez-Mampaso E, Gonzalez R, Hoffmann H, Hsueh PR, Indra A, Jagielski T, Jamieson F, Jankovic M, Jong E, Keane J, Koh WJ, Lange B, Leao S, Macedo R, Mannsåker T, Marras TK, Maugein J, Milburn HJ, Mlinkó T, Morcillo N, Morimoto K, Papaventsis D, Palenque E, Paez-Peña M, Piersimoni C, Polanová M, Rastogi N, Richter E, Ruiz-Serrano MJ, Silva A, da Silva MP, Simsek H, van Soolingen D, Szabó N, Thomson R, Tórtola Fernandez T, Tortoli E, Totten SE, Tyrrell G, Vasankari T, Villar M, Walkiewicz R, Winthrop KL, Wagner D (2013) Nontuberculous Mycobacteria Network European Trials Group. The geographic diversity of nontuberculous mycobacteria isolated from pulmonary samples: an NTM-NET collaborative study. Eur Respir J 42:1604-13.
Hoxmeier JC (2014) The pathogenesis and environmental maintenance of *Mycobacterium ulcerans*. PhD thesis. Colorado State University, Colorado, USA.
Huygen K, Adjei O, Affolabi D, Bretzel G, Demangel C, Fleischer B, Johnson RC, Pedrosa G, Phanzu DM, Phillips RO, Pluschke G, Siegmund F, Singh M, van der Werf TS, Wansbrough-Jones M, Portaels F (2009) Buruli ulcer disease: prospects for a vaccine. Med Microbiol Immunol

(Berl) 198:69-77.

Jackson K, Edwards R, Leslie DE, Hayman J (1995) Molecular method for typing *Mycobacterium ulcerans*. J Clin Microbiol 33:2250-3.

Johansen MD, Herrmann JL, Kremer L (2020) Non-tuberculous mycobacteria and the rise of *Mycobacterium abscessus*. Nat Rev Microbiol 18:392-407.

Kambarev S, Corvec S, Chauty A, Marion E, Marsollier L, Pecorari F (2017) Draft genome sequence of *Mycobacterium ulcerans* S4018 isolated from a patient with an active Buruli ulcer in Benin, Africa. Genome Announc 5:e00248-17.

Käser M, Rondini S, Naegeli M, Stinear T, Portaels F, Certa U, Pluschke G (2007) Evolution of two distinct phylogenetic lineages of the emerging human pathogen *Mycobacterium ulcerans*. BMC Evol Biol 7:177.

Käser M, Pluschke G (2008) Differential gene repertoire in *Mycobacterium ulcerans* identifies candidate genes for patho-adaptation. PLoS Negl Trop Dis 2:e353.

Kweon K, Kim SJ, Kim JH, Nho SW, Bae D, Chon J, Hart M, Baek DH, Kim YC, Wang W, Kim SK, Sutherland JB, Cerniglia CE (2020) CYPminer: an automated cytochrome P450 identification, classification, and data analysis tool for genome data sets across kingdoms. BMC Bioinformatics 21:160.

Kwofie SK, Dankwa B, Odame EA, Agamah FE, Doe LPA, Teye J, Agyapong O, Miller 3rd WA, Mosi L, Wilson MD (2018) *In silico* screening of isocitrate lyase for novel anti-Buruli ulcer natural products originating from Africa. Molecules 23:1550.

Liu Y, Gao Y, Liu J, Tan Y, Liu Z, Chhotaray C, Jiang H, Lu Z, Chiwala G, Wang S, Makafe G, Islam MM, Hameed HMA, Cai X, Wang C, Li X, Tan S, Zhang T (2019) The compound TB47 is highly bactericidal against *Mycobacterium ulcerans* in a Buruli ulcer mouse model. Nat Commun 10:524.

Luo Y, Degang Y, Ohtsuka M, Ishido Y, Ishii N, Suzuki K (2015) Detection of *Mycobacterium ulcerans* subsp. *shinshuense* DNA from a water channel in familial Buruli ulcer cases in Japan. Future Microbiol 10:461-469.

Maman I, Tchacondo T, Kere AB, Beissner M, Badziklou K, Tedihou E, Nyaku E, Amekuse K, Wiedemann FX, Karou DS, Bretzel G (2018) Molecular detection of *Mycobacterium ulcerans* in the environment and its relationship with Buruli ulcer occurrence in Zio and Yoto districts of maritime region in Togo. PLoS Negl Trop Dis 12:e0006455.

Mangas KM, Tobias NJ, Marion E, Babonneau J, Marsollier L, Porter JL, Pidot SJ, Wong CY, Jackson DC, Chua BY, Stinear TP (2020) High antibody titres induced by protein subunit vaccines using *Mycobacterium ulcerans* antigens Hsp18 and MUL_3720 with a TLR-2 agonist fail to protect against Buruli ulcer in mice. Peer J 8:e9659.

Manry J, Vincent QB, Johnson C, Chrabieh M, Lorenzo L, Theodorou I, Ardant MF, Marion E, Chauty A, Marsollier L, Abel L, Alcais A (2020) Genome-wide association study of Buruli ulcer in rural Benin highlight's role of two LncRNAs and the autophagy pathway. Commun Biol 3:177.

Morris A, Gozlan R, Marion E, Marsollier L, Andreou D, Sanhueza D, Ruffine R, Couppie P, Guegan JF (2014) First Detection of *Mycobacterium ulcerans* DNA in environmental samples from South America. PLoS Negl Trop Dis 8:e2660.

Mujovo SF, Hussein AA, Meyer JJM, Fourie B, Muthivhi T, Lall N (2008) Bioactive compounds from *Lippia javanica* and *Hoslundia opposita*. Nat Prod Res 22:1047-1054.

Nakanaga K, Ishii N, Suzuki K, Tanigawa K, Goto M, Okabe T, Imada H, Kodama A, Iwamoto T, Takahashi H, Saito H (2007) "*Mycobacterium ulcerans* subsp. *shinshuense*" isolated from a skin ulcer lesion: identification based on 16S rRNA gene sequencing. J Clin Microbiol 45:3840-3843.

Nakanaga K, Ogura Y, Toyoda A, Yoshida M, Fukano H, Fujiwara N, Miyamoto Y, Nakata N, Kazumi Y, Maeda S, Ooka T, Goto M, Tanigawa K, Mitarai S, Suzuki K, Ishii N, Ato M, Hayashi T, Hoshino Y (2018) Naturally occurring a loss of a giant plasmid from *Mycobacterium ulcerans* subsp. *shinshuense* makes it non-pathogenic. Sci Rep 8:8218.

Nain Z, Karim MM, Sen MK, Adhikari UK (2020) Structural basis and designing of peptide vaccine using PE-PGRS family protein of *Mycobacterium ulceran*s - An integrated vaccinomics approach. Mol Immunol 120:146-163.

Narh CA, Mosi L, Quaye C, Tay SCK, Bonfoh B, deSouza DK (2014) Genotyping tools for *Mycobacterium ulcerans* drawbacks and future prospects. J Mycobac Dis 4:149.

Nuhamunada M, Pratama GA, Wikanthi S, Anam MK, Rizki RLP, Wijayanti N (2018) Data mining and comparative analysis of human skin microbiome from EBI metagenomics database. In 1st International Conference on Bioinformatics, Biotechnology, and Biomedical Engineering-Bioinformatics and Biomedical Engineering, 1-6, doi:10.1109/BIOMIC.2018.8610588.

O'Brien DP, Murrie A, Meggyesy P, Priestley J, Rajcoomar A, Athan E (2019) Spontaneous healing of *Mycobacterium ulcerans* disease in Australian patients. PLoS Negl Trop Dis 13:e0007178.

Ohtsuka M, Kikuchi N, Yamamoto T, Suzutani T, Nakanaga K, Suzuki K, Ishii N (2014) Buruli ulcer caused by *Mycobacterium ulcerans* subsp. *shinshuense*: a rare case of familial concurrent occurrence and detection of insertion sequence 2404 in Japan. JAMA Dermatol 150:64-67.

Omansen TF, van der Werf TS, Phillips RO (2019) Antimicobial treatment of *Mycobacterium ulcerans* infection. In Pluschke G, Röltgen K, Eds, Buruli Ulcer, Springer, Switzerland, 203-220.

Parvez M, Qhanya LB, Mthakathi NT, Kgosiemang IK, Bamal HD, Pagadala NS, Xie T, Yang H, Chen H, Theron CW, Monyaki R, Raselemane SC, Salewe V, Mongale BL, Matowane RG, Abdalla SM, Booi WI, van Wyk M, Olivier D, Boucher CE, Nelson DR, Tuszynski JA, Blackburn JM, Yu JH, Mashele SS, Chen W, Syed K (2016) Molecular evolutionary dynamics of cytochrome P450 monooxygenases across kingdoms: Special focus on mycobacterial P450s. Sci Rep 6:33099.

Phillips R, Horsfield C, Laing MK, Awuah EP, Nyarko K, Osei-Sarpong F, Butcher P, Lucas S, Wansbrough-Jones M (2006) Cytokine mRNA expression in *Mycobacterium ulcerans*-Infected human skin and correlation with local inflammatory response. Infect Immun 74:2917-2924.

Pidot SJ, Porter JL, Marsollier L, Chauty A, Migot-Nabias F, Badaut C, Benard A, Ruf MT, Seemann T, Johnson PDR, Davies JK, Jenkin GA, Pluschke G, Stinear TP (2010) Serological evaluation of *Mycobacterium ulcerans* antigens identified by comparative genomics. PLoS Negl Trop Dis 4:872.

Qi W, Käser M, Röltgen K, Yeboah-Manu D, Pluschke G (2009) Genomic diversity and evolution of *Mycobacterium ulcerans* revealed by next-generation sequencing. PLoS Pathog 5:e1000580.

Reva O, Koroteitskiy I, Ilin A (2015) Role of the horizontal gene exchange in evolution of pathogenic Mycobacteria. BMC Evol Biol 15:S2.

Reynaud Y, Fresia P, Iraola G (2019) Phylogenetic analyses of *Mycobacterium ulcerans* from French Guiana using combination of core and accessory genomes. Caribbean Science and Innovation Meeting 2019, Pointe-à-Pitre (Guadeloupe), France. (hal-02453184). https://hal.univ-antilles.fr/hal-02453184.

Röltgen K, Qi W, Ruf MT, Mensah-Quainoo E, Pidot SJ, Seemann T, Stinear TP, Käser M, Yeboah-Manu D, Pluschke G (2010) Single nucleotide polymorphism typing of *Mycobacterium ulcerans* reveals focal transmission of Buruli ulcer in a highly endemic region of Ghana. PLoS Negl Trop Dis 4:e751.

Röltgen K, Pluschke G (2015) Epidemiology and disease burden of Buruli ulcer: a review. Res Rep Trop Med 6:59-73.

Saad J, Combe M, Hammoudi N, Couppié P, Blaizot R, Jedir F, Gozlan RE, Drancourt M, Bouam A (2019) Whole-genome sequence of *Mycobacterium ulcerans* CSURP7741, a French Guianan clinical isolate. Microbiol Resour Announc 8:e00215-19.

Saad J, Hammoudi N, Zghieb H, Anani H, Drancourt M (2020) Geographic microevolution of *Mycobacterium ulcerans* sustains Buruli ulcer extension, Australia. bioRxiv doi: https://doi.org/10.1101/2020.11.03.366435.

Sarpong FN (2018) Proteomics of Buruli Ulcer Disease Healing. Master's Thesis. Kwame Nkrumah University of Science and Technology, Kumasi, Ghana.

Senate LM, Tjatji MP, Pillay K, Chen W, Zondo NM, Syed PR, Mnguni FC, Chiliza ZE, Bamal HD, Karpoormath R, Khoza T, Mashele SS, Blackburn JM, Yu JH, Nelson DR, Syed K (2019) Similarities, variations, and evolution of cytochrome P450s in *Streptomyces* versus *Mycobacterium*. Sci Rep 9:3962.

Simpson H, Deribe K, Tabah EN, Peters A, Maman I, Frimpong M, Ampadu E, Phillips R, Saunderson P, Pullan RL, Cano J (2019) Mapping the global distribution of Buruli ulcer: a systematic review with evidence consensus. Lancet Glob Health 7:e912-e922.

Smith PG, Revill WD, Lukwago E, Rykushin YP (1977) The protective effect of BCG against *Mycobacterium ulcerans* disease:a controlled trial in an endemic area of Uganda. Trans R Soc Trop Med Hyg 70:449-457.

Stinear TP, Jenkin GA, Johnson PDR, Davies JK (2000) Comparative genetic analysis of *Mycobacterium ulcerans* and *Mycobacterium marinum* reveals evidence of recent divergence. J Bacteriol 182:6322-6330.

Stinear TP, Mve-Obiang A, Small PLC, Frigui W, Pryor MJ, Brosch R, Jenkin GA, Johnson PDR, Davies JK, Lee RE, Adusumilli S, Garnier T, Haydock SF, Leadlay PF, Cole ST (2004) Giant plasmid-encoded polyketide synthases produce the macrolide toxin of *Mycobacterium ulcerans.* Proc Natl Acad Sci USA 101:1345-1349.

Stinear TP, Pryor MJ, Porter JL, Cole ST (2005) Functional analysis and annotation of the virulence plasmid pMUM001 from *Mycobacterium ulcerans*. Microbiology 151:683-692.

Stinear TP, Seemann T, Pidot S, Frigui W, Reysset G, Garnier T, Meurice G, Simon D, Bouchier C, Ma L, Tichit M, Porter JL, Ryan J, Johnson PDR, Davies JK, Jenkin GA, Small PLC, Jones LM, Tekaia F, Laval F, Daffe M, Parkhill J, Cole ST (2007) Reductive evolution and niche adaptation inferred from the genome of *Mycobacterium ulcerans*, the causative agent of Buruli ulcer. Genome Res 17:192-200.

Sugawara M, Ishii N, Nakanaa K, Suzuki K, Umebayashi Y, Makigami K, Aihara M (2015) Exploration of a standard treatment for Buruli ulcer through a comprehensive analysis of all cases diagnosed in Japan. J Dermatol 42:581-595.

Sur S, Bothra AK, Sen A (2010) Symbiotic nitrogen fixation-a bioinformatics perspective. Biotechnology 9:257-273.

Sur S (2021) Understanding the nature and dynamics of *Mycobacterium ulcerans* cytochrome P450 monooxygenases (CYPs)–a bioinformatics approach. Acta Biol Szeged 65:93-103.

Tai AYC, Athan E, Friedman ND, Hughes A, Walton A, O'Brien DP (2018) Increased Severity and Spread of *Mycobacterium ulcerans*, Southeastern Australia. Emerg Infect Dis 24:58-64.

Tanghe A, Dangy JP, Pluschke G, Huygen K (2008) Improved

protective efficacy of a species-specific DNA vaccine encoding mycolyl-transferase Ag85A from *Mycobacterium ulcerans* by homologous protein boosting. PLoS Negl Trop Dis 2:e199.

Vandelannoote K, Meehan CJ, Eddyani M, Affolabi D, Phanzu DM, Eyangoh S, Jordaens K, Portaels F, Mangas K, Seemann T, Marsollier L, Marion E, Chauty A, Landier J, Fontanet A, Leirs H, Stinear TP, de Jong BC (2017) Multiple introductions and recent spread of the emerging human pathogen *Mycobacterium ulcerans* across Africa. Genome Biol Evol 9:414-426.

Vandelannoote K, Phanzu DM, Kibadi K, Eddyani M, Meehan CJ, Jordaens K, Leirs H, Portaels F, Stinear TP, Harris SR, de Jong BC (2019) *Mycobacterium ulcerans* population genomics to inform on the spread of Buruli ulcer across Central Africa. mSphere 4:e00472-18.

Vandelannoote K, Eddyani M, Buultjens A, Stinear TP (2019a) Population genomics and molecular epidemiology of *Mycobacterium ulcerans.* In Pluschke G, Röltgen K, Eds, Buruli Ulcer, Springer, Switzerland, 107-115.

Van Leuvenhaege C, Vandelannoote K, Affolabi D, Portaels F, Sopoh G, de Jong BC, Eddyani M, Meehan CJ (2017) Bacterial diversity in Buruli ulcer skin lesions: challenges in the clinical microbiome analysis of a skin disease. PLoS ONE 12:e0181994.

Van der Werf TS, Van der Graaf WT, Tappero JW, Asiedu K (1999) *Mycobacterium ulcerans* infection. Lancet 354:1013-1018.

Walsh DS, Portaels F, Meyers WM (2011) Buruli ulcer: Advances in understanding *Mycobacterium ulcerans* infection. Dermatol Clin 29:1-8.

Wolinsky E (1992) Mycobacterial diseases other than tuberculosis. Clin Infect Dis 15:1-10.

Yoshida M, Nakanaga K, Ogura Y, Toyoda A, Ooka T, Kazumi Y, Mitarai S, Ishii N, Hayashi T, Hoshino Y (2016) Complete genome sequence of *Mycobacterium ulcerans* subsp. *shinshuense*. Genome Announc 4:e01050-16.

Yotsu RR, Murase C, Sugawara M, Suzuki K, Nakanaga K, Ishii N, Asiedu K (2015) Revisiting Buruli ulcer. J Dermatol 42:1033-1041.

Zakham F, Belayachi L, Ussery D, Akrim M, Benjouad A, Aouad RE, Ennaji MM (2011) Mycobacterial species as a case-study of comparative genome analysis. Cell Mol Biol 57(Supp):OL1462-OL1469.

Zakham F, Aounae O, Ussery D, Benjouad A, Ennaji MM (2012) Computational genomics-proteomics and phylogeny analysis of twenty-one mycobacterial genomes (Tuberculosis & non Tuberculosis strains). Microb Inform Exp 2:7.

Zhu X, Chang S, Fang K, Cui S, Liu J et al. (2009) MyBASE: a database for genome polymorphism and gene function studies of *Mycobacterium*. BMC Microbiol 9:40.

Zingue D, Bouam A, Tian RBD, Drancourt M (2018) Buruli ulcer, a prototype for ecosystem-related infection, caused by *Mycobacterium ulcerans*. Clin Microbiol Rev 31:e00045-17.

Acta Biologica Szegediensis

Volume 65(2):247-252, 2021
Acta Biologica Szegediensis
http://abs.bibl.u-szeged.hu/index.php/abs

DOI:10.14232/abs.2021.2.247-252

ARTICLE

Investigation of efficacy of asenapine on passive avoidance learning and memory and oxidative stress in animal model of seizure-induced with pentylenetetrazole

Elham Farhadi[1], Naser Mirazi[1]*, Abdolkarim Hosseini[2]

[1]Department of Biology, Faculty of Basic Sciences, Bu-Ali Sina University, Hamedan, Iran
[2]Department of Animal Sciences and Biotechnology, Faculty of Life Sciences and Biotechnology, Shahid Beheshti University, Tehran, Iran.

ABSTRACT Asenapine (ASE) has been used for treatment of bipolar disorder. There is also evidence that it may be useful in the treatment of neurodegenerative disorders. In this regard, the efficacy of ASE in an experimental model of seizure and memory impairment caused by seizures in rats has been investigated in the present study. Seizures in male Wistar rats (200-250 g) were induced by pentylenetetrazole (PTZ, 60 mg/kg, intraperitoneally (i.p.)), and the anticonvulsant effect of ASE (0.5 and 1 mg/kg, i.p.) was evaluated. The effect on memory was assessed using passive avoidance (PA) test in a shuttle box apparatus. After behavioral tests, the animals underwent deep anesthesia and were euthanized painlessly. Serum was isolated for oxidative stress assays (nitric oxide (NO), and glutathione (GSH)). Intraperitoneal injection of ASE decreased the mean number of myoclonic jerks and duration of generalized tonic clonic seizures (GTCS) and increased the mean latency of myoclonic jerk and GTCS compared to the PTZ group. Moreover, in the PA test, ASE caused a significant increase in retention latency (RL) and total time spent in the light compartment (TLC) compared to the PTZ group. Biochemical tests showed that ASE was able to significantly increase GSH serum levels and significantly reduce NO serum levels compared to the PTZ group. Overall, this study suggests the potential neuroprotective effects of ASE in a model of memory impairment caused by seizures via the mechanism of inhibition of the oxidative stress pathway.
Acta Biol Szeged 65(2):247-252 (2021)

KEY WORDS
asenapine
oxidative stress
passive avoidance learning
rat
seizure

ARTICLE INFORMATION
Submitted
08 October 2021
Accepted
28 November 2021
***Corresponding author**
E-mail: mirazi205@gmail.com

Introduction

Seizure is a condition in which nerve cells make sudden and simultaneous discharges and is often accompanied by changes in the network and neural function. The term epilepsy – one of the most common diseases in the world – is defined as the presence of two or more seizures (Katyayan and Diaz-Medina 2021). Along with seizures, epilepsy is also associated with several other comorbidities, including cognitive deficits, which are very common in patients with epilepsy (Suleymanova 2021). At present, most cases of epilepsy are treated or controlled with anti-epileptic drugs (AEDs), which, as has been shown, have limitations in performance, safety, and efficacy (Fattorusso et al. 2021).

Although there are many studies on how comorbidities with epilepsy develop, there is little information on how a generalized or acute seizure causes memory impairment associated with learning (Carter et al. 2017). In addition to memory impairment, studies have indicated that acute generalized seizures are associated with increased oxidative stress (OS) and the production of reactive oxygen species (ROS). There is ample evidence that OS plays a pivotal role in promoting seizures and epilepsy, causing membrane lipid peroxidation and depletion of antioxidant enzyme levels (Olowe et al. 2020).

Asenapine (ASE) is an antipsychotic drug developed to treat schizophrenia and bipolar disorder. ASE exhibits its pharmacological effects by acting on serotonergic, dopaminergic, alpha-adrenergic, and histaminergic receptors. Having these pharmacological properties, it has been shown to have anti-anxiety, anti-stress, sedative, and anti-depressant properties (Grossini et al. 2014; Marazziti et al. 2019; Marston et al. 2009; Vieta and Montes 2018). ASE has also been shown to improve phencyclidine-induced object recognition deficiency in rats due to its antagonistic properties on the dopamine d1 receptor (Snigdha et al. 2011).

To the best of our knowledge, so far, there has been no

report on the effect of ASE on the seizure process, as well as on the memory impairment associated with seizures in humans or animal models; likewise, how it affects OS is still unknown. Thus, this study was designed and performed to identify the neuroprotective properties of ASE in rats with seizure and consequent memory deficit induced by pentylenetetrazole (PTZ), and to investigate the possible antioxidant mechanisms that ASE may suggest.

Materials and methods

Animals

Locally bred male Wistar rats (8 weeks old, 200-250 g) were used in the present study. These rodents were kept in standard cages in the animal room under controlled conditions (room temperature 22 ± 2 °C and 12 h light/dark cycle). Standard food for rats (Pars Animal Feed Co., Iran) as well as water were made available to the animals in an unlimited manner. All the experiments were performed between 9 and 12 a.m. to reduce the effect of the light cycle on the susceptibility to seizures. Working with animals and the implementations of the experiments were completely done in accordance with the international ethical principles. The research protocol was also approved by the University's Animal Ethics Committee (IR.BASU.REC.1400.003).

Drugs and chemicals

Asenapine (ASE) (10 mg) was obtained from Hikma Pharma, Egypt. Pentylenetetrazole (PTZ) was purchased from Sigma Company as a crystalline, white powder.

Experimental design and treatment protocol

Twenty rats were randomly divided into four groups. Seizures were inducted by intraperitoneal (i.p.) injection of PTZ (60 mg/kg) dissolved in normal saline (Kumar et al. 2018). ASE was administrated at doses of 0.1 and 0.5 mg/kg (Huang et al. 2008). The volume of injections in all animals was constant at 0.5 ml. The test protocol used to evaluate the effect of ASE on the behavioral activities was as follows:

- -Group I (control group): Rats that received only normal saline.
- -Group II (PTZ group): Rats that received normal saline half an hour before the PTZ injection.
- -Group III (ASE 0.1 group): Rats that received asenapine (0.1 mg/kg) half an hour before the PTZ injection.
- -Group IV (ASE 0.5 group): Rats that received asenapine (0.5 mg/kg) half an hour before the PTZ injection.

Table 1. Racine's scale for pentylenetetrazole (PTZ)-induced seizure in rats.

Score	Behavioral manifestation
0	No behavioral sign
1	Ear and facial twitching
2	Head nodding and myoclonic jerks
3	Unilateral forelimb clonus with lorditic posture
4	Bilateral forelimb clonus with rearing and falling
5	Generalized tonic-clonic seizure (GTCS) with loss of postural tone

Behavioral evaluation of seizure manifestation

The motor behavior of the animals in each group was recorded in the plexiglass box (the box cleaned and dried before each test) and stored by a computer-connected camera for half an hour after the PTZ injection and was examined by researcher in a blind fashion. The latency and number of myoclonic jerks, and latency and duration of generalized tonic clonic seizure (GTCS) in animals was evaluated based on the stereotypical behavioral manifestations that were displayed after PTZ injections in six stages (Table 1) (Hosseini et al. 2021).

Evaluation of passive avoidance memory

The rate of memory recovery in animals was assessed by a shuttle box (Borj Sanaat Co., Iran) (Hosseini et al. 2021). The device consists of a dark and a light compartment, separated by a guillotine door. The floor of the dark chamber has steel rods that can transmit electric shock to the feet of the rats. Briefly, on the first day of the acquisition phase, each rat was placed separately in a clear compartment. After 30 s of habituation, the guillotine door was opened and initial latency (IL) was measured to enter the dark chamber. The rats that showed IL for more than 60 s were excluded from further analysis. When the rats entered the dark area, the guillotine door would quickly be closed, and an electric foot shock (75 V, 0.2 mA, 50 Hz) was applied to them for 3 s. The animal would be transferred to its cage 30 s after the electric shock and this operation was repeated 5 min later. The rats were shocked every time they put all four limbs in the dark side. The training would end when the animal stayed in the bright area for 120 consecutive seconds. The number of shocks (SN) was measured until acquisition. Twenty-four hours later, like before, retention latency (RL) as well as total light compartment (TLC) time was measured after seizure induction, but no electric shock was applied. Retention time was measured in 300 s.

Animal euthanasia and serum extraction

After behavioral tests, the animals underwent deep an-

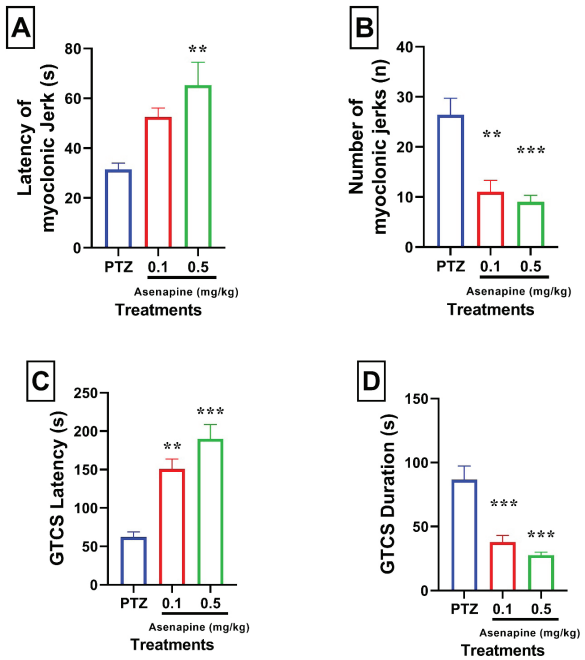

Figure 1. The effect of ASE (0.1, and 0.5 mg/kg, 30 min prior to testing) after PTZ treatment (60 mg/kg, i.p.) on latency of myoclonic jerk (**A**), number of myoclonic jerks (**B**), GTCS latency (**C**), and GTCS duration (**D**) in male Wistar rats. The data represents as the mean ± SEM (n = 5 rats per group). **p < 0.01; ***p < 0.001 significant difference between ASE (0.1 or 0.5 mg/kg) treatment with PTZ group.

ASE: asenapine, GTCS: generalized tonic clonic seizure, PTZ: pentylenetetrazole.

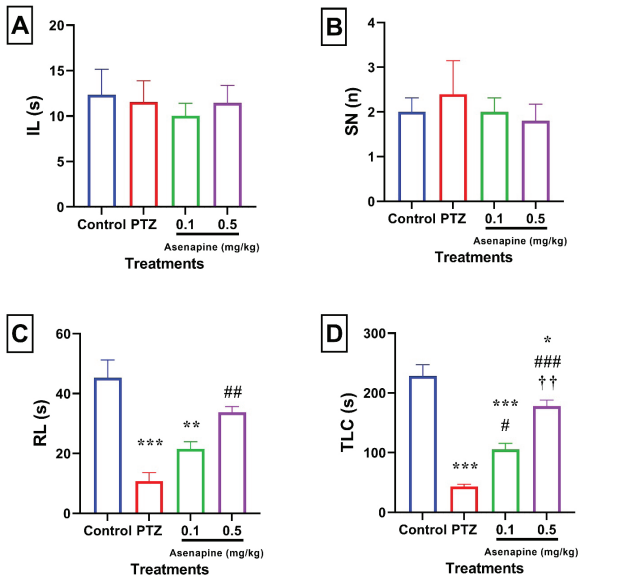

Figure 2. The effect of ASE (0.1, and 0.5 mg/kg, 30 min prior to testing) after PTZ treatment (60 mg/kg, i.p.) on IL (**A**), SN (**B**), RL (**C**), and TLC (**D**) in male Wistar rats. The data represents as the mean ± SEM (n = 5 rats per group). *p < 0.05; **p < 0.01; ***p < 0.001 significant difference between PTZ or ASE (0.5 or 1 mg/kg) treatment with control group. #p < 0.05; ##p < 0.01; ###p < 0.001 significant difference between ASE (0.1 or 0.5 mg/kg) treatment with PTZ group. ††p < 0.01 significant difference between ASE (0.1 mg/kg) treatment with ASE (0.5 mg/kg) group.

ASE: asenapine, IL: initial latency, PTZ: pentylenetetrazole, RL: retention latency, SN: shock number, TLC: total light compartment.

esthesia with ketamine and xylazine, and their blood was collected after cardiac puncture by a sterile syringe. The blood was allowed to clot for half an hour at room temperature and then the serums were separated by a centrifuge at 3000 rpm for 15 min and stored at -20 °C.

Measurement of oxidative stress markers

To measure GSH and NO oxidative stress indices, animal serum samples and conventional kits (Novin Navand Salamat Co., Iran) available in the market were used. The activity of GSH was measured according to the kit instructions at a wavelength of 340 nm by microplate reader (BioteTek ELx808, USA) and was reported in mU/mL. In addition, the amount of NO was measured according to the instructions of the kit and at a wavelength of 550 nm by the same microplate reader and was reported in terms of nmol/mL.

Statistical analysis of data

The results of the present study were shown as mean ± SEM. The normality of the data was tested by Shapiro-Wilk test. If the data were normal, then one-way ANOVA and Tukey's post hoc test were used to examine the differences between the groups. If the hypothesis of normality of the data was rejected, then non-parametric Kruskal-Wallis test and Dunn's test post hoc test were used to examine the differences between the groups. All statistical analyses were performed by GraphPad Prism software. In all analyses, the value of *P* was set at less than 0.05.

Results

The effect of ASE on the activity of PTZ-induced seizure

The effect of different treatments on the manifestations of PTZ-induced convulsive behavior is displayed in Fig. 1(A-D). Regarding the latency of myoclonic jerk, statistical analysis revealed a significant increase in the group IV, but not the group III, vs. group II (Fig. 1A). As shown in Fig. 1B, the number of myoclonic jerks in different groups was affected; the effect was a significant decrease in the group III and group IV compared to the group II. Regarding the GTCS latency, a significant increase was observed in the group III and group IV compared to the group II

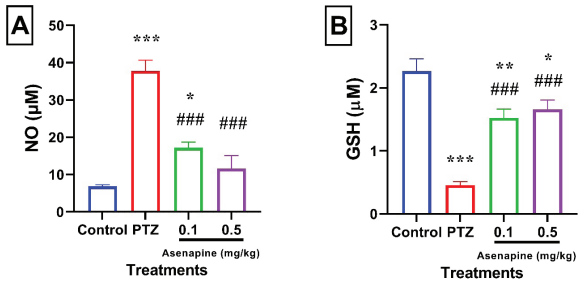

Figure 3. The effect of ASE (0.1, and 0.5 mg/kg, 30 min prior to testing) after PTZ treatment (60 mg/kg, i.p.) on serum level of NO (**A**), and GSH (**B**), in male Wistar rats. The data represents as the mean ± SEM (n = 5 rats per group). *p < 0.05; **p < 0.01; ***p < 0.001 significant difference between PTZ or ASE (0.1 or 0.5 mg/kg) treatment with control group. ###p < 0.001 significant difference between ASE (0.1 or 0.5 mg/kg) treatment with PTZ group.

ASE: asenapine, PTZ: pentylenetetrazole, NO: nitric oxide, GSH: glutathione.

(Fig. 1C). GTCS duration was significantly decreased in the group III and group IV vs. group II (Fig. 1D).

The effect of ASE on passive avoidance memory

There was no statistically significant difference between IL (Fig. 2A) and SN (Fig. 2B) in different treatment groups. However, RL in the PTZ group was significantly decreased compared to the control group, indicating memory impairment ($P < 0.001$). RL in the group III was not significantly different compared to the group II. On the contrary, in the group III, RL was increased significantly vs, group II ($P = 0.002$) (Fig. 2C). Regarding TLC time, the group II exhibited a significant decrease compared to the group I ($P < 0.001$). In both group III and group IV, TLC significantly increased vs. group II ($P = 0.010$ and $P < 0.001$, respectively) (Fig. 2D).

The effect of ASE on oxidative stress markers

As shown in Fig. 3A, there was a significant increase in serum NO levels in the group II compared to group I ($P < 0.001$); but in the group III and group IV a significant decrease was observed in serum NO level compared to the group II ($P < 0.001$). In case of serum GHS levels, the effects were similar (Fig. 3B).

Discussion

In the present study, the effect of ASE on seizures and PTZ-induced avoidance memory deficits in rats was investigated. The results revealed that ASE has a statistically significant effect on behavioral manifestation of PTZ-induced seizures. The PA test also showed that PTZ caused memory impairment resulting in reduced RL and TLC. The results of this study are in line with reports on memory impairment due to PTZ-induced seizures (Aghaie et al. 2021; Hosseini et al. 2021; Nagib et al. 2018). By inducing significant increase in RL and TLC compared to the PTZ group, ASE reversed the effect of PTZ-induced memory impairment, indicating its protective role against seizures and seizure-induced memory impairment. While no studies have been reported on the anticonvulsant effect or the effect on memory of ASE so far, there are some reports on the inhibitory effects of ASE on experimental models of psychosis or bipolar disorder (BD) as well as on the progression of underlying diseases associated with psychosis or BD (Marston et al. 2009; McLean et al. 2010; Snigdha et al. 2011).

Various mechanisms have been proposed for how PTZ injection causes seizures and the associated memory impairment. One of the most important factors in the development of seizures and resulting behavioral changes is OS and shift in the ROS level (Olowe et al. 2020). In the present study, the results showed a decrease in the GSH and an increase in NO serum levels following PTZ injection. The present study, similar to various prior studies, showed that the injection of PTZ in animal models increases OS and NO and decreases antioxidant levels (Hosseini et al. 2021; Kawakami et al. 2021; Kumar et al. 2018). Glutathione as an antioxidant helps protect cells against free radical damage. Glutathione is present inside cells in states of reduced GSH and oxidized GSSG. In healthy cells and tissues, more than 90% of total glutathione is in reduced form, and less than 10% as GSSG disulfide. The high concentration of GSH is due to the fact that the glutathione reductase enzyme (which transforms it from the oxidized state) is very active. Increase in GSSG to GSH is indicative of oxidative stress (Cárdenas-Rodríguez et al. 2014). NO is a molecular mediator which is made by the nitric oxide synthase (NOS) enzyme from L-arginine, oxygen, and NADPH and participates in vascular homeostasis by inhibiting vascular smooth muscle contraction, platelet aggregation, and leukocyte adhesion to endothelium, inflammation, thrombosis, immunity and neurotransmission. People with atherosclerosis, diabetes, and high blood pressure often manifest NO pathway disorders (Ghimire et al. 2017). NO has also been reported to be increased in PTZ-induced seizures (Kawakami et al. 2021). The effects of ASE on NO and GSH have not been reported in the status epilepticus condition, but in a previous study, ASE modulate inducible NOS (iNOS) and protected porcine coronary endothelial cells against oxidative stress by preventing ROS production and GSH loss (Grossini et al. 2014). Therefore, the positive effects of ASE on seizures as well as the improvement of memory impairment caused by seizures which were observed in the

present study can be partially ascribed to the antioxidant properties of the agent.

The present study for the first time examined the antioxidant effects of ASE, as well as its possible pathway. The elicited results could pave the way for future studies. Despite this strength, the present study had a limitation: this study did not investigate the molecular pathway or inflammatory cytokines due to the small number of samples and time constraints. This issue can be addressed in future research designs.

Conclusion

Overall, the present study provided evidence for the potential neuroprotective effects of the ASE drug. In addition, it was shown that ASE can be protective against oxidative stress induced during seizures. Therefore, a treatment strategy that could address the potential therapeutic effect of ASE with AEDs in the treatment of seizures as well as memory impairment associated with seizures calls for further research. Additional study designs are also needed to fully elucidate the mechanisms of anticonvulsant function as well as safety in their chronic use.

Acknowledgments

This study is financially supported by Bu-Ali Sina University. The research protocol was approved by the University's Animal Ethics Committee (IR.BASU.REC.1400.003). The datasets used and/or analyzed during the current study are available from the corresponding author on reasonable request.

References

Aghaie F, Shemshaki A, Rajabi M, Khatami P, Hosseini A (2021) Rapamycin alleviates memory deficit against pentylenetetrazole-induced neural toxicity in Wistar male rats. Mol Biol Rep 48(6):5083-5091.

Cárdenas-Rodríguez N, Coballase-Urrutia E, Pérez-Cruz C, Montesinos-Correa H, Rivera-Espinosa L, Sampieri A, 3rd, Carmona-Aparicio L (2014) Relevance of the glutathione system in temporal lobe epilepsy: evidence in human and experimental models. Oxid Med Cell Longev 2014:759293.

Carter AN, Born HA, Levine AT, Dao AT, Zhao AJ, Lee WL, Anderson AE (2017) Wortmannin attenuates seizure-induced hyperactive PI3K/Akt/mTOR signaling, impaired memory, and spine dysmorphology in rats. eNeuro 4:ENEURO.0354-16.2017.

Fattorusso A, Matricardi S, Mencaroni E, Dell'Isola GB, Di Cara G, Striano P, Verrotti A (2021) The pharmacoresistant epilepsy: An overview on existant and new emerging therapies Front Neurol 12:674483.

Ghimire K, Altmann HM, Straub AC, Isenberg JS (2017) Nitric oxide: what's new to NO? Am J Physiol Cell Physiol 312:C254-C262.

Grossini E, Gramaglia C, Farruggio S, Bellofatto K, Anchisi C, Mary D, Vacca G, Zeppegno P (2014) Asenapine increases nitric oxide release and protects porcine coronary artery endothelial cells against peroxidation. Vascul Pharmacol 60:127-141.

Hosseini A, Allahyari F, Azizi V (2021) Effects of *Tanacetum polycephalum* on passive avoidance learning and oxidative stress in epileptic model of memory impairment in the male Wistar rats. Adv Tradit Med 21:545–552.

Huang M, Li Z, Dai J, Shahid M, Wong EH, Meltzer HY (2008) Asenapine increases dopamine, norepinephrine, and acetylcholine efflux in the rat medial prefrontal cortex and hippocampus. Neuropsychopharmacology 33:2934-2945.

Katyayan A, Diaz-Medina G (2021) Epilepsy: Epileptic syndromes and treatment. Neurol Clin 39:779-795.

Kawakami Y, Murashima YL, Tsukimoto M, Okada H, Miyatake C, Takagi A, Ogawa J, Itoh Y (2021) The roles of dominance of the nitric oxide fractions nitrate and nitrite in the epilepsy-prone EL mouse brain. J Nippon Med Sch 88:189-193.

Kumar R, Arora R, Agarwal A, Gupta YK (2018) Protective effect of *Terminalia chebula* against seizures, seizure-induced cognitive impairment and oxidative stress in experimental models of seizures in rats. J Ethnopharmacol 215:124-131.

Marazziti D, Mucci F, Falaschi V, Dell'Osso L (2019) Asenapine for the treatment of bipolar disorder. Expert Opin Pharmacother 20:1321-1330.

Marston HM et al. (2009) Asenapine effects in animal models of psychosis and cognitive function. Psychopharmacology (Berl) 206:699-714.

McLean SL, Neill JC, Idris NF, Marston HM, Wong EH, Shahid M (2010) Effects of asenapine, olanzapine, and risperidone on psychotomimetic-induced reversal-learning deficits in the rat. Behav Brain Res 214:240-247.

Nagib MM, Tadros MG, Al-Khalek HAA, Rahmo RM, Sabri NA, Khalifa AE, Masoud SI (2018) Molecular mechanisms of neuroprotective effect of adjuvant therapy with phenytoin in pentylenetetrazole-induced seizures: Impact on Sirt1/NRF2 signaling pathways. Neurotoxicology 68:47-65.

Olowe R, Sandouka S, Saadi A, Shekh-Ahmad T (2020) Approaches for reactive oxygen species and oxidative stress quantification in epilepsy. Antioxidants (Basel) 9(10):990.

Snigdha S, Idris N, Grayson B, Shahid M, Neill JC (2011)

Asenapine improves phencyclidine-induced object recognition deficits in the rat: evidence for engagement of a dopamine D1 receptor mechanism. Psychopharmacology (Berl) 214:843-853.

Suleymanova EM (2021) Behavioral comorbidities of epilepsy and neuroinflammation: Evidence from experimental and clinical studies. Epilepsy Behav 117:107869.

Vieta E, Montes JM (2018) A review of asenapine in the treatment of bipolar disorder. Clin Drug Investig 38:87-99.

Acta Biologica Szegediensis

Volume 65(2):247-260, 2021
Acta Biologica Szegediensis
http://abs.bibl.u-szeged.hu/index.php/abs
DOI:10.14232/abs.2021.2.247-260

ARTICLE

Predatory mites fauna on medicinal and aromatic plants from Sundarban Biosphere Reserve, West Bengal, India

Indrani Samaddar[1], Sanjoy Podder[1], Santanu Chakrabarti[2], Himani Biswas[3]*

[1]Department of Zoology, The University of Burdwan, Golapbag, Burdwan, West Bengal, India
[2]Singur Government, General Degree College, Singur, Hoogly-712409, West Bengal, India
[3]Post Graduate Department of Zoology, Krishnagar Government College, Krishnagar, Nadia, PIN-741101, West Bengal, India

ABSTRACT A regular survey was conducted in different places of Sundarban Biosphere Reserve (SBR) region of West Bengal on 32 different medicinal and aromatic plants. A total of 41 species of predatory mites belonging to 19 genera, 7 families, under 2 orders were observed during this study. Collection data, distribution and keys are given for all taxonomic categories. Many of the species and habitats reported here are new records. Ecological and behavioral remarks on all the predatory mite species reported from Sundarban Biosphere Reserve are also presented.
Acta Biol Szeged 65(2):247-260 (2021)

KEY WORDS
Acari
distribution
key
medicinal and aromatic plant
Mesostigmata
Prostigmata

ARTICLE INFORMATION
Submitted
17 September 2021
Accepted
19 October 2021
***Corresponding author**
E-mail: himanibiswas@gmail.com

INTRODUCTION

In India, Sundarban Biosphere Reserve (21°9497'N 89.11833'E) is one of the world heritage sites declared by UNESCO in 1997. It is in the Ganga-Bramhaputra delta of Bay of Bengal, and it is the largest single tract of mangrove systems covering 4100 km^2 of which 2/3rd falls under Bangladesh and 1/3rd portion lies under Indian territory. It is one of the richest biodiversity zones of India having luxuriant growth of mangrove plants, many of which are having medicinal values and are being used by local population in day–to-day healthcare system. In many fringe areas of Sundarban Biosphere Reserve, which are having habitation also possesses many non-mangrove plants such as, medicinal and aromatic plants (MAP). MAP possess a serious threat of being attacked by a number of herbivores among which insects and mites play significant role.

Among the major pests of MAPs in Sundarban, phytophagous mites are undoubtedly the worst, and their attack sometimes becomes so severe that the entire plant turns yellowish- brown to reddish, falling of leaves, and in some cases plant may die. The attack of phytophagous mites on these plants causes depletion and deterioration of their active ingredients and induce mild to hazardous damage to them. Damage to the plant may show adverse effect on the occurrence of predatory mites, which are present on the plant along with the phytophagous mite species. Most of the predatory mites considered as food generalists due to their feeding abilities on number of prey species along with plant exudates, pollen, and fungi (Tixier 2018). The predatory mites are natural enemies and can regulate the growth rate of phytophagous mite at low equilibrium densities and thus, can be utilized as biocontrol agents (McMurtry and Croft 1997; Gerson et al. 2003). Diversity of species, phylogenetic patterns and evolutionary processes play a pivotal role for identification of species which in turn is very significant for development of biological pest management strategy. Application of morphological taxonomic method would be advantageous for proper identification of mites. For proper implementation of biocontrol strategies against phytophagous mites, detailed knowledge of predatory mite biodiversity is essential and required (Tixier 2018). The information in all aspect are not available from our country specially from Sundarban Biosphere Reserve. So, the present study was designed to make a comprehensive list of predatory mites infesting MAPs along with a detailed taxonomic key, habitat, and distribution.

This information will be helpful for stakeholders to find out some predatory mites having great potentiality in utilizing as biological control for phytophagous mites infested MAPs.

Survey

A regular extensive survey of predatory mites was done in different, selected places of Sundarban Biosphere Reserve in the following localities: Sagar Island (21°7269'N 88°1096'E), Gosaba (22°1652'N 88°8070'E), Dhamakhali (22°3615'N 88°8645'E), Jeliakhali (22°3615'N 88°8645'E), Jharkhali (22°0306'N 88°7013'E), Balikhal (22°0307'N 88°7014'E), Sarberia (22°2675'N 88°4446'E), Hasnabad (22°5745'N 88°9174'E), Taki (22°5864'N 88°9097'E), during February 2017 to May 2018. During the surveys, various MAPs were investigated for the occurrence of predatory mites.

Collection

For collection of predatory mites, direct examination of leaves plucked from plants of our interest was done in the field with 20X hand lens, and after confirmation of mites, 25-30 leaves were taken in polythene zipper bags for proper examination in the laboratory under stereo-binocular microscope (MSZ-TR 70T0842). During the collection of plants, field observations were made regarding their association with phytophagous mites and the predatory importance of predatory mites, if any. All the measurements given in the text are in microns and entire collection was made by extensive survey by all the authors.

Preservation

The collected mites were preserved in 70% ethyl alcohol and subsequently, mounted in Hoyer's medium (Walter and Krantz 2009). Permanently mounted mites were identified under OLYMPUS CH-20i microscope. Identification was done consulting the updated literature. The keys of Gupta (2003), Moraes et al. (2004), and Chant and McMurtry (2007) were followed for the phytoseiid mite and Gupta (2002) was followed for identification and classification for other families. All the identified materials have been deposited in the Entomological Collection of Krishnagar Government College and those will be submitted to the National Collection Unit (Zoological Survey of India, Kolkata) in due course.

RESULTS

Taxonomic accounts

The identified collection of predatory mites belonged to 41 species of 19 genera, 7 families, under 2 orders from 32 species of medicinal and aromatic plants. The most dominating predatory mites associated with different species of phytophagous mite species were *Amblyseius largoensis, Amblyseius herbicolus*, *Euseius ovalis, Paraphytoseius bhadrakaliensis, Euseius coccinae, Euseius alstoniae, Euseius ovalis,* in the Phytoseiidae family and *Agistimus fleschneri* in the Stigmaidae family. The detailed taxonomic account with keys is given below.

Key to the superorders, orders and suborders of "Acari":

1. With 1-4 pairs of dorsolateral or ventrolateral stigmata posterior to coxa II, coxae of legs free usually movable, tarsi of leg II-IV with peripodomeric fissure associated with slit organs tarsus of leg I with dense dorsal cluster of solidiform setae subdistally ....**Superorder: Parasitiformes**

*Venter of subcapitulum with maximum of IV pairs of setae, triotosternum usually present with a distinctly base, 1-2 setuloselacini and valves of adult ------ or at most with 1 pair of setae, base of chelicerae enclosed by a sclerotised ring usually with epistome..... ..... **Order: Mesostigmata**

Idiosoma of adult female with 38 or fewer pairs of setae, dorsal shield with 23 or fewer pairs of setae including setae of r3 and R1; caudo-ventral area of female with 10 or fewer pairs of setae; corniculae slender, triotosternum well developed with two lacinae, chelicerae well developed with two digits, having variable dentition, interior margin of tectum smooth or minutely denticulate. .... Family: Phytoseiidae**

- Without visible stigmata posterior to coxae II, coxae of legs integrated with venter of podosoma and often forming coxi-sternum, tarsai of leg II-IV without peri-podomeric fissure and slit organ, tarsus of leg I with a pair of dorsal setae distally and subdistally..... .....**Superorder: Acariformes, 2**

2. Chelicera rarely chelate, fixed digit often regressed and movable digit often a hook-like needle or style-like structure, cheliceral bases sometimes face medially, palp simple or modified into a thumb-claw process, sometimes reduced, subcapitulum without rutella , ambulacra of at least legs II and III usually with 2 pair of lateral claws and with or rarely without a medium or empodium, may be pad-like or rayed and often sucker-like opisthsoma, lacking paired lateral glands , one pair of stigmata opens between base of chelicerae or on anterior prodorsum , usually present and sometimes associated with peretreme

dorsally on cheliceral bases or on the anterior margin of prodorsum.....**Order: Trombidiformes**
*Tracheal system with one pair of stigmata, opening between the bases of chelicerae or on anterior pro-dorsum usually present, usually with fixed digit sheath-like or completely regressed, coxal fields, contiguous or II-III separated.....**Suborder: Prostigmata**

Order: Mesostigmata

Family: Phytoseiidae

Phytoseiidae Baker and Wharton (1952) An Introduction to Acarology, The McMillan Co., USA, p. 87.

Key to the subfamilies of Phytoseiidae:

1. Setae z3 and S6 absent..... **Amblyseiinae**
- Either or both of setae z3 and S6 present..... **2**

2. Setae Z1, S2, S4, and S5 absent ..... **Phytoseiinae**
- At least one of setae Z1, S2, S4, S5 present ..... **Typhlodrominae**

Key to the tribes of subfamily Amblyseiinae:

1. Sternal shield with median posterior projection, deutosternal groove wider (>5 μm in width), some forward migration of preanal setae, JV2 and ZV2, preanal setae on male, preanal setae usually arranged in tangential row rather than a triangular pattern .....**Euseiini** ..... **Genus: *Euseius***
- Sternal shield without posterior projection, deutosternal groove narrower without forward migration of preanal setae on male usually arranged in a triangular pattern rather than in a tangential row **2**

2. S4 absent.*
*Some dorsolateral setae thickened, serrate, arising from tubercles. Setae J2, S2 present, setae j6 short not longer than setae Z2 with 3 pairs of preanal setae..... **Kampidomini** .....**Genus: *Paraphytoseius***
- Seta S 4 present **3**

3. Ratio of seta S4:Z1<3.0:1.0, setae S4, Z4, Z5 not greatly longer than other dorsal setae.....**4**
- Ratio of setae S4:Z1<3.1:1.0, setae S4, Z5, Z4 marked longer than other dorsal setae.....**Amblyseiini** .....**Genus: *Amblyseius***

4. Genu II without and genu III rarely with a macrosetae, fixed digit of chelicerae with fewer than 6 teeth, rarely multidentate in structure..... **Genus: *Neoseiulus***
- Genu II and genu III rarely without macrosetae, fixed digit of chelicerae usually with more than 6 teeth..... .....**Typhlodromipsini** .....**Genus: *Scapulaseius*** ..... ***Scapulaseius suknaensis***

Genus *Amblyseius* Berlese

Amblyseius Berlese (1914) Acari nuovi. Manipulus IX. Redia 10:113-150.

Key to the species groups of genus Amblyseius:

1. Cervix of spermatheca tubular or with various modifications.....**2**
- Cervix not tubular or with various modifications. **3**

2. Cervix of spermatheca pocular and with parallel walls and nodular atrium. .....***obtusus* group** .....***Amblyseius obtusus***
- Cervix elongated with fundibuliform wall and nodular atrium. .....***coffeae* group** .....***Amblyseius coffeae***
- Cervix long, narrow, tubular, flared internally and atrium nodular type. ..... ***sundi* group** ..... ***Amblyseius paraaerialis***
- Cervix short or long, tubular and with a nodular atrium .....***aerialis* group** .....***Amblyseius aerialis***
- Spermatheca with slightly corniform cervix. ....***Amblyseius cucurbitae***
- Cervix long, slender, tubular with nodular, triangular or waforied atrium. .....***largoensis* group, 5**

3. Cervix of spermatheca saccular with various modifications.....**4**
- Cervix not saccular or not saccular with various modification.....***ipomeae* group** .....***Amblyseius ipomeae***

4. Cervix of spermatheca long, saccular, swollen externally or distinctly flared internally and differentiated to slightly flared internally and differentiated to slightly nodular atrium.....***punctatus* group** ..... ***Amblyseius kulini***
- Cervix saccular with nodular or undifferentiated atrium. .....***orientalis* group** .....***Amblyseius orientalis***

5. Spermatheca with tubular cervix..... .....***Amblyseius largoensis***
- Spermatheca with fundibular cervix. **6**

6. Z5 < 300 μm. 7
- Z5 approximately 300 μm or longer..... **8**
7. s4 approximately 100 μm, Z5 < 200 μm, ST4 75 μm... .....***Amblyseius herbicolus***
- s4 longer than 100 μm, Z5 longer than 250 μm, ST4 less than 70 μm. .....***Amblyseius adhatodae***

8. Z4 less than 100 μm.....***Amblyseius herbicoloides***
- Z4 longer than 100 μm.....***Amblyseius fletcheri***

Amblyseius aerealis (Muma)

Collection data: 2 females; India: West Bengal, Dist. South 24 Paraganas, Jharkhali on *Datura metel*; Dt. 23.ix.2017.

Distribution: India (Karnataka, Bihar, West Bengal), Mexico, Brazil, USA, Jamaica

Remarks: The economic importance of the species is unknown in India though it has been reported to feed upon *Panonychus citri* on citrus (Gupta 2003). In the present study it was associated with *Brevipalpus rica* on *Datura metel.*

Amblyseius adhatodae Muma

Collection data: 1 female; India: West Bengal, Dist. North 24 Paraganas, Hasnabad on *Heliotropium indicum*; Dt. 5.xi.2017.

Distribution: India (Maharashtra, West Bengal), Pakistan.

Remarks: The economic importance is unknown.

Amblyseius coffeae De Leon

Collection data: 1 female; India: West Bengal, Dist. South 24 Paraganas, Gosaba on *Cinnamomum tamala;* Dt. 4.vi.2017.

Distribution: Mexico, India (new record).

Remarks: This species as well as the habitat on which it was collected is a new record for India.

Amblyseius cucurbitae Rather

Collection data: 2 females; India: West Bengal, Dist. South 24 Paraganas, Jeliakhali on *Capparis zeylanica*; Dt. 16.iv.2017.

Distribution: India (Jammu and Kashmir, West Bengal).

Remarks: This species is the second report for India and the habitat is also new for the species.

Amblyseius fletcheri Schicha

Collection data: 1 female; India: West Bengal, Dist. South 24 Paraganas, Dhamakhali on *Scuttelaria javanica*; Dt. 25.v.2017.

Distribution: New Caledonia, India (new record)

Remarks: The species has been unknown from India and hence is a new record. The habitat also forms a new record.

Amblyseius herbicoloides McMurtry

Collection data: 2 females, 1 male; India: West Bengal, Dist. South 24 Paraganas, Gosaba on *Cleome viscosa;* Dt. 26.iii.2017.

Distribution: Fiji, India.

Remarks: The occurrence of this species was casual, but *Cleome viscosa* is a new habitat record for this species. The presence of the species in India was reported earlier by Gupta and Karmakar (2015). The record of this species for West Bengal is made here for the first time.

Amblyseius herbicolus (Chant)

Collection data: 2 females, 1 male; India: West Bengal, Dist. South 24 Paraganas, Tangrakhali on *Cocos nucifera;* Dt. 6.xi.2017.

Distribution: India (West Bengal, Tripura, Mizoram, Sikkim, Tamil Nadu), USA, Brazil, Mexico, Australia, South Africa, Japan, Thailand.

Remarks: This is one of the commonest phytoseiid mites present on a wide range of plants (Gupta 2003). In our study, it was associated with the coconut perianth mite, *Acaria guerreronis* and fed on its eggs.

Amblyseius ipomeae Ghai and Menon

Collection data: 1 female, 1 nymph; India: West Bengal, Dist. South 24 Paraganas, Jharkhali on *Ricinus communis;* Dt. 19.viii.2017.

Distribution: India (Maharastra).

Remarks: Its occurrence was casual and no economic importance has been observed, although, Ghai and Menon (1967) reported its occurrence in association with tetranychids mites.

Amblyseius largoensis (Muma)

Collection data: 5 females; India: West Bengal, Dist. South 24 Paraganas, Sagar Island on *Justicia adhatoda;* Dt. 25.ii.2017; 2 females; Jeliakhali on *Ixora coccinea*; Dt. 15.iv.2017; 1 male; Dhamakhali on *Ricinus communis*; Dt.16. iv.2017; 6 females and 2 males; Jharkhali on *Avicenia alba*; Dt. 23.ix.2017; 24.x.2017, 14.i.2018, 2 females; Dist. North 24 Paraganas, Hasnabad on *Occimum sanctum*; Dt. 5.xi.2017.

Distribution: India (Himachal Pradesh, Odisha, Gujarat, West Bengal, Andaman Nicobar Island, Karnataka, Manipur, Assam, Meghalaya, Nagaland, Kerala, Bihar), Brazil, Costa Rica, New Zealand, S. Africa, Japan, Angola, USA.

Remarks: This is another common phytoseiid mite species present on many plants feeding mostly in immature phytophagous mites. In the present study it was seen in the colony of *Oligonychus iseilemae* on *Avicenia alba* and in the colony of *Brevipalpus californicus* on *Justicia adhatoda* and in both cases its feeding was observed on the immature stages.

Amblyseius kulini Gupta

Collection data: 1 male, 2 females; India: West Bengal, Dist. South 24 Paraganas, Jharkhali on *Cocos nucifera;* Dt. 23.ix.2017.

Remarks: In the recent study it was found feeding upon eriophyid mites on *Cocos nucifera*.

Amblyseius obtusus (Koch)

Collection Data: 1 female; India: West Bengal, Dist. North 24 Paraganas, Hasnabad on *Butea monosperma*; Dt. 23.xii.2017.

Distribution: Indonesia, Europe Australia, Canada, India (new record).

Remarks: The record of this species is made here for the first time.

Amblyseius orientalis Ehara

Collection data: 1 female; India: West Bengal, Dist. North 24 Paragana, Mini Sundarban on *Avicenia alba*; Dt. 12.v.2017.

Distribution: India (Assam, West Bengal), Japan

Remarks: The occurrence of this species has been reported as casual occurrence. Earlier studies reported this mite from Assam (Gupta 1978). Its feeding behavior was not observed.

Amblyseius paraaerialis Muma

Collection data: 2 females; India: West Bengal, Dist. South 24 Paraganas, Jharkhali on *Vitex negundo;* Dt. 23.ix.2017.

Distribution: India (Arunachal Pradesh, Assam, Meghalaya, Sikkim, Kerala), Thailand.

Remarks: Although this species has been reported from India on a number of plants feeding upon phytophagous mite (Gupta 2003), it was recorded just only showing no predatory importance in the present study.

Genus *Euseius* Wainstein

Amblyseius (Amblyseius) section *Euseius* Wainstein (1962) Acarologia 4:15.

Euseius, Chant and McMurtry (2007) p.118.

Key to the species of genus Euseius:

1. All setae on dorsal shield minute except j1 and Z5.... **3**
- Besides j1 and Z5 some other setae also long..... **2**

2. S2-S5 equal.....***Euseius ovalis***
- S2-S5 unequal.....***Euseius rhododendronis***

3. j1, j3 either equal or j3 longer than j1..... **4**
- j1 longer than j3 ..... **5**

4. j3 longer than j1.....***Euseius alstoniae***
- j3 as long as j1 .....***Euseius coccinae***

5. Leg chaetotaxy on genu III 1 2 2 1; tibia III 1 2 2 1.
0 0 1 1.....
.....***Euseius prasadi***
- Genu III 1 1 1 1; tibia III 1 2 1 1
1 1 1 1..... ***Euseius finlandicus***

Euseius alstoniae Gupta

Collection data: 1 female; India: West Bengal, Dist. South 24 Paraganas, Sagar Island on *Gmelina arborea;* Dt. 18.vi.2017.

Distribution: India (West Bengal, Odisha, Bihar, Uttar Pradesh, Punjab, Jammu and Kashmir)

Remarks: This species was in close association with *Oligonychus bihariensis* on *Gmelina arborea* and feeding upon its immature stages.

Euseius coccineae Gupta

Collection data: 2 females; India: West Bengal, Dist. South 24 Paragana, Sagar Island on *Justicia adhatoda*; Dt. 18.vi.2017

Distribution: India (Arunachal Pradesh, Meghalaya, Tripura, Gujrat, Odisha, West Bengal)

Remarks: This species was in close association with *Brevipalpus californicus* on *Justicia adhatoda* but both in field and laboratory examination its feeding was not noticed.

Euseius finlandicus Oudemans

Collection data: 1 male; India: West Bengal, Dist. South 24 Paraganas, Jeliakhali on *Heliotropium indicum;* Dt. 16.iv.2017.

Distribution: India (Karnataka, West Bengal, Bihar, Sikkim, Punjab, Jammu and Kashmir), Pakistan, Canada, Mexico, Russia, Europe, USA, Japan.

Remarks: This mite is known to be an important predator of tetranychids (Hoy 2011) but in the present study no such behavior was noticed.

Euseius ovalis (Evans)

Collection data: 2 females; India: West Bengal, Dist. South 24 Paraganas, Gosaba on *Murraya koenigii;* Dt. 23.viii.2017.

Distribution: India (Arunachal Pradesh, Assam, Sikkim, Mizoram, West Bengal, Gujarat, Punjab, Tamil Nadu, Kerala, Andaman & Nicobar Islands), Philippines, Taiwan, Hawaii, Mexico, Malaysia, Japan, New Zealand, Australia.

Remarks: This species is known to be a very important predator of a number of phytophagous mites (Gupta 2003). In the present study the species was found feeding upon the eggs of *Schizotetranychus cajani* on the leaf of *Murraya koenigii*. The infested leaf of *Murraya koenigii* infested with *Schizotetranychus cajani* when examined

under stereo-binocular microscope, the predator was found feeding upon eggs.

Euseius prasadi Gupta

Collection data: 2 females, 1 male; India: West Bengal, Dist. South 24 Paraganas, Jharkhali on *Heritiera fomes*; Dt. 23.ix.2017. 1 male, 1 nymph; India: West Bengal, North 24 Paraganas, Taki on *Ocimum gratssiimum;* Dt. 14.iv.2018.

Distribution: India (West Bengal, Arunachal Pradesh, Assam, Meghalaya, Sikkim, Tripura Mizoram, Punjab, Himachal Pradesh, Jammu & Kashmir).

Remarks: This is a very common phytoseiid mite, known to be occurring on wide range of plants but its economic importance has not been observed in the field.

Euseius rhododendronis (Gupta)

Collection data:1 male, 1 female; India-West Bengal, Dist. South 24 Paraganas, Balikhal on *Acacia auriculiformis*; Dt. 23.x.2017.

Distribution: India (West Bengal, Tripura, Sikkim, Tamil Nadu, Karnataka), Thailand.

Remarks: This species has no known economic importance.

Genus *Neoseiulus* Hughes

Neoseiulus Hughes (1948) Min Agr Fish Lond, p. 141.

Neoseiulus longispinosus (Evans)

Collection data: 1 female; India: West Bengal, Dist. South 24 Paraganas, Jeliakhali on *Mangifera indica*; Dt. 16.iv.2017.

Distribution: India (West Bengal, Odisha, Bihar, Sikkim, Uttar Pradesh, Karnataka, Andaman and Nicobar Islands), Taiwan, Indonesia, Japan, Pakistan, Australia, Malaysia, Jamaica.

Remarks: This is one of the well-known and established predatory mites feeding upon phytophagous mites in India, and it is known to feed upon several tetranychid mites on a wide range of host plants. In the present study, this species was seen actively feeding upon *Oligonychus mangiferus* on mango.

Genus *Paraphytoseius* Swirski and Schechter

Paraphytoseius Swiriski and Schechter (1961) Israel J Agric Res 11:113.

Key to the species of genus Paraphytoseius:

1. Setae z2 and z4 serrate.....
.....***Paraphytoseius scleroticus***

- Setae z2 and z4 smooth .....
.....***Paraphytoseius bhdrakaliensis***

Paraphytoseius scleroticus Gupta and Ray

Collection data: 1 female; India: West Bengal, Dist. South 24 Paraganas, Jeliakhali on *Vitex negundo*; Dt. 16.iv.2017.

Distribution: India (West Bengal)

Remarks: This was earlier described from hilly area of North East India (Gupta and Ray 1981) and its presence in Gangetic plain of West Bengal in very interesting. Predatory behavior was not noticed.

Paraphytoseius bhadrakaliensis (Gupta)

Collection data: 1 male 2 female; India: West Bengal, Dist. South 24 Paragana, Gosaba on *Ficus racemose*; Dt. 26.iii.2017.

Distribution: India (West Bengal)

Remarks: This species was found associated with *Eotetranychus hirsti* on *Ficus racemosa*. It was seen attacking the immature stages of fig mite when the infested leaves were examined under stereo binocular microscope.

Tribe Typhlodromipsini

Genus *Scapulaseius* Karg and Oomen-Kalsbeck

Amblyseius (*Scapulaseius*) Karg and Oomen- Kalsbeck (1987) Zool Jahr Syst 114(1):131-140.

Scapulaseius suknaensis (Gupta)

Collection data: 4 females, 1 male; India: West Bengal, Dist. South 24 Paraganas, Kakdwip on *Uraria picta*; Dt. 14.i.2018.

Distribution: India (Arunachal Pradesh, Assam, Sikkim, Mizoram, Meghalaya, West Bengal, Odisha).

Remarks: The species is well distributed in various states of India and more so in the eastern and north eastern part of India. It has been recorded on a large number of plants often in association with phytophagous mite. In the present study, its feeding was observed on immature stages of *Tetranychus neocaledonicus* infesting *Rauvolfia sarpentina* and *Solanum melongena*. This appears to be a potential predator of phytophagous mites.

Subfamily Phytoseiinae

Genus *Phytoseius* Ribaga

Phytoseius Ribaga (1904) Gamasidi Planticoli Rivista Patalogia Vegetale, Italy 10:175-178.

Key to the species of subfamily Phytoseiinae

1. Setae R1 present ..... ***Phytoseius minutus***
- Setae R1 absent ..... ***Phytoseius swirskii***

Phytoseius minutus Narayanan, Kaur and Ghai

Collection data: 1 male; India: West Bengal, Dist. South 24 Paraganas, Jharkhali on *Derris indica;* Dt. 24.ix.2017.

Distribution: India (Delhi, Punjab, Himachal Pradesh, Uttar Pradesh)

Remarks: Predatory importance not known.

Phytoseius swirskii Gupta

Collection data: 3 females; India: West Bengal, Dist. North 24 Paraganas, Hasnabad on *Ocimum gratssiimum*; Dt. 5.xi.2017.

Distribution: India (West Bengal, Karnataka).

Remarks: In present study this species was closely associated with larval stages of *Brevipalpus mitrofanovi* occurring on *Ocimum gratssiimum*.

Subfamily Typhlodrominae

Genus *Typhlodromus* Scheuten

Typhlodromus Scheuten (1857) Arch Nutur, Germany 23:104-112.

Typhlodromus fleshneri (Chant)

Collection data: 2 females; India: West Bengal, Dist. South 24 Paraganas, Sarberia on *Justicia adhatoda*; 3 females; Jharkhali, Sardar More on *Holarrhena pubescens*; Dt. 23.vii.2017.

Distribution: India (Assam, Meghalaya, West Bengal, Karnataka, Bihar).

Remarks: This species is well distributed in the eastern, north eastern and southern part of India associated with phytophagous mites. However, its predatory behavior was not reported neither in the present study nor in former studies.

Superorder: Acariformes

Order: Trombidiformes

Suborder: Prostigmata

Key to the families of sub order Prostigmata

1. Without a palpal thumb-claw complex 2
- With a palpal thumb-claw complex 5

2. Rod-like solenidion on tarsus usually lying flush with tarsus in a specialized membranous depression; anteriorly the propodosoma with a tubercle, bearing 1 pair of setae .....**Eupodidae**
- Rod like solinidion on tarsus erect arising from a small circular membranous base 3

3. Cheliceral bases fused or if not fused, not capable of lateral scissors-like motion over gnathosoma Iolinidae
- Chelicerae free attached at base and free to move scissors-like laterally across gnathosoma 4

4. With two pairs of genital suckers, the relatively long palpi curved inwards, distal segment usually claw-like, free living.....**Cunaxidae**
- With 3 pairs of genital suckers, the relatively long palpi elbow like with distal setae, free living .....**Bdellidae**

5. Body dorsally densely covered with setae, larvae heteromorphic .....**Erythraeidae**
- Body setae relatively few, arranged in transverse row, larvae heteromorphic 6

6. Chelicera formed a stylophore, coxae II and III contiguous ..... **Raphignathidae**
- Chelicera generally independently movable but may be adnate or stylophore-like, in a few genera, coxae II and III not contiguous; leg I and II directed anteriorly and leg III and IV directed posteriorly ..... **Stigmaeidae**

Family Bdellidae

Key to the subfamilies of Bdellidae

1. Venter of hypostome with 6-7 pairs of strong setae and 2 pairs of small adornal setae, without well-developed genital tracheae 2
- Venter of hypostome with 2 pairs of strong setae and 2 pairs of small adornal setae with well-developed genital tracheae ..... **Spinibdellinae**
..... **Genus *Biscirus***
.....***Biscirus* sp.**

2. Trichoboth absent on tibia II, palpaltibio-tarsus expanded distally ..... **Bdellinae**
.....**Genus *Hexabdella***
.....***Hexabdella unusoculata***
- Trichoboth present on tibia II, palpaltibio-tarsus cylindrical or elongated ..... **Odontoscrirnae**
..... **Genus *Bdellodes***
.....***Bdellodes* sp.**

Genus *Biscirus* Thor

Biscirus Thor (1913) Zool Anzeig 42:28-30.

Biscirus sp.

Biscirus sp. Gupta (1992) In Contributions to Acarological Researchers in India, p.440.

Collection data: 1 male; India: West Bengal, Dist. South 24 Paraganas, Sarberia on *Cocos nucifera*; Dt. 14.xii.2017.

Distribution: India (Arunachal Pradesh, West Bengal)

Remarks: A damaged specimen was collected on *Cocos nucifera*.

Genus *Bdellodes*

Bdellodes Oudemans (1937) Kritsch Historisch Overzitchtder Acarologic 3(C):12-17.

Bdellodes sp.

Collection data: 1 female; India: West Bengal, Dist. North 24 Paraganas, Taki Mini Sundarban on *Justicia adhatoda*; Dt. 5.xi.2017.

Distribution: India (West Bengal, Haryana)

Remarks: An undetermined species of this genus was collected but species identification could not be ascertained due to the for damaged condition of the specimen.

Genus *Hexabdella*

Hexabdella van Den Schyff, Theron & Uckermann (2004) Afr Plant Protect 9(1):19-22.

Hexabdella unuscoluta van Der Schyff

Collection data: 1 female; India: West Bengal, Dist. South 24 Paraganas, Dhamakhali on *Vitex negundo*; Dt. 15.iv.2017.

Distribution: South Africa, India (new record)

Remarks: Originally this species was described from Natal in South Africa from soil habitat and the occurrence of this species on *Vitex negundo* in Sundarban area is quite interesting providing a new distributional data.

Family Cunaxidae

Key to the genera and species of family Cunaxidae:

1. Palpal genu apically without elongate apophysis, tarsai I-IV long, slender and attenuate, without conspiqous lateral bilobed flanges terminally ..... ***Cunaxa*, 2**

- Palpal genu apically with elongate apophysis, tarsus I-IV long, stout and terminating in conspiqous bilobed lateral flanges ..... **Genus *Dactyloseiurus***
.....***Dactyloseiurus* sp.**

2. Propodosomal and hysterosomal shields smooth 3
- Propodosomal shield reticulate, smooth or striated and hysterosoma striated or with reticulate shield .....
.....***Cunaxa currasavica***

3. Palpal telofemur inner surface without flange or apophysis .....***Cunaxa evansi***
- Palpal telofemur inner surface with flange orapophysis
..... 4

4. Palpal telofemur inner surface with an uncinate or truncate apophysis .....***Cunaxa capriolus***
- Palpal telofemur inner surface with a distally rounded or sharply pointed apophysis or a rod like blunt finger like apophysis ..... ***Cunaxa terrula***

Genus *Cunaxa* von Heyden

Cunaxa von Heyden 1826, ISIS of Oken 18(6):609.

Cunaxa capreolus Berlese

Collection data: 2 females, India-West Bengal, Dist-South 24 Paraganas, Jharkhali on *Justicia adhatoda,* Dt.14.i.2018.

Distribution: India (Arunachal Pradesh, Meghalaya), cosmopolitan.

Remarks: Although it is a good predator of phytophagous mite (Smiley 1992) but in the present study its occurrence was scanty and therefore its predatory character was not observed.

Cunaxa currasavica Gupta

Collection data: 1 female; India: West Bengal, Dist. South 24 Paragana, Tangrakhali (Hasnabad) on *Abelmoschus esculentus*; Dt. 19.xi.2017.

Distribution: India (Arunachal Pradesh)

Remarks: This predator mite was described from north-east India. In this present case, its occurrence was casual.

Cunaxa evansi Smiley

Collection data:1 female; India: West Bengal, Dist. South 24 Paragana, Sagar Island on *Occimum sanctum*; Dt. 25.ii.2017.

Distribution: Mexico, Texas, India (new record)

Remarks: This species was earlier described from Mexico (Smiley 1992). It has been unknown from India. Its occurrence was casual on the undersurface of leaves. No predatory behavior was noticed.

Cunaxa terrula Den Heyer

Collection data: 1 male; India: West Bengal, Dist. South 24 Paraganas, Sagar Island on *Murraya koenigii*; Dt. 26.ii.2017

Distribution: South Africa, India (new record)

Remarks: This species has not been reported from India and hence the present is a new record.

Genus *Dactyloscirus* Berlese

Scirus (*Dactyloscirus*) Berlese, Redia 12(1):131.
Dactyloscirus Smiley (1975) Ann Ent Soc Amer 68(2):230.

Dactyloscirus sp.

Collection data: 1 male; India: West Bengal, Dist. South 24 Paraganas, Gosaba on *Ricinus communis*; Dt. 26.iii.2017.

Remarks: From India only 3 species of this genus is known. The chaetotaxy of palp and relative length of setae on dorsal surface did not match with any of the species from India or abroad. This is likely to be a new species and further studies are being made for confirmation.

Family Erythraeidae

Key to the subfamilies of Erythraeidae:

1. Two eyes on each side ..... **Erythraeinae**
..... **Genus *Erythraeus***
..... ***Erythraeus orientalis***
- One eye on each side ..... **Balustiinae**
..... **Genus *Balustium***
..... ***Balustium putmani***

Genus *Balustium*

Balustium von Heyden (1826) K.H.O.A 111P:309.

Balustium putmani Smiley

Collection data: 1 female; India: West Bengal, Dist. South 24 Paraganas, Jeliakhali on *Mangifera indica*; Dt. 16.iv.2017.

Distribution: Europe, USA, India (new record).

Remarks: This is a well-known predator of phytophagous mite. It was found feeding on immatures of *Oligonychus mangiferus.* The infested leaf when examined under stereo-binocular microscope revealed this. This mite has not earlier been reported from India.

Genus *Erythraeus*

Erythraeus orientalis (Khot)

Collection data: 1 female; India: West Bengal, Dist. South 24 Paragana, Jeliakhali on *Oxalis corniculate*; Dt. 16.iv.2017.

Distribution: India (Maharashtra, West Bengal, new record)

Remarks: This species was reported casually, and its predatory importance has not been noticed in the field.

Family Eupodidae

Genus *Eupodes*

Eupodes Koch (1842) Heft 1-40.

Eupodes sigmoidensis Strandmann & Goff

Collection data: 1 female; India: West Bengal, Dist. South 24 Paraganas, Jeliakhali on *Bixa orellana*; Dt. 15.iv.2017.

Distribution: India (West Bengal, Mizoram, Lakshadweep Island, Sikkim)

Remarks: This mite is frequently encountered on different plants in India and has been observed in the field to jump as soon as disturbed. Its feeding habits could not be ascertained in the present study.

Family Iolinidae

Genus *Pronematus*

Pronematus Canestrini (1886), Att. 1st Veneto Ser. 6, 4:698.

Pronematus sextoni Baker

Collection data*:* 1 female; India: West Bengal, Dist. South 24 Paragana, Jharkhali, *Datura metel*; Dt. 14.i.2018.

Distribution: India (West Bengal, Delhi, Uttar Pradesh, Karnataka), Africa.

Remarks: This species was reported from various states of India (Gupta 1992) but it was not recorded on the plant found in the present study. During laboratory examination it was found that the species actively fed on eggs on of *P. latus* occurring on infested *Datura* leaves.

Family Raphignathidae

Genus *Raphignathus*

Raphignathus Duges (1834) Ann Sci Nat 29:1-46.

Raphignathus sp.

Collection data: 1 female; India: West Bengal, Dist. South 24 Paragana, Jeliakhali on *Acacia auriculifomes*; Dt. 16.iv.2017.

Remarks: The non-availability of concerned literature

made it unable to determine the identity of this specimen up to species level.

Family Stigmaeidae

Key to the genera of Stigmaeidae:

1. Dorsal setae la on median plate proper; this plate also carries setae a, b, c and lm .....**Genus *Agistemus*** .....***Agistemus fleschneri***

- Setae la distributed on small independent plates, median plate carries 4 pairs of setae or five pairs if intercalary plates are integrated with it.*

*13 pairs of dorsal setae, suranals included individuals of pair lm always brone on small independent plates. Three or more pairs of paragenital setae .....**Genus *Stigmaeus*** .....***Stigmaeus* sp.**

Genus *Agistemus*

Agistemus Summers (1960) Proc Ent Soc Wash 62:234.

Agistemus fleschneri Summers

Collection data: 2 females, 1 male; India: West Bengal, Dist. South 24 Paraganas, Jharkhali on *Carica papaya*, *Solanum melangona*; Dt. 23.ix.2017.

Distribution: India (Arunachal Pradesh, Assam, Meghalaya, Sikkim, Tripura, West Bengal, Delhi, Punjab), USA, Chile, Mexico.

Remarks: This is a well-known predator of several phytophagous mites. In the present study this was found associated with eggplant infested with *Tetranychus urticae* as well as *Euyetranychus orientalis* on *Carica papaya*. However, field observations did not indicate any feeding on the respective phytophagous mites.

Genus *Stigmaeus*

Stigmaeus sp.

Collection data: 1 female; India: West Bengal, Dist. South 24 Paraganas, Jharkhali on *Citrus limon*; Dt. 20.vii.2017.

Distribution: India.

Remarks: This undetermined species of *Stigmaeus* was recorded on lemon tree for the first time. Due to damaged condition its specific identity could not be ascertained.

DISCUSSION

A very few attempts have been made earlier to document predatory mite fauna in Sunderban Biosphere Reserve. Gupta et al. (2004) provided a preliminary faunistic data on predatory mite fauna in some region of Sunderban. They found 28 species of predatory mites from Mangrove vegetation and agri-horticultural crops. Another study made by Kar and Karmakar (2021) reported 3 new species of phytoseiid mite from Sundarban. The present study on the predatory mites occurring on MAPs from Sundarban Biosphere Reserve revealed the occurrence of 41 species from 19 genera, 7 families and 2 orders. The diversity of predatory mites found in this study was high and this may be possible that such high diversity is a function of considerable diversity of plants sampled. A great diversity of plants leads to the great diversity of microhabitats that in turn allow a high number of mite species (Walter and O'Dowd 1995). The results of this study also suggest that the Sunderban Biosphere Reserve is an important reservoir of predatory mites, some of which may be helpful in controlling pest mites in different agro-ecosystem of Sunderbans. The occurrence of 7 species, 2, 3, 1 and 1, from *Cunaxa*, *Amblyseius*, *Balustium,* and *Hexabdella*, respectively, is new for India. This study also enlightens 25 plants that are acted as new habitats for some mites identified in this study (Table 1). Out of the 41 species, the occurrence of 12 species from West Bengal was hitherto unknown. Among these predatory mites *Amblyseius largoensis, Amblyseius herbicolus* and *Euseius ovalis* were active feeders of different stages of spider mites (Tetranychidae). The occurrence of other predatory mites was of causal nature. Some members of the genus *Stigmaeus*, *Dactyloscirus*, *Bdella*, and *Raphignathus* appear to be undescribed species and their taxonomic identities will be ascertained by further study. The data pertaining to the occurrence of predatory mites from Sundarban on MAPs is still fragmentary and thus, present paper will enrich the detailed taxonomic account of predatory mites from medicinal and aromatic plants of Sunderban Biosphere Reserve.

ACKNOWLEDGEMENTS

Sincere thanks are due to the Department of Science and Technology, Government of West Bengal (Sanc No:107(sanc)/S & T/1G-30/2016 to Dr. Himani Biswas), for providing financial assistance for this study. Thanks are also due to the Principal, Krishnagar Government College and Head, Department of Zoology, The University of Burdwan for providing infrastructural facilities for this study. The authors are highly thankful to Dr. S. K. Gupta, Former Emeritus Scientist of Zoological Survey of India for his guidance in identification of specimens.

Table 1. Location and habitat wise distribution list of predatory mites collected on medicinal and aromatic plants of Sundarbans area, West Bengal. Abbreviations: + denotes presence of mite species in that location, - denotes absence of mite species in that particular location.

No	Species	Location and habitat									Remarks
		Sagar Isl.	Gosaba	Dhamakali	Jelia Khali	Jharkhali	Bali Khal	Sar Beria	Hasnabad	Taki	
						Phytoseiidae					
1	*Amblyseius aerealis* (Muma)	-	-	-	-	+; *Datura metel*	-	-	-	-	Casual occurrence
2	*Amblyseius adhatodae* Muma	-	-	-	-	-	-	-	+; *Heliotropicum indicum*	-	New habitat record
3	*Amblyseius coffeae* De Leon	-	+; *Cinnamomum tamala*	-	-	-	-	-	-	-	New report in India
4	*Amblyseius cucurbitae* Rather	-	-	-	+; *Cappari zelyrica*	-	-	-	-	-	New habitat record
5	*Amblyseius fletcheri* Schicha	-	-	+; *Scuttelaria javanica*	-	-	-	-	-	-	New report from India
6	*Amblyseius herbicoloides* McMurtry	-	+; *Cleome viscosa*	-	-	-	-	-	-	-	New habitat record
7	*Amblyseius herbicolus* (Chant)	-	-	-	-	-	-	+; *Cocos nucifera*	-	-	Potential Predator
8	*Amblyseius ipomeae* Ghai and Menon	-	-	-	-	+; *Ricinus communis*	-	-	-	-	Casual occurrence
9	*Amblyseius kulini* Gupta	-	-	-	-	+; *Cocos nucifera*	-	-	-	-	Casual occurrence
10	*Amblyseius largoensis* (Muma)	*Justicia adhatodae*	-	*Ricinus communis*	*Ixora coccinea*	*Avicenia alba*	-	-	+; *Occimum sanctum*	-	Potent predator
11	*Amblyseius obtusus* (Koch)	-	-	-	-	-	-	-	+; *Butea monosperma*	-	New habitat record
12	*Amblyseius (Amblyseius) orientalis* Ehara	-	-	-	-	-	-	-	-	+; *Avicenia alba*	Casual occurrence
13	*Amblyseius paraaerialis* Muma	-	-	-	-	-	+; *Vitex nigundo*	-	-	-	Casual occurrence
14	*Euseius alstoniae* Gupta	+; *Gmelina arborea*	-	-	-	-	-	-	-	-	New habitat record
15	*Euseius coccineae* Gupta	+; *Justicia adhatodae*	-	-	-	-	-	-	-	-	Common predator
16	*Euseius finlandicus* Oudemans	-	-	-	+; *Heliotropium indicum*	-	-	-	-	-	Good predator of Tetranychids
17	*Euseius ovalis* (Evans)	-	+; *Murraya koenigii*	-	-	-	-	-	-	-	Important predator
18	*Euseius prasadi* Gupta	-	-	-	-	+; *Heritiera fomes*	-	-	-	+; *Ocimum gratssiimum*	Common and economically important predator
19	*Euseius rhododendronis* (Gupta)	-	-	-	-	-	+; *Acacia auriculiformis*	-	-	-	Casual occurrence
20	*Neoseiulus longispinosis* (Evans)	-	-	-	+; *Mangifera indica*	-	-	-	-	-	Well known predator
21	*Paraphytoseius bhadrakaliensis* (Gupta)	-	+; *Ficus racemosa*	-	-	-	-	-	-	-	Casual occurrence
22	*Paraphytoseius scleroticus* Gupta and Ray	-	-	-	+; *Vitex negundo*	-	-	-	-	-	Casual occurrence
23	*Scapulaseius suknaensis* (Gupta)	+; *Uraria picta*	-	-	-	-	-	-	-	-	New habitat record

Table 1. Continued.

No	Species	Location and habitat									Remarks
		Sagar Isl.	Gosaba	Dhamakali	Jelia Khali	Jharkhali	Bali Khal	Sar Beria	Hasnabad	Taki	
						Phytoseiidae					
24	*Phytoseius minutus* Narayanan, Kaur & Ghai	-	-	-	-	+; *Derris indica*	-	-	-	-	Predatory importance unknown
25	*Phytoseius swirskii* Gupta	-	-	-	-	-	-	-	+; *Ocimum gratsiimum*	-	Predatory importance unknown
26	*Typhlodromus fleshneri* Chant	-	-	-	-	-	-	+; *Justicia adhatoda*	-	-	New habitat record
						Bdellidae					
27	*Biscirus* sp.	-	-	-	-	-	-	+; *Cocos nucifera*	-	-	Casual occurrence
28	*Bdellodes* sp.	-	-	-	-	-	-	-	-	+; *Justicia adhatoda*	Predatory importance unknown
29	*Hexabdella unuscoluta* van Der Schyff	-	-	+; *Vitex negundo*	-	-	-	-	-	-	New record in India
						Cunaxidae					
30	*Cunaxa capreolus* Berlese	-	-	-	-	+; *Justicia adhatoda*	-	-	-	-	Good predator
31	*Cunaxa currasavica* Gupta	-	-	-	-	-	-	-	+; *Abelmoschus esculentus*		Casual occurrence
32	*Cunaxa evansi* Smiley	+; *Occimum sanctum*	-	-	-	-	-	-	-	-	New record in India
33	*Cunaxa terrula* Den Heyer	+; Murraya koenigii	-	-	-	-	-	-	-	-	New report from India
34	*Dactyloscirus* sp.	-	+; *Ricinus communis*	-	-	-	-	-	-	-	Casual occurrence
						Erythraeidae					
35	*Balustium putmani* Smiley	-	-	-	+; *Mangifera indica*	-	-	-	-	-	Potent predator
36	*Erythraeus orientalis* (Khot)	-	-	-	+; *Oxalis corniculata*	-	-	-	-	-	New habitat record
						Eupodidae					
37	*Eupodes sigmoidensis* Strandmann & Goff	-	-	-	+; *Bixa orellana*	-	-	-	-	-	Casual occurrence
						Iolenidae					
38	*Pronematus sextoni* Baker	-	-	-	-	+; *Datura metel*	-	-	-	-	Potential predator
						Raphignathidae					
39	*Raphignathus* sp.	-	-	+; *Acacia auriculifomes*	-	-	-	-	-	-	Casual occurrence
						Stigmaeidae					
40	*Agistemus fleschneri* Summers	-	-	-	-	+; *Carica papaya*	-	-	-	-	Important predator
41	*Stigmaeus* sp.	-	-	-	-	+; *Citrus limon*	-	-	-	-	Casual occurrence

REFERENCES

Baker EW, Wharton GW (1952) An Introduction to Acarology. The MacMillan Company, New York.

Berlese A (1914) Acari nuovi. Manipulus IX. Redia 10:113-150.

Canestrini G (1886) Prospetto dell'acarofauna Italiana. Famiglia degli Eupodini. Atti del Reale Istituto Venrto de Scienze. Lettere ed Arti 4:693-734.

Chant DA, McMurtry JA (2007) Illustrated Keys and Diagnoses for the Genera and Subgenera of the Phytoseiidae of the World (Acari: Mesostigmata). Indira Publishing House, West Bloomfield, USA.

Duges A (1834) Recherches sur l'ordre des Acariens en général et la famille des Trombides en particulier. Ann Sci Nat Zool S2 1:5-46.

Ghai S, Menon RMG (1967) Taxonomic studies on Indian mites of the family Phytoseiidae (Acarina). I. New species and new records of the genus *Amblyseius* Berlese from India (Acarina: Phytoseiidae) with a key to Indian species. Orient Insect 1:65-79.

Gerson U, Smiley RL, Ochoa T (2003) Mites (Acari) for Pest Control. Blackwell Science, Oxford, UK.

Gupta SK (1978) Studies on Indian Phytoseiidae (Acarina: Mesostigmata): some *Typhlodromus* mites from South India with descriptions of new species. Bull Zool Surv Ind 1:47-54.

Gupta SK, Ray S (1981) Species of the subgenera *Paraphytoseius* and *Asperoseius* from India with description of a new species of *Paraphytoseius*. *Bull Zool Surv India* 4:41-46.

Gupta SK (1992) Arachnida: Plant mites (Acari). State Fauna Series 3: Fauna of West Bengal. Vol. 3. Zoological Survey of India, Calcutta, pp. 61-211.

Gupta SK (1992a) Report on plant mite fauna of Arunachal Pradesh, India. Contr 10 Acarol Res India 433-445.

Gupta SK (2002) A monograph on plant inhabiting predatory mites of India Part I: Orders: Prostigmata, Astigmata and Cryotostigmata. Mem Zool Surv India 19:1-183.

Gupta SK (2003) A monograph on plant inhabiting predatory mites of India Part II: Order: Mesostigmata. Mem Zool Surv India 20:1-185.

Gupta SK, Ghoshal S, Choudhury A, Mukherjee B (2004) Phytophagous and predatory mite fauna of Sundarban Biosphere Reserve: II. Some Predatory mites occurring on mangrove vegetation and agrihorticultural crops. Rec Zool Surv India 103:33-45.

Gupta SK, Karmakar K (2015) An updated checklist of Indian Phytoseiid mites (Acari: Mesostigmata). Rec Zool Surv India 115:51-72.

Hoy MA (2011) Agricultural Acarology: Introduction to Integrated Mite Management. CRC Press, Boca, Raton, USA.

Hughes AM (1948) The Mites Associated with Stored Food Products. Ministry of Agriculture and Fisheries, London, UK.

Kar A, Karmakar K (2021) Description of three new species of phytoseiid mites (Acari: Mesostigmata) from Sundarban, West Bengal, India. Int J Acarol 47:51-60.

Karg W, Oomen-Kalsbeek F (1987) Neue Raubmilbenarten der Gattung Amblyseius Berlese (Acarina, Parasitiformes, Phytoseiidae). Antagonisten der unechten Spinnmilbe *Brevipalpus phoenicis* Geijskes. Zool Jahrbücher 114:131-140.

Koch CL (1842) Ubersicht des Arachnidensystems. JL Lotzberk, Nürnberg, 1-72.

de Moraes GJ, McMurtry JA, Denmark HA, Campos CB (2004) A revised catalog of the mite family Phytoseiidae. Zootaxa 434:1-494.

McMurtry JA, Croft BA (1997) Life-styles of phytoseiid mites and their roles in biological control. Annu Rev Entomol 42:291-321.

Oudemans AC (1937) Kritisch Historisch Overzicht der Acarologie III: 1805-1850: C: Leiden, Brill EJ, pp.1240-1253.

Ribaga C (1904) Gamasidi planticoli. Riv Patol Veget 10:175-178.

Scheuten A (1857) Einiges unber Milben. Arch F Naturgesch 23:104-112.

Smiley RL (1975) A generic revision of the mites of the family Cunaxidae (Acarina). Ann Entomol Soc Am 68:227-244.

Smiley RL (1992) The Predatory Mite Family Cunaxidae (Acari) of the World with a New Classification. Indira Publishing House, Michigan. pp 356.

Summers FM (1960) Several stigmaeid mites formerly included in *Mediolata* redescribed in *Zetzellia* Ouds, and *Agistemus*, new genus. Proc Ent Soc Wash 62:233-247.

Swirski E, Shechter R (1961) Some phytoseiid mites (Acarina: Phytoseiidae) of Hong Kong, with a description of a new genus and seven new species. Israel J Agric Res 11:97-117.

Tixier MS (2018) Predatory mites (Acari: Phytoseiidae) in agro-ecosystems and conservation biological control: A review and explorative approach for forecasting plant-predatory mite interactions and mite dispersal. Front Ecol Evol 6:192.

Thor S (1913) *Biscirus* genus novum. Eine neue Bdelliden-Gattung und zwei neue Untergattungen. Zoolog Anzeig 42:28-30.

Van der Schyff J, Theron PD, Ueckermann EA (2004) *Hexabdella*, a new mite genus of Bdellidae (Acari: Prostigmata) from southern Africa, with descriptions of five new species. Afr Plant Prot 9:19-22.

Von Heyden C (1826) Versuch einer systematischen Eintheilung der Acariden. Isis of Oken 18:608-613.

Wainstein BA (1962) Révision du genre *Typhlodromus* Scheuten, 1857 et systématique de la famille des Phytoseiidae (Berlese 1916) (Acarina: Parasitiformes). Acarologia 4:5-30.

Walter DE, O'Dowd DJ (1995) Life on the forest phylloplane:

hairs, little houses, and myriad mites. In Lowman MD, Nadkarni N, Eds., Forest Canopies. Academic Press, New York, 325-351.

Walter DE, Krantz GW (2009) Collecting, rearing and preparing specimens. A Manual of Acarology. Tech University Press, Texas 3:83-94.

Acta Biologica Szegediensis

Volume 65(2):253-261, 2021
Acta Biologica Szegediensis
http://abs.bibl.u-szeged.hu/index.php/abs
DOI:10.14232/abs.2021.2.253-261

ARTICLE

Expression of sialyltransferases from the *St3gal*, *St6gal* and *St6galnac* families in mouse skeletal muscle and mouse C2C12 myotubes

Rositsa S. Milcheva*, Any K. Georgieva, Katerina S. Todorova, Svetlozara L. Petkova

Institute of Experimental Morphology, Pathology and Anthropology with Museum, Bulgarian Academy of Sciences, Sofia, Bulgaria

ABSTRACT In skeletal muscles, the sialic acids have a great significance for their functional maintenance and proper structural organization. Our work described the expressions of *St3gal*, *St6gal* and *St6galnac* sialyltransferases specific for glycoproteins in mouse skeletal muscles and murine C2C12 myotubes. Lectin histochemistry, cytochemistry and lectin blot were used to demonstrate the membrane localization and the electrophoretic profiles of α-2,3- and α-2,6-sialylated glycoproteins. The expression levels of sialyltransferases were analysed by real time RT-PCR and western blot. The enzymes *St6gal2* and *St6galnac1* were not expressed in skeletal muscle tissue and C2C12 myotubes. In both experimental groups, mRNAs of the *St3gal* family prevailed over the mRNA expressions of the *St6gal* and *St6galnac* families. The profiles of sialyltransferase expressions showed differences between the two experimental groups, illustrated by the absence of expressions of the mRNA for the *St3gal6* and *St6galnac3* genes in the C2C12 cell samples and by the different shares of the enzymes *St3gal3* and *St3gal4* in both experimental groups. The different patterns of enzyme expressions in both experimental groups corresponded with differences between their α-2,3- and α-2,6-sialylated glycoprotein profiles. These results could be a useful addendum to the knowledge concerning the glycosylation of the skeletal muscle tissue.

Acta Biol Szeged 65(2):253-261 (2021)

KEY WORDS
C2C12 myotubes
sialylation
sialyltransferases
skeletal muscles

ARTICLE INFORMATION
Submitted
12 July 2021
Accepted
19 October 2021
***Corresponding author**
E-mail: rosicamilcheva@abv.bg

Introduction

The attachment of monosaccharide residues is one of the most complicated co- or post translational modifications that proteins can undergo, resulting in an abundant, diverse, and highly regulated repertoire of cellular glycans. Two major classes of oligosaccharides are defined according to the nature of the linkage between the carbohydrate chain and the polypeptide region. An O-glycan (O-linked oligosaccharide) is usually bound to the polypeptide via N-acetylgalactosamine (GalNAc) to a serine (Ser) or threonine (Thr) residue and can be extended into a variety of different structural core classes. An N-glycan (N-linked oligosaccharide) is a sugar chain covalently linked to an asparagine (Asn) residue of a polypeptide chain within the consensus peptide sequence: Asn-X-Ser/Thr (Brockhausen and Stanley 2017; Stanley et al. 2017).

One of the most fascinating building units of the oligosaccharide constructions are the sialic acids. They represent a family of over 40 modifications of the N-acetylneuraminic acid (Neu5Ac). The sialic acids typically occupy the terminal position of the glycoconjugate sugar chains, usually via α-2,3-, α-2,6-, or α -2,8- glycosidic bond (Varki 1992; Harduin-Lepers et al. 2001; Schauer 2004). The glycosidic bonds are generated by highly specific enzymes that belong to four sialyltransferase families. The members of the families, beta-galactoside alpha-2,3-sialyltransferase (ST3Gal), beta-galactoside alpha-2,6-sialyltransferase (ST6Gal) and N-acetylgalactosaminide alpha-2,6-sialyltransferase (ST6GalNAc) are widely spread in different tissues, while the enzymes from the alpha-N-acetyl-neuraminide alpha-2,8-sialyltransferase family (ST8SiA) are mostly expressed in the brain (Harduin-Lepers et al. 2005). The sialylation of glycoproteins or glycolipids always occurs into the Golgi, and afterwards they are transported to the cell membrane. Because of their terminal position on the oligosaccharide chains, the sialic acids participate in almost all types of recognition phenomena and adhesion mechanisms (Varki 2007; Schauer 2009).

In skeletal muscles the sialic acids are very important for the functional maintenance of glycoproteins involved in fibre structure and neuromuscular junctions, develop-

ment and regeneration, muscle excitability and exercise performance (McDearmon et al. 2003; Combs and Ervasti 2005; Broccolini et al. 2008; Johnson et al. 2004; Schwetz et al. 2011; Hanish et al. 2013).

Even if the sialylation is not as much abundant as in other tissues, the muscles are very sensitive to sialic acid deficiency due to mutations, which results in a variety of diseases with a severe and progressive loss of motility as a common feature (Tajima et al. 2005; Broccolini et al. 2009). Histological expressions of sialylated glycoproteins in adult human skeletal muscles were already described in detail (Marini et al. 2014). By now, however, the only identified sialylated glycoprotein in skeletal muscles is the α-dystroglycan, a member of the dystrophin-associated glycoprotein complex (Barresi and Campbell 2006). Comprehensive information about the expression of enzymes from the sialyltransferase families is also missing in the available literature.

The aim of this work was to investigate the sialylation in mouse skeletal muscle tissue and C2C12 mouse myotubes in the aspect of localization of α-2,3- and α-2,6-sialylated glycoproteins, relative quantification of sialyltransferase expressions and comparison of the α-2,3- and α-2,6-sialylated glycoprotein profiles.

Material and methods

Ethical procedures

All animal experiments were performed in compliance of Regulation No 20/01.11.2012 on the minimum requirements for protection and welfare of experimental animals and the requirements for the sites for their use, breeding and/or delivery, issued by the Ministry of Agriculture and Food of Republic of Bulgaria.

Mouse tissue samples collection

Five male white laboratory mice, 6-8 weeks old, were humanely euthanized. Tissue specimens were excised from the femoral and gluteal muscles and fixed with freshly prepared modified methacarn fixative (Cox et al. 2006) or stored at -80 °C for further studies. Specimens from lungs, spleen, brain, liver, intestine, colon, and kidneys were archived in low temperatures, too. After processing, the fixed specimens were embedded in paraffin.

Cell cultures

C2C12 mouse myoblast cell line (ATCC® CRL-1772™) was purchased from LGC Standards USA (Manchester, NH, USA). The cells were cultured for 48 h in Dulbecco's Modified Eagle's Medium (DMEM, Sigma-Aldrich, St. Louis, MO, USA) with a high glucose content of 4.0 g/L supplemented with 10% fetal bovine serum (FBS, Gibco-Thermo Fisher Scientific, Waltham, MA, USA), penicillin 100 IU/ml and streptomycin 100 μg/ml, (AppliChem, Darmstadt, Germany) into plastic tissue culture flasks (Orange Scientific, Braine-l`Alleu, Belgium) or onto 12 mm oval glass cover slips (Glaswarenfabrik Karl Hecht, Sondheim, Germany), until 90% confluence of the monolayer was achieved. Further differentiation into myotubes was induced by changing the growth medium to differentiation medium – Dulbecco's Modified Eagle's Medium, supplemented with 2% horse serum (Sigma-Aldrich, Merck, Darmstadt, Germany). After a routine estimation of the fusion index, the mature myotubes were dissociated by 0.05% solution of trypsin (Gibco, Thermo Fisher Scientific) with 0.025% ethylenediaminetetraacetic acid (AppliChem, Darmstadt, Germany) and counted with an automatic cell counter (Countess™, Invitrogen™, Thermo Fisher Scientific). Samples with approximate concentration of 5 x 10^6 cells/ml were stored at -80 °C for further molecular and proteomic studies. The myotube layers onto the cover slips (Glaswarenfabrik Karl Hecht, Sondheim, Germany) were submitted for lectin cytochemistry.

Lectin histo- and cytochemistry

Cover slips with myotube cultures and skeletal muscle tissue sections were treated with biotinylated lectins – *Maackia amurensis* lectin-II (MAL-II, Vector Laboratories, Burlingame, CA, USA), specific for α-2,3-sialic acids (Knibbs et al. 1991) and *Sambucus nigra* agglutinin (SNA, Vector Laboratories), specific for α-2,6-bound sialic acids (Kaku et al 2007). The tissue sections were first rehydrated, and the myotubes were treated with 0.3% Triton in buffer. The further steps were performed in dark. All samples were incubated for 30 min with 1 μg/mL methanol solution of 4′,6-diamidino-2-phenylindole (DAPI, AppliChem), then with SNA or MAL-II (1 μg/mL) for 60 min, and finally with Streptavidin-FITC (1:100, Sigma-Aldrich) for 30 min. Control samples were treated with buffer instead of lectins. The samples were mounted in Vectashield mounting medium (Vector Laboratories) and observed with light microscope Leica DM 5000B (Leica Camera AG, Wetzlar, Germany) under UV, blue, green and UV/violet fluorescent filters. The obtained parallel images of each sample were merged using ImageJ (version 1.48h3; developed at the U.S. National Institutes of Health (Bethesda, MD, USA) by W. Rasband, and available at https://imagej.net/Downloads; Schneider et al., 2012).

Gene expression analyses

The experiments described in this section were designed to evaluate the expression of mRNA of mouse sialyltransferases *St3gal1, 2, 3, 4* and *6*, *St6gal1* and *2*, and *St6galnac1, 2, 3* and *4* in mouse skeletal muscle tissue samples and mouse C2C12 myotubes. The levels of expressions were

estimated via normalization versus the expressions of peptidyl prolyl isomerase A (*Ppia*) and glyceraldehyde 3-phosphate dehydrogenase (*Gapdh*) as reference genes. All primers were designed using the NCBI Blast Tool (Ye et al. 2012) in a way to span at least one intron sequence. The full names of investigated genes, the primer sequences and the size of the amplified products are available in Table 1, as a supplementary file. The oligonucleotides were purchased from HVD Biotech Vertriebs (Vienna, Austria). The substrate specificities of all sialyltransferases, analyzed in this study, are shown in Table 2.

Five skeletal muscle tissue samples with approximate weight of 30 mg each and five aliquots of C2C12 cell cultures from different passages with approximate concentration of 5 x 10^6 cells/ml were homogenized using TissueRuptur II homogenizer (Qiagen, Hilden, Germany) on ice. Total RNA was isolated and purified by GeneMatrix Universal RNA Purification Kit (EurX®, Gdansk, Poland), strictly following the corresponding protocols recommended by the producer. The yield and purity of the collected RNA were measured using S-300 spectrophotometer (Boeco, Hamburg, Germany).

Approximately 2 μg total RNA from each sample were used for first strand cDNA synthesis. The reverse transcription reaction mixture contained 5 x reaction buffer, 20 U RiboLock Rnase Inhibitor, 1 mM dNTPs, 100 pmol random hexamer primers, 200 U RevertAid Reverse Transcriptase (all of them Fermentas; Thermo Fisher Scientific, Waltham, MA, USA) and diethylpyrocarbonate (DEPC)-treated water (Sigma-Aldrich). The reaction mixture was first incubated at room temperature for 10 min, then at 42 °C for 1 h, and the reaction was terminated at 70 °C for 10 min. The generated cDNA was quantified, and the samples were stored at -80 °C.

Table 1. The full names of the investigated genes and their primers sequences used in this study.

Gene	Abbreviation	Accession number	Primers sequences (5`-3`)	Product size (bp)
Peptidylprolyl isomerase A	*Ppia*	NM_008907.1	TTCGAGCTCTGAGCACTGG – F CCAGTGCCATTATGGCGT – R	115
Glyceraldehyde 3-phosphate dehydrogenase	*Gapdh*	NM_001289726 transcript variant 1	TCCTCGTCCCGTAGACAAAATG – F AATCTCCACTTTGCCACTGC – R	103
ST3 beta-galactoside alpha-2,3-sialyltransferase 1	*St3gal1*	NM_009177.4	ACCATCACTCACACCTATGTCC – F CCTGAAGCCAGTTGTCAAAGAC – R	112
ST3 beta-galactoside alpha-2,3-sialyltransferase 2	*St3gal2*	NM_009179	TCCTTCCTTCGAGTGGACAAAG – F ACCAGCATTCCTGTGGAAGG – R	116
ST3 beta-galactoside alpha-2,3-sialyltransferase 3	*St3gal3*	NM_001161774.2 transcript variant 2	AACTTTTCCGAGGGAGCTTG – F TAGCCCACTTGCGAAAGGAG – R	118
ST3 beta-galactoside alpha-2,3-sialyltransferase 4	*St3gal4*	NM_009178.4	TGGGTAAAGACGCCATCCAC – F TCGAGGCTCTTTATGCTCTCAG – R	119
ST3 beta-galactoside alpha-2,3-sialyltransferase 6	*St3gal6*	NM_018784.2	TCCCAGCTGAAGAAATGAGGAC – F TCAGCTCTGCACAGAAATGG – R	112
ST6 beta-galactoside alpha-2,6-sialyltransferase 1	*St6gal1*	NM_145933.3	GCCGTCGTGTCTTCTGCAGGAT – F TGGAAGTTGTCTGTAGGTGCCCC – R	107
ST6 beta-galactoside alpha-2,6-sialyltransferase 2	*St6gal2*	NM_172829.2	CTGCGCAGTTGTCATGTCTG – F TTTCTCATAGCCACGTGTAGGG – R	115
ST6 (alpha-N-acetyl-neuraminyl-2,3-beta-galactosyl-1,3)1-acetogalactosaminide alpha-2,6-sialyltransferase 1	*St6galnac1*	NM_011371.2	TCCTGCTTCTGACTGTGTTGGCA – F TCTCCTGGGCACTTGCGTCA –R	117
ST6 (alpha-N-acetyl-neuraminyl-2,3-beta-galactosyl-1,3)1-acetogalactosaminide alpha-2,6-sialyltransferase 2	*St6galnac2*	NM_009180.3	CCCACGAGCATTCTTTGACCCCA – F TCAAACAGGCTGCGGAAGCGA – R	117
ST6 (alpha-N-acetyl-neuraminyl-2,3-beta-galactosyl-1,3)1-acetogalactosaminide alpha-2,6-sialyltransferase 3	*St6galnac3*	NM_011372.2	CAGGCAGCCTCTTCGAACTCACT – F ACCTTCTGCCCGACCATTTGACC – R	117
ST6 (alpha-N-acetyl-neuraminyl-2,3-beta-galactosyl-1,3)1-acetogalactosaminide alpha-2,6-sialyltransferase 4	*St6galnac4*	NM_011373.3 transcript variant 1	TTCACTGAACGCATGATGGC – F AGGGCCAGAATCATGGTGAAC – R	116

Real-time PCR was designed on approximately 700 ng cDNA as a template in 20 µl total volume of reaction using SG qPCR Master Mix (2x), 0.25 U uracyl-N-glycolase (UNG), nuclease free water (all from EurX) and 0.2 µM R- and F-primers specific for amplification of fragments of *Gapdh*, *Ppia*, *St3gal1*, *2*, *3*, *4* and *6*, *St6gal 1* and *2*, and *St6galnac1*, *2*, *3* and *4*. Three real-time PCR reactions/sample in duplicate were performed for amplification of each fragment of interest using RotorGene™ 6000 Real-time Analyzer (Corbett Life Science-Qiagen).

The data were analysed using Rotor Gene Q Series Software (Qiagen) and the relative quantification of the sialyltransferase expressions was calculated by the ΔΔCt method (Zhang et al. 2014) versus *Ppia* and *Gapdh* as reference genes. After each run, a High-Resolution Melting Curve Analysis (HRM) was performed to verify the specificity of the amplified products, which were visualized on 2.5% agarose gel supplemented with Simply Safe nucleic acid stain (EurX) versus 100-1000 bp DNA Ladder (EurX) and the gels were photographed with a gel documentation system Vision (Scie-Plas Ltd, Cambridge, UK).

Statistical analysis of the gene expression quantification

Statistical analysis of the data was performed using GraphPad Prism 5.03 software (San Diego, CA, USA). One Way Anova analysis with test of Bonferroni was computed to detect statistically significant differences between the Ct values of the qPCR products, and the results were interpreted as follows: $P < 0.001$ = highly significant; $P < 0.01$ = very significant; $P < 0.05$ = significant.

SDS-PAGE, lectin- and western blotting

Skeletal muscle tissue samples with an approximate weight of 30 mg each and aliquots of C2C12 myotubes from different passages with an approximate concentration of 5 x 10^6 cells/ml were homogenized in 0.6 M Tris buffer, containing 150 mM NaCl, 5 mM EDTA and 1% CHAPS (all purchased from Sigma-Aldrich), supplemented with Proteinase inhibitor cocktail, set 3 (Sigma-Aldrich), using TissueRuptur II homogenizer (Qiagen) on ice, and then centrifuged at 21 000 g, for 1 h at 4 °C. The supernatants were used for methanol/chloroform protein precipitation, as described by Fic et al. (2010). The protein pellet was reconstituted in 6 M urea buffer, containing 1.5 M thiourea, 3% CHAPS, and 66 mM DTT (all purchased from Sigma-Aldrich), and stored at -20 °C. The protein content was measured by the method of Bradford (1976) on spectrophotometer S-300 (Boeco).

Approximately 30 µg from each sample were mixed with 4 x Loading buffer (EurX), samples were heated at 98 °C for 10 min and were then loaded on 10% polyacrylamide gel. SDS-PAGE was performed under reducing conditions as described by Laemmli (1970).

Gels were then stained with colloidal Coomassie Brilliant Blue (Jahn et al. 2013) or were forwarded to western blotting on 0.45 µm nitrocellulose membranes (Sigma-Aldrich), as described by Towbin et al. (1979). The membranes designated for lectin-affino blots were blocked with 5% non-fat dry milk (Sigma-Aldrich) for 1 h, then

Table 2. Substrate specificity of the sialyltransferases, operating on glycoproteins (Markos et al. 2004; Takashima 2008), investigated in this study. The monosaccharides in bold indicate a residue onto which a sialic acid is transferred via α-2,3- or α-2,6-glycosidic linkage. Gal – galactose, GalNAc – N-acetyl-D-galactosamine, GlcNAc – N-acetyl-D-glucosamine, SiA – sialic acid, Ser – serine, Thr – threonine.

β-Galactoside-α-2,3-sialyltransferase family (ST3Gal)	
ST3Gal1	**Gal**-β-1,3-GalNAc
ST3Gal2	**Gal**-β-1,3-GalNAc
ST3Gal3	**Gal**-β-1,3-GlcNAc > **Gal**- β-1,4-GlcNAc > **Gal**-β-1,3-GalNAc
ST3Gal4	**Gal**-β-1,3-GalNAc > **Gal**- β-1,4-GlcNAc > **Gal**-β-1,3-GlcNAc
ST3Gal6	**Gal**- β-1,4-GlcNAc > **Gal**-β-1,3-GlcNAc
β-Galactoside-α-2,6-sialyltransferase family (ST6Gal)	
ST6Gal1	**Gal**- β-1,4-GlcNAc
ST6Gal2	**Gal**- β-1,4-GlcNAc
GalNAc α-2,6-sialyltransferase family (ST6GalNAc)	
ST6GalNAc1	**GalNAc**-α-1-Ser/Thr (Tn Ag) > Gal-β-1,3-**GalNAc**-α-1-Ser/Thr (T Ag)
	SiA-α-2,3-Gal-β-1,3-**GalNAc**-α-1-Ser/Thr (sialyl-T Ag)
ST6GalNAc2	Gal-β-1,3-**GalNAc**-α-1-Ser/Thr > **GalNAc**-α-1-Ser/Thr
	SiA-α-2,3-Gal-β-1,3-**GalNAc**-α-1-Ser/Thr
ST6GalNAc3	SiA-α-2,3-Gal-β-1,3-**GalNAc**-
ST6GalNAc4	SiA-α-2,3-Gal-β-1,3-**GalNAc**-

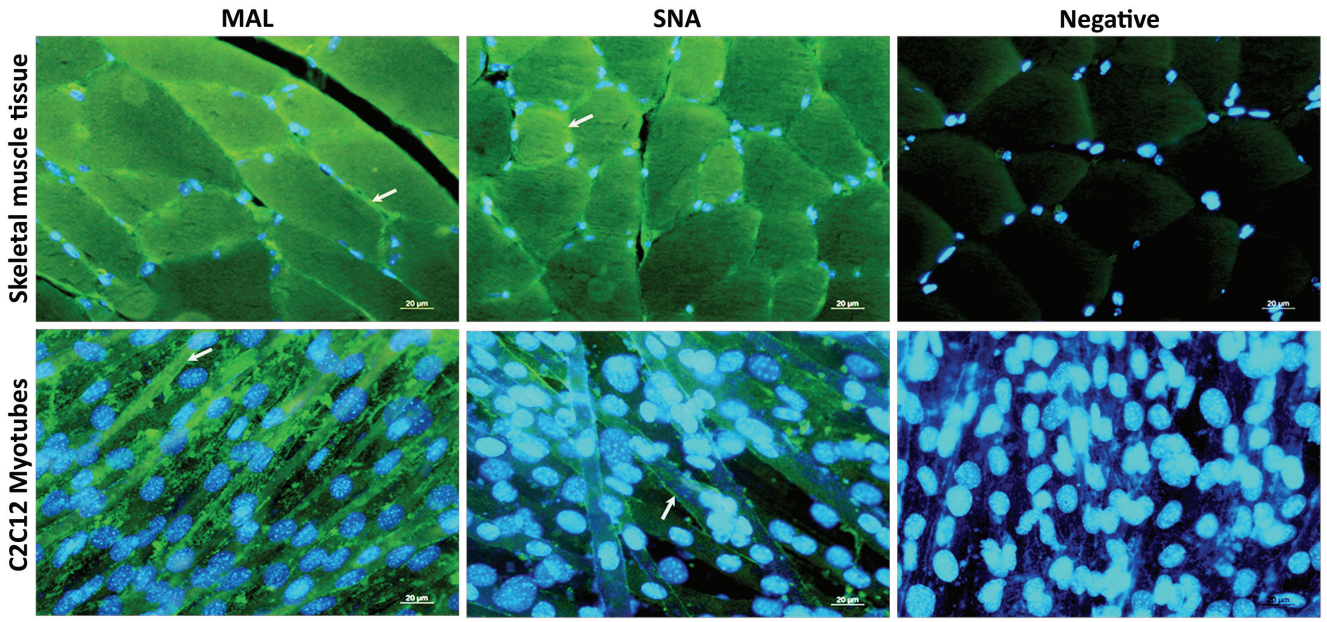

Figure 1. Sialylated glycorpoteins in mouse skeletal muscle tissue and mouse C2C12 myotubes. Skeletal muscle tissue sections and C2C12 myocyte cultures were stained with lectins MAL-II and SNA specifically recognizing α-2,3- and α-2,6-sialylated glycoproteins located on the cell membranes (arrows). Streptavidin-FITC, DAPI. Scale bar: 20 µm.

incubated with biotinylated SNA (Vector Laboratories) or MAL-II (Vector Laboratories) (1 µg/mL) for 1 h, and finally treated with streptavidin horseradish peroxidase (HRP, Vector Laboratories) for 30 min at room temperature. The membranes designated for western blots were treated with goat blocking serum (Vector Laboratories) for 1 h, then incubated with polyclonal rabbit antibodies against GAPDH (1:2000, Thermo Fisher Scientific), ST3Gal VI (1 µl/mL) and ST6GalNAc III (2 µl/mL) (Sigma-Aldrich) for 2 h, and finally treated with WestVision Peroxidase Polymer Anti-Rabbit IgG (Vector Laboratories) for 30 min at room temperature. The colour reaction on all membranes was developed after exposure to DAB Peroxidase Substrate solution (Vector Laboratories). The approximate molecular weight of the detected protein bands was estimated versus Perfect™ Tricolor Protein Ladder (EurX), ranging from 11 to 245 kDa.

Results

Localization and protein profiles of α-2,3- and α-2,6-sialylated glycoproteins

The lectin histochemistry and cytochemistry in our study demonstrated the membrane localization of α-2,3- and α-2,6-sialylated glycoproteins in mouse skeletal muscle samples and the C2C12 cell line (Fig. 1). The cell line samples were much more reactive towards MAL-II in comparison with SNA. Both experimental groups showed similar protein profiles with a slight difference between the patterns of the α-2,3-sialylated glycoproteins, demonstrated by MAL-II affino-blot. The C2C12 cell culture samples showed a higher number of α-2,6-sialylated glycoproteins, as demonstrated by the SNA affino-blot. In both experimental groups, the lectin affino-blots revealed

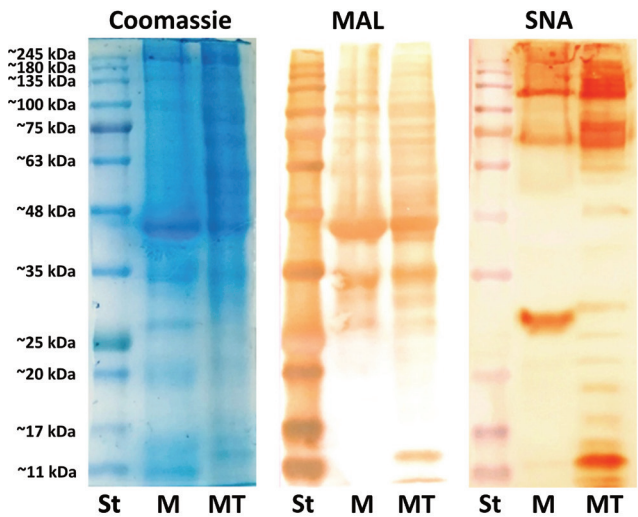

Figure 2. SDS-PAGE, MAL-II and SNA lectin affino-blot of mouse skeletal muscle tissue (M) and C2C12 myotube samples (MT), loaded on 10% gels versus Perfect™ Tricolor Protein Ladder (EurX) ranging from 11 to 245 kDa (line L), showing different patterns of sialylation. Streptavidin-HRP, DAB.

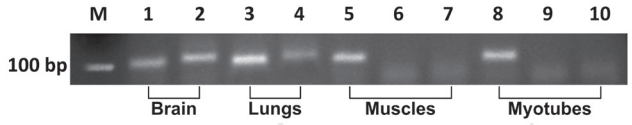

Figure 3. Absence of amplification products specific for mouse *St6gal2* and *St6galnac1* sialyltransferases in mouse skeletal muscles and C2C12 myotubes. Mouse brain and lungs were used as positive expression controls. Lanes: M – 100 bp fragment of DNA Ladder, 1 and 2 – *Gapdh* (103 bp) and *St6gal2* (115 bp) expressions in brain, 3 and 4 – *Gapdh* and *St6galnac1* (117 bp) expressions in mouse lungs, 5, 6 and 7 – *Gapdh*, *St6gal2* and *St6galnac1* expressions in mouse skeletal muscles, 8, 9 and 10 – *Gapdh*, *St6gal2* and *St6galnac1* expressions in C2C12 myotubes.

sialylated glycoproteins with an approximate molecular weight between 120 and 15 kDa (Fig. 2).

Expression of sialyltransferases

Our study was designed to analyse the expressions of members from the β-galactoside α-2,3-sialyltransferase (*St3gal*), β-galactoside α-2,6-sialyltransferase (*St6Gal*) and GalNAc α-2,6-sialyltransferase (*St6galnac*) families, operating on glycoproteins (Takashima 2008), which substrate preferences were described in Table 2.

The mRNAs of *St6gal2* and *St6galnac1* didn't show products of amplification in the skeletal muscle samples and in the C2C12 cell line (Fig. 3). Expressions of mRNAs for all the rest of the sialyltransferases were detected in mouse skeletal muscle samples (Fig. 4A). Expressions of mRNA for the genes *St3gal6* and *St6galnac3* were not detected in the C2C12 muscle cell samples (Fig. 4B) and this was confirmed also by protein western blot (Fig. 4C).

According to the percent distribution analysis of the expressions of investigated sialyltransferases in both experimental groups (Fig. 5), mRNAs of the *St3gal* family prevailed over the mRNA expressions of the *ST6gal* and *St6galnac* families. The profiles of sialyltransferase

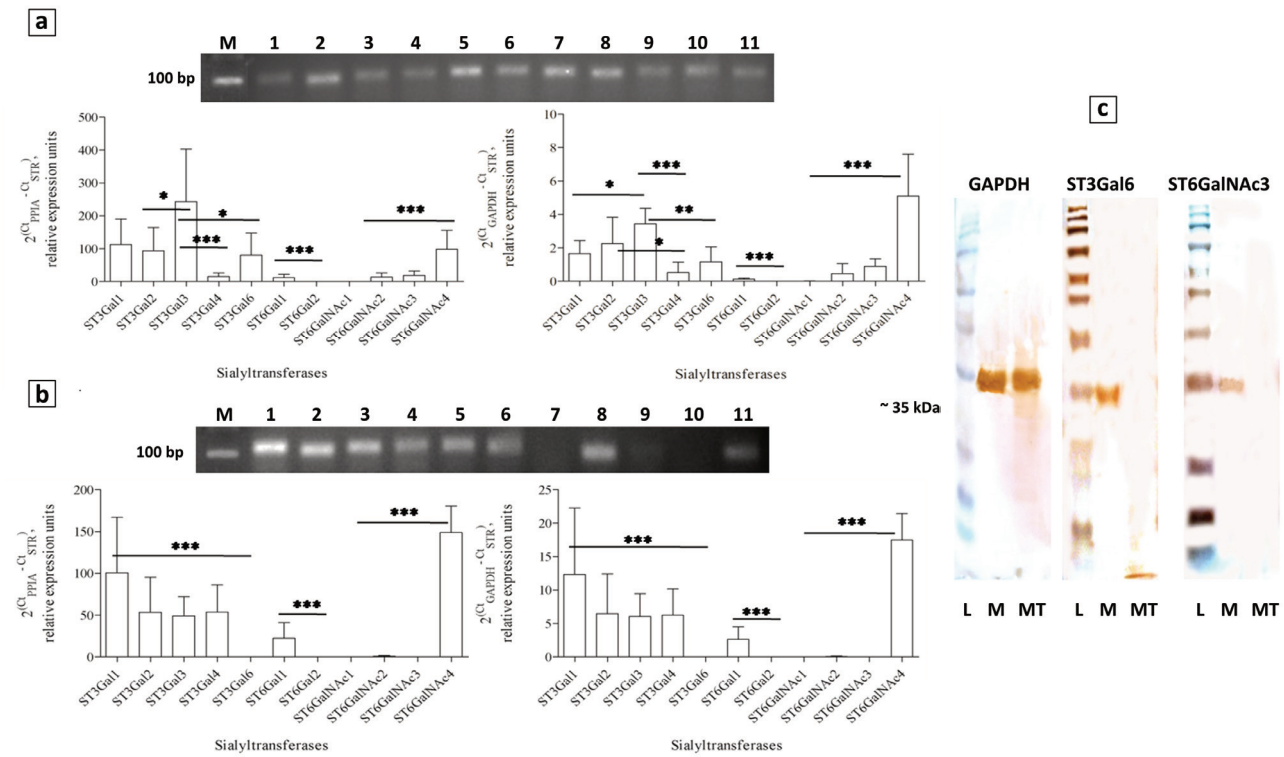

Figure 4. Expressions of mouse sialyltransferases analyzed by real time RT-PCR in skeletal muscle tissue (a) and C2C12 myotube cultures (b), and by western blot (c). Panels a and b – The photographs show amplification products specific for mouse sialyltransferases on 2.5% agarose gel: M – 100 bp fragment of DNA Ladder, 1 – **Ppia** (115 bp), 2 – *Gapdh* (103 bp), 3 – *St3gal1* (112 bp), 4 – *St3gal2* (116 bp), 5 – *St3gal3* (118 bp), 6 – *St3gal4* (119 bp), 7 – *St3gal6* (112 bp), 8 – *St6gal1* (107 bp), 9 – *St6galnac2* (117 bp), 10 – *St6galnac3* (117 bp), 11 – *St6galnac4* (116 bp). The charts represent a relative quantification of sialyltransferase expressions calculated by the ΔΔCt method versus *Ppia* (left) and *Gapdh* (right) as reference genes from six individual samples in triplicate. The bars show the standard deviation. The stars indicate statistically significant difference between sialyltransferase expressions in each family: *** P < 0.001, ** P< 0.01, * P< 0.05. Panel c – Western blots of mouse skeletal muscle tissue (M) and C2C12 myotube samples (MT), with polyclonal rabbit antibodies against GAPDH Thermo Fisher Scientific), ST3Gal VI and ST6GalNAc III (Sigma-Aldrich) sialyltransferases, loaded on 10% gels versus Perfect™ Tricolor Protein Ladder (EurX) ranging from 11 to 245 kDa (line L), showing absence of expression of both enzymes by the C2C12 myotubes. ImPress™ HRP Anti-Rabbit IgG, DAB.

expressions were different between skeletal muscle tissue samples and C2C12 cell cultures, illustrated by the missing expressions of the mRNA for the *St3gal6* and *St6galnac3* genes in the C2C12 cell samples and by the different shares of the genes *Stgal3* and *Stgal4* in both experimental groups. Among the members of the *St6galnac* family, the expression of *St6galnac4* gene prevailed strongly in both experimental groups. The expression of the *St6galnac2* sialyltransferase was also significantly lower in the C2C12 myotubes. Both experimental groups showed expression of only *St6gal1* but not *St6gal2* (data not shown).

Discussion

Apart from the broad knowledge about the extracellular proteoglycan components and their role in the muscle growth and development (Velleman 2002), most of the information concerning glycosylation of the skeletal muscle tissue is related to inherited disease states (Grewal and Hewitt 2003; Martin-Rendon and Blake 2003) and actually very little is known about its normal glycoproteome.

As already mentioned, the only sialylated glycoprotein discovered in the skeletal muscle tissue by now, was the α-dystroglycan bearing α-2,3-linked sialic acid residues (Barresi and Campbell 2006). Our results showed however the presence of at least several α-2,3- and α-2,6-sialylated glycoproteins, still not identified.

A very important aspect in this scientific topic is the expression of sialyltransferases in muscles. The great variety of the oligosaccharide constructions used as acceptors by the sialyltransferases predetermines the diversity of these enzymes, which were grouped into four families according to the glycosidic linkages they synthesize. From amino acid sequence similarities, substrate specificities and gene structures, the members of each sialyltransferase family were classified into subfamilies (Harduin-Lepers et al. 2005).

In mice and humans, ST6Gal II is one of the two members of the ST6Gal family. Both members utilize the Gal-β-1,4-GlcNAc structure on glycoproteins and oligosaccharides as acceptor substrates. The *St6gal1* gene has a wide range of tissue expression; however, the *St6gal2* gene is expressed in a stage-specific (embryonic stage) and a tissue-specific (adult brain) manner (Takashima et al. 2003), as confirmed also by our results.

The enzymes ST6GalNac I and ST6GalNAc II were classified into a common subfamily of the ST6GalNAc family. Both enzymes exhibit similar substrate specificity, utilizing GalNAc- (Tn antigen), Gal-β-1,3-GalNAc- (T antigen) and SiA-α-2,3-Gal-β-1,3-GalNAc- (sialyl-T antigen) structures on O-glycans of glycoproteins as acceptor substrates (Kono et al. 2000). However, ST6GalNAc I

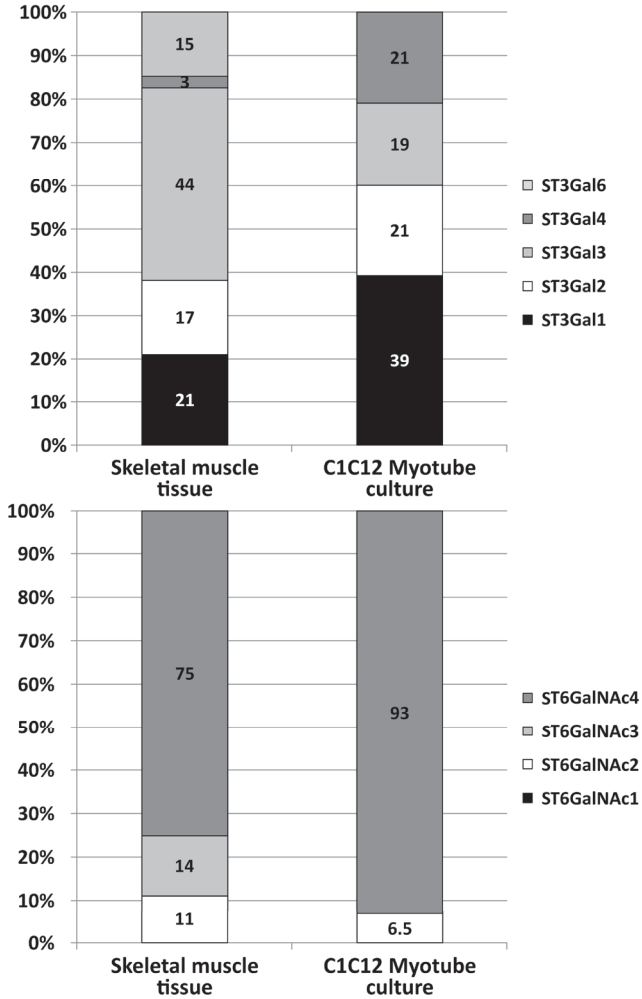

Figure 5. Percent distribution of the gene expressions of the enzymes sialyltransferases from the *St3gal* and *St6galnac* families in mouse skeletal muscle and mouse C2C12 myotubes. Normalization shown versus *Ppia* as a reference gene.

was reported as a major sialyl-Tn synthase, whereas the ST6GalNAc II acts preferentially on T antigen (Markos et al. 2004). In our study, we observed a positive signal of amplification of *St6galnac1* specific product in mouse lung tissue, but not in our experimental muscle and myotube samples.

ST3Gal VI is a member of the ST3Gal family and utilizes preferentially the Gal-β-1,4-GlcNAc structure on glycoproteins and glycolipids as an acceptor substrate (Okajima et al. 1999). ST6GalNAc III together with ST6GalNAc IV was classified into a common subfamily from the corresponding sialyltransferase family. These two enzymes utilize the SiA-α2,3-Gal-β-1,3-GalNAc (sialyl-T antigen) structure on glycoproteins as an acceptor substrate (Lee et al. 1999). Our results definitively showed absence of expression of *St3gal6* and *St6galnac3*

and their encoded proteins in C2C12 myotubes, a finding that is in agreement with similar results predicted by Janot et al. (2009).

Another intriguing difference between the muscle tissue and the cell culture was the different expression levels of the genes *St3gal3* and *St3gal4*, which belong to the same subfamily of α-2,3-sialyltransferases. Both enzymes utilize the same oligosaccharide structures as substrate acceptors, but with quite opposite preferences (Takashima 2008).

The development of new technologies in life sciences opened in the late 1980s a new division of molecular biology named "glycobiology". Since then, huge knowledge was accumulated concerning the chemistry of carbohydrates, the enzymology of glycan biosynthesis and degradation, the structure of glycoconjugates, the recognition of glycans by specific proteins and the roles that the glycans occupy in complex biological systems. In this rapidly growing field in the natural sciences, however, the skeletal muscles remained somehow not quite well explored object of investigation. The results from our work could be a useful addendum to the knowledge concerning the glycosylation of this tissue. In addition, this report would be helpful and informative for any research in future where the C2C12 cell cultures will take a place as an experimental model.

Acknowledgements

This work was financially supported by the Bulgarian National Science Fund under Grant DN01/16.

References

Barresi R, Campbell KP (2006) Dystroglycan: from biosynthesis to pathogenesis of human disease. J Cell Sci 119:199-207.

Bradford MM (1976) A rapid and sensitive method for the quantification of microgram quantities of protein utilizing the principle of protein-dye binding. Anal Biochem 72:248-254.

Broccolini A, Gidaro T, De Cristofaro R, Morosetti R, Gliubizzi C, Ricci E, Tonali PA, Mirabella M (2008) Hyposialylation of neprilysin possibly affects its expression and enzymatic activity in hereditary inclusion-body myopathy muscle. J Neurochem 105:971-981.

Broccolini A, Gidaro T, Morosetti R, Mirabella M (2009) Hereditary inclusion-body myopathy: clues on pathogenesis and possible therapy. Muscle Nerve 40:340-349.

Brockhausen I, Stanley P (2017) O-GalNAc Glycans. In Varki A, Cummings RD, Esko JD, Stanley P, Hart GW, Aebi M, Darvill AG, Kinoshita T, Parcker NH, Prestegard JH, Schnaar RL, Seeberger PH, Eds., Essentials of Glycobiology, 3rd ed. Cold Spring Harbor Laboratory Press, New York. 2015-2017.

Combs AC, Ervasti JM (2005) Enhanced laminin binding by alpha-dystroglycan after enzymatic deglycosylation. Biochem J 390:303-309.

Cox ML, Schary CL, Luster CW, Stewart ZS, Korytko PJ, Khan KNM, Paulauskis JD, Dunston RW (2006) Assessment of fixatives, fixation, and tissue processing on morphology and RNA integrity. Exp Mol Pathol 80:183-91.

Fic E, Kerdarcka-Krok S, Jankowska U, Pirog A, Dziedzicka-Wasylewska M (2010) Comparison of protein precipitation methods for various rat brain structures prior to proteomic analysis. Electrophoresis 31:3573-3579.

Grewal PK, Hewitt JE (2003) Glycosylation defects: a new mechanism for muscular dystrophy? Hum Mol Gen 12:259-264.

Hanisch F, Weidemann W, Großmann M, Joshi PR, Holzhausen HJ, Stoltenburg G, Weis J, Zierz S, Horstkorte R (2013) Sialylation and muscle performance: Sialic acid is a marker of muscle ageing. PLoS ONE 8(12): e80520.

Harduin-Lepers A, Mollicone R, Delannoy P, Oriol R (2005) The animal sialyltransferases and sialyltransferase-related genes: a phylogenetic approach. Glycobiology 15:805-817.

Harduin-Lepers A, Vallejo-Ruiz V, Krzewinski-Recchi MA, Samyn-Petit B, Julien S, Delannoy P (2001) The human sialyltransferase family. Biochimie 83:727-737.

Jahn O, Tenzer S, Bartsch N, Patzig J, Werner HB (2013) Myelin proteome analysis: Methods and implications for the myelin cytoskeleton. In Dermietzel R, Ed., The cytoskeleton: Imaging, isolation, and interaction. Neuromethods 79:335-354.

Janot M, Audfray A, Loriol C, Germot A, Maftah A, Dupuy F (2009) Glycogenome expression dynamics during mouse C2C12 myoblast differentiation suggests a sequential reorganization of membrane glycoconjugates. BMC Genomics BMC Genomics 10:483.

Johnson D, Montpetit ML, Stocker PJ, Bennett ES (2004) The sialic acid component of the β_1 subunit modulates voltage-gated sodium channel function. J Biol Chem 279:44303-44310.

Kaku H, Kaneko H, Minamihara N, Iwata K, Jordan ET, Rojo MA, Minami-Ishii N, Minami E, Hisajima S, Shibuya N (2007) Elderberry Bark lectins evolved to recognize Neu5Acα2,6Gal/GalNAc sequence from Gal/GalNAc binding lectin through the substitution of amino-acid residues critical for the binding to sialic acid. J Biochem 142:393-401.

Knibbs RN, Goldstein IJ, Ratclife RM, Shibuya N (1991) Characterization of the carbohydrate binding specificity of the leukoagglutinin lectin from *Maackia amurensis*.

Comparison with the other sialic acid-specific lectins. J Biol Chem 266:83-88.

Kono M, Tsuda T, Ogata S, Takashima S, Liu H, Hamamoto T, Hrkowitz SH, Nishimura S, Tsuji S (2000) Redefined substrate specificity of ST6GalNAc II: a second candidate sialyl-Tn synthase. Biochem Biophys Res Commun 272:94-97.

Laemmly UK (1970) Cleavage of structural proteins during the assembly of the head of bacteriophage T4. Nature 227:680-685.

Lee YC, Kaufmann M, Kitazume-Kawaguchi S, Kono M, Takashima S, Kurosawa N, Liu H, Pricher H, Tsuji S (1999) Molecular cloning and functional expression of two members of mouse NeuAcα2,3Galβ1,3GalNAc GalNAcα2,6-sialyltransferase family, ST6GalNAcIII and IV. J Biol Chem 274:11957-11967.

Marcos NT, Pinho S, Grandela C, Cruz A, Samyn-Petit B, Harduin-Lepers A, Almeida R, Silva F, Morais V, Costa J, Kihlberg J, Clausen H, Reis CA (2004) Role of the human ST6GalNAc-I and St6GalNAc-II in the synthesis of the cancer-associated sialyl-Tn Antigen. Can Res 64:7050-7057.

Marini M, Ambrosini S, Sarchielli E, Thyrion GD, Bonaccini L, Vannelli GB, Sgambati E (2014) Expression of sialic acids in human adult skeletal muscle tissue. Acta Histochem 116:926-935.

Martin-Rendon E, Blake DJ (2003) Protein glycosylation in disease: new insights into the congenital muscular dystrophies. Trends Pharmacol Sci 24:178-183.

McDearmon EL, Combs AC, Ervasti JM (2003) Core 1 glycans on α-dystroglycan mediate laminin-induced acetylcholine receptor clustering but not laminin binding. J Biol Chem 278:44868-44873.

Okajima T, Fukumoto S, Miyazaki H, Ishida H, Kiso M, Furukawa K, Urano T, Furukawa K (1999) Molecular cloning of a novel α-2,3-sialyltransferase (ST3GalVI) that sialylates type II lactosamine structures of glycoproteins and glycolipids. J Biol Chem 274:11479-11486.

Schauer R (2004) Sialic acids: fascinating sugars in higher animals and man. Zoology 107:49-64.

Schauer R (2009) Sialic acids as regulators of molecular and cellular interactions. Curr Opin Struct Biol 19:507-514.

Schneider CA, Rasband WS, Eliceiri KW (2012) NIH Image to ImageJ: 25 years of image analysis. Nat Methods 9:671-675.

Schwetz TA, Norring NA, Ednie AR, Bennett ES (2011) Sialic acids attached to O-glycans modulate voltage-gated potassium channel gating. J Biol Chem 286:4123-4132.

Stanley P, Taniguchi N, Aebi M (2017) N-glycans. In Varki A, Cummings RD, Esko JD, Stanley P, Hart GW, Aebi M, Darvill AG, Kinoshita T, Parcker NH, Prestegard JH, Schnaar RL, Seeberger PH, Eds., Essentials of Glycobiology, 3rd ed. Cold Spring Harbor Laboratory Press, New York. 2015-2017.

Tajima Y, Uyama E, Go S, Sato C, Tao N, Kotani M, Hino H, Suzuki A, Sanai Y, Kitajima K, Sakuraba H (2005) Distal myopathy with rimmed vacuoles: Impaired O-glycan formation in muscular glycoproteins. Am J Pathol 166:1121-1130.

Takashima S (2008) Characterization of mouse sialyltransferase genes: their evolution and diversity. Biosci Biotechnol Biochem 72:1155-1167.

Takashima S, Tsuji S, Tsujimoto M (2003) Comparison of the enzymatic properties of mouse β-galactoside α-2,6-sialyltransferases, ST6GalI and II. J Biochem 134:287-296.

Towbin H, Staehelin T, Gordon T (1979) Electrophoretic transfer of proteins from polyacrylamide gels to nitrocellulose sheets: procedure and some applications. PNAS 79:4350-4354.

Varki A (1992) Diversity in the sialic acids. Glycobiology 2:25-40.

Varki A (2007) Glycan-based interactions involving vertebrate sialic-acid-recognizing proteins. Nature 446:1023-1029.

Velleman SG (2002) Role of the extracellular matrix in muscle growth and development. J Anim Sci 80:E8-E13.

Ye J, Coulouris G, Zaretskaya I, Cutcutache I, Rozen S, Madden T (2012) Primer-BLAST: A tool to design target-specific primers for polymerase chain reaction. BMC Bioinform 13:134.

Zhang JD, Ruschhaupt M, Biczok R (2014) ddCt method for qRT-PCR data analysis. Available: http://bioconductor.jp/packages/2.14/bioc/vignettes/ddCt/inst/doc/rtPCR.pdf. Accessed 15 May 2021.

Acta Biologica Szegediensis

Volume 65(2):263-270, 2021
Acta Biologica Szegediensis
http://abs.bibl.u-szeged.hu/index.php/abs

DOI:10.14232/abs.2021.2.263-270

ARTICLE

Ammonia ambiance induces SIRT5 regulated expression of EGF-AKT-mTOR axis in Asian stinging catfish *Heteropneustes fossilis* (Bloch) 1974

Sabarna Chowdhury and Surjya K Saikia*

Aquatic Ecology and Fish Biology Laboratory, Department of Zoology, Centre for Advanced Studies, Visva-Bharati (A Central University), Santiniketan, West Bengal, India

ABSTRACT The present study was aimed to understand whether ammonia exposure induces oxidative stress in *Heteropneustes fossilis* and what is the fate of the excess ammonia in the skeletal muscle of the fish. The experiments were performed in two different sets as control and treated (repeated three times with fresh specimens) of aquaria with 25 mM of ammonium chloride treatment and the tissues were collected in different time intervals (24 h, 72 h and 7 days). The collected tissues were studied to understand the change of SIRT5 levels in liver and skeletal muscle tissues. The results that were obtained from investigation of MDA (malondialdehyde) and superoxide dismutase (SOD) revealed that the fish undergoes extensive oxidative stress when exposed to ammonia ambiance. Further, after 7 days of ammonia exposure increase in the levels of glutamate and glutamine revealed the fate of excess ammonia in the skeletal muscle of the fish. Moreover, the levels of cell proliferator proteins like EGF, AKT and mTOR were also analysed and found an increase in their expression with a time dependent manner. It indicates that the excess ammonia could be utilised in synthesising protein and triggering cell growth and proliferation even under such harsh condition of ambient ammonia.
Acta Biol Szeged 65(2):263-270 (2021)

KEY WORDS
glutamate
glutamine
malondialdehyde
oxidative stress
SIRT5

ARTICLE INFORMATION
Submitted
11 December 2021
Accepted
30 December 2021
***Corresponding author**
E-mail: surjyasurjya@gmail.com

Introduction

An increase in ammonia (concentration) can generate reactive oxygen and nitrogen species in tissues. It is an already established fact that ammonia accumulation in the brain due to dysfunction in the liver can contribute to the pathogenesis of liver encephalopathy (Bobermin et al. 2015; Skowronska and Albrecht 2013). Ammonia, which is mainly produced from the deamination of amino acids is a toxic component in blood and tissues. It can significantly reduce cell viability and induce apoptosis in the cells (Wang et al. 2018). Ammonia is produced during protein catabolism and is an essential component for nucleic acid and protein biosynthesis. Inadequate ammonia detoxification can have adverse effects on muscle size and strength in mammals. On the other hand, ammonia can be utilized for muscle growth in avian species (Stern and Mozdziak 2019).

Among the teleosts, catfishes can tolerate stress to a great extent like thermal stress, salinity stress, heat stress, bacterial exposure, environmental and abiotic stressors like hypoxia (Burleson and Silva 2011; Meritha et al. 2018; Nepal and Fabrizio 2019; Saha et al. 2011; Sarma et al. 2012; Tan et al. 2019; Zhou et al. 2018). The walking catfish (*Clarias batrachus*) can survive in very high ambient ammonia concentration (25 mM) during certain seasons of the year in the natural habitat (Banerjee et al. 2019). They are predominantly ammoniotelic but can totally turn into ureotelism when exposed to higher ambient ammonia. This can be significantly evident from the increase of some of the key urea cycle enzymes from hepatic and non-hepatic tissues (Banerjee et al. 2020). That is why it is considered as a potential ureogenic teleost because of its significantly functional ornithine urea cycle (Saha et al. 2003; Saha and Das 1999). There are various other fish species that can tolerate ammonia stress. Detoxification of ammonia to urea has also been observed in elasmobranchs (Randall and Tsui 2002).

It is evident that a rise in the expression of inducible nitric oxide takes place in catfishes when exposed to ambient ammonia which is considered to be a potential strategy to enhance the adaptive capacity and survivability of catfish under various adverse environmental conditions in nature (Ajani 2008; Kumari et al. 2018; Zhang et al. 2018). Fish like *Clarias magur* and *Clarias batrachus* show a

differential expression of multiple glutamine synthetase genes and carbamoyl phosphate synthetase III gene during excess ambient ammonia condition (Banerjee et al. 2018). Studies have reported that ammonia toxicity can induce glutamine accumulation in catfishes (Li et al. 2016; Saha et al. 2007). Catfishes like *H. fossilis* and *C. batrachus* have immense capacity and physiological adaptive strategies related to amino acid metabolism along with the presence of functional and regulatory urea cycle when exposed to very high ambient ammonia in the air, water or in the mud in their habitat (Saha and Ratha 1998; Saha et al. 2000; Saha et al. 2002).

However, a strong metabolic support is necessary for acquiring necessary energy pool to appropriately response such behaviours of catfish. The metabolic backup is further required to augment growth in catfish under stressed ammonia ambiance. In this context, deficiency of SIRT5 is reported to suppress mitochondrial NADH oxidation as well as inhibition of ATP synthase activity resulting in reduced formation of ATP and subsequently activates AMPK in cultured cells and mouse hearts (Zhang et al. 2019). Understanding SIRT 5 is important because it has a strong control over mitochondrial energy metabolism and its level regulated by PGC1 α and AMPK (Buler et al. 2014). This information are hardly available in fish, although energy supplement is shown as vital criteria in fish group. Understanding these kinds of adaptations to withstand adverse situation by catfish may further enlighten possibility of other similar strategy of fish growth in aquaculture practice.

With this background, we attempted to detect the oxidative stress in ambient ammonia in *Heteropneustes fossilis,* accordingly, and change in expression of mammalian SIRT5. To understand the growth under ammonia ambiance, expression of growth factors like epidermal growth factor (EGF) in skeletal muscle tissue and few of its downstream proteins AKT (Protein kinase B) and mTOR (Mechanistic target of rapamycin) of a specific pathway in *H. fossilis* exposed to ammonia ambiance were also analyzed. The amino acids like glutamate and glutamine are also measured in skeletal muscle tissue in ammonia exposed *H. fossilis*.

Materials and Methods

Animals

Live samples of *H. fossilis* (50 ± 10 g body mass) were purchased from commercial sources and acclimatized in the laboratory approximately for 15 days at 28 ± 2 °C with 12 h:12h light dark photoperiod before experiments. Minced pork liver and rice bran (5% of body wt) were given as food, and the water was changed on alternate days. Food was withdrawn 24 h prior to the experiment.

Experimental protocol

A set of fish (n = 15) of similar sizes (Length = 25 ± 5 cm, Weight = 50 ± 10 g) was weighed and placed in aquarium containing 1 L of 25 mM NH_4CL solution prepared in fresh water (pH 6.82 ± 0.11). Another set of fish (n = 15) were kept in aquarium containing 1 L of fresh water (pH 7.04 ± 0.10) that served as controls. Both NH_4CL solution and the fresh water from each aquarium (treated and control) were replaced with a fresh medium every day at a fixed time. On first, third and seventh day, 5-5 fish (n = 5) from each treatment were removed and sacrificed. No mortality of fish was observed during the period of experiment. Before tissue collection, fishes were narcotized using MS222. The overall experiment was repeated three times. Liver and skeletal muscle tissues were dissected out from all the treated as well as control fish and tissue samples were stored at -20 °C. All the assays were completed within 2 weeks of collecting the tissue.

Tissue collection and processing

Tissues (skeletal muscle, and liver) were collected from *H. fossilis* and processed for further analysis. The skeletal muscle tissues were collected from head region (HM), trunk region (TRM) and tail region (TLM) for estimating the total protein in these regions separately. Before every analysis, the pooled tissues (100 mg) kept in lysis buffer (0.1M phosphate buffer, pH 7.2) were homogenized (10% homogenate) using micro tissue homogenizer. The tissues homogenized were then centrifuged in 10000 g for 15 min. The supernatant of the 10% homogenate was collected and used for all biochemical assessments (MDA, SOD, glutamate and glutamine). For western blot analysis, tissue proteins of 100 μg from the lysate were used.

Biochemical assays

The biochemical assessment was performed for estimating total skeletal muscle protein, MDA (malondialdehyde), antioxidant enzyme SOD (superoxide dismutase), glutamate and glutamine. The total skeletal muscle protein was estimated using Lowry's (1951) method of protein estimation. MDA assay was performed according to the method of Aust (1985). MDA is a product of lipid peroxidation and reacts with TBA (thiobarbituric acid) to give a red species named TBARS (thiobarbituric acid reactive substance). The antioxidant enzyme SOD assay was performed following the method of Ewing and Janero (1995) while glutamate assay together with glutamine quantification were performed using assay kit (CCK037-100).

Electrophoresis and immunoblotting

The desired quantity of tissue protein (100 μg) was used in

Table 1. Antibodies used for immunoblotting of tissues from *H. fossilis*.

Primary antibody	Company	Art No.	Secondary antisera for immunoblotting	Company	Art No.
SIRT5	Elabscience	E-AB-15844	Anti-rabbit antibody	Sigma Aldrich	A3687
EGF	Abclonal	A2720			
AKT	Abclonal	A5523			
mTOR	Abclonal	A2445			
α-tubulin	Affinity Biosciences	AF7010			

10% SDS-PAGE and was transferred to PVDF membranes through transfer buffer (25 mM Tris, 193 mM glycine, 20% methanol, pH 8.5) for 1.5 h. Western blot analysis was performed for the proteins like SIRT5, EGF, AKT, mTOR using specific antibodies (Table 1). Membrane bound primary antibodies were visualized using corresponding secondary antibodies at 1:1000 dilutions, which was tagged with alkaline phosphatase and developed with corresponding substrates, 5-bromo-3-chloro-3-indolyl phosphate/ nitrobluetetrazolium (BCIP/NBT). Band intensities were quantified by utilizing Image J software (NIH, Bethesda, MD).

Statistical analysis

Homogeneity of variances of data sets was tested using Levene's statistics. The Kruskal-Wallis H test was computed where Levene's statistics did not comply to $p > 0.05$.

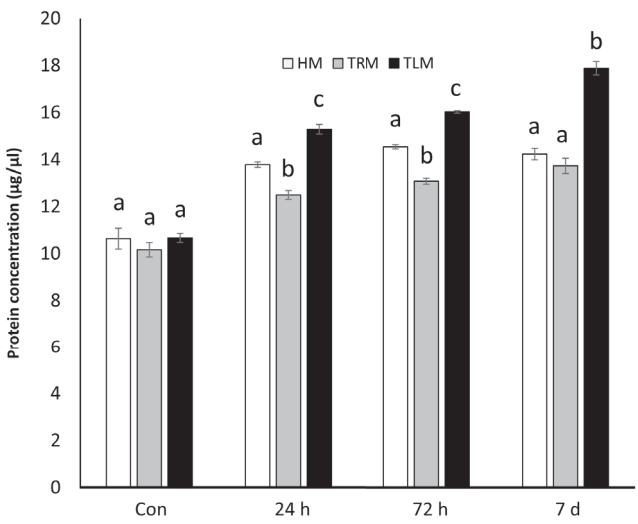

Figure 1. Determination of total protein concentration (µg/µl) in skeletal muscle of *H. fossilis* under three different time intervals of 25 mM ammonia exposed conditions compared with control: Control, 24 h, 72 h and 7 days. Data are shown as Mean ± SE. Comparison of mean are performed following Kruskal-Wallis non-parametric test. Bars with different lower-case letters (a, b, c) show statistically significant difference at $p < 0.05$. HM: Head Region Muscle; TRM: Trunk Region Muscle; TLM: Tail Region Muscle.

In case of all statistical analyses, α level was fixed at 0.05. SPSS 16.0 was used for all statistical analyses.

Results

The present study observed some effects in *H. fossilis* on exposure to ammonia (25 mM/L) for three different time intervals. On exposure for 7 days to ammonia, the total muscle protein level in the skeletal muscle showed an increase in concentration of protein. When analysed in head, trunk, and tail regions, from the skeletal muscles of *H. fossilis,* the treatments showed overall significant increase of protein concentration compared to the control (Kruskal-Wallis H Test, $\chi 2 = 113.96$, $p = 0.00$; Fig. 1). However, skeletal muscle from tail region, showed comparatively high level of protein concentration than the skeletal muscle of head and trunk regions. It was also observed that the fish was under oxidative stress during ammonia exposure, indicated, in terms of increase in MDA and antioxidant enzyme SOD in liver and skeletal muscle tissue (Fig. 2). In liver tissue, the MDA level was maximum and significantly increased at 24 h of ammonia exposure as compared to the control (One-way ANOVA, $F = 131.093$; 3, 36; $p < 0.05$; Fig. 2). Another significant increase of MDA was observed after 7 days of ammonia exposure giving a minor hint of chronic oxidative stress in the fish. The antioxidant enzyme SOD was found to increase prominently after 7 days of ammonia exposure in liver tissue (Kruskal-Wallis H Test, $\chi 2 = 36.585$, $p = 0.00$; Fig. 2). In skeletal muscle, significant increase of MDA was observed after 72 h of ammonia exposure as compared to the control which confirms that the fish was under oxidative stress, until it falls sharply after 7 days of ammonia exposure (One-way ANOVA, $F = 114.503$; 3, 36; $p < 0.05$; Fig. 2). In liver the results of antioxidant enzyme SOD showed a similar pattern in skeletal muscle signifying a constant stress at 7 days of ammonia exposure (Kruskal-Wallis H Test, $\chi 2 = 36.585$, $p = 0.00$; Fig 2). A more or less similar pattern of expression of SOD was also observed in skeletal muscle of the fish (Fig. 2).

In both liver and skeletal muscle tissues, increase in expression of SIRT 5 after 24 h of ammonia exposure

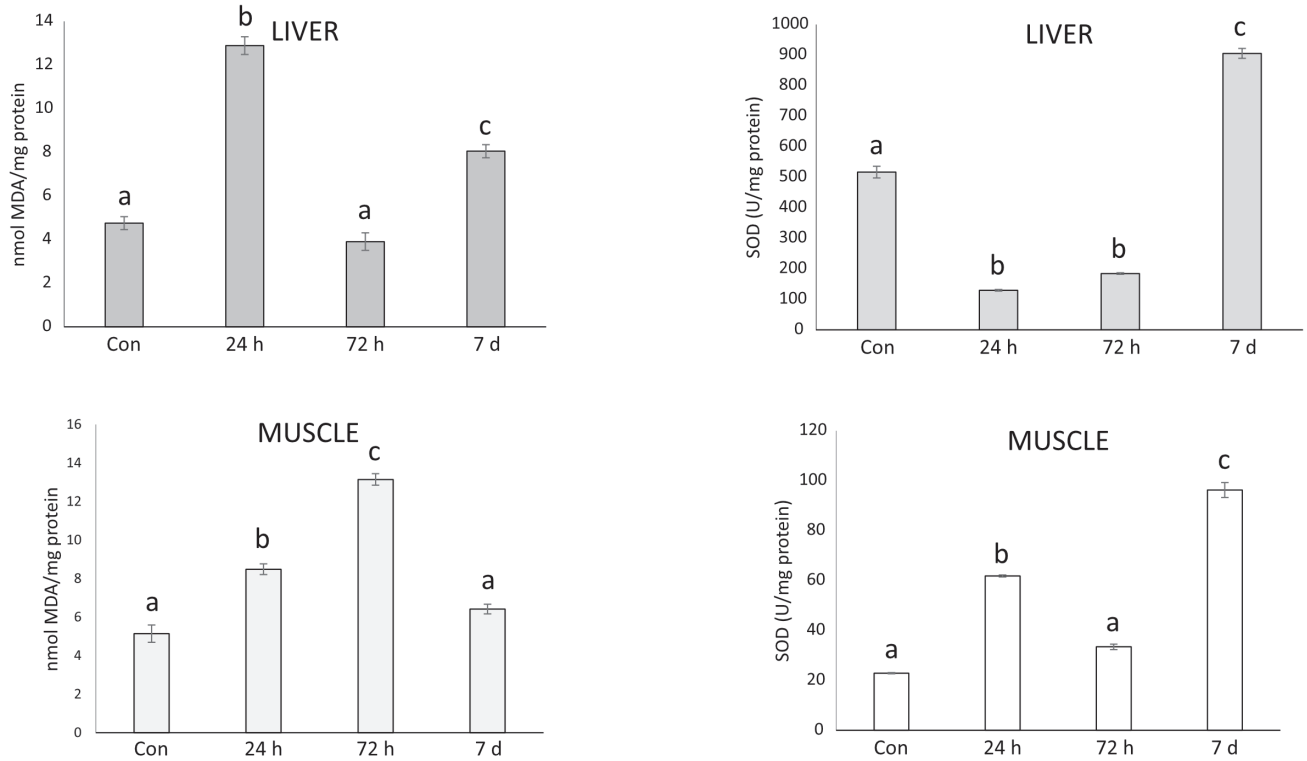

Figure 2. Determination of SOD (U/mg protein) and MDA (nmol/mg protein) in liver and skeletal muscle of *H. fossilis* under three different time intervals of 25 mM ammonia exposed conditions compared with control: Control, 24 h, 72 h and 7 days. Data are shown as Mean ± SE. Comparison of mean are performed following Kruskal-Wallis non-parametric test for SOD and Comparison of mean are performed following One-way ANOVA parametric test for MDA. Bars with different lower-case letters (a, b, c) show statistically significant difference at $p < 0.05$.

was prominent. Similar to MDA, the expression of SIRT 5 was peaked again after 7 days of ammonia exposure (One-way ANOVA, $F = 36.191$; 3, 20; $p < 0.05$ for SIRT5 in liver tissue; One-way ANOVA, $F= 195.803$; 3, 20; $p < 0.05$ for SIRT5 in skeletal muscle tissue; Fig. 3). On the other hand, proteins which are involved in the pathway of cell proliferation and growth (EGF, AKT, mTOR) were examined after exposure to ammonia at 24 h, 72 h and 7 days and found to exhibit time dependent significant upregulation in their expression (Kruskal-Wallis H Test, $\chi2 = 19.547$, $p = 0.00$ for EGF in skeletal muscle; One-way ANOVA, $F = 28.035$; 3, 20; $p < 0.05$ for AKT in skeletal muscle tissue and One-way ANOVA, $F = 76.588$; 3, 20; $p < 0.05$ for mTOR in skeletal muscle tissue; Fig. 4). Simultaneously, the levels of glutamate and glutamine also showed gradual increase from 24 h to 7 days of ammonia exposure (Kruskal-Wallis H Test, $\chi2 = 9.974$, $p = 0.019$ for glutamate in skeletal muscle tissue; Kruskal-Wallis H Test, $\chi2 = 10.385$, $p = 0.016$ for glutamine in skeletal muscle tissue; Fig. 5).

Discussion

It is obvious from the results that *H. fossilis* experiences oxidative stress when exposed to 25 mM of ambient ammonia. Oxidative indicators like MDA and SOD showed clear indication, both in skeletal muscle and liver that on 7th day of ammonia exposure, the fish underwent oxidative stress. Both MDA and SOD are already considered as efficient stress marker for animals. However, the results also depict that under ammonia exposure the total protein of the skeletal muscle increase significantly, which markedly visible from the tail region. How the augmentation of such increase in total protein under ammonia ambiance in catfish happens needs a clarification.

It led us to investigate the expression of a mammalian protein called SIRT5, one of the seven members of the nicotinamide adenine dinucleotide (NAD^+)-dependent sirtuin family of lysine deacetylases in mammals. SIRT5 is localized in the mitochondrial matrix and removes succinyl, malonyl, and glutaryl groups from protein targets in the mitochondrial matrix and other subcellular compartments (Bringman-Rodenbarger et al. 2018; Nakagawa et al. 2009). SIRT5 interacts with carbamoyl phosphate syn-

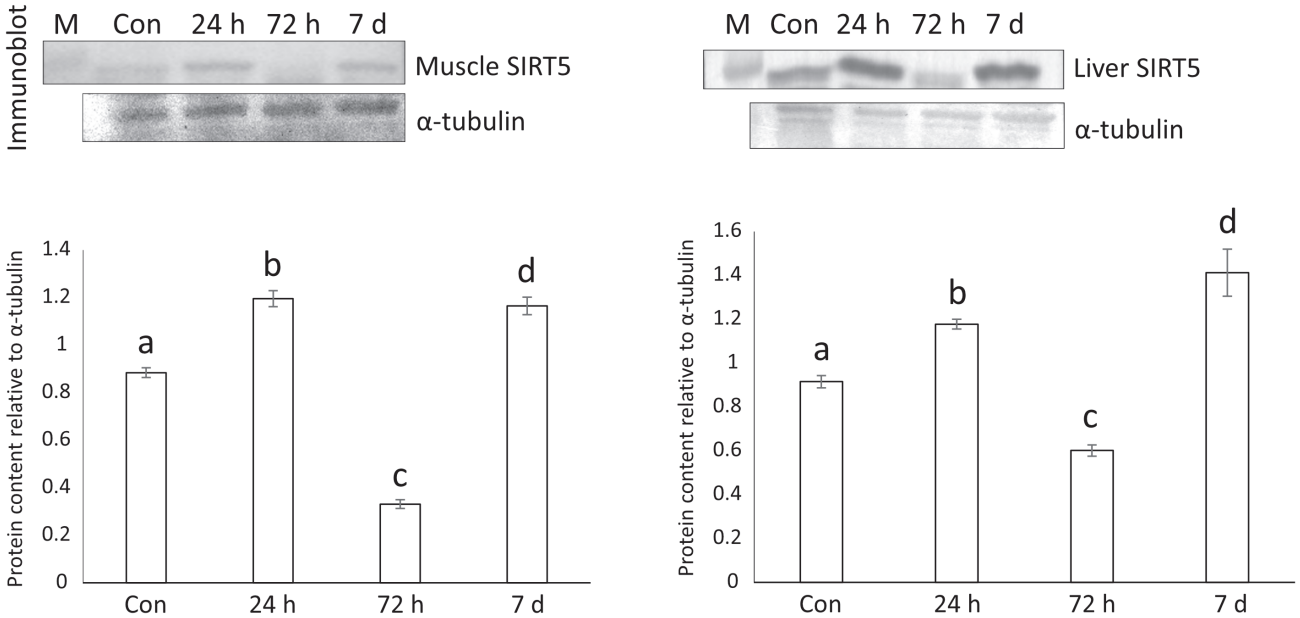

Figure 3. Immunoblot of SIRT5 in liver and skeletal muscle of *H. fossilis* under three different time intervals of 25 mM ammonia exposed conditions compared with control and its densitometry analysis: control, 24 h, 72 h and 7 days. Data are shown as Mean ± SE. Comparison of mean are performed following One-way ANOVA parametric test. Bars with different lower-case letters (a, b, c, d) show statistically significant difference at $p < 0.05$. M: molecular weight marker; Con: Control.

thetase 1 (CPS1), an enzyme that catalyzes the initial step of the urea cycle for ammonia detoxification and disposal (Saha and Ratha 1998). SIRT5 mainly deacetylates CPS1 (carbamoyl phosphate synthetase I) and upregulates its activity and plays a major role in ammonia detoxification and disposal by activating CPS1 (Nakagawa et al. 2009). There are studies which has reported the fact that catfishes under ammonia ambience upregulates SIRT5 and triggers the urea cycle for ammonia detoxification (Li et al. 2016). Increase of SIRT5 also is reported to be linked to ROS detoxification (Kumar and Lombard 2018). In the present study, it was found that SIRT5 expression was significantly upregulated in the liver and skeletal muscle of fish exposed to ammonia ambiance. The expression of SIRT5 was hiked twice with an intermittent gap at 72 h. The gap, at 72 h between these two hikes. i.e., at 24 h and 7 days of SIRT5 upregulation is significant, as the MDA during this period also remained high in both skeletal muscle and liver tissues. In a study, Liu et al. (2013) has showed that SIRT5 regulates oxidative stress induced apoptosis in cardiomyocytes. A similar function of SIRT5 may also be advocated here. As already mentioned in the introduction, the SIRT5 is mainly involved in activating the detoxification process through CPS1. It was necessary to examine the fate of glutamate and glutamine, being the substrate of the enzyme CPS1 through which it initiates detoxification cycle. It is possible that, as soon as the exposure of fish to ammonia toxicity, the SIRT5 gets upregulated in defence of the skeletal muscle cells, resulting in an increase in almost all the measured parameters. However, a chronic exposure may always induce a secondary defensive mechanism, which is visible from the occurrence of second spike of SIRT5. For first instance, safeguarding against the oxidative stress would be the best appropriate and possible explanation in the skeletal muscle cell. Consequently, the second instance may direct towards an alternative pathway of detoxification through protein metabolism.

This led us to measure the levels of glutamate and glutamine in the skeletal muscle of the fish. Both glutamate and glutamine are known to play important roles in metabolism. From the result, it is clear that, both glutamate and glutamine levels were increased from the first day with a significantly high level on 7th day in fish exposure to ammonia. It indicates that, these two by-products, advocates an alternative defence mechanism might be contributing to protein metabolism. Thus, under chronic ammonia exposure, the levels of glutamate and glutamine increased indicating that the excess ammonia not directed towards detoxification might be routed towards synthesis of glutamate and glutamine. This helps to maintain proteostasis under stress condition. If this is the case, there is possibility, that major growth proteins would be upregulated during this period.

Of the numerous protein synthesis and cell proliferation pathways, a significant pathway is the EGF-AKT-

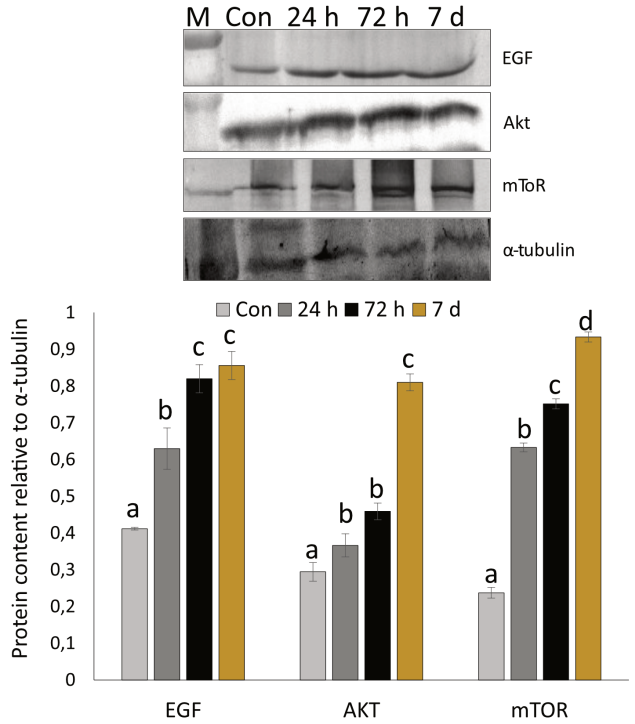

Figure 4. Immunoblot of EGF, AKT and mTOR in skeletal muscle of *H. fossilis* under three different time intervals of 25 mM ammonia exposed conditions compared with control and its densitometry analyses: control, 24 h, 72 h and 7 days. Data are shown as Mean ± SE. Comparison of mean are performed following Kruskal-Wallis non-parametric test for EGF. Comparison of mean are performed following One-way ANOVA parametric test for AKT and mTOR. Bars with different lower-case letters (a, b, c, d) show statistically significant difference at $p < 0.05$. M: molecular weight marker; Con: control.

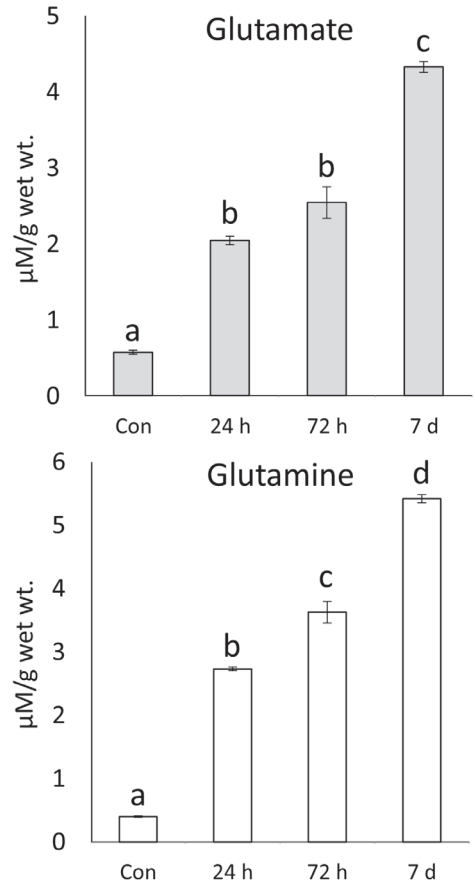

Figure 5. Determination of glutamate and glutamine (μM/g wet weight) in skeletal muscle of *H. fossilis* under three different time intervals of 25 mM ammonia exposed conditions compared with control: control, 24 h, 72 h and 7 days. Data are shown as Mean ± SE. Comparison of mean are performed following Kruskal-Wallis non-parametric test. Bars with different lower-case letters (a, b, c, d) show statistically significant difference at $p < 0.05$. Con: control.

mTOR pathway. In mammals, this pathway has been shown to play crucial role in cell differentiation, muscle development, environmental adaptation, cell growth, proliferation, apoptosis and promotes insulin-stimulated glucose uptake and storage which establishes a link between growth and development with metabolism (Xu et al. 2020). This study of the pathway also elucidates the pathogenesis of cerebrovascular diseases, neurodegenerative diseases, diabetes mellitus and other malignant tumours. It is a vital signalling pathway for growth that provides new molecular targets for diagnosis and treatments of various human diseases like ovarian cancer, haematologic malignancy, colorectal cancer, endometrial cancer, and lung tumorigenesis (Dobbin and Landen 2013; Kawauchi et al. 2009; Memmott and Dennis 2009; Slomovitz and Coleman 2012; Xu et al. 2020). In our study, it was observed that proteins in this pathway were upregulated on 7th day compared to control, reflecting a recovery of skeletal muscle growth compensating the loss during the exposure at 72 h. We could say that there is a time dependent increase in expression of these proteins. Thus, through the contributors like glutamate and glutamine, protein syntheses might get accelerated in *H. fossilis* under ammonia ambiance. Glutamine can even directly upregulate mTOR for cell growth and proliferation (Csibi et al. 2013; Zhu et al. 2020). So, from these outcomes, a relation of the increased levels of glutamate and glutamine under ammonia ambience indirectly initiated by SIRT5 may be established. With the increase in the levels of these amino acids, help us to explain the possible mechanism of growth and survival of stinging catfish in ammonia rich environment.

Conclusion

From the results it may be said that under chronic exposure to ammonia for 7 days the fish experiences oxidative stress, but the excess ammonia in the body of the fish is not directed towards detoxification, rather is used in synthesis of glutamate and glutamine which indirectly regulated by expression of SIRT5 and in turn, promotes protein synthesis and thereby cell growth and proliferation. From this, it may be said that even under chronic exposure to ammonia for 7 days, the catfish, *H. fossilis* has the potential to bypass the excess ammonia from the detoxification pathway by utilizing it in inducing protein synthesis and upregulating the pathway of cell growth and proliferation.

Acknowledgements

Authors acknowledge National Agriculture Science Fund (NASF) [Project Ref. NASF/ABA/7011/2018-19/241], The Indian Council of Agricultural Research (ICAR) for financial assistance and DIST FIST- II and CAS-II of Department of Zoology, Visva-Bharati for instrumental assistance. Authors are also thankful to DST-PURSE of Siksha Bhavana, Visva-Bharati for technical assistance.

References

Ajani F (2008) Hormonal and haematological responses of *Clarias geriepinus* (Burchell 1822) to ammonia toxicity. Afr J Biotechnol 7:3466-3471.

Aust SD (1985) Lipid peroxidation. In Greenwald RA, Ed., Handbook Methods for Oxygen Radical Research. CRC Press Revivals, Florida, 203-210.

Banerjee B, Koner D, Bhuyan G, Saha N (2018) Differential expression of multiple glutamine synthetase genes in air-breathing magur catfish, *Clarias magur*and their induction under hyper-ammonia stress. Gene 671:85-95.

Banerjee B, Koner D, Hasan R, Bhattacharya S, Saha N (2019) Transcriptome analysis reveals novel insights in air-breathing magur catfish (*Clarias magur*) in response to high environmental ammonia. Gene 703:35-49.

Banerjee B, Koner D, Hasan R, Saha N (2020) Molecular characterization and ornithine-urea cycle genes expression in air-breathing magur catfish (*Clarias magur*) during exposure to high external ammonia. Genomics 112:2247-2261.

Bobermin LD, Wartchow KM, Flores MP, Liete MC, Quincozes-Santos A, Goncalves G (2015) Ammonia-induced oxidative damage in neurons is prevented by resveratrol and lipoic acid with participation of heme oxygenase 1. Neurotoxicology 49:28-35.

Bringman-Rodenbarger LR, Guo AH, Lyssiotis CA, Lombard DB (2018) Emerging roles for SIRT5 in metabolism and cancer. Antioxid Redox Signal 28:677-690.

Buler M, Aatsinki SM, Izzi V, Uusimaa J, Hakkola J (2014) SIRT5 is under the control of PGC-1α and AMPK and is involved in regulation of mitochondrial energy metabolism. FASEB 28:3225-3237.

Burleson ML, Silva PE (2011) Cross tolerance to environmental stressors: Effects of hypoxic acclimation on cardiovascular responses of Channel Catfish (*Ictalurus punctatus*) to a thermal challenge. J Therm Biol 36:250-254.

Csibi A, Fendt SM, Li C, Poulogiannis G, ChooAY, Chapski DJ, Jeong SM et al (2013) The mTORC1 pathway stimulates glutamate metabolism and cell proliferation by repressing SIRT4. Cell 153:840-854.

Dobbin ZC, Landen CN (2013) The importance of the PI3K/AKT/mTOR pathway in the progression of ovarian cancer. Int J Mol Sci 14:8213-8227.

Ewing JF, Janero DR (1995) Microplate superoxide dismutase assay employing a nonenzymatic superoxide generator. Anal Biochem 232:243-248.

Kawauchi K, Ogasawara T, Yasuyama M, Otsuka K, Yamada O (2009) Regulation and importance of the PI3K/Akt/mTOR signaling pathway in hematologic malignancies. Anticancer Agents Med Chem 9:1024-1038.

Kumar S, Lombard DB (2018) Functions of the sirtuin deacylase SIRT5 in normal physiology and pathobiology. Crit Rev Biochem Mol Biol 53:311-334.

Kumari S, Choudhury MG, Saha N (2018) Hyper-ammonia stress causes induction of inducible nitric oxide synthase gene and more production of nitric oxide in air-breathing catfish, *Clarias magur* (Hamilton). Fish Physiol Biochem 45:907-920.

Li M, Gong S, Li Q, Yuan L, Meng F, Wang R (2016) Ammonia toxicity induces glutamine accumulation, oxidative stress and immunosuppression in juvenile yellow catfish *Pelteobagrus fulvidraco*. Comp biochem Physiol Part C 183:1-6.

Liu B, Che W, Zheng C, Liu W, Wen J, Fu H, Tang K, Zhang J, Xu Y (2013) SIRT5: a safeguard against oxidative stress-induced apoptosis in cardiomyocytes. Cell Physiol Biochem 32:1050-1059.

Lowry OH, Rosebrough NJ, Farr AL, Randall RJ (1951). Protein measurement with the Folin phenol reagent. J Biol Chem 193:265-275.

Memmott RM, Dennis PA (2009) The role of the Akt/mTOR pathway in tobacco carcinogen-induced lung tumorigenesis. Clin Cancer Res 16:4-10.

Meritha WW, Suprayudi MA, Ekasari J (2018) The growth performance and resistance to salinity stress of striped catfish *Pangasius* sp. juvenile in biofloc system with different feeding rates. JAI 17:113-119.

Nakagawa T, Lomb DJ, Haigis MC, Guarente L (2009) SIRT5 deacetylates carbamoyl phosphate synthetase 1 and regulates the urea cycle. Cell 137:560-570.

Nepal V, Fabrizio MC (2019) High salinity tolerance of invasive blue catfish suggests potential for further range expansion in the Chesapeake Bay region. Plos One 14:1-20.

Randall DJ, Tsui TKN (2002) Ammonia toxicity in fish. Mar Pollut Bull 45:17-23.

Saha N, Das L (1999) Stimulation of ureogenesis in the perfused liver of an Indian air-breathing catfish, *Clarias batrachus*, infused with different concentrations of ammonium chloride. Fish Physiol Biochem 21:303-311.

Saha N, Datta S, Bhattacharjee A (2002) Role of amino acid metabolism in an air-breathing catfish, *Clarias batrachus* in response to exposure to a high concentration of exogenous ammonia. Comp Biochem Physiol Part B 133:235-250.

Saha N, Datta S, Biswas K, Kharbuli ZY (2003) Role of ureogenesis in tackling problems of ammonia toxicity during exposure to higher ambient ammonia in the air-breathing walking catfish *Clarias batrachus*. J Biosci 28:733-742.

Saha N, Datta S, Haussinger D (2000) Changes in free amino acid synthesis in the perfused liver of an air-breathing walking catfish, *Clarias batrachus* infused with ammonium chloride: A strategy to adapt under hyperammonia stress. J Exp Zool 286:13-23.

Saha N, Datta S, Kharbuli ZY, Biswas K, Bhattacharjee A (2007) Air-breathing catfish, *Clarias batrachus* upregulates glutamine synthetase and carbamyl phosphate synthetase III during exposure to high external ammonia. Comp Biochem Physiol Part B 147:520-530.

Saha N, Jyrwa LM, Das M, Biswas K (2011) Influence of increased environmental water salinity on gluconeogenesis in the air-breathing walking catfish, *Clarias batrachus*. Fish Physiol Biochem 37:681-692.

Saha N, Ratha BK (1998) Ureogenesis in Indian air-breathing teleosts: adaptation to environmental constraints. Comp Biochem Physiol Part A 120:195-208.

Sarma K, Prabakaran K, Krishnan P, Grinson G, Kumar AA (2012) Response of a freshwater air-breathing fish, *Clarias batrachus* to salinity stress: an experimental case for their farming in brakishwater areas in Andaman, India. Aquacult Int 21:183-196.

Skowronska M, Albrecht J (2013) Oxidative and nitrosative stress in ammonia neurotoxicity. Neurochem Int 62:1-7.

Slomovitz BM, Coleman RL (2012) The PI3K/ AKT/mTOR pathway as a therapeutic target in endometrial cancer. Clin Cancer Res 18:5856-5864.

Stern RA, Mozdziak PE (2019) Differential ammonia metabolism and toxicity between avian and mammalian species, and effect of ammonia on skeletal muscle: A comparative review. J Anim Physiol Anim Nutr 103:774-785.

Tan S, Wang W, Tian C, Niu D, Zhou T, Jin Y, Yang Y, Gao D, Dunham R, Liu Z (2019) Heat stress induced alternative splicing in catfish as determined by transcriptome analysis. Comp Biochem Physiol Part D Genom Proteom 29:166-172.

Wang F, Chen S, Jiang Y, Zhao Y, Sun L, Zheng B, Chen L, Liu Z, Zheng X, Yi K, Li C, Zhou X (2018) Effects of ammonia on apoptosis and oxidative stress in bovine mammary epithelial cells. Mutagenesis 33:291-299.

Xu F, Na L, Li Y, Chen L (2020) Roles of the PI3K/AKT/mTOR signalling pathways in neurodegenerative diseases and tumours. Cell Biosci 10:1-12.

Zhang M, Li M, Wang R, Qian Y (2018) Effects of acute ammonia toxicity on oxidative stress, immune response and apoptosis of juvenile yellow catfish *Pelteobagrus fulvidraco* and the mitigation of exogenous taurine. Fish Shellfish Immunol 79:313-320.

Zhang M, Wu J, Sun R, Tao X, Wang X, Kang Q, Wang H, Zhang L, Liu P, Zhang J, Xia Y, Zhao Y, Yang Y, Xiong Y, Guan K-L, Zou Y, Ye D (2019) SIRT5 deficiency suppresses mitochondrial ATP production and promotes AMPK activation in response to energy stress. Plos One 14:1-25.

Zhou T, Yuan Z, Tan S, Jin Y, Yang Y, Shi H, Wang W, Niu D, Gao L, Jiang W, Gao D, Liu Z (2018) A review of molecular responses of catfish to bacterial diseases and abiotic stresses. Front Physiol 9:1-16.

Zhu M, Qin YC, Gao CQ, Yan HC, Wang XQ (2020) L-Glutamate drives porcine intestinal epithelial renewal by increasing stem cell activity via upregulation of the EGFR-ERK-mTORC1 pathway. Food Funct 11:2714-2724.

Acta Biologica Szegediensis

Volume 65(2):271-283, 2021
Acta Biologica Szegediensis
http://abs.bibl.u-szeged.hu/index.php/abs

DOI:10.14232/abs.2021.2.271-283

ARTICLE

Inflammatory and bone biomarkers/composites as a predictive tool for clinical characteristics of rheumatoid arthritis patients

Hameed Hussein Ali[1], Muna Mohammed Yaseen[2], Khalid F. AL-Rawi[1], Shakir F. T. Alaaraji[3], Hussein Kadhem Al-Hakeim[4]*

[1]Department of Chemistry, College of Science, University of Anbar, Iraq
[2]Department of Basic Science, College of Dentistry, University of Anbar, Iraq
[3]Department of Chemistry, College of Education for Pure Science, University of Anbar, Iraq
[4]Department of Chemistry, College of Science, University of Kufa, Iraq

ABSTRACT Rheumatoid arthritis (RA) is related to alterations in different inflammatory and connective tissue biomarkers. The diagnostic values and the factors affecting these biomarkers are conflicting. In the present study, a bone-related composite (B-composite), made from the z-score of stromelysin-1 (MMP3), colony-stimulating factor *2* (CSF2), and osteopontin (OPN), and I-composite, reflecting immune activation, made from the z-score of tumor necrosis factor-*α* (TNFα), interferon-γ (INFγ), and vascular endothelial growth factor-A (VEGF) were examined in RA patients. The biomarkers were measured by ELISA technique in 102 RA patients and 58 age-matched healthy control subjects. Serum MMP3, TNFα, IFNγ, and CSF2 showed significant elevation in RA patients. Multivariate general linear model (GLM) analysis revealed a significant high effect of diagnosis on biomarkers' level (partial $\eta^2 = 0.415$). Duration of disease is significantly associated with VEGF, OPN, and B-composite and negatively correlated with TNFα. B-composite is significantly associated with CRP. A significant fraction of the DAS28 score variance can be explained by the regression on zlnINFγ. The variance in the CRP was explained by zlnOPN and B-composite. More than half of anti-citrullinated protein antibodies (ACPA) variation can be explained by the regression on serum MMP3 and I-composite. The top 3 sensitive predictors for RA disease are INFγ, MMP3, and TNFα. B-composite is associated with the duration of disease and CRP. At the same time, I-composite is negatively associated with the ACPA level. The biomarker composites have potential use as RA disease characteristic biomarkers.

KEY WORDS
diagnosis
inflammation
rheumatoid arthritis
stromelysin-1
osteopontin

ARTICLE INFORMATION
Submitted
28 July 2021
Accepted
26 November 2021
***Corresponding author**
E-mail: headm2010@yahoo.com

INTRODUCTION

Rheumatoid arthritis (RA) is a chronic autoimmune-inflammatory disorder that affects joints mostly in women and older subjects (Tobón et al. 2010; Agarwal 2011). RA is associated with systemic complications, progressive disability, socioeconomic costs, and even early death (Firestein 2003; Choy 2012). RA patients suffer from chronic inflammation, swollen and painful joints, stiffness following prolonged inactivity, fatigue, burning sensations, and loss of motor control (Alamanos and Drosos 2005; Stack et al. 2014). The etiology of RA remains ambiguous but is attributed to a package of genetic and environmental factors (Vickers 2017). Many parameters were measured and examined for their potential applicability as a factor of diagnosis, prognosis, or RA disease follow-up. Among those parameters, scientists have measured adipokines (Ali et al. 2020), trace elements (Al-Hakeim et al. 2019), various pro- and anti-inflammatory cytokines (Mateen et al. 2016; Wu et al. 2021). Because RA is characterized by inflammation of the synovial membrane that leads to the pulverization and destruction of the joints (Anandarajah 2011), estimation of different inflammation-related cytokines is still an interesting field of study. Due to the increasing production of free radicals in the inflamed joints, inflammation and tissue damage have also been involved in RA's pathogenesis (Mateen et al. 2016; Quiñonez-Flores et al. 2016). Multiple cellular elements, adhesion molecules, soluble mediators, and autoantibodies lead to inflammation of the joints and internal organs and structural changes (McInnes and Schett 2017; Giannini et al. 2020). However, the results of most parameters are not completely decisive and conclusive. Among these measured cytokines in RA is a colony-stimulating factor (CSF2), stromelysin-1 (MMP3), tumor necrosis factor-*α*

(TNFα), osteopontin (OPN), vascular endothelial growth factor-A (VEGF) and interferon-γ (INFγ). TNFα is secreted by monocytes, B cells, and multiple T cell subsets (Zhang et al. 2019). TNFα is bounteously present in RA patients' serum and joint synovium as an essential and significant cytokine upsetting the controlled harmony between pro-inflammatory and anti-inflammatory cytokines (Brennan and McInnes 2008). In one study, TNFα secreted from B-cells, among multiple osteoblasts' inhibitors, can inhibit bone formation in RA's animal model (Sun et al. 2018).

It is known that MMP3 is expressed in the synovium of RA patients (Kanbe et al. 2011; Chen et al. 2014) and represents a potential indicator of early diagnosis and the activity of the disease (Chen et al. 2014; Lerner et al. 2018). During tissue remodeling in RA, MMP3 participates in the breakdown of extracellular matrix proteins (Page-McCaw et al. 2007). Serum levels of MMP3 reflect the activity of RA disease, bone and joint injury and predict drug responsiveness and disease outcome (Vistoli et al. 2013; Lerner et al. 2018; Liu et al. 2018). These findings encouraged some researchers to suggest MMP3 monitoring in the routine assessment to accompany therapeutic modalities in RA management (Lerner et al. 2018).

CSF2 is a cytokine that can rise to high levels in response to immune stimuli (Borriello et al. 2019) to regulate inflammatory responses (Wicks and Roberts 2016). CSF2 is essential for developing inflammatory and arthritic pain in RA models (Cook et al. 2013). It is also increased locally in inflammation sites such as asthmatic patients' lungs and allergic patients' skin (Hamilton 2020). CSF2 has also been detected significantly in the arthritic synovial fluid, where it is expected to destroy bone and joint (Cook et al. 2013).

The binding of vascular endothelial growth factor (VEGF) to its receptor activates a series of signal transduction events that ultimately lead to the secretion of various inflammatory and growth factors that stimulate the proliferation and migration of the endothelial cells to produce new blood vessels (Hicklin and Ellis 2005). VEGF is widely expressed in RA patients' serum and synovial fluid (Lee and Bae 2018; Xu et al. 2019), where it is responsible for vascular growth and blood vessel invasion of the synovial lining membrane in RA (Malemud 2007). VEGF is considered a critical angiogenic factor that causes a synovitis continuous reaction and mainly results in tissue hypoxia (Zimna and Kurpisz 2015). Inflammation in synovium and hypoxia enhances the production of pro-inflammatory cytokines such as IL-1β and TNFα, activating VEGF production (Cho et al. 2006).

The bone matrix contains OPN that connects osteoclasts and hydroxyapatite to bolster bone resorption (Horton et al. 1995). This fact was supported by experiments on OPN-null mice that showed a resistance to the inflammatory joint destruction in collagen-induced arthritis (Yumoto et al. 2002). In a previous study, a manifest elevation of OPN concentration in RA patients' synovial fluid was found, which is suggested to play a significant role in the pathogenesis of RA (Ohshima et al. 2002). Furthermore, plasma OPN was considered an inflammatory bone damage biomarker in RA patients (Iwadate et al. 2014). The presence of the anti-OPN antibodies has been associated with the severity of RA.

In the immune system, IFNγ plays a role in producing cytokine, antigen presentation, cellular differentiation, metabolic pathways, macrophage activation, and cell growth and survival (Lees 2015). The activated T cells and natural killer (NK) cells are the primary cells that secrete IFNγ in plasma (Billiau 1996; Billiau and Matthys 2009), while the dominant source of IFNγ in RA synovium is CD8+ T cells (Zhang et al. 2019). INFγ enhances antigen presentation, mediates antiviral and antibacterial immunity, orchestrate the activation of the innate immune system, regulates Th1/Th2 balance, promotes macrophage activation, and controls cellular proliferation and apoptosis (Billiau 1996; Billiau and Matthys 2009). A previous attempt to use recombinant IFNγ to treat RA without any benefit (Veys et al. 1997). Therefore, the exact effect of these parameters on the RA is not fully understood by studying every parameter alone. In the present study, we built two biomarkers composite from bone biomarkers from MMP3, OPN, and VEGF, reflecting the bone status (B-composite). The second composite (I-composite) was built from TNFα, INFγ, and CSF2, reflecting immune activation. The current study aims to examine the diagnostic role of the above biomarkers and their composites in the RA patients and study the factors affecting their level in the sera of RA patients.

MATERIAL AND METHODS

Participants

The present case-control study was performed in Fallujah General Hospital in Anbar, Iraq, from October 2019 till December 2020. The study included 102 males with RA patients and 58 healthy control subjects. The criteria of the "American College of Rheumatology" and the "European League against Rheumatism" were used for RA diagnosis (Aletaha et al. 2010). Every patient achieved a score higher than six from the results of the four domains: the number and site of the painful joints, positive serologic results (rheumatoid factor (RF), and anti-citrullinated protein antibodies (ACPA)), elevations of inflammatory markers (C-reactive protein (CRP) and/or erythrocyte sedimentation rate (ESR)), and the duration of RA symptoms. The clinical characteristics of the

Table 1. Clinical and demographic characteristics rheumatoid arthritis patients (RA) and healthy controls (HC).

Variables	HC (n = 58)	RA (n = 112)	F/χ^2	df	p
Age (years)	47.128 ± 6.017	48.222 ± 5.941	1.139	1/158	0.289
BMI (kg/m^2)	24.923 ± 2.623	25.917 ± 2.348	2.325	1/158	0.082
DAS28	-	7.406 ± 1.374	-	-	-
Duration of disease (years)	-	9.275 ± 4.788	-	-	-
ACPA (+ve/-ve)	0/58	87/15	59.626	1	<0.001
CRP (+ve/-ve)	0/58	82/20	52.111	1	<0.001
RF (+ve/-ve)	0/58	88/14	61.747	1	<0.001
Urea (mg/dl)	34.258 ± 5.192	35.357 ± 6.028	2.135	1/158	0.272
Creatinine (mg/dl)	0.820 ± 0.201	0.890 ± 0.194	3.164	1/158	0.247
Uric acid (mg/dl)	5.258 ± 1.237	5.891 ± 1.138	3.874	1/158	0.041
T.Protein (g/dl)	7.222 ± 0.949	7.305 ± 0.817	1.127	1/158	0.297
Albumin (g/dl)	4.552 ± 0.610	4.666 ± 0.624	0.817	1/158	0.304
T.Ca (mM)	2.160 ± 0.191	2.168 ± 0.210	0.035	1/158	0.853
I.Ca (mM)	1.254 ± 0.053	1.255 ± 0.058	0.016	1/158	0.901
MMP3 (ng/ml)	16.054 ± 6.557	22.827 ± 9.112	27.305	1/158	<0.001
TNFα (pg/ml)	31.123 ± 8.528	43.471 ± 16.235	14.058	1/158	<0.001
VEGF (pg/ml)	155.258 ± 37.124	159.068 ± 36.848	0.127	1/158	0.685
OPN (ng/ml)	4.777 ± 2.185	5.025 ± 2.681	2.024	1/158	0.122
IFNγ (pg/ml)	58.588 ± 23.582	104.309 ± 31.253	46.951	1/158	<0.001
CSF2 (pg/ml)	66.852 ± 22.136	91.265 ± 38.302	11.027	1/158	0.001
B-Composite	-0.248 ± 1.783	0.238 ± 1.609	1.806	1/158	0.183
I-Composite	0.407 ± 1.847	0.158 ± 1.948	0.380	1/158	0.539

BMI: Body mass index; DAS28: Disease activity score-28; T.Ca: Total calcium; I.Ca: Ionized calcium; CSF2: Colony-stimulating factor; MMP3 (Stromelysin-1): Matrix metalloproteinase-3; TNFα: Tumor necrosis factor-alpha; OPN: Osteopontin; INFγ: Interferon gamma; VEGF: Vascular endothelial growth factor; z: z-score; ln: natural logarithm; B-Composite: Bone cytokines composite = zlnMMP3+zlnVEGF+zlnOPN; I-Composite: Inflammatory cytokines composite = zlnTNFα+zlnINFγ+zlnCSF2.

RA disease and socio-demographic information were recorded from all patients. Disease Activity Score was calculated by using (DAS28-ESR) calculator available online at https://www.mdcalc.com/disease-activity-score-28-rheumatoid-arthritis-esr-das28-esr. The Clinical Disease Activity Index (CDAI) of all patients' RA disease activity was more than 10, indicating moderate to high disease activity. Body mass index (BMI) was calculated by dividing body weight (kilograms) by the squared length of subjects (squared meter). The study was approved by the ethical approval committee (IRB) of the University of Anbar, Iraq (Document number 103/2019), which complies with the "International Guideline for Human Research" standards as mandatory by the Declaration of Helsinki.

A complete medical history evaluated all subjects to exclude any systemic diseases that might influence the measured parameters' results, particularly liver and renal disease, infection, diabetes, cardiovascular events. The smoking subjects were also excluded from the study.

Measurements

After overnight fasting, five millilitres of venous blood were collected from all subjects without a tourniquet and, after complete clotting at 37 °C, centrifuged at 3000 rpm for 15 min. Sera were isolated and stored at -80 °C until analysis. Serum CRP and RF were measured by semi-quantitative kits (Spinreact®, Girona, Spain) based on the latex agglutination principle. A semi-quantitative ACPA test was carried out by kits provided by Hotgen Biotech (Beijing, China). Serum CSF2, INFγ, MMP3, OPN, TNFα, and VEGF were determined by sandwich ELISA assay kits (Mybiosource®, CA, USA). Serum albumin, total protein, calcium, urea, creatinine, and uric acid were measured spectrophotometrically using ready-to-use kits (Spinreact®, Girona, Spain). Ionized calcium (I.Ca) in serum was calculated from the following equation "$I.Ca = 0.813 \times T.Ca^{0.5} - 0.006 \times Albumin^{0.75} + 0.079$" (Mateu-de Antonio 2016), which give the best approximate result. The sensitivities of the ELISA kits were: CSF2 < 1 pg/ml, INFγ < 4 pg/ml, MMP3 < 0.068 ng/ml, OPN < 0.1 pg/ml, TNFα < 1 pg/ml, and VEGF < 1 pg/ml. The intra-assay coefficients of variance of all kits were less than 10%.

Table 2. Multivariate GLM analysis examining the differences in biomarkers between rheumatoid arthritis patients and normal controls.

Tests	Dependent variables	Explanatory variables	F	df	p	Partial η^2
Multivariate	All 8 biomarkers	Diagnosis	14.112	8/149	<0.001	0.415
		Sex	1.124	8/149	0.352	0.102
		BMI	1.224	8/149	0.307	0.911
		Age	1.248	8/149	0.411	0.090
Between-subject effects	T.Ca	Diagnosis	1.714	1	0.194	0.021
	I.Ca	Diagnosis	1.695	1	0.197	0.020
	MMP3	Diagnosis	13.173	1	<0.001	0.141
	TNFγ	Diagnosis	1.687	1	0.207	0.023
	VEGF	Diagnosis	0.988	1	0.294	0.032
	OPN	Diagnosis	0.214	1	0.516	0.017
	IFNγ	Diagnosis	23.777	1	<0.001	0.227
	CSF2	Diagnosis	2.945	1	0.078	0.049

All results of multivariate GLM analysis with the biomarkers as dependent variables and diagnosis as an explanatory variable while adjusting for extraneous variables. Diagnosis: RA versus healthy controls; BMI: Body mass index; DAS28: Disease Activity Score-28; T.Ca: Total calcium; I.Ca: Ionized calcium; CSF2: Colony-stimulating factor; MMP3 (Stromelysin-1): Matrix metalloproteinase-3; TNFα: Tumor necrosis factor-alpha; OPN: Osteopontin; INFγ: Interferon-gamma; VEGF: Vascular endothelial growth factor.

Statistical analysis

The distribution of all biomarkers results was found normal, as examined by the Kolmogorov-Smirnov test. Therefore, all results were presented as mean ± standard deviation. Chi-square test (χ^2-test) was used to estimate the associations between categorical variables, and analysis of variance (ANOVA) test was used for checking the differences in scale variables between groups. Correlations among biomarkers and between biomarkers and clinical and demographic parameters were assessed using Pearson's product-moment correlation analysis. Associations between RA diagnosis and the measured biomarkers were examined using the multivariate general linear model (GLM) analysis while directing for age and BMI as confounding variables. Accordingly, tests for between-subject effects were performed to explain the associations between diagnosis and every biomarker. The effect size of the analysis was expressed as partial eta-squared (η^2). Various z-unit weighted composite scores were calculated based on the levels of the biomarkers. Firstly, we computed the sum of z values of three normalized inflammatory biomarkers values (zlnTNFα) + zlnINFγ + zlnCSF2) reflecting immune activation (I-composite). Secondly, we computed the sum of z values of three normalized bone-related biomarkers (zlnMMP3) + zlnVEGF + zlnOPN) reflecting bone tissue status (B-composite).

The multiple regression analysis was employed to assess the most significant biomarkers that predict some measured biomarkers. Receiver Operating Curve (ROC) was used to study the measured biomarkers' diagnostic ability for RA. We estimated the best cut-off value of the parameters that produce the best sensitivity and specificity. A two-tailed test was used, and a p-value <0.05 would be considered as a statistical significance. The IBM SPSS package for windows-10, version 25, was used for performing all analyses.

RESULTS

Demographic, clinical and blood parameters characteristics

The demographic data of RA patients in comparison with the healthy controls are shown in Table 1. No significant differences in BMI and age between the groups. Table 1 also shows no significant difference in the levels of urea, creatinine, total protein, albumin, T.Ca and I.Ca between groups. Serum uric acid showed a slight significant increase (p = 0.041) in the RA group compared with the control group. Serum MMP3, TNFα, IFNγ, and CSF2 were significantly increased in RA patients than in the control group. While the serum level of VEGF and OPN showed no significant difference between groups. The weighted composites of bone tissue (B-composite) and inflammatory state (I-composite) showed no significant difference in the RA group than the control group. Co-varying for the drug state did not alter the results.

GLM analysis

The multivariate GLM analysis results, in Table 2, did not show any significant effect of age (F = 1.248, df = 8/149, p = 0.411), and BMI (F = 1.244, df = 8/149, p = 0.307) on the eight biomarkers. The presence of RA (diagnosis) has a highly significant effect (F = 14.112, df = 8/149, p<0.001) on the levels of the biomarkers with a high effect size

Table 3. Correlation matrix of the measured biomarkers with the demographic and among other biomarkers in all the study subjects.

Parameter	zlnMMP3	zlnTNFα	zlnVEGF	zlnOPN	zlnINFγ	zlnCSF2	B-Composite	I-Composite
Age	-0.094	-0.152	-0.055	-0.168	-0.151	-0.156	-0.191	0.256*
BMI	-0.110	-0.025	0.048	-0.003	-0.148	-0.089	-0.035	-0.146
T. Ca	-0.261*	-0.053	-0.121	-0.129	-0.027	-0.150	-0.308**	-0.131
I. Ca	-0.210*	-0.100	-0.150	-0.141	-0.082	-0.151	-0.304**	-0.187
S. Uric acid	-0.122	-0.029	0.085	-0.024	-0.061	-0.098	-0.030	-0.106
zlnMMP3	1	-0.061	-0.166	0.093	0.174	0.124	0.531**	0.134
zlnTNFα	-0.061	1	0.013	-0.002	0.075	-0.075	-0.028	0.541**
zlnVEGF	-0.166	0.013	1	-0.078	-0.052	-0.103	0.504**	-0.082
zlnOPN	0.093	-0.002	-0.078	1	0.100	0.154	0.606**	0.144
zlnINFγ	0.174	0.075	-0.052	0.100	1	0.111	0.128	0.649**
zlnCSF2	0.124	-0.075	-0.103	0.154	0.111	1	0.098	0.604**
B-Composite	0.531**	-0.028	0.504**	0.606**	0.128	0.098	1	0.112
I-Composite	0.134	0.541**	-0.082	0.144	0.649**	0.604**	0.112	1

*: Significant correlation (p<0.01); **: Significant correlation (p<0.001); BMI: Body mass index; DAS28: Disease Activity Score-28; T.Ca: Total calcium; I.Ca: Ionized calcium; CSF2: Colony-stimulating factor; MMP3 (Stromelysin-1): Matrix metalloproteinase-3; TNFα: Tumor necrosis factor-alpha; OPN: Osteopontin; INFγ: Interferon gamma; VEGF: Vascular endothelial growth factor; z: z-score; ln: natural logarithm; B-Composite: Bone cytokines composite expressed as zlnMMP3+zlnVEGF+zlnOPN; I-Composite: Inflammatory cytokines composite expressed as zlnTNFα+zlnINFγ+zlnCSF2.

(partial $\eta^2 = 0.415$). Tests for between-subject showed that the diagnosis has the major effects on the levels of IFNγ ($F = 23.777$, df = 1, $p<0.001$, partial $\eta^2 = 0.227$), followed by MMP3 ($F = 13.173$, df = 1, $p < 0.001$, partial $\eta^2 = 0.141$). Other biomarkers parameters showed lower effects by diagnosis with low-size effects.

Intercorrelation matrix

Table 3. shows the intercorrelation matrix of the measured parameters in 170 subjects. There were significant negative associations between the zlnMMP3 and T.Ca ($r = -0.261$, $p<0.01$) and I.Ca ($r = -0.210$, $p<0.05$) across the entire study group. I-composite is significantly correlated with age ($r = 0.256$, $p<0.01$).

In the RA patients group only, the zlnMMP3 was correlated with ACPA ($r = 0.379$, $p<0.01$), while negatively associated with T.Ca ($r = -0.311$, $p<0.01$) and I.Ca ($r = -0.318$, $p<0.01$). Duration of disease is significantly associated with zlnVEGF ($r = 0.325$, $p<0.01$), zlnOPN ($r = 0.383$, $p<0.001$), and B-composite ($r = -0.433$, $p<0.001$). While zlnTNFα is negatively and significantly associated with the duration of disease ($r = -0.303$, $p<0.01$), and zlnTNFα ($r = -0.281$, $p<0.05$). CRP is significantly associated with B-composite ($r = -0.375$, $p<0.01$) and zlnVEGF ($r = -0.357$,

Table 4. Results of multiple regression analysis with the routinely measured parameters in rheumatoid arthritis patients in addition to DAS28 and the duration of disease as dependent variables.

Regression	Explanatory variables	β	t	p	F_{model}	p	R^2
#1. DAS28	**Model**				5.235	0.012	0.127
	zlnINFγ	0.313	-2.208	0.015			
#2. Duration of disease	**Model**				7.323	<0.001	0.259
	zlnMMP3	-0.234	-3.0021	<0.001			
	Sex	0.244	2.877	<0.001			
#3. CRP	**Model**				5.912	0.006	0.218
	zlnOPN	-0.106	2.168	0.027			
#4. RF	**Model**				6.432	0.001	0.311
	GM-CSF	1.848	2.025	<0.001			
#5. ACPA	**Model**				7.927	<0.001	0.501
	zlnMMP3	0.281	3.077	0.002			

DAS28: Disease Activity Score-28; CSF2: Colony-stimulating factor; MMP3 (Stromelysin-1): Matrix metalloproteinase-3; OPN: Osteopontin; INFγ: Interferon gamma; CRP: C-reactive protein; RF: Rheumatoid factor; ACPA: anti-citrullinated protein antibodies; z: z-score (standard score); ln: natural logarithm.

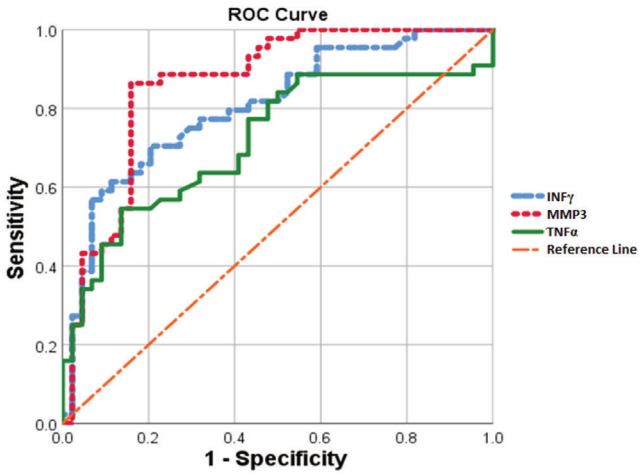

Figure 1. ROC analysis curve for the biomarkers (IFNγ, MMP3, and TNFα) that have the highest area under the curve as predictors for rheumatoid arthritis compared with the reference line.

p<0.01). DAS28 is associated with the zlnINFγ. ACPA is significantly and negatively associated with I-composite (r = -0.336, p<0.01).

Table 4. presents the results of different automatic multiple regression analyses with the routine measured parameters (ACPA, CRP, and RF) in addition to DAS28 and the duration of disease as dependent variables. Regression #1 explained that 12.7% of the variance in the DAS28 score on zlnINFγ. Regression #2 shows that the regression can explicate 25.9% of the variance in disease duration on B-composite (positively associated) and zlnMMP3 (inversely associated). Regression #3 shows that 21.8% of the CRP variance was explicated by zlnOPN (inversely associated) and B-composite (positively associated). Regression #4 shows that 31.1% of the RF variance was explained by zlnCSF2 (positively associated). More than half (50.1%) of the variation in ACPA level can be explained by the regression on serum calcium, MMP3, and I-composite in Regression #5.

Effects of background variables

We also examined the effects of drugs taken on the serum levels of the measured parameters in RA patients by using univariate-GLM analysis. The analysis shows no significant effects of taking sulfasalazine (F = 2.981, df = 1/100, p=0.071) and methotrexate (F = 2.110, df = 1/100, p=0.971) on the serum level of the eight measured biomarkers. There was a slight significant effect of prednisolone on TNFα (p = 0.032; partial η^2 = 0.048) and INFγ (p = 0.047, partial η^2 = 0.066), naproxen on CSF2 (p = 0.039, partial η^2 = 0.072), and tofacitinib on TNFα (p = 0.0292 partial η^2 = 0.061). The other administered drugs have no remarkable effect. The drug administration's overall effects on the measured parameters were only minimum (partial η^2< 0.059).

Predictive value of the measured biomarkers

Table 5. shows the ROC parameters of the measured biomarkers for the diagnosis of rheumatoid arthritis. Only the biomarkers that showed a significant efficacy was cited in Table 5. Figure 1. shows only the top 3 sensitive biomarkers (p<0.001) for RA's diagnosis in a suspected subject. The serum concentration of 62.7 pg/ml represents the cut-off value that when the suspected subjects have higher serum INFγ than it, may refer to the presence of RA with sensitivity = 86.4% and specificity = 84.1%. The cut-off value of MMP3 was 17.7 ng/ml with sensitivity = 70.5% and specificity = 79.5%. While TNFα have sensitivity = 65.6% and specificity = 68.2% at cut-off value of 36.2 pg/ml. While the other biomarkers (CSF2, OPN, and VEGF) showed lower sensitivities and specificities than the top 3 biomarkers.

DISCUSSION

The initial stage in ensuring the quality of the research was to enroll subjects who were not suffering from renal issues with normal urea and creatinine levels as seen in Table 1. The most important finding of the current study is the increased serum MMP3, TNFα, IFNγ, and CSF2 in RA patients compared with the HC group. The elevation in these biomarkers values suggested a more inflammatory state in RA group. Tissue damage is thought to be controlled by cytokines (Alstergren and Kopp 2006). TNFα is commonly acknowledged as a pro-inflammatory cytokine involved in RA pathophysiology (Vervoordeldonk and Tak 2002; Yamanaka 2015; Guo et al. 2019). The outcome of other previous research showed higher levels of TNFα in RA patients (Thilagar et al. 2018). As a result of elevated TNFα, osteoclast precursor cells are stimulated, causing bone resorption (Bartold et al. 2005). TNFα triggers an infection or inflammatory immunological response. However, it promotes an increase in osteoclast precursors and osteoclast development, causing bone resorption (Cessak et al. 2014). A comprehensive evaluation confirmed the advantages of anti-TNF medication for RA patients' rheumatic joints (Zamri and de Vries 2020).

The rise in IFNγ levels in the patients' group is attributable to the inflammatory character of RA, as several cell types, including T-cells, B-cells, NK cells, and monocytes/macrophages, produce IFN (Lees 2015). CD8+ T lymphocytes in the RA synovium are the primary source of IFNγ. T cells, on the other hand, are required for the generation of tissue-degrading enzymes and proinflammatory cytokines, and CD4 T cells are an important regulator of

Table 5. Receiver operating characteristic-area under curve analysis of the measured biomarkers for the diagnosis of rheumatoid arthritis.

Variable	Cut-off concentration	Sensitivity %	Specificity %	Youden's J statistics	AUC	95% CI of AUC	p-value
IFNγ	62.7 pg/ml	86.4	84.1	0.67	0.863	0.784-0.942	<0.001
MMP3	17.7 ng/ml	70.5	79.5	0.46	0.804	0.713-0.896	<0.001
TNFα	36.2 pg/ml	65.6	68.2	0.40	0.718	0.609-0.828	<0.001
CSF2	69.2 pg/ml	53.6	52.4	0.31	0.668	0.556-0.780	0.017
OPN	4.65 ng/ml	44.4	47.4	0.27	0.624	0.505-0.743	0.038
VEGF	167.2 pg/ml	42.3	49.8	0.24	0.480	0.357-0.602	0.042

AUC: area under curve; CI: Confidence interval; CSF2: Colony-stimulating factor; MMP3 (Stromelysin-1): Matrix metalloproteinase-3; TNFα: Tumor necrosis factor-alpha; OPN: Osteopontin; INFγ: Interferon-gamma; VEGF: Vascular endothelial growth factor.

these processes (Klimiuk et al. 1999, Petrasca et al. 2020). IFNγ signaling can regulate many genes (Rusinova et al. 2013) that may affect the inflammatory process and the destruction or degeneration of synovial membranes. The presence of IFNγ receptors is associated with RA symptoms, and an increase in IFNγ-induced inflammation is a sign of therapy success and RA remission (Page et al. 2010; Lee et al. 2017).

MMP3 levels were found to be elevated in our RA patients' group, which was previously reported (Czeczuga and Zajkowska 2008; Mamehara et al. 2010; Ma et al. 2015; Tuncer et al. 2019). However, one study showed no significant difference in MMP3 in RA and control groups (Abd-Allah et al. 2012). When it comes to bone damage detection, the serum level of MMP3 is a good predictor, and suppressing MMP3 levels may be an essential treatment approach for individuals with early RA (Fiedorczyk et al. 2006; Houseman et al. 2012; Tokai et al. 2018). According to a recent research, serum MMP3 levels are better at predicting clinical remission of RA disease than CRP levels (Hattori et al. 2019). It is possible that serum MMP3 will serve as a biomarker for histological synovitis and the diagnosis of RA (Ma et al. 2014), joint erosions in the early stages of the disease, and monitoring disease activity (Tuncer et al. 2019).

As seen previously, RA patients have a higher serum level of CSF2 than the control group (Fiehn et al. 1992; Nakamura et al. 2000). CSF2 is expressed in the synovial membrane and is higher in the synovial fluid of patients with RA (Field and Clinton 1993; Bell et al. 1995). CSF2 receptors are also upregulated by RA subjects in synovial tissue and circulating mononuclear cells (Field and Clinton 1993; Berenbaum et al. 1994). Populations of synovial tissue macrophages are associated with articular damage, and a drop in macrophage numbers is a responsive biomarker for treatment response in RA patients (Haringman et al. 2005). Since CSF2 plays a central role in macrophages' differentiation, activation, and survival, inhibiting CSF2 activity may affect the function of macrophages and provide RA with clinical benefit. In RA pathogenesis, CSF2 contributes to the differentiation and pathogenicity of Th17 cells (Wijbrandts et al. 2007; Codarri et al. 2011; El-Behi et al. 2011).

According to the results of Table 2, multivariate GLM analysis showed no significant effects of the cofounders (age and BMI) on the levels of the measured biomarkers. The biomarkers' levels are significantly affected only by RA disease in the subject with a big effect size (partial $\eta^2 = 0.415$). Tests for between-subject effects revealed that 22.7% of the variance in the IFNγ level. At the same time, 14.1% of the variance in the MMP3 level was due to the RA disease. This analysis excluded any effect of the cofounders on the levels of the measured parameters. A multivariate general linear model (GLM) analysis was used to delineate the relationships between diagnosis and biomarkers while controlling for confounding variables (age and BMI). As a result, to establish the relationship between diagnosis and each biomarker, we conducted an inter-subject effect analysis. This analysis revealed the importance of activating monocytes/macrophages in RA because IFNγ activates monocytes/macrophages activated in RA and contributes to the progression and advancement of the disease (Udalova et al. 2016). Furthermore, IFNγ deficiency or defects in the IFNγ-receptors may have an important effect on the activity and the serum level of IFNγ in RA disease (Lee et al. 2017; Sharma et al. 2018).

MMP3 enzyme can degrade collagen molecules, laminin, proteoglycans, elastin, and fibronectin (Verma and Hansch 2007), which are components of the connective tissues' matrix joints, bones, tendons, and their reduction causes destruction in the joints and exaggerate the RA state. The increase in MMp3 from the synovial fibroblasts or B cells is well-known as a producer of MMP3 (Tetlow et al. 1993). Since MMP3 has a major role in connective tissue remodeling, it may affect their calcium contents and even serum calcium level, as seen in Table 3. However, previously, serum MMP3 is correlated with systemic inflammation and not an independent joint damage marker (So et al. 1999). In previous work, plasma OPN levels were strongly associated with MMP3

levels, and after treatment, the responders' plasma OPN levels decreased dramatically (Iwadate et al. 2014). Also, B-composite showed a significant negative correlation with serum calcium. As B-composite represents the bone biomarkers, it is important to notice that bone biomarkers' elevation, as a composite, is more indicative than each biomarker alone. Previous work showed that circulating pro-inflammatory molecules are inversely correlated with the calcium status parameters and serum calcium level (Poddar et al. 2016). The increase in the inflammatory composite (I-composite) with age is due to each component's cumulative effects. Therefore, I-composite is better than each parameter separately as a tool for studying inflammatory effects. The TNFα level presented a positive correlation with age (Milan-Mattos et al. 2019). Because age is considered a major risk factor for many chronic inflammatory diseases (Larbi et al. 2008; Ferrucci and Fabbri 2018), immune aging contributes to many autoimmune diseases.

The results of Table 4. indicated the direct effect of INFγ on the severity of disease expressed as DAS28. This result indicated the importance of pro-inflammatory biomarkers INFγ on disease progression (Meyer et al. 2010). Duration of the disease depends on the magnitude of the MMP3 and B-composite. As the disease extends, the bone composite increases with time. In one study, MMP3 level was not correlated to the age, disease duration, and the DAS28 scores. However, MMP3 is significantly correlated to CRP and ESR, which are markers of inflammation (Sun et al. 2014). MMP3 was associated with age (Kodama et al. 2018). Furthermore, CRP was explained by B-composite. These results indicated the dependence of the level of bone-related cytokines on the inflammation state biomarkers. However, other researchers showed that raised serum biomarkers might not act as a risk factor for low bone mineral density (Sponholtz et al. 2014). A significant fraction of the RF level can be explained by CSF2. The same explanations can be used, i.e. the inflammation state in RA is the major cause of the biomarker's changes. ACPA level is affected by serum calcium, MMP3, and I-composite levels, as seen in Regression #5 of Table 4. Previously, ACPA had the highest predictive value for RA development (van de Stadt et al. 2011; van Heemst et al. 2015). However, the concomitant existence of RF could increase the risk of RA production. (Rantapää-Dahlqvist et al. 2003; Kokkonen et al. 2011). A significant correlation between ACPA-positivity status and arthritis progression has also been confirmed in multiple patients that have subsequently developed RA. (van Gaalen et al. 2004; Rakieh et al. 2015).

Figure 1. and Table 5. showed a good predictive value of the serum INFγ, MMP3, and TNFα for the presence of RA in a suspected subject. MMP3 is a biomarker for connective tissues, while INF and TNF are inflammatory parameters. Thus, RA is a result of a cascade of inflammatory processes in the joints and bone tissues. However, the diagnostic cut-off value is rather high. MMP3 expression is a good indicator for disease activity in patients with RA (Ma et al. 2015). MMP3 levels elevated as the stage and type of RA progressed and eventually reduced after effective therapy (Uemura et al. 2015). MMP3 levels in the serum were favorably linked with serum CRP or RF levels or with joint destruction (Li et al. 2013). However, a statistically significant correlation was observed between MMP3 and CRP and ESR (So et al. 1999; Hattori et al. 2019). Elevation of serum MMP3 in RA patients is a sign of inflammation (Mamehara et al. 2010) and serves as an early marker of developing joint destruction and a good prognostic indicator of active rheumatoid arthritis illness (Ma et al. 2014; Ma et al. 2015; Galil et al. 2016). Joint injury may be detected with the use of a blood test for serum MMP3, which is linked to systemic inflammation (Mamehara et al. 2010).

Different immune cells, such as neutrophils, release pro-inflammatory indicators, such as prostaglandins, cytokines, and reactive oxygen intermediates, which contribute to synovitis (Cascao et al. 2010). Mast cells in the synovium also release large quantities of cytokines, chemokines, proteases, and vasoactive amines, all of which are harmful to the joint tissues (Nigrovic and Lee 2007; Hueber et al. 2010). ACPA has been widely accepted as a biomarker for RA activity and types (Schuerwegh et al. 2010). ACPA has been widely used to diagnose RA with specificity (Hill et al. 2008). ACPA endorsed inflammatory cytokines production in RA patients and accumulated at the citrulline site, causing bone damage (Umeda et al. 2017).

CONCLUSION

The top 3 sensitive predictors for RA are INFγ, MMP3, followed by TNFα. A significant part of CRP variance was explained by zlnOPN and B-composite, while CSF2 can explain a significant RF variance. Duration of the disease can be explained and B-composite (positively associated). About half (50.1%) of the variation in ACPA level can be explained by the regression on serum calcium, MMP3, and I-composite. B-composite is associated with the duration of disease and CRP. I-composite is negatively associated with the ACPA level. The overall results indicated the importance of composite from the biomarkers with common properties as a new biomarker for estimating disease characteristics.

Concerning the limitations of the study, the first drawback is the small scale of the research sample. Test

experiments with a larger sample size will be needed to ensure sufficient generalization of the analysis' results. The second limitation is that the study recruited only male subjects, and we excluded women to eliminate the effect of the estrogens on the measured parameters. The third limitation is the relatively significant inter-assay CV% of the ELISA kits, which were less than 10% for all kits.

ACKNOWLEDGMENT

The authors acknowledge Fallujah General Hospital's staff in Anbar Governorate, Iraq to help with sample collection and the biochemical measurements.

REFERENCES

Abd-Allah SH, Shalaby SM, Pasha HF, El-Shal AS, Abou El-Saoud AM (2012) Variation of matrix metalloproteinase 1 and 3 haplotypes and their serum levels in patients with rheumatoid arthritis and osteoarthritis. Gen Test Mol Biomark 16(1):15-20.

Agarwal SK (2011) Biologic agents in rheumatoid arthritis: an update for managed care professionals. J Manag Care Pharm 17(9 Suppl B):S14-18.

Al-Hakeim HK, Moustafa SR, Jasem KM (2019) Serum cesium, rhenium, and rubidium in rheumatoid arthritis patients. Biol Trace Elem Res 189(2):379-386.

Alamanos Y, Drosos AA (2005) Epidemiology of adult rheumatoid arthritis. Autoimmun Rev 4(3):130-136.

Aletaha D, Neogi T, Silman AJ, Funovits J, Felson DT, Bingham CO, Birnbaum NS, Burmester GR, Bykerk VP, Cohen MD (2010) 2010 rheumatoid arthritis classification criteria: an American College of Rheumatology/European League Against Rheumatism collaborative initiative. Arthritis Rheum 62(9):2569-2581.

Ali DM, Al-Fadhel SZ, Al-Ghuraibawi NHA, Al-Hakeim HK (2020) Serum chemerin and visfatin levels and their ratio as possible diagnostic parameters of rheumatoid arthritis. Reumatologia 58(2):67-75.

Alstergren P, Kopp S (2006) Insufficient endogenous control of tumor necrosis factor-alpha contributes to temporomandibular joint pain and tissue destruction in rheumatoid arthritis. J Rheumatol 33(9):1734-1739.

Anandarajah AP (2011) Clinical aspects of rheumatoid arthritis: highlights from the 2010 ACR conference. Int J Clin Rheumatol 6(3):267.

Bartold PM, Marshall RI, Haynes DR (2005) Periodontitis and rheumatoid arthritis: a review. J Periodontol 76(11 Suppl):2066-2074.

Bell AL, Magill MK, McKane WR, Kirk F, Irvine AE (1995) Measurement of colony-stimulating factors in synovial fluid: potential clinical value. Rheumatol Int 14(5):177-182.

Berenbaum F, Rajzbaum G, Amor B, Toubert A (1994) Evidence for GM-CSF receptor expression in synovial tissue. An analysis by semi-quantitative polymerase chain reaction on rheumatoid arthritis and osteoarthritis synovial biopsies. Eur Cytokine Netw 5(1):43-46.

Billiau A (1996) Interferon-gamma: biology and role in pathogenesis. Adv Immunol 62:61-130.

Billiau A, Matthys P (2009) Interferon-gamma: a historical perspective. Cytokine Growth Fact Rev 20(2):97-113.

Borriello F, Galdiero MR, Varricchi G, Loffredo S, Spadaro G, Marone G (2019) Innate immune modulation by GM-CSF and IL-3 in health and disease. Int J Mol Sci 20(4):834.

Brennan FM, McInnes IB (2008) Evidence that cytokines play a role in rheumatoid arthritis. J Clin Invest 118(11):3537-3545.

Cascao R, Rosário H, Souto-Carneiro M, Fonseca J (2010) Neutrophils in rheumatoid arthritis: more than simple final effectors. Autoimmun Rev 9(8):531-535.

Cessak G, Kuzawińska O, Burda A, Lis K, Wojnar M, Mirowska-Guzel D, Bałkowiec-Iskra E (2014) TNF inhibitors - Mechanisms of action, approved and off-label indications. Pharmacol Rep 66(5):836-844.

Chen JJ, Huang JF, Du WX, Tong PJ (2014) Expression and significance of MMP3 in synovium of knee joint at different stage in osteoarthritis patients. Asian Pac J Trop Dis 7(4):297-300.

Cho ML, Jung YO, Moon YM, Min SY, Yoon CH, Lee SH, Park SH, Cho CS, Jue DM, Kim HY (2006) Interleukin-18 induces the production of vascular endothelial growth factor (VEGF) in rheumatoid arthritis synovial fibroblasts via AP-1-dependent pathways. Immunol Lett 103(2):159-166.

Choy E (2012) Understanding the dynamics: pathways involved in the pathogenesis of rheumatoid arthritis. Rheumatology (Oxford) 51(Suppl-5):v3-11.

Codarri L, Gyülvészi G, Tosevski V, Hesske L, Fontana A, Magnenat L, Suter T, Becher B (2011) RORγt drives production of the cytokine GM-CSF in helper T cells, which is essential for the effector phase of autoimmune neuroinflammation. Nat Immunol 12(6):560-567.

Cook AD, Pobjoy J, Sarros S, Steidl S, Durr M, Lacey DC, Hamilton JA (2013) Granulocyte-macrophage colony-stimulating factor is a key mediator in inflammatory and arthritic pain. Ann Rheum Dis 72(2):265-270.

Czeczuga A, Zajkowska J (2008) [Usefulness of examinations of serum levels of matrix metalloproteinases 1, MMP-3, MMP-9, tissue inhibitor of metalloproteinases 1, hyaluronic acid and antibodies against cyclic citrullinated peptide in Lyme arthritis, rheumatoid arthritis and patients with arthritic complaints]. Przegl Epidemiol

62 (Suppl 1):20-29.
El-Behi M, Ciric B, Dai H, Yan Y, Cullimore M, Safavi F, Zhang GX, Dittel BN, A Rostami (2011) The encephalitogenicity of TH 17 cells is dependent on IL-1-and IL-23-induced production of the cytokine GM-CSF. Nat Immunol 12(6):568-575.
Fiedorczyk M, Klimiuk PA, Sierakowski S, Gindzienska-Sieskiewicz E, Chwiecko J (2006) Serum matrix metalloproteinases and tissue inhibitors of metalloproteinases in patients with early rheumatoid arthritis. J Rheumatol 33(8):1523-1529.
Fiehn C, Wermann M, Pezzutto A, Hüfner M, Heilig B (1992) [Plasma GM-CSF concentrations in rheumatoid arthritis, systemic lupus erythematosus and spondyloarthropathy]. Z Rheumatol 51(3):121-126.
Field M, Clinton L (1993) Expression of GM-CSF receptor In rheumatold arthritis. Lancet 342(8881):1244.
Firestein GS (2003) Evolving concepts of rheumatoid arthritis. Nature 423(6937):356-361.
Galil SM, El-Shafey AM, Hagrass HA, Fawzy F, Sammak AE (2016) Baseline serum level of matrix metalloproteinase-3 as a biomarker of progressive joint damage in rheumatoid arthritis patients. Int J Rheum Dis 19(4): 377-384.
Giannini D, Antonucci M, Petrelli F, Bilia S, Alunno A, Puxeddu I (2020) One year in review 2020: pathogenesis of rheumatoid arthritis. Clin Exp Rheumatol 38:387-397.
Guo X, Wang S, Godwood A, Close D, Ryan PC, Roskos LK, White WI (2019) Pharmacodynamic biomarkers and differential effects of TNF- and GM-CSF-targeting biologics in rheumatoid arthritis. Int J Rheum Dis 22(4):646-653.
Hamilton JA (2020) GM-CSF in inflammation. J Exp Med 217(1).
Haringman JJ, Gerlag DM, Zwinderman AH, Smeets TJ, Kraan MC, Baeten D, McInnes IB, Bresnihan B, Tak PP (2005) Synovial tissue macrophages: a sensitive biomarker for response to treatment in patients with rheumatoid arthritis. Ann Rheum Dis 64(6):834-838.
Hattori Y, Kida D, Kaneko A (2019) Normal serum matrix metalloproteinase-3 levels can be used to predict clinical remission and normal physical function in patients with rheumatoid arthritis. Clin Rheumatol 38(1):181-187.
Hicklin DJ, Ellis LM (2005) Role of the vascular endothelial growth factor pathway in tumor growth and angiogenesis. J Clin Oncol 23(5):1011-1027.
Hill JA, Bell DA, Brintnell W, Yue D, Wehrli B, Jevnikar AM, Lee DM, Hueber W, Robinson WH, Cairns E (2008) Arthritis induced by posttranslationally modified (citrullinated) fibrinogen in DR4-IE transgenic mice. J Exp Med 205(4):967-979.
Horton MA, Nesbit MA, Helfrich MH (1995) Interaction of osteopontin with osteoclast integrins. Ann N Y Acad Sci 760:190-200.
Houseman M, Potter C, Marshall N, Lakey R, Cawston T, Griffiths I, Young-Min S, Isaacs JD (2012) Baseline serum MMP-3 levels in patients with rheumatoid arthritis are still independently predictive of radiographic progression in a longitudinal observational cohort at 8 years follow up. Arthritis Res Ther 14(1):R30.
Hueber AJ, Asquith DL, Miller AM, Reilly J, Kerr S, Leipe J, Melendez AJ, McInnes IB (2010) Cutting edge: mast cells express IL-17A in rheumatoid arthritis synovium. J Immunol 184(7):3336-3340.
Iwadate H, Kobayashi H, Kanno T, Asano T, Saito R, Sato S, Suzuki E, Watanabe H, Ohira H (2014) Plasma osteopontin is correlated with bone resorption markers in rheumatoid arthritis patients. Int J Rheum Dis 17(1):50-56.
Kanbe K, Chiba J, Nakamura A (2011) Decrease of CD68 and MMP-3 expression in synovium by treatment of adalimumab for rheumatoid arthritis. Int J Rheum Dis 14(3):261-266.
Klimiuk PA, Yang H, Goronzy JJ, Weyand CM (1999) Production of cytokines and metalloproteinases in rheumatoid synovitis is T cell dependent. Clin Immunol 90(1):65-78.
Kodama R, Muraki S, Iidaka T, Oka H, Teraguchi M, Kagotani R, Asai Y, Hashizume H, Yoshida M, Kawaguchi H, Nakamura K, Akune T, Tanaka S, Yoshimura N (2018) Serum levels of matrix metalloproteinase-3 and autoantibodies related to rheumatoid arthritis in the general Japanese population and their association with osteoporosis and osteoarthritis: the ROAD study. J Bone Miner Metab 36(2):246-253.
Kokkonen H, Mullazehi M, Berglin E, Hallmans G, Wadell G, Ronnelid J, Rantapaa-Dahlqvist S (2011) Antibodies of IgG, IgA and IgM isotypes against cyclic citrullinated peptide precede the development of rheumatoid arthritis. Arthritis Res Ther 13(1):R13.
Lee SH, Kwon JY, Kim SY, Jung K, Cho ML (2017) Interferon-gamma regulates inflammatory cell death by targeting necroptosis in experimental autoimmune arthritis. Sci Rep 7(1):10133.
Lee YH, Bae S-C (2018) Correlation between circulating VEGF levels and disease activity in rheumatoid arthritis: a meta-analysis. Zeitsch Rheumatol 77(3):240-248.
Lees JR (2015) Interferon gamma in autoimmunity: A complicated player on a complex stage. Cytokine 74(1):18-26.
Lerner A, Neidhofer S, Reuter S, Matthias T (2018) MMP3 is a reliable marker for disease activity, radiological monitoring, disease outcome predictability, and therapeutic response in rheumatoid arthritis. Best Pract Res Clin Rheumatol 32(4):550-562.
Li L, Cai B, Liao J, Yang B, Huang Z, Wang L (2013) [Clinical value of serum matrix metalloproteinase-3 in evaluating joint destruction and therapeutic effect in rheumatoid arthritis patients]. Chinese J Cell Mol Immunol 29(9): 966-969.

Liu MK, Wang LC, Hu FL (2018) [Value of serum matrix metalloproteinase 3 in the assessment of early rheumatoid arthritis]. Beijing Da Xue Xue Bao Yi Xue Ban 50(6): 981-985.

Ma J, Wang X, Mo Y, Chen L, Zheng D, Wei X, Dai L (2015) [Value of serum matrix metalloproteinase-3 in the assessment of active disease in patients with rheumatoid arthritis]. Zhonghua Yi Xue Za Zhi 95(47):3823-3828.

Ma JD, Zhou JJ, Zheng DH, Chen LF, Mo YQ, Wei XN, Yang LJ, Dai L (2014) Serum matrix metalloproteinase-3 as a noninvasive biomarker of histological synovitis for diagnosis of rheumatoid arthritis. Mediators Inflamm 2014:179284.

Ma M, Liu H, Qu X, Wang J (2015) Matrix metalloproteinase-3 gene polymorphism and its mRNA expression in rheumatoid arthritis. Genet Mol Res 14(4):15652-15659.

Malemud CJ (2007) Growth hormone, VEGF, FGF: Involvement in rheumatoid arthritis. Clin Chim Acta 375(1):10-19.

Mamehara A, Sugimoto T, Sugiyama D, Morinobu S, Tsuji G, Kawano S, Morinobu A, Kumagai S (2010) Serum matrix metalloproteinase-3 as predictor of joint destruction in rheumatoid arthritis, treated with non-biological disease modifying anti-rheumatic drugs. Kobe J Med Sci 56(3):E98-107.

Mateen S, Moin S, Khan AQ, Zafar A, Fatima N (2016) Increased Reactive Oxygen Species Formation and Oxidative Stress in Rheumatoid Arthritis. PLoS One 11(4):e0152925.

Mateen S, Zafar A, Moin S, Khan AQ, Zubair S (2016) Understanding the role of cytokines in the pathogenesis of rheumatoid arthritis. Clin Chim Acta 455:161-171.

Mateu-de Antonio J (2016) New predictive equations for serum ionized calcium in hospitalized patients. Med Princ Pract 25(3):219-226.

McInnes IB, Schett G (2017) Pathogenetic insights from the treatment of rheumatoid arthritis. Lancet 389(10086):2328-2337.

Meyer PW, Hodkinson B, Ally M, Musenge E, Wadee AA, Fickl H, Tikly M, Anderson R (2010) Circulating cytokine profiles and their relationships with autoantibodies, acute phase reactants, and disease activity in patients with rheumatoid arthritis. Mediators Inflamm 2010:158514.

Milan-Mattos JC, Anibal FF, Perseguini NM, Minatel V, Rehder-Santos P, Castro CA, Vasilceac FA, Mattiello SM, Faccioli LH, Catai AM (2019) Effects of natural aging and gender on pro-inflammatory markers. Braz J Med Biol Res 52(9):e8392.

Nakamura H, Ueki Y, Sakito S, Matsumoto K, Yano M, Miyake S, Tominaga T, Tominaga M, Eguchi K (2000) High serum and synovial fluid granulocyte colony stimulating factor (G-CSF) concentrations in patients with rheumatoid arthritis. Clin Exp Rheumatol 18(6):713-718.

Nigrovic PA, Lee DM (2007) Synovial mast cells: role in acute and chronic arthritis. Immunol Rev 217(1):19-37.

Ohshima S, Yamaguchi N, Nishioka K, Mima T, Ishii T, Umeshita-Sasai M, Kobayashi H, Shimizu M, Katada Y, Wakitani S, Murata N, Nomura S, Matsuno H, Katayama R, Kon S, Inobe M, Uede T, Kawase I, Saeki Y (2002) Enhanced local production of osteopontin in rheumatoid joints. J Rheumatol 29(10):2061-2067.

Page-McCaw A, Ewald AJ, Werb Z (2007) Matrix metalloproteinases and the regulation of tissue remodelling. Nat Rev Mol Cell Biol 8(3):221-233.

Page CE, Smale S, Carty SM, Amos N, Lauder SN, Goodfellow RM, Richards PJ, Jones SA, Topley N, Williams AS (2010) Interferon-γ inhibits interleukin-1β-induced matrix metalloproteinase production by synovial fibroblasts and protects articular cartilage in early arthritis. Arthritis Res Ther 12(2):R49.

Petrasca A, Phelan JJ, Ansboro S, Veale DJ, Fearon U, Fletcher JM (2020) Targeting bioenergetics prevents CD4 T cell-mediated activation of synovial fibroblasts in rheumatoid arthritis. Rheumatology (Oxford) 59(10):2816-2828.

Poddar A, Behera DD, Ray S (2016) Serum alkaline phosphatase activity & serum calcium levels: an assessment tool for disease activity in rheumatoid arthritis. IJBAMR 5(4):1324.

Quiñonez-Flores CM, González-Chávez SA, Del Río Nájera D, Pacheco-Tena C (2016) Oxidative stress relevance in the pathogenesis of the rheumatoid arthritis: a systematic review. BioMed Res Int 2016:6097417.

Rakieh C, Nam JL, Hunt L, Hensor EM, Das S, Bissell LA, Villeneuve E, McGonagle D, Hodgson R, Grainger A, Wakefield R J, Conaghan PG, Emery P (2015) Predicting the development of clinical arthritis in anti-CCP positive individuals with non-specific musculoskeletal symptoms: a prospective observational cohort study. Ann Rheum Dis 74(9):1659-1666.

Rantapää-Dahlqvist S, de Jong BA, Berglin E, Hallmans G, Wadell G, Stenlund H, Sundin U, van Venrooij WJ (2003) Antibodies against cyclic citrullinated peptide and IgA rheumatoid factor predict the development of rheumatoid arthritis. Arthritis Rheum 48(10):2741-2749.

Rusinova I, Forster S, Yu S, Kannan A, Masse M, Cumming H, Chapman R, Hertzog PJ (2013) Interferome v2.0: an updated database of annotated interferon-regulated genes. Nucleic Acids Res 41(Database issue):D1040-1046.

Schuerwegh AJ, Ioan-Facsinay A, Dorjee AL, Roos J, Bajema IM, van der Voort EI, Huizinga TW, Toes RE (2010) Evidence for a functional role of IgE anticitrullinated protein antibodies in rheumatoid arthritis. Proc Natl Acad Sci USA 107(6):2586-2591.

Sharma V, Pope BJ, Bolland M, Reynolds R, Sun D, Bridges SL, Raman C (2018). Enhanced interferon gamma re-

sponse contributes to disease remission in rheumatoid arthritis. J Immunol 200(Suppl 1):45.18.
So A, Chamot AM, Peclat V, Gerster JC (1999) Serum MMP-3 in rheumatoid arthritis: correlation with systemic inflammation but not with erosive status. Rheumatology (Oxford) 38(5):407-410.
Sponholtz TR, Zhang X, Fontes JD, Meigs JB, Cupples LA, Kiel DP, Hannan MT, McLean RR (2014) Association between inflammatory biomarkers and bone mineral density in a community-based cohort of men and women. Arthritis Care Res 66(8):1233-1240.
Stack RJ, van Tuyl LD, Sloots M, van de Stadt LA, Hoogland W, Maat BMallen CD, Tiwana R, Raza K, van Schaardenburg D (2014) Symptom complexes in patients with seropositive arthralgia and in patients newly diagnosed with rheumatoid arthritis: a qualitative exploration of symptom development. Rheumatol 53:1646-1653.
Sun S, Bay-Jensen A-C, Karsdal MA, Siebuhr AS, Zheng Q, Maksymowych WP, Christiansen TG, Henriksen K (2014) The active form of MMP-3 is a marker of synovial inflammation and cartilage turnover in inflammatory joint diseases. BMC Musculoskelet Disord 15:93.
Sun W, Meednu N, Rosenberg A, Rangel-Moreno J, Wang V, Glanzman J, Owen T, Zhou X, Zhang H, Boyce BF, Anolik JH, Xing L (2018) B cells inhibit bone formation in rheumatoid arthritis by suppressing osteoblast differentiation. Nat Commun 9(1):5127.
Tetlow LC, Lees M, Ogata Y, Nagase H, Woolley DE (1993) Differential expression of gelatinase B (MMP-9) and stromelysin-1 (MMP-3) by rheumatoid synovial cells in vitro and in vivo. Rheumatol Int 13(2):53-59.
Thilagar S, Theyagarajan R, Sudhakar U, Suresh S, Saketharaman P, Ahamed N (2018) Comparison of serum tumor necrosis factor-α levels in rheumatoid arthritis individuals with and without chronic periodontitis: A biochemical study. J Indian Soc Periodontol 22(2):116-121.
Tobón GJ, Youinou P, Saraux A (2010) The environment, geo-epidemiology, and autoimmune disease: rheumatoid arthritis. Autoimmun Rev 9(5):A288-A292.
Tokai N, Yoshida S, Kotani T, Yoshikawa A, Kimura Y, Fujiki Y, Matsumura Y, Takeuchi T, Makino S, Arawaka S (2018) Serum matrix metalloproteinase 3 levels are associated with an effect of iguratimod as add-on therapy to biological DMARDs in patients with rheumatoid arthritis. PLoS One 13(8):e0202601.
Tuncer T, Kaya A, Gulkesen A, Kal GA, Kaman D, Akgol G (2019) Matrix metalloproteinase-3 levels in relation to disease activity and radiological progression in rheumatoid arthritis. Adv Clin Exp Med 28(5):665-670.
Udalova IA, Mantovani A, Feldmann M (2016) Macrophage heterogeneity in the context of rheumatoid arthritis. Nat Rev Rheumatol 12(8):472-485.
Uemura Y, Hayashi H, Takahashi T, Saitho T, Umeda R, Ichise Y, Sendo S, Tsuji G, Kumagai S (2015) [MMP-3 as a biomarker of disease activity of rheumatoid arthritis]. Rinsho Byori 63(12):1357-1364.
Umeda N, Matsumoto I, Sumida T (2017) The pathogenic role of ACPA in rheumatoid arthritis. Japan J Clin Immunol 40(6):391-395.
van de Stadt LA, de Koning MH, van de Stadt RJ, Wolbink G, Dijkmans BA, Hamann D, van Schaardenburg D (2011) Development of the anti-citrullinated protein antibody repertoire prior to the onset of rheumatoid arthritis. Arthritis Rheum 63(11):3226-3233.
van Gaalen FA, Linn-Rasker SP, van Venrooij WJ, de Jong BA, Breedveld FC, Verweij CL, Toes RE, Huizinga TW (2004) Autoantibodies to cyclic citrullinated peptides predict progression to rheumatoid arthritis in patients with undifferentiated arthritis: a prospective cohort study. Arthritis Rheum 50(3):709-715.
van Heemst J, Trouw LA, Nogueira L, van Steenbergen HW, van der Helm-van Mil AH, Allaart CF, Serre G, Holmdahl R, Huizinga TW, Toes RE, van der Woude D (2015) An investigation of the added value of an ACPA multiplex assay in an early rheumatoid arthritis setting. Arthritis Res Ther 17:276.
Verma RP, Hansch C (2007) Matrix metalloproteinases (MMPs): chemical-biological functions and (Q)SARs. Bioorg Med Chem 15(6):2223-2268.
Vervoordeldonk MJ, Tak PP (2002) Cytokines in rheumatoid arthritis. Curr Rheumatol Rep 4(3):208-217.
Veys EM, Menkes CJ, Emery P (1997) A randomized, double-blind study comparing twenty-four-week treatment with recombinant interferon-gamma versus placebo in the treatment of rheumatoid arthritis. Arthritis Rheum 40(1):62-68.
Vickers NJ (2017) Animal communication: when i'm calling you, will you answer too? Curr Biol 27(14):R713-R715.
Vistoli G, De Maddis D, Cipak A, Zarkovic N, Carini M, Aldini G (2013) Advanced glycoxidation and lipoxidation end products (AGEs and ALEs): an overview of their mechanisms of formation. Free Radic Res 47(Suppl 1):3-27.
Wicks IP, Roberts AW (2016) Targeting GM-CSF in inflammatory diseases. Nat Rev Rheumatol 12(1):37-48.
Wijbrandts CA, Vergunst CE, Haringman JJ, Gerlag DM, Smeets TJ, Tak PP (2007) Absence of changes in the number of synovial sublining macrophages after ineffective treatment for rheumatoid arthritis: Implications for use of synovial sublining macrophages as a biomarker. Arthritis Rheum 56(11):3869-3871.
Wu J, Li Q, Deng J, Zhao JJ, Yu QH (2021) Association between IL-33 and other inflammatory factors in patients with rheumatoid arthritis and in fibroblast-like synoviocytes in vitro. Exp Ther Med 21(2):161.
Xu J, Feng Z, Chen S, Zhu J, Wu X, Chen X, Li J (2019) Taxol

alleviates collagen-induced arthritis in mice by inhibiting the formation of microvessels. Clin Rheumatol 38(1):19-27.

Yamanaka H (2015) TNF as a target of inflammation in rheumatoid arthritis. Endocr Metab Immune Disord Drug Targets 15(2):129-134.

Yumoto K, Ishijima M, Rittling SR, Tsuji K, Tsuchiya Y, Kon S, Nifuji A, Uede T, Denhardt DT, Noda M (2002) Osteopontin deficiency protects joints against destruction in anti-type II collagen antibody-induced arthritis in mice. Proc Natl Acad Sci USA 99(7):4556-4561.

Zamri F, de Vries TJ (2020) Use of TNF inhibitors in rheumatoid arthritis and implications for the periodontal status: for the benefit of both? Front Immunol 11:591365.

Zhang F, Wei K, Slowikowski K, Fonseka CY, Rao DA, Kelly S, Goodman SM, Tabechian D, Hughes L B, Salomon-Escoto K, Watts GFM, Jonsson AH, Rangel-Moreno J, Meednu N, Rozo C, Apruzzese W, Eisenhaure TM, Lieb DJ, Boyle DL, Mandelin AM, 2nd, A Accelerating Medicines Partnership Rheumatoid, C Systemic Lupus Erythematosus, Boyce BF, DiCarlo E, Gravallese EM, Gregersen PK, Moreland L, Firestein GS, Hacohen N, Nusbaum C, Lederer JA, Perlman H, Pitzalis C, Filer A, Holers V M, Bykerk V P, Donlin LT, Anolik JH, Brenner MB, Raychaudhuri S (2019) Defining inflammatory cell states in rheumatoid arthritis joint synovial tissues by integrating single-cell transcriptomics and mass cytometry. Nat Immunol 20(7):928-942.

Zimna A, Kurpisz M (2015) Hypoxia-Inducible Factor-1 in physiological and pathophysiological angiogenesis: applications and therapies. Biomed Res Int 2015:549412.